Zeitschrift: IABSE reports = Rapports AIPC = IVBH Berichte
Band: 79 (1998)

Rubrik: Tall buildings

Plenary Session

High-Rise Buildings

Keynote Lectures

Leere Seite
Blank page
Page vide

Architecture and Urban Responsibility in High-Rise Design

Jun MITSUI
Cesar Pelli & Assoc., Japan
Jun Mitsui & Assoc., Architects
Tokyo, Japan

Jun Mitsui, born 1955 received his Bachelor of Science degree from University of Tokyo in 1978 and Master of Architecture from Yale University in 1982 with awards. He is currently heading Cesar Pelli & Assoc., Japan and Jun Mitsui & Assoc. He is also a member of Japan Institute of Architects and American Institute of Architects and is licensed in both countries. He practices in architectural design and urban design.

Summary

High-rise buildings became possible through technological innovations, however at the same time their impact to our living space has been astronomical and changing our look of cities dramatically. Technology should be for the better quality of our life. Therefore as an architect Cesar Pelli has been struggling hard to make this very modern building type as part of our friendly partner. Technology is becoming very internationally recognized and understood however, urban culture of each place is very much attached to the place and strongly connected to the tradition and custom of the district. The job of architect is to negotiate those conflicting phenomena of modern age and create a better cities for people.

The Era of High-Rise Building

High-rise Building or so-called Skyscraper is a new invention of the modern society. They became able to exist by the modern technology which did not exist before the modern time. Office space before the skyscrapers were low to mid height office buildings with the light well (exterior courtyard in the middle) in the center.

Skyscrapers became possible on a group of technologies, such as fast elevator technology, air conditioning and electrical technology and structural technology. Especially in Japan, compared to other areas of the world, the idea of real skyscraper had to be a very new idea, because of the strong seismic consideration.

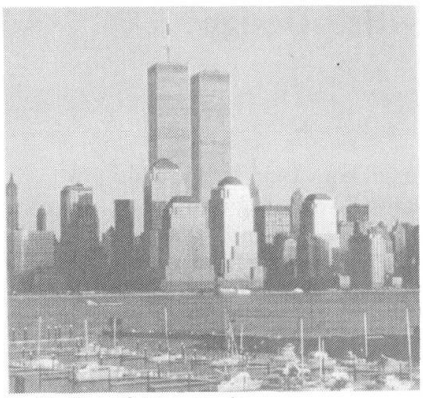

1 Skyline of New York

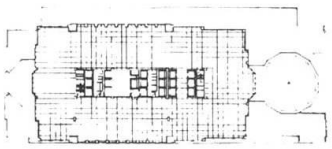

2 North West Center Plan

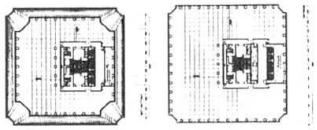

3 Mori Building Plan

4 NCNB Plan

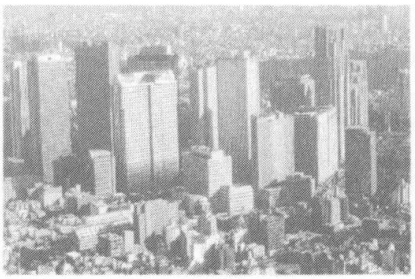

5 Bird's-eye view of Shinjuku

6 Bird's-eye view of Firenze

At the same time high-rise buildings became also possible by the economical reasons of the land development. One was a great need for white-color work space and the other was a pressure to maximize the limited urban property. As the commercial activities get centralized and very dense in terms of the per square feet value in cities, the pressure to maximize the every inch of the property became very important. At the same time with the development of the hi-speed elevatoring system, it actually became economically more efficient to do high-rises than doing flat and large floor plate buildings. The leasing depth of the tower high-rises were around 40 ft and it was a comfortable dimension as a office space.

In any case, the idea of skyscraper became a very common idea in the modern world supported both by economy and technology and they are changing the traditional idea of urban space and urban development planning method.

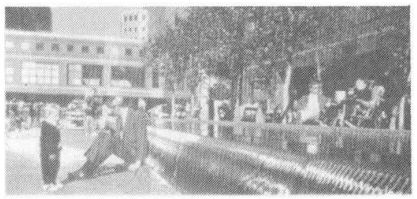

7 World Financial Center

Urban Impact by High-Rise Buildings

Because of its immense scale and volume as well as the numbers of the people living in the building and the energy consumed there, high-rise buildings have been always controversial issues in our society. Here I would like to focus my attention on the visual impact of the high-rise to the city both as part of our culture and as part of the tools to create comfortable city.

Cities are places for people not for buildings. Therefore the urban space such as street, piazza, plaza and others are so de-

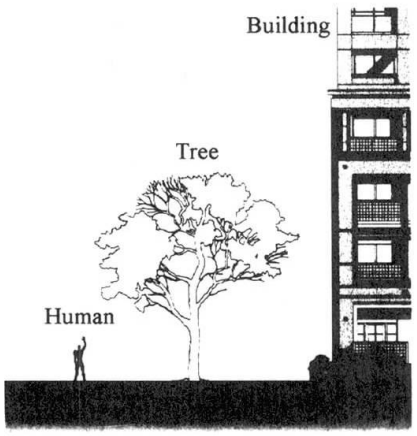

8 Comparing Scales

signed that people in there feel comfortable and can enjoy their life in the city. And people has certain scale. Human scale, although they may be slightly different by generations, or country, they are in a certain height range. And trees are also in a certain height ranges too. As a result the scale of the buildings should fit to the scale of people and trees not vise versa.

9 A contemporary city for 3 million people.

In the process of urban planning studies for high-rise buildings, incentive method were created to minimize the negative impact of the high-rise buildings. This was to achieve more comfortable open spaces around the building by giving more FAR to the building as a bonus. As Le Corbusier tried in his "La Ville Radieuse" book, towers surrounded by green open space was one of the first try to solve the high-rise building and human scale, in which he tried to solve the scale problem by placing park around the tower. This method however as a result did eliminate the development of urban street space and made the space around the tower very barren. People needed street activities on the street not a very windy open plaza or just trees. From a urban activity (nigiwai) view points, the high-rise shape controlling method should be carefully studied.

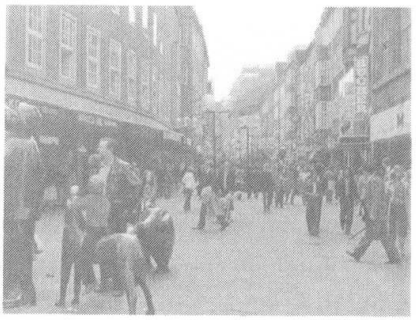

10 Urban Street Space formed by human scaled buildhing fronts

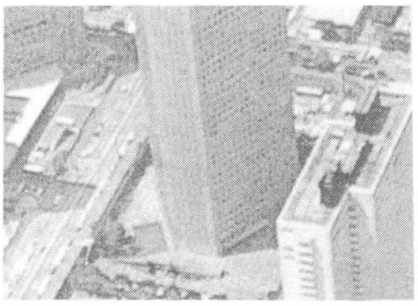

11 Lack of attention to surrrounding space

Because of its immense volume, the wind moves around the tower sometimes in a very unexpected way and can cause uncomfortable micro-climatic conditions. Wind, after hitting the tower can be a very strong down-draft on the street and the velocity of the wind around the tower could be very annoying and sometimes can become physically very dangerous. The consideration to the micro-climate conditions which will are caused by the towers are a new urban problems and needs careful design responses to solve the problem.

Roles of High-Rises in the Urban Space Planning.

Because of its height, high-rise towers can play important role which mid-rise buildings could not play. One thing which it can achieve is the sense of landmark of the area. Height itself already gives a strong visibility and people get very much inspired by the height. There has been always a desire in people to go higher and taller structure. The KLCC towers which Cesar Pelli

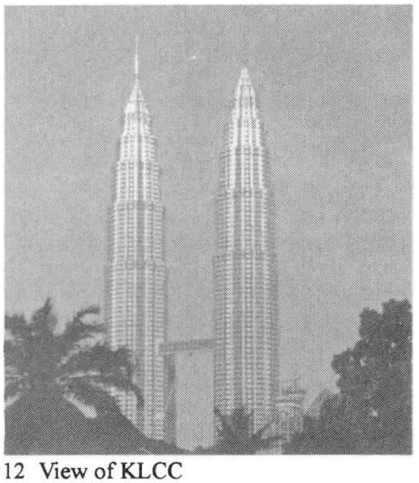

12 View of KLCC

& Associates (CPA) designed are the highest skyscraper in the world as of 1998 and the fact has been actually very much appreciated as a national pride by Malaysian people.

-KLCC Towers Kuala Lumpur, Malaysia-

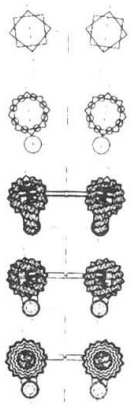

13 Plans of KLCC

Because of its very visible presence, not only the height but the design of the tower is also very important. In the KLCC tower we tried to achieve cultural metaphor in the tower design. First the floor plan of the tower is the overlap of the two squares rotated by 45 degrees. This combination is the basic set of geometry for Islamic visual culture which does not have icon figure in their life. The pattern with comfortable leasing depth and other mechanical space comfortably planned became a very reasonable floor plans for towers. The floor plans are fine adjusted depend on the floor and created a modern symbol for Kuala Lumpur. This project has two tower in symmetry and 70 meters space in-between. Each tower embodies the modern translation of the Islamic culture and the in-between space implies the gateway to the city.

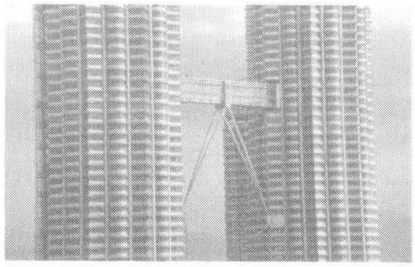

14 Bridge of KLCC

At the 52nd floor level two towers are connected by the double deck bridge for functional reasons. This large scale design configuration is obviously an urban response by Cesar Pelli, accomplishing its role. At the same time this tower has a huge commercial function base which makes the street life much more active and comfortable. People needs excitements and lots of people on the street to enjoy their life.

15 Base

High-rise buildings have basically two different appearances in urban-scape. One is the long distance view which could be also called sky-line shape and the other is the base of the tower which defines the street space and very much related to human scale. Although the tower structure may be purer and simpler if it is isolated from the other structure, it is more comfortable for people if it has a smaller scale base attached to the high-rise structure.

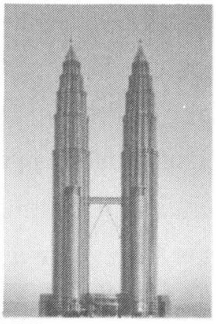

16 Full view of KLCC

At the beginning stage of the high-rise structure history, structural consideration prevailed and essentially decided its form.

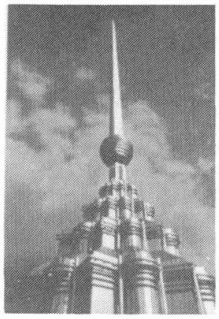

17 Detail of top

However now we are finding out that the technology and science is for people not just for technology and science and those are tools to achieve thinking of human-being. Even the high-rise buildings should be designed and should reflect the local culture of the place, and then they could be a cultural symbol of the place.

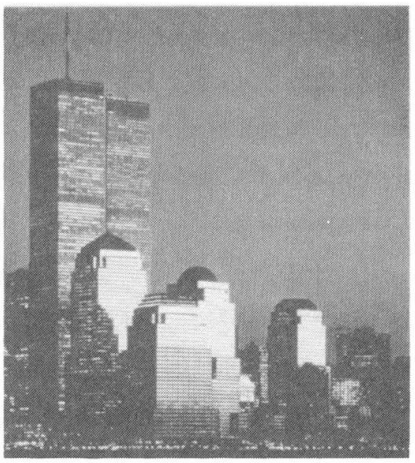

18 View of the World Financial Center

-World Financial Center NY, USA-

High-rise buildings in some cases are designed and planned in groups. When there are so many towers planned in the city, obviously the design and planning coordination of the towers are very important. In the early stage of the high-rise structure, it was not a consideration to make the tower much more sympathetic to the culture of the place. However we are realizing that it is actually very important to design towers carefully in coordination with other developments and urban context because the quality of the urban space will be decided not by a single building but the collection of the buildings in that area. In this project CPA was trying to balance the skyline form which will be created by both World Trade Center and WFC. It was not important to have a stronger presence or distinguished presence than the World Trade Center but to create a better Manhattan skyline and urban space together with the surrounding buildings. The end result, we believe is amazing. The new addition created a much better urban space in New York and added a great life to Manhattan skyline.

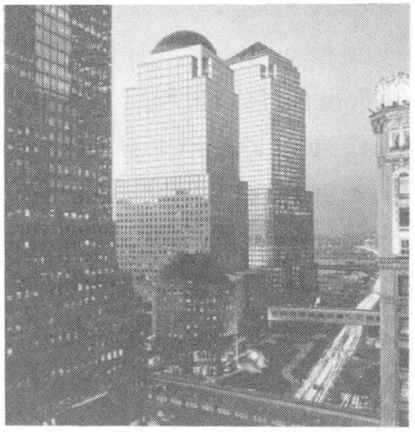

19 View of the World Financial Center

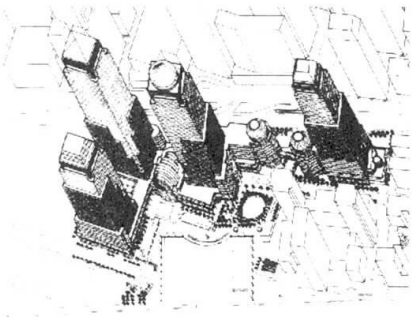

20 Axonometric

In this project there are four office towers and each has different shape roof as a metaphor to old New York skyscrapers. The floor plate sizes were adjusted so that basic tower floor plate sizes are very similar to World Trade Center. And there are setbacks in tower forms to create a sense of gradual height increase of the towers towards World Trade Center.
By this massing consideration, the World Financial Center and adjacent buildings became very interrelated urban buildings, those are together creating a exciting urban space.

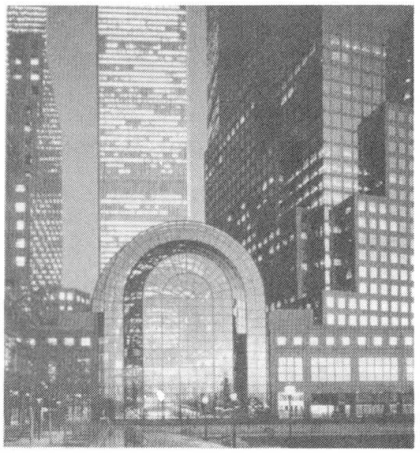

21 Base of the World Financial Center

Buildings are so interlaced in the modern cities and collaborating spatial effect of the multiple buildings in the city is becoming

very important especially in the large scale high-rise buildings. As an architect we feel that it is our responsibility to create better city and better buildings for future by adapting the presence of high-rise bldgs. and by adjusting its scale and make it more gentle to people.

-Sea Hawk Hotel, Fukuoka, Japan-

This project is right on a beautiful bay called Hakata Bay, and next to the huge indoor baseball dome structure called "Fukuoka Dome". When the design started for this hotel, the baseball dome was already designed and our goal was to create a good resort hotel and beautiful skyline for the entire complex including the future Fantasy Dome. Since the massing of the Dome Stadium is so large and chunky that we felt that the design of the hotel high-rise tower should be rather thin in profile and should look visually light. In the end the floor plan of the tower became a ship-like form with the pointed top. This shape also achieved a view to the Hakata Bay from all the guest rooms. We also added a vertical articulation to the tower. Since the structure became so thin, we had to put the seismic mass damper a the top of the tower.

From the bay, the high-rise tower poses a very strong and characteristic presence and it is a very visible landmark of this area. The height of the tower is limited by the airport near-by, however it is the highest structure in that area. When people approach from air or on the sea or by car, the shape of the structure is so designed that from every angle, the structure appears almost as a sculpture and gives a new addition to Fukuoka culture.

Cesar Pelli & Associates have done many skyscrapers all over the world and what interests us most whenever we design high-rise building is to contribute to creating a comfortable and pleasant living environment through architectural design and urban design. When we design skyscrapers, we see people working there, shopping there and enjoying the buildings and the environment which the skyscrapers creates.

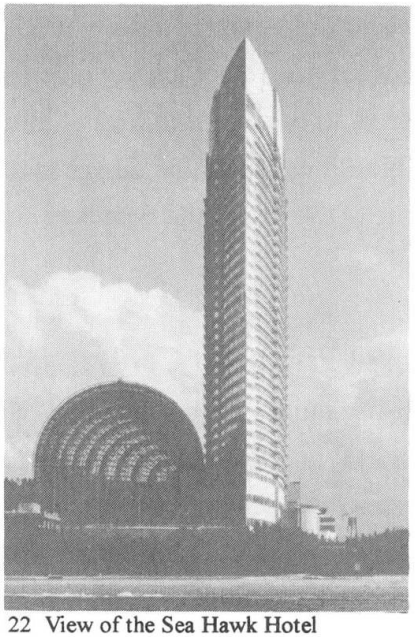

22 View of the Sea Hawk Hotel

23 Plan

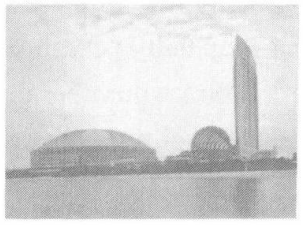

24 The view from Hakata Bay

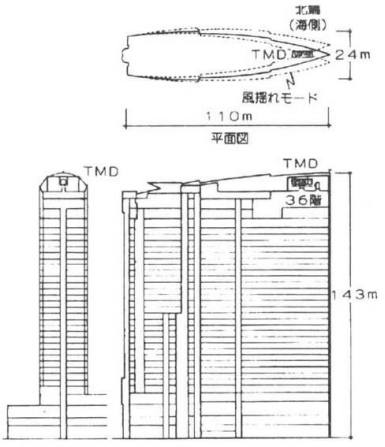

25 Seismic Damper System

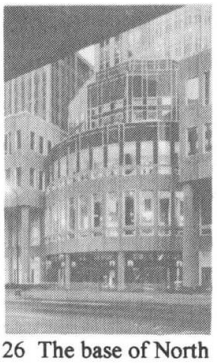

26 The base of North West Tower

27ShoppingAcade in the North WestTower

New high-strength steel and high speed computer controlled elevator system will
soon make a kilometer tall high-rise possible. And at that time we will have to
ask ourselves why we are building such a tall tower? Do we really need it for our better life or is it simply for a technological challenge or a desire of human-being to show its pride and achievement. However when economy or technology decides to build the next generation structure, as an architect we are committed to design the new structure to make our city more comfortable and livable space.

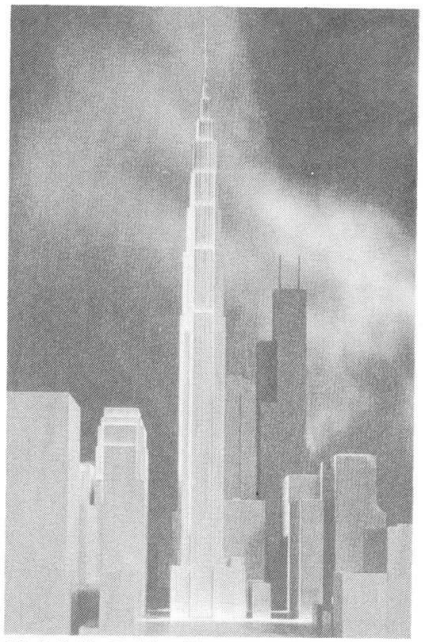

29 Miglin Beitler Tower

Quotation

1. Photo No.1 taken from "The Master Architect's Series-Cesar Pelli," published by Sigma Union, 1993 page 55
2. Photo No.5 taken from "The Development of Complex Renovation," published by Syoukokusya, 1995 page 47
3. Photo No.6 taken from "The Street and Roof of Europe, " published by Creo Corporation, 1995 page 103
4. Photo No.7 taken from "The Master Architect's Series-Cesar Pelli," published by Sigma Union, 1993 page 63
5. Photo No.9 taken from "Le Corbusier," published by A.D.A. EDITA, 1975 page 15
6. Photo No.10 taken from "Public Design Dictionary," published by Sngyo Cyosakai , 1991 page 148
7. Photo No.11 taken from "Public Design Dictionary," published by Sngyo Cyosakai , 1991 page 72
8. Photo No.17 taken from "The Master Architect's Series-Cesar Pelli," published by Sigma Union, 1993 page 131
9. Photo No.18 taken from "The Master Architect's Series-Cesar Pelli," published by Sigma Union, 1993 page 54
10. Photo No.21 taken from "The Master Architect's Series-Cesar Pelli," published by Sigma Union, 1993 page 56
11. Photo No.26 taken from "The master Architect's Series-Cesar Pelli," published by Sigma Union, 1993 page 5 0
12. Photo No.27 taken from "The Master Architect's Series-Cesar Pelli," published by Sigma Union, 1993 page 53
13. Photo No.29 taken from " Cesar Pelli,Buildings and Projects" published by Rizzoli inter National Publications,Inc, 1993 page 187

Leere Seite
Blank page
Page vide

Building Where They Said It Couldn't Be Done!

R. Shankar NAIR
Senior Vice President
Teng & Associates, Inc.
Chicago, IL, USA

R. Shankar Nair received his Ph.D. in civil engineering from the University of Illinois in 1969. In nearly three decades of practice with engineering and architecture firms in the USA, he developed the structural designs of numerous tall buildings of 30 to 70 stories and many major bridges. He is chairman of the Council on Tall Buildings and Urban Habitat

Summary

Construction of tall buildings in the centers of the world's large cities almost invariably involves working within severe site constraints. The constraints can involve all aspects of architectural and engineering design. As illustrated with examples drawn from the author's practice, many different structural engineering concepts are available for overcoming limitations imposed by site conditions. Creating opportunities for development of "impossible" sites through innovative design represents a unique — and uniquely rewarding — challenge to the structural engineer.

1. Introduction

Innovations and refinements in the structural analysis and design of tall buildings can make the building structure more efficient by providing the required strength and serviceability at less cost. But important as they are, these improvements in analysis and design (which may save the project owner a few dollars per square meter in construction cost) will rarely have a decisive effect on the economic feasibility of an urban development.

There are situations, however, where the structural engineer's contribution to the success of a project can be decisive. Most often, these situations involve the use of innovative structural engineering to overcome or circumvent constraints imposed by site conditions.

It is the rare tall building these days that can be placed on a "green field" location. Typically, the new urban building project has to conform to constraints imposed by existing conditions at the site. Site conditions can require that a building have a structurally-inefficient shape (e.g., unsymmetric or very slender). And site conditions can create a situation where there is no clear and direct path along which to transmit structural loads into the ground from floors located where they are functionally most desirable. It is the latter situation that is the primary subject of this paper.

Some of the main classes of solutions to the problem of transferring structural loads to the ground along indirect paths will be outlined. This will be followed by a discussion of a few unusual load-transfer challenges and solutions from the author's practice.

2. Types of Structural Transfers

At the most basic level, structural load transfer systems can be classified according to the type of load that is to be transferred — vertical force, horizontal force, or overturning moment. Transfer systems for vertical load and those for horizontal force and overturning moment will be discussed separately.

2.1 Transfer of Vertical Load

When the direct downward transfer of vertical load to the ground is prevented by an obstruction, the solutions include spanning across the obstruction or cantilevering out over the obstruction, as illustrated in Figure 1. The transfer trusses or girders (trusses shown) used for the span or cantilever could be located near the bottom of the building or at the top (or anywhere in between).

Locating the transfer trusses or girders at the bottom will usually result in lower construction cost. When the transfer elements are at the top, floor loads have to be carried up to the top through hangers and then down to the ground through the support columns. The extra distance through which the loads have to be transmitted will be reflected in increased column and hanger material and cost. Also, the construction sequence can be awkward. Yet another difficulty with the hung-from-above design is proper control of floor elevation, since floor loading simultaneously stretches the hangers and compresses the support columns.

Despite these drawbacks, transfer trusses or girders are sometimes placed at the top, either within the building envelope or exposed above the roof. This is done when transfer components at the lower floors would have an unacceptable effect on the functional or architectural design of the project.

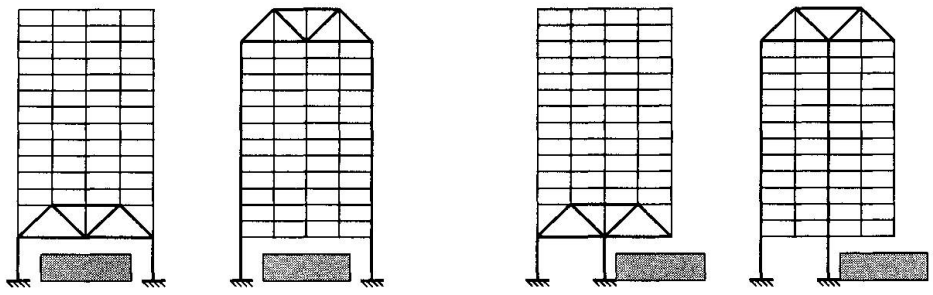

Fig. 1. Structural transfer concepts for vertical load

A possible alternative to the transfer cantilever shown in Fig. 1 is the "tied-back shear panel" transfer system shown in Fig. 2. In this design, vertical load is shifted laterally by means of a vertical wall panel (or diagonally-braced truss panel) loaded in essentially pure shear. The corresponding moment is restrained by a tension tie at the top of the panel and a compression strut at the bottom, both connected to the building's main lateral load-resisting system.

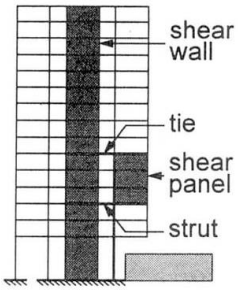

Tied-Back Shear Panel

Fig. 2. Tied-back shear panel transfer concept for vertical load

In many situations the shear panel will be less disruptive of the use of the building than conventional cantilever trusses or girders. The drawback is that the moment imposed on the building's lateral load-resisting system can be substantial. (Of course, balanced panels on both sides of the building would avoid this problem.)

2.2 Transfer of Horizontal Shear and Overturning Moment

Structural design concepts for transfer of horizontal shear and overturning moment from one part of a building structure to another are illustrated in Fig. 3. In the picture on the left, shear alone is transferred, while the moment continues down to the ground. In the picture on the right, both horizontal shear and overturning moment are transferred. (The building's lateral load-resisting system is shown as a truss or braced frame in the illustration; it could be a shear wall or rigid frame instead.)

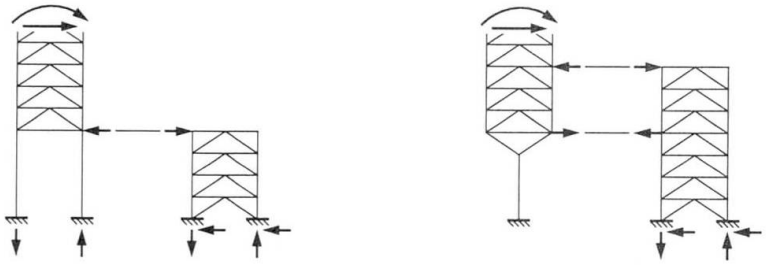

Transfer of Shear Alone Transfer of Shear and Moment

Fig. 3. Structural transfer concepts for horizontal shear and overturning moment

Transfer of horizontal shear in a building structure (left side of Fig. 3) is usually a simple matter. Building floors are typically very stiff and strong in their own plane, and can be designed to transmit large in-plane forces at little additional cost.

Overturning moment can be transferred from one part of the building to another as a horizontal couple, using floors to transmit horizontal force in one direction at one floor and the opposite direction at another floor (right side of Fig. 3).

3. Examples

The use of innovative structural transfer systems will be illustrated with four examples drawn from the author's consulting engineering practice. One of the projects was not actually built; it succumbed to changes in market conditions late in the design process. The other three examples are buildings that have been completed.

In the following discussion of the four projects, there will be some simplification and idealization of actual conditions, for purposes of clarity. Additional information on the three completed buildings can be found in the database of the Council on Tall Buildings and Urban Habitat. (The database is accessible to Council members through the Internet.)

3.1 Morton International Building

The Morton International Building (Reference 1), at 100 North Riverside in Chicago, is a 36-story, 101,000 m^2 office building. The lower 12 floors, of 4,300 m^2 each, hold lobbies, parking space for 435 cars, and a 26,000 m^2 computer center for the local telephone company. The upper floors hold rental office space.

The entire project is above an active rail yard, which had defeated all previous attempts at developing the site, though it is at a prime location on the Chicago River. As shown in the schematic site plan in Fig. 4, the rail tracks cover almost the entire site. The streets in the area are about 10 m above the tracks.

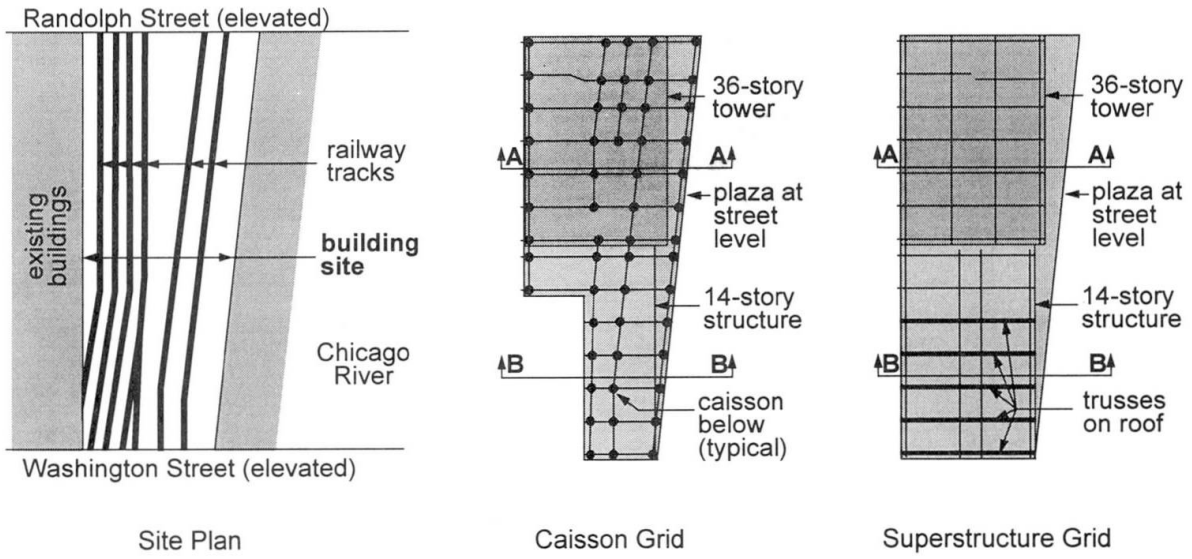

Fig. 4. Schematic layout of Morton International Building

Development of the Morton International site was made possible by a comprehensive transfer system. Foundation caissons (drilled piers) and track-level columns were located where track clearances were adequate, as shown in the caisson grid in Fig. 4. The caisson locations did not coincide with column locations in the building above (see superstructure grid in Fig. 4).

A complete grid of concrete transfer girders, about 2.5 m deep and between 1.0 and 2.5 m wide, transfers load from the building columns above to the track-level columns and caissons below. The top of the girder grid is at street level. The columns below the girders are of reinforced concrete (and are, in effect, extensions of the caissons). The building above the girders is framed in steel. Schematic Section A-A in Fig. 5 shows the relationship between building columns, transfer girders and caissons.

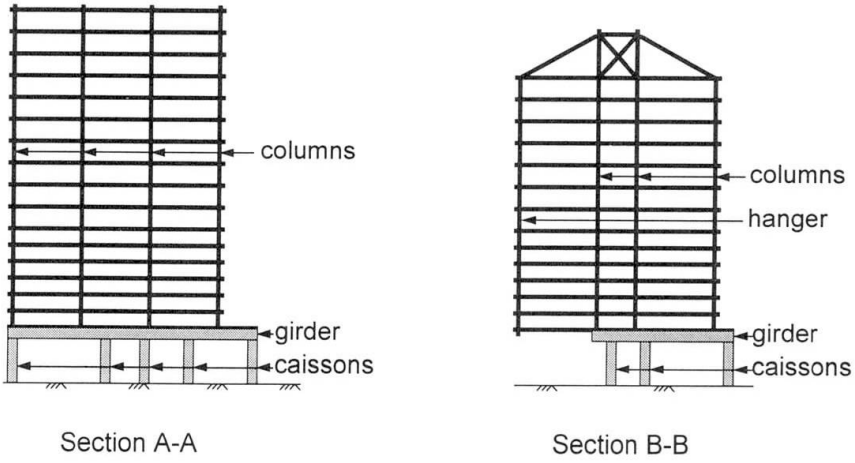

Fig. 5. Schematic sections through Morton International Building (see Fig. 4 for location of sections)

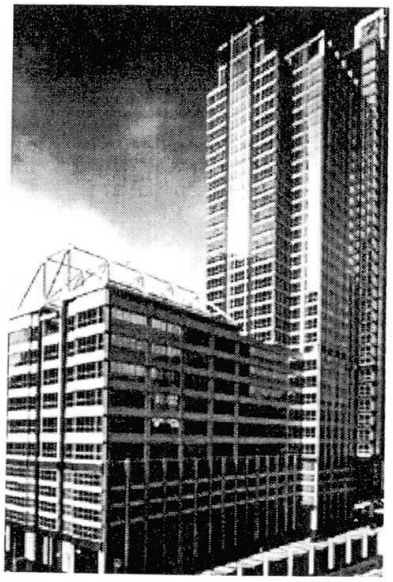

Fig. 6. Morton International Building

There was no room for caissons or columns among the tracks in a 20 m x 46 m area at the southwest corner of the site (see caisson grid in Fig. 4). In early planning concepts, this area was left unbuilt. However, it proved to be very important that there be floors above this foundation-

less area. The telephone company demanded full 4,300 m^2 floors; efficiency of the parking layout also required full floors, without a cut-out in the corner. The solution was to provide a cantilever transfer system to support the part of the building below which there could be no caissons. Cantilever trusses at the bottom, just above the tracks, would have been most economical but would have disrupted the parking layout. So the trusses were placed on the roof, where they became part of the architectural expression of the building, as indicated in Section B-B in Fig. 5 and the photograph in Fig. 6.

The Morton International Building is a good example of the use of an innovative structural transfer system to create an opportunity for development of a site that had previously been judged to be undevelopable. The entire building superstructure, both the 36-story tower and the low-rise portion, is supported on the grid of concrete girders above the railway tracks. The cost of the girder system, distributed over the floor area that it supports, was fairly modest.

The cantilever trusses support only a small fraction of the total floor area in the project. The additional floor area made possible by the cantilevers came at a very high price, if expressed in dollars per square meter of additional space. But this $\$/m^2$ figure does not tell the whole story. The cantilever system played an important role in the success of the entire project by creating the floor size demanded by a major tenant and by allowing an efficient parking layout.

3.2 Chicago Mercantile Exchange Center

The Chicago Mercantile Exchange Center (Reference 2), at 10 and 30 South Wacker Drive in Chicago, includes two 40-story, 116,000 m^2 office towers and two stacked column-free trading halls, of about 4,000 m^2 and 3,000 m^2 respectively. Parking is provided on four floors below street level. The photograph in Fig. 7 shows one of the two towers and part of the structure enclosing the trading halls.

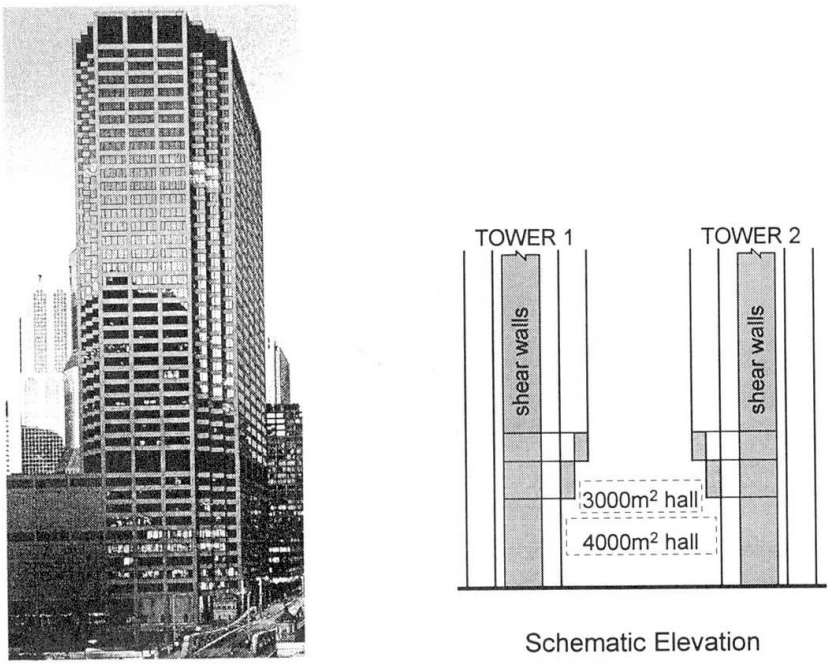

Fig. 7. Chicago Mercantile Exchange Center

Typical floors in the office towers are of just under 3,000 m^2, a size considered optimum in the local office leasing market. The challenge to the structural engineer on this project was to accommodate two 3,000 m^2 office towers and a 4,000 m^2 column-free trading hall on a site with a total area of under 8,000 m^2. The solution was to cantilever each tower about 10 m over the trading hall, as shown in the schematic elevation in Fig. 7.

The building is constructed of reinforced concrete, except that steel framing is used for the long-span floor above the lower trading hall and the roof above the upper trading hall. The lateral load-resisting system is a shear wall core in each tower. The project was completed in two phases: Phase I consisted of one tower and the trading halls; Phase II was the second tower.

Since the office towers overhang the trading halls by 10 m, it was necessary to transfer load out of one row of exterior columns in each tower. Transfer girders or trusses spanning across the halls would have been very expensive because of the long spans involved, and would have been further complicated by the phased construction of the project. Cantilever girders or trusses supported on the first row of interior columns and extending back into the building was another possibility. But this would have resulted in a large amount of wasted space. The cantilevers would have had to extend back into the elevator cores, which would have required a larger back-to-back spacing of elevators and wasted area on all floors in the towers.

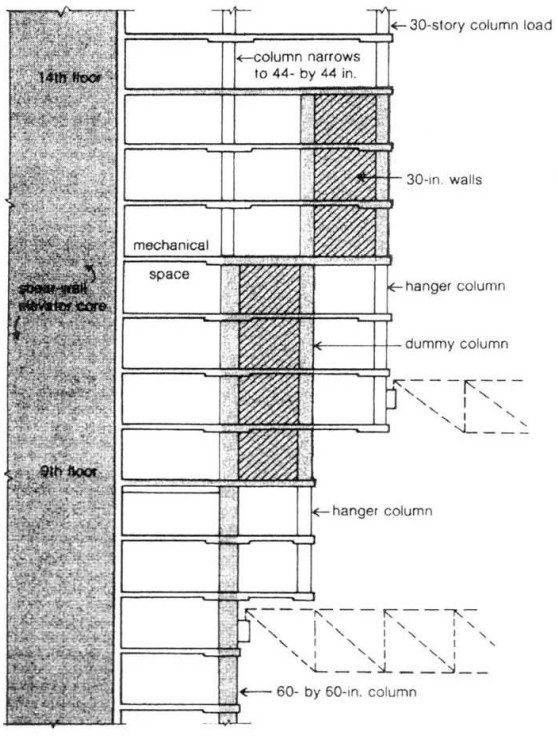

Fig. 8. Shear panel transfer system at Chicago Mercantile Exchange Center

The solution adopted was the tied-back shear panel concept explained in Section 2.1 and shown schematically in Fig. 2. The application of the concept to this project is shown in Fig. 8. The 10-m horizontal transfer is achieved in two steps over seven stories (with a total height of 25 m). The shear panels are reinforced concrete walls 760 mm thick. The tension tie at the top and the

compression strut at the bottom transfer overturning moment in the form of a horizontal couple to the shear wall core.

One of the interesting structural engineering details in the Chicago Mercantile Exchange Center project is that the overturning moments imposed by the transfer system cause lateral deformation of the shear cores. The towers were erected out-of-plumb by up to 100 mm to compensate for this. Subsequent lateral displacements, including long-term effects, brought the towers to a plumb condition.

3.3 Unbuilt Mixed-Use Project

This example will deal with a very large mixed-use project that involved extensive transferring of both vertical and lateral load. The project was not built, but the engineering concepts were fully developed (and tested for cost) before work was stopped.

The general layout of the project, simplified and idealized for clarity, is indicated in Fig. 9. It includes a 70-story office tower, two 40-story office towers and a 20-story hotel, with a common 6-story base or podium holding retail space. Parking is accommodated in several below-ground basement levels. The total floor area in the project is about 500,000 m^2. The project was to be constructed in two phases. The first phase, of about 250,000 m^2, included the entire basement and podium (including the lower floors of all the office towers), one 40-story office tower and the hotel.

Architectural and engineering design had been completed to the point of receiving a construction manager's Guaranteed Maximum Price for Phase I when the project was stopped because of changes in market conditions.

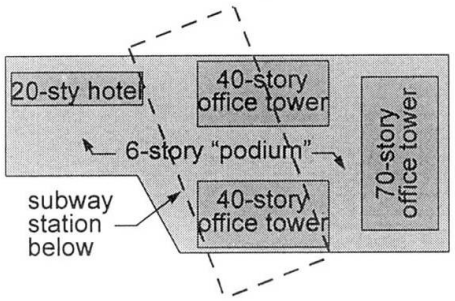

Fig. 9. Overall layout of unbuilt mixed-use project

The most obvious site-related engineering challenge on this project was the presence of a subway station running diagonally across the middle of the property (see Fig. 9). This had discouraged all previous attempts at developing the site, even though it was at a prime location. The top of the concrete roof slab of the subway station structure is about 2 m below the surrounding ground surface.

The solution to the problem posed by the subway was a grid of cast-in-place concrete transfer girders just above the station roof slab. The girders were supported on the station walls, some existing columns within the station where additional capacity was available, and new columns

inserted where possible within the station. The concept is similar to that adopted for the Morton International Building (see Section A-A in Fig. 5), but without the cantilevers and hangers.

Early designs for the project included expansion joints through the 6-story "podium" structure to separate it into four segments, one at each tower, as indicated in Fig. 10. This permitted the four towers to act independently in resisting lateral load, in conformance with conventional practice. But the joints gave rise to certain problems. The most obvious difficulty was that relative movement at the joints could be as much as 200 mm as the towers oscillated out of phase with one another during the design wind event. This was especially problematic in that some of the joints went right through ballrooms and other finished spaces.

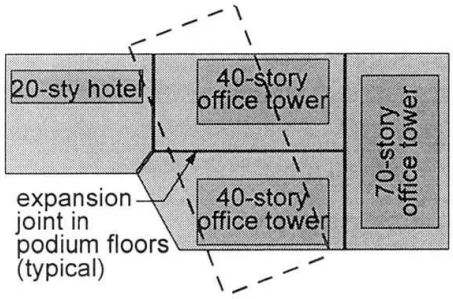

Fig. 10. Conventional expansion joint configuration

The office towers used braced-frame cores with outriggers to "supercolumns" as their lateral load-resisting systems. The initial structural design, again following conventional practice, carried the lateral forces from the towers straight down through the podium floors to the foundation. The problem here was that the diagonal bracing could not be carried down through the lower six stories since the retail space below the tower cores needed to be open. So instead of braced frames, massive steel rigid frames were proposed in the podium floors below the tower cores.

The problems posed by the large movement at expansion joints and the massive (and expensive) rigid frames below the tower cores were eliminated by a redesign that eliminated the expansion joints, causing the entire four-tower project to act as a single structure.

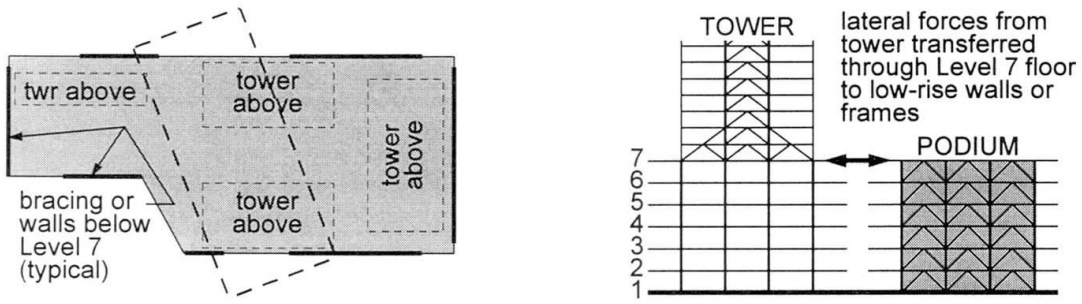

Fig. 11. Design concept with no expansion joints

With expansion joints eliminated, a separate bracing system was not needed below each tower in the podium floors. Bracing and walls were provided wherever they would fit conveniently, scattered throughout the project, below Level 7 (at the top of the podium), as shown on the left side of Fig. 11. The Level 7 slab was designed to transfer horizontal shear forces from the tower bracing systems to the podium bracing as shown on the right side of Fig. 11.

The redesign to eliminate the expansion joints and transfer lateral loads as indicated in Fig. 11, together with a few other structural engineering refinements, reduced the estimated cost of this project by $60 million.

3.4 Boulevard Towers

The Boulevard Towers office development, at 205 and 225 North Michigan Avenue in Chicago, consists of a 44-story, 86,000 m^2 South Tower and a 24-story, 82,000 m^2 North Tower. Up to the 19th level, a 30 m wide infill structure spans the 12 m space between the two towers, resulting in floors of over 5,600 m^2 each. The structure is constructed of reinforced concrete, with shear wall cores as the lateral load-resisting system.

Both towers straddle an existing commuter train station, which had to remain open throughout the construction period. A comprehensive grid of concrete girders supports tower columns and shear walls and transfers load to columns between the tracks and on the station platforms. The main subject of this discussion, however, will be not the transfer over the railway station but the linkage between the two towers. (The linked design anticipated some of the concepts proposed for the unbuilt mixed-use project discussed in Section 3.3.)

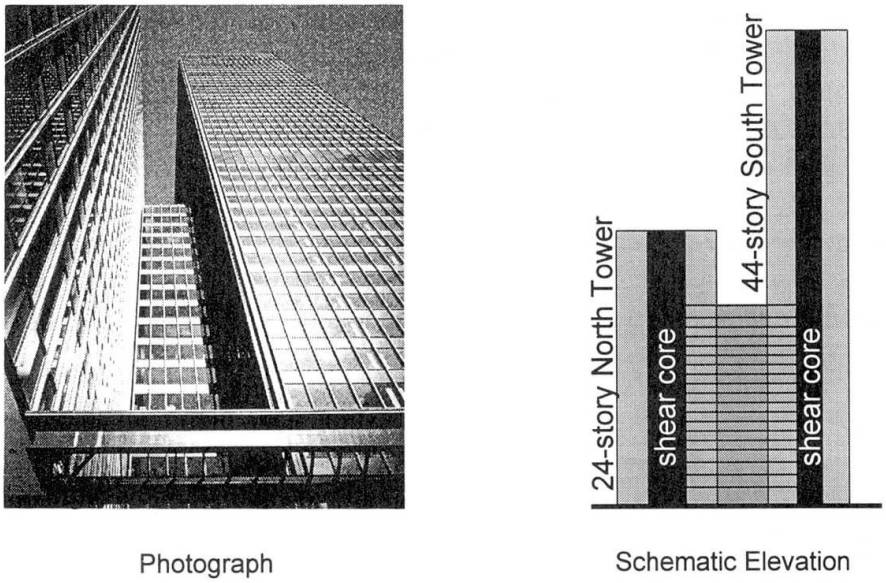

Fig. 12. Boulevard Towers

The 19-story infill between the two towers (see Fig. 12) links the towers structurally. There are no expansion joints between the infill structure and either tower. A joint at the infill would have been subject to very large relative movements — of the order of 300 mm at the 19th floor —

which would have been difficult to accommodate in the architectural and functional design of the project. Moreover, use of the infill floors to link the two towers structurally offered important benefits.

The lower North Tower has much larger floors than the taller South Tower. (Typical floor areas are 3,200 m^2 in the North Tower and 2,100 m^2 in the South Tower.) Architectural and space-planning requirements made it possible to have a deep shear core in the stubby North Tower, but only a shallow core in the slender South Tower. If the two towers had been structurally independent, the lateral load-resisting system of the taller tower would have been extremely inefficient and expensive. Linking the towers (see schematic elevation in Fig. 12) allowed the deeper, stiffer core in the lower building to resist most of the combined lateral loading imposed on the two towers.

The link floors represent a transfer system for both shear and moment, as shown schematically on the right side of Fig. 3, except that not all the moment is transferred from the taller to the shorter tower. However, sufficient moment is transferred that the moment in the shear core of the South Tower is greater at the 20th floor (just above the link) than further down in the building. At the base, the two shear cores share overturning moment roughly in proportion to their stiffness, with the core of the lower building supporting significantly more than half the total.

The project was built in two phases. The shorter North Tower was built first; the taller South Tower was completed four years later. Compared to a design with the towers structurally separated by expansion joints, the linked design resulted in modest additional cost in the shorter tower and major savings in the cost of the taller tower.

4. Conclusions

Innovative structural transfer systems can create opportunities for development where they didn't exist before. This is illustrated by the Morton International Building and the unbuilt mixed-use project discussed in this paper. Existing conditions at the sites of both these projects had defeated all previous attempts at development. At the Chicago Mercantile Exchange Center, an unusual transfer system made it possible to place two office towers and a trading hall where it would otherwise have been economically possible to develop only one tower adjacent to the hall. In all these situations, the purpose of the transfer system was to carry to the ground, along indirect load paths, gravity loads from floors located where they were most useful.

Structural transfer systems can also be used to transfer horizontal shear and overturning moment from one part of a project to another. Transfers of this type can produce major reductions in the cost of the overall development, as illustrated by the unbuilt mixed-use project and the Boulevard Towers buildings. In both these cases, the transfer system integrated into a single structure towers that would, in a conventional design, have behaved as independent structural units.

As cities become ever more densely developed, structural engineers will have increasing opportunities to make decisive contributions to the economic feasibility of projects ' y conceiving innovative transfer systems.

5. References

1. "Confident Times Revisited: Morton International Building," by John Morris Dixon, *Progressive Architecture*, July 1991, pp. 94-98.

2. "Unique cantilevers carry 400,000 sq ft of tower," *Architectural Record*, November 1983, pp. 136-139.

Working Session

High-Rise Buildings and Towers

Papers and Posters

Leere Seite
Blank page
Page vide

Simplified Model for Wind Speed/Height Relationship and Design of High Rise Structures

Alfred B.O. SOBOYEJO
Prof.
The Ohio State Univ.
Columbus, OH, USA

Prof. Alfred B.O. Soboyejo born 1938, BS 1962 in C.E. Univ. of London, UK; MS 1963 Pd.D. 1965 in Structural Eng. and Mechanics, Stanford Univ., California, USA; UNESCO Post Doctoral Fellow at M.I.T.; Princeton Univ., Univ. of Pennsylvania, USA and Imperial College, Univ. of London, UK. Special Fields: Engineering Design, Structural Mechanics and Materials, and Probabilistic Mechanics Methods in Eng. Analysis and Design; Life Member and Fellow ASCE; Fellow ASME; Member IABSE.

Summary

A new simplified model for wind speed/height relationship is hereby reported in this technical paper. The applications of the model to the development of wind engineering codes and standards for the specifications of design wind speeds and dynamic wind pressures, for the structural design of high-rise structures, in different parts of the world, with different climatic conditions, are discussed briefly.

Introduction

The need to provide simplified but accurate models for extreme wind speed/height relationship is an important consideration in the development of appropriate design methodology in structural engineering design application. A new simplified model which can easily be linearized, in order to simplify computational work, has been developed and hereby presented in this technical paper. Having identified the wind profile for any topographical zone: namely, urban, semi-urban, or rural zone, and using appropriate field data, good statistical correlations have been established between the actual predictions of the model and recommended field data which can be used in structural engineering design.

THE NEW MODEL

Results of recent research are hereby presented for the characterization of wind speed/height relationship which can be used in structural design of high-rise structures. The new model gives results, which agree with Davenport's power laws model (1); which can be represented by:

$$y(h) = \frac{V(h)}{V(H_G)} = \left| \frac{h}{H_G} \right|^C \qquad (1)$$

In equation (1), V(h) is the wind speed at a height h above the ground level, H_G is known as the gradient height. C and H_G are constants which depend on environmental surface roughness of any of the three topographical zones; namely (i) urban, (ii) semi-urban and (iii) rural. The variable, y(h), is a function of the height h, as shown in equation (1). The values of these constants are as follows (1):

	Zone	The Exponent C	Gradient Height, H_G (feet)	The Drag Coefficient, K
(i)	Urban	0.40	1700	0.050
(ii)	Semi-Urban	0.28	1300	0.015
(iii)	Rural	0.16	900	0.005

In general, wind speed is generally a function of height h and wind gust duration t; however at a given value of wind gust duration, the mathematical form of the new simplified model is as follows; for any particular zone:

$$y(h) = \frac{h}{a_1 h + b_1} = \frac{1}{a_1 + \frac{b_1}{h}} \qquad (2)$$

Where a_1 and b_1 are constants for any particular zone. Equation (2) can be linearized to give the simple expression:

$$\left(\frac{h}{y(h)} \right) = a_1 h + b_1 \qquad (3)$$

When multivariate regression analysis was carried out on the data of h/y(h) against h excellent correlations were recorded, thereby demonstrating the validity of the model of equation (2). Results of the multivariate regression analysis are as follows:

	Zone	a_1	b_1	Correlation Coefficient
(i)	Urban	0.9184	336.44	0.988
(ii)	Semi-Urban	0.9433	165.92	0.985
(iii)	Rural	0.9647	62.81	0.992

The data of y(h) were generated using equation (1) and the recommended values of C and H_G given above.

In the above analysis h is in feet. Equations (1) and (2) are indeed simple mathematical models, which can be linearized, and easily applied to the prediction of wind speed/height relationship, for a given wind gust duration t and for any of the three zones indicated. Using this model, the variations of wind speed/height relationships, for each of these three zones are as shown in Figure 1. These wind speed/height profiles are applicable to both normal and extreme wind speeds.

Some important characteristics of the model given by equation (2) are as follows: When h is large the value of y(h) tends to a_1^{-1}. This means practically that when h approaches the gradient height H_{G1} where the gradient wind speed V_{G1} occurs, y(h) becomes 1.0, when $a^{-1} = V_G$, the gradient wind speed V_G relevant to the zone. This aspect of the model agrees with the field data (3). Furthermore by differentiation, it can also be shown that the value of the slope d/dh [y(h)] is b_1^{-1} when h=0.

STATISTICAL MODEL FOR EXTREME WIND SPEEDS

Using Type I Gumbel asymptotic distribution of extreme values in mathematical statistics, the maximum annual wind speed V(h,t) at a given height h and gust duration t can be shown to have a cumulative distribution function, which can be expressed as (2):

$$G[V(h,t)] = \exp[-\alpha \exp[-\beta V(h,t)]] \tag{4}$$

Where α and β are constants which can be obtained from field data; by linearizing equation (4) to give:

$$\ln(-\ln G[v(h,t)]) = \ln\alpha - \beta V(h,t) \tag{5}$$

By carrying out multivariate regression analysis on ln {-ln G [v(h,t)]} against V(h,t) we can obtain the constants α and β. Having obtained α and β for any given location, the return period in years, T_V, for any annual maximum wind speed V(h,t) can be expressed as (2) for the same location.

$$T_V = \frac{1}{\alpha} \exp[\beta V(h,t)] \tag{6}$$

The values of the constants α and β for any given location can also be computed from the mean μ and the standard deviation σ of the recorded data of the annual maximum extreme wind speeds which are (2).

$$\mu = \frac{1}{\beta}(\ln\alpha + 0.577) \tag{7}$$

$$\sigma = \frac{1.282}{\beta} \tag{8}$$

From equations (7) and (8), the values of the constants α and β can be evaluated. In general, the annual maximum wind speed data for V(h, t) are normally collected at height h = h_1 = 33 feet (10 m) at several meteorological stations. Equations (1) and (2) can be made use of in order to evaluate the corresponding maximum wind speed at any other height, for the same location, and for the same wind gust period.

In order to allow for the possible statistical variabilities in the maximum wind speeds V(h,t), it is necessary to evaluate the relationship between the intensity of wind turbulence, I_V, at a height h, and the normalized spectrum of wind turbulence evaluated at a height h_1 = 33 feet (10 m), as follows (1):

$$I_V = \frac{\sigma_V(h,t)}{V(h,t)} = 2.45K^{\frac{1}{2}}\left(\frac{h}{h_1}\right)^{-\gamma} \tag{9}$$

where K is the drag coefficient, of the particular zone, as indicated earlier in this technical paper.

APPLICATIONS IN STRUCTURAL DESIGN

In practical design of high rise structures against wind loads the Codes of Structural Engineering Practices have always recognized the major variables which can account for design wind speed. A typical specification of design wind speed, V(h,t), at a given height h in meters and wind gust duration, t, is as follows (3):

$$V_D(h,t) = V_B(h_1,t)F_1 \times F_2(h,t) \times F_3 \tag{10}$$

Where $V_B(h_1,t)$ is referred to as basic wind speed, which is the maximum wind speed, on the average, which occurs once in 50 years, (i.e. Tv = 50 years), see equation (6). F_1 is the design factor or constant due to topographic influences of the environment; $F_2(h,t)$ is a design factor or variable due to surface roughness of the environment, wind gust duration t appropriate to the size of the structure, and the height h of the structure and components above the ground level, where the wind loading is to be considered; F_3 is a design factor or constant due to the probabilistic considerations of the design life of the structure. Relevant tables (3) have also been provided in these Codes of Practices which had specified appropriate values of F_1, $F_2(h,t)$ and F_3 which should be used in the design of high-rise structures. Design wind pressure, P, is also defined as follows:

$$P = \frac{\rho}{2g}[V_D(h,t)]^2 \tag{11}$$

Where ρ is the density of the air, and g is the acceleration due to gravity appropriate to the location. From equation (10), it is quite clear that the appropriate specification of the random variable $F_2(h,t)$ is a critical issue in the characterization of the design wind speed, for structural design application. Based on results of recent research in this field, which can be verified using appropriate statistical data this paper therefore proposes the use of the same mathematical form of the model in equation (2), which will now be built into the process of defining the appropriate random variable $F_2(h,t)$ as follows:

$$F_2(h,t) = h[m(t)h + n(t)]^{-1} \tag{12}$$

Where m(t) and n(t) are the model constants at a specific value of wind gust duration, t, relevant to the height h, where the design wind loading is acting on the structure. Equation (12) can be linearized as follows:

$$\frac{h}{F_2(h,t)} = m(t)h + n(t) \tag{13}$$

Multivariate statistical regression analysis of the variable $h/F_2(h,t)$ has been carried out against the variable, h; using appropriate data from the British Code of Practice, see Reference (3) for the different zones of (I) urban, (ii) semi-urban and (iii) rural zones. This statistical analysis yields excellent correlation coefficients, see Table I, which therefore confirms that the new simplified linearized model of equation (13) from equation (12), gives results which agree very well with recommended practical field data.

The statistical analyses also give the relevant values of the new model constants m(t) and n(t) at different values of wind gust duration, t. The summary of the significant results of the statistical analyses are shown in Table I of this paper. Similar studies carried out on recommended field data of other regions of the world have yielded encouraging excellent correlations in the ongoing research in this field, at The Ohio State University, Columbus, Ohio, USA.

CONCLUSIONS AND RECOMMENDATIONS

The new simplified model developed in this paper is recommended for use in different parts of the world. The same statistical studies, which have been carried out in this paper should also be carried out on similar field data in different regions of the world, with different climatic conditions, in order to establish the relevant constants of this model which can be applied in practical structural engineering design of high-rise structures, in different parts of the world. The results of such studies should also be made available to the international technical groups and organizations in structural engineering.

ACKNOWLEDGMENT

The author is grateful to The Department of Aerospace Engineering, Applied Mechanics, and Aviation, and The Department of Food, Agricultural, and Biological Engineering at The Ohio State University, Columbus, Ohio, USA, for the facilities, funding and the encouragement which the author has received in carrying out this research.

REFERENCES

1) Davenport, A. G. "Use of Application of Statistical Concepts to the Wind Loading on Structures". Proc. Inst. Of Civil Engineers, Vol. 19, August 1961, pp. 449-472.

2) Soboyejo, A. B. O. "Probabilistic Structural Mechanics and Design for the High Wind Environment". Proc. Structures, Structural Dynamics and Materials Conference, American Institute of Aeronautics and Astronautics, Paper No. 97-1027, Kissimmee, Florida, USA, 1997.

3) British Standard Code of Practice CP3. Code of Basic Data for the Design of Buildings. Chapter V Loadings: Part 2: 1972. Wind Loads. British Standards Institution, London.

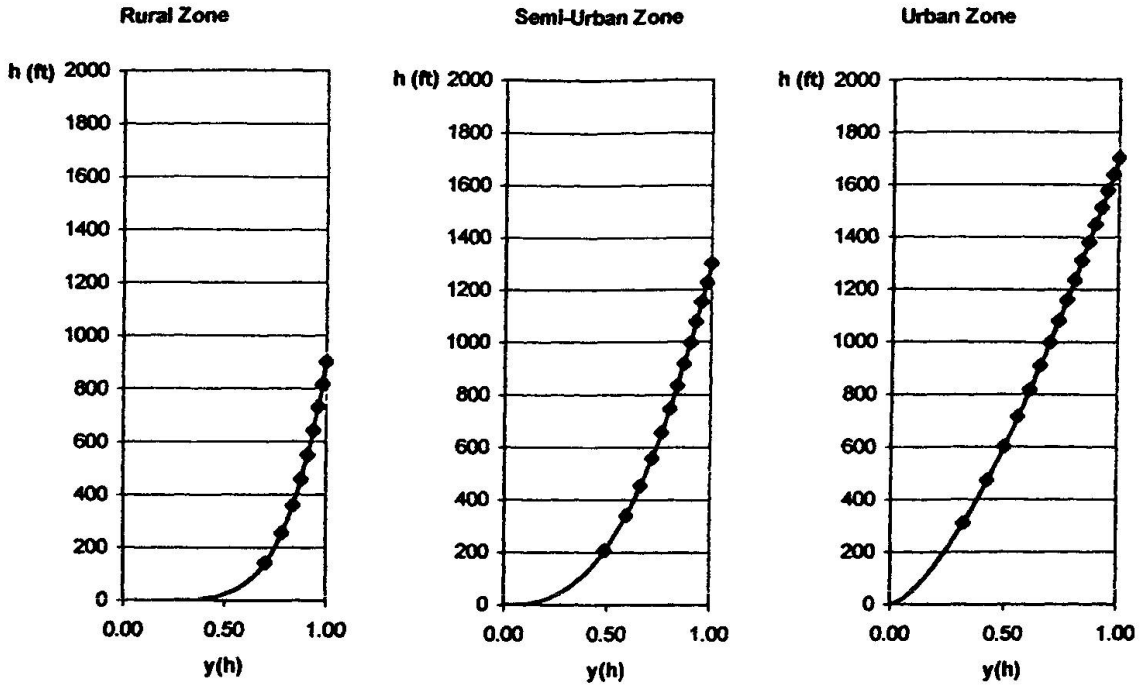

FIGURE 1: MEAN VELOCITY PROFILE, y(h) USING THE NEW MODEL.

Table I: Statistical Analyses of Data of Reference (3)

$$\frac{h}{F_2(h,t)} = m(t)h + n(t); \qquad \text{(h in meters)}$$

Zone	t=3 secs gust		t=5 secs gust		t=15 secs gust		Correlation Coefficient
	m(t)	n(t)	m(t)	n(t)	m(t)	n(t)	
Urban	0.7943	7.8190	0.8088	9.1890	0.8222	10.4981	0.9974
Semi Urban	0.7917	5.3979	0.7948	6.0970	0.8173	7.0315	0.9986
Rural	0.7804	3.5050	0.7984	3.9210	0.8166	4.6122	0.9988

Design Seismic Motions and Wind Loads for 1000 m High, 1000 Year Use Building

Jun KANDA
Prof.
Univ. of Tokyo
Tokyo, Japan

Toshihiko KUBOTA
Man. Dir.
Kobori Research Complex Inc.
Tokyo, Japan

Mitsugu ASANO
Gen. Mgr
Nikken Sekkei Ltd
Tokyo, Japan

Shin-ichi HIRASHIMA
Gen. Mgr
Shimizu Corp.
Tokyo, Japan

Yoshihiro MATAKI
Sen. Chief Research Eng.
Takenaka Corp.
Chiba, Japan

Summary

Construction of 1,000-meter-high hyper buildings for 1,000-year use having a total floor area of 10 million square meters in Japan requires studies on structural safety against earthquakes and winds. In this study, flowcharts for checking the structural safety of hyper buildings taking into consideration their characteristics, namely height and service life, were proposed, through comparison with typical flowcharts for high-rise buildings. Target performance and methods for determining design values of seismic and wind loads were also studied. This paper presents the basic concepts thus developed, along with a list of subjects of further study.

1. Introduction

Starting in 1995, a group of organizations including the Ministry of Construction, the Building Center of Japan, general contractors, and design firms conducted a two-year joint study as a step toward the realization of the scheme for hyper buildings, which are 1,000 m high and have a service life of 1,000 years and a total floor area of 10 million square meters. The study covered 13 fields of research, and the subject of design ground motions and wind loads was adopted as one of them.

Needless to say, a 1,000m-high building for 1,000-year use requires a more comprehensive structural safety evaluation than a conventional 300m-high 100-year-or-so-useful-life high-rise building does.

In this study, considering the construction of hyper buildings in Japan, methods for evaluating their structural performance and target structural performance are proposed. An example of calculation of a measure of safety common to seismic loads and wind loads is also presented. Finally, the basic concepts of seismic- and wind-resistant design and flowcharts for the proposed design procedures are presented.

2. Basic concept of structural safety

2.1 Image of a hyper building

Structural safety of a hyper building is considered for its three major components: main structure, secondary structure, and infrastructure. The main structure is the part of the hyper building that is supposed to remain unchanged in performance throughout the service life of the building. The secondary structure is any structure inside the main structure that may be changed, often more than once during the service life of the building, depending on performance requirements. The infrastructure is the part of the building that supports the circulation of people, vehicles, energy, and the like and computer-based control functions and is therefore subject to change depending on the performance needs of the time.

2.2 Flowchart for structural performance evaluation

Structural performance evaluation of hyper buildings requires a life-cycle approach because the construction period and service life of hyper buildings are longer than those of conventional high-rise buildings.
A flowchart for a life-cycle structural performance evaluation of hyper buildings against ground motions and wind loads is shown in Fig. 1.

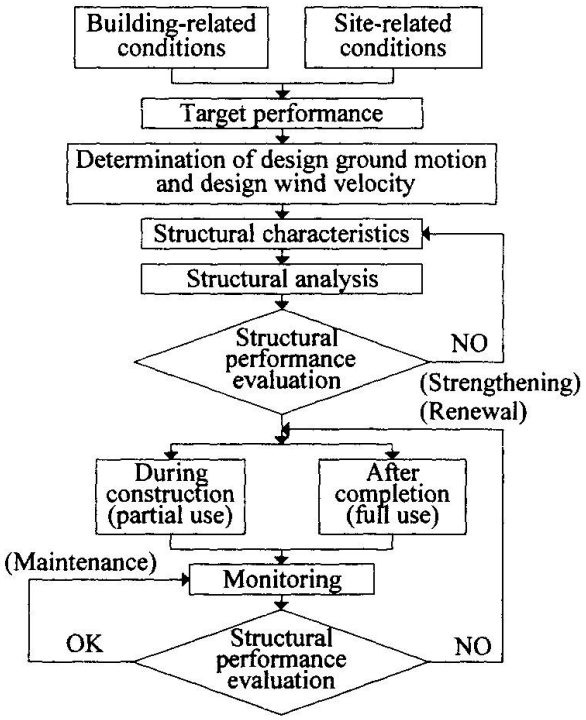

Fig.1 Flowchart for life-cycle structural performance evaluation of a hyper building

2.3 Target performance

The target performance of a hyper building is its ability to remain safe, restorable, and functional against natural and artificial phenomena that can occur during the assumed service life of 1,000 years. From the engineering point of view, it is considered reasonable to determine load conditions needed for structural design by statistically treating data on past natural and artificial phenomena and estimating phenomena which can take place in future. Specific target performance of each component of a hyper building for the three purposes that the building must fulfill is shown in Table 1.

Table 1 Definitions of target performance of hyper building by key word

Load category		L	P	F
Key word		Safety	Restorability	Functionality
Purpose		Protect life	Protect property	Maintain functions
Target performance	General	The structure neither collapses nor undergoes lifethretening damage under the maximum load expected during the service life of the main structure.	The secondary structure undergoes only minor damage under the maximum load expected during the service life of secondary structure.	The building is able to maintain its functions without making users feel uncomfortable under loads expected about once in several years
	Main Structure	The main structure behaves,for the most part,elastically under loads expected two or more times during the service life of the main structre.	The main structure responds elastically.	Attainment of habitability goals
	Secondary Structure	The secondary structure neither collapses nor undergoes life-thretening damage.	Mostly elastic response Minor repairs	Attainment of habitability goals
	Infra-structure	Rescue and evacuation are possible.	Easy restoration	Normal traffic, communications,etc.

2.4 Calculation of design load based on optimum reliability and checks of structural safety

1) Optimum reliability index

Using Kanda's method,[1] the optimum reliability index β_{OPT} is calculated from the equation

$$\beta_{OPT} = -\alpha_Q V_Q + \sqrt{(\alpha_Q V_Q)^2 + 2\ln(\frac{g}{\sqrt{2\pi\kappa}\alpha_Q V_Q})}$$

where α_Q : separation factor
V_Q : coefficient of variation of load effect
g : normalized failure cost
κ : normalized cost ratio

The design load X_D can be given as

$$X_D = \exp(\alpha_Q \beta_{OPT})\mu_{QT}$$

where μ_{QT} is the mean value of maximum loads per T years.
In this study, α_Q=0.85, g=2, and κ=0.05[2] are assumed for both seismic loads and wind loads.

2) Seismic load

The means of maximum values per 50, 100, and 1,000 years for ground surface velocity in Tokyo and Osaka were calculated, using Kanda's distribution parameters. The design ground motion velocity V_D based on the optimum reliability index was then calculated accordingly.
The mean μ_{QT} of the maximum values per T years of ground surface velocity and the optimum design ground motion velocity V_D for each site are shown in Table 2.

3) Wind load

The Gumbel distribution parameters for the annual maximum wind velocity at each site were calculated on the basis of Nakahara et al. (1984).[3] Then, the mean of the maximum values of the basic wind velocity (ground roughness category II for open space such as rural district, 10 m above ground surface) and the coefficient of variation at each site were calculated. For the evaluation of optimum reliability, dynamic pressure, which can be regarded as the load effect, was used, and the optimum design value was converted to a basic design wind velocity.
The coefficient of variation of the basic wind velocity was assumed to be

$$V_Q = \sqrt{(V_V^2 + 0.2^2)}$$ [4]

using the coefficient of variation, V_V, of the maximum value per T years.
The mean μ_{QT} of the maximum values per T years of ground surface velocity and the optimum design basic wind velocity U_D at each site are shown in Table 3. Since no upper limit is imposed on load values as in the case of seismic loads, the design load increases as the service period becomes longer.

4) Checks of structural safety

The probability of exceedance during the service period for each component is established, and structural safety is checked accordingly.

Table2 Mean of maximum values per T years of ground surface velocity and optimum design ground motion velocity (unit:cm/s)

T / Site	50		100		1000	
	μ_{QT}	V_D	μ_{QT}	V_D	μ_{QT}	V_D
Tokyo	14.8	41.3	17.8	44.6	21.9	50.6
Osaka	11.2	52.6	16.5	69.9	45.9	135.5

Table3 Mean of maximum values per T years of basic wind velocity and optimum design wind velocity (unit:m/s)

T / Site	50		100		1000	
	μ_{QT}	U_D	μ_{QT}	U_D	μ_{QT}	U_D
Tokyo	40.5	65.0	43.4	69.1	52.7	82.8
Osaka	46.7	76.9	50.8	82.7	64.4	102.5

3. Design ground motion

Because of the height and service life of hyper buildings which far exceed conventional ones considered for current seismic design practices, a study was undertaken for the development of a flowchart for the seismic design of a hyper building. The flowchart thus developed is shown in Fig. 2.(The steps common to seismic design and wind-resistant design are omitted, and only the steps between C and D in Fig.4 is shown)

The most important technical consideration in seismic design is how to determine the design ground motion. Therefore, various design input ground motions specified or proposed by laws, academic societies, or other institutions[5], and studies on source processes were examined, and a framework for the evaluation and determination of design ground motion was developed (Fig. 3).

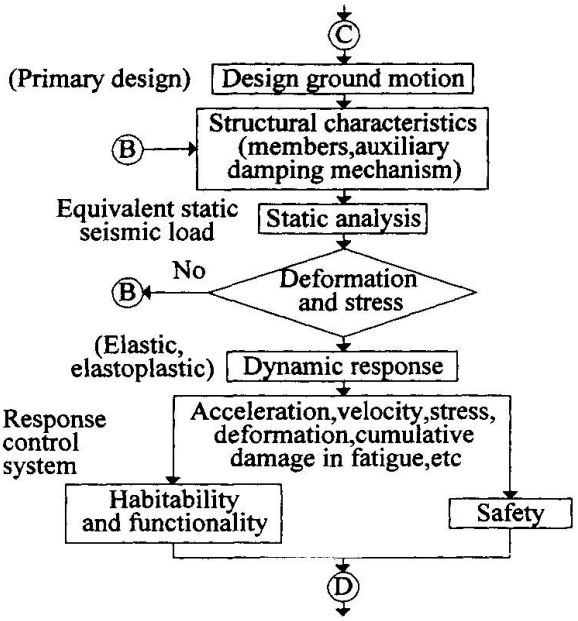

Fig.2 Flowchart for seismic design (part)

Site Investigation		
Seismological condition	Ground condition	Earthquake observation
Historical earthquake Active fault Seismo-tectonic structure	Bedrock Sedimentary basin Surface geology / topografy	Array observation

Characteristics of hyper building
Importance Size (1000m, period 20sec.) Service period (1000years) Design criteria classification

Design criteria		
Category L	Category P	Category F
Protection of life	Protection of property	Maintenance of functions(daily) Normal traffic and communication

Selection of study earthquake (a simplified method to be used for estimation of ground motion at the time of selection)		
Historical earthquakes	Active faults	Seismo-tectonic structure

Evaluation of ground motion	
Method 1 : Theoretical method Method 2 : Emperical method Method 3 : Semiemperical method	Method 4 : Hybrid method Method 5 : Other method

Determination of design ground motion		
Evaluation of ground motion characteristics	Determination of time history	Comparison with lower-limit ground motion for safety
Maximum amplitude Response spectrum Duration time Nonstationary chracteristics	Two or more time histories obtained by different methods Selection of representative one from two or more time histories Simulated ground motion compatible with two or more time histories	Definition of lower-limit ground motion for safety

Fig.3 Framework for evaluation and determination of design ground motion

4. Design wind loads

The proposed wind-resistant design procedure (Fig. 4) differs greatly from that for conventional high-rise buildings in the following aspects:

a) The method of determining the design wind velocity through estimation using a typhoon simulation model[6] is also applicable.
b) Wind observation[7,8] at altitudes of more than 1,000 m using doppler radar or doppler sodar is necessary.
c) In order to protect life, inelastic response analysis[9] is carried out as part of the studies conducted for the prevention of collapse.
d) Additional damping mechanisms are adopted wherever appropriate.
e) Checking fatigue damage[10] is essential.
f) The importance of maintenance not only during but also after construction is shown.

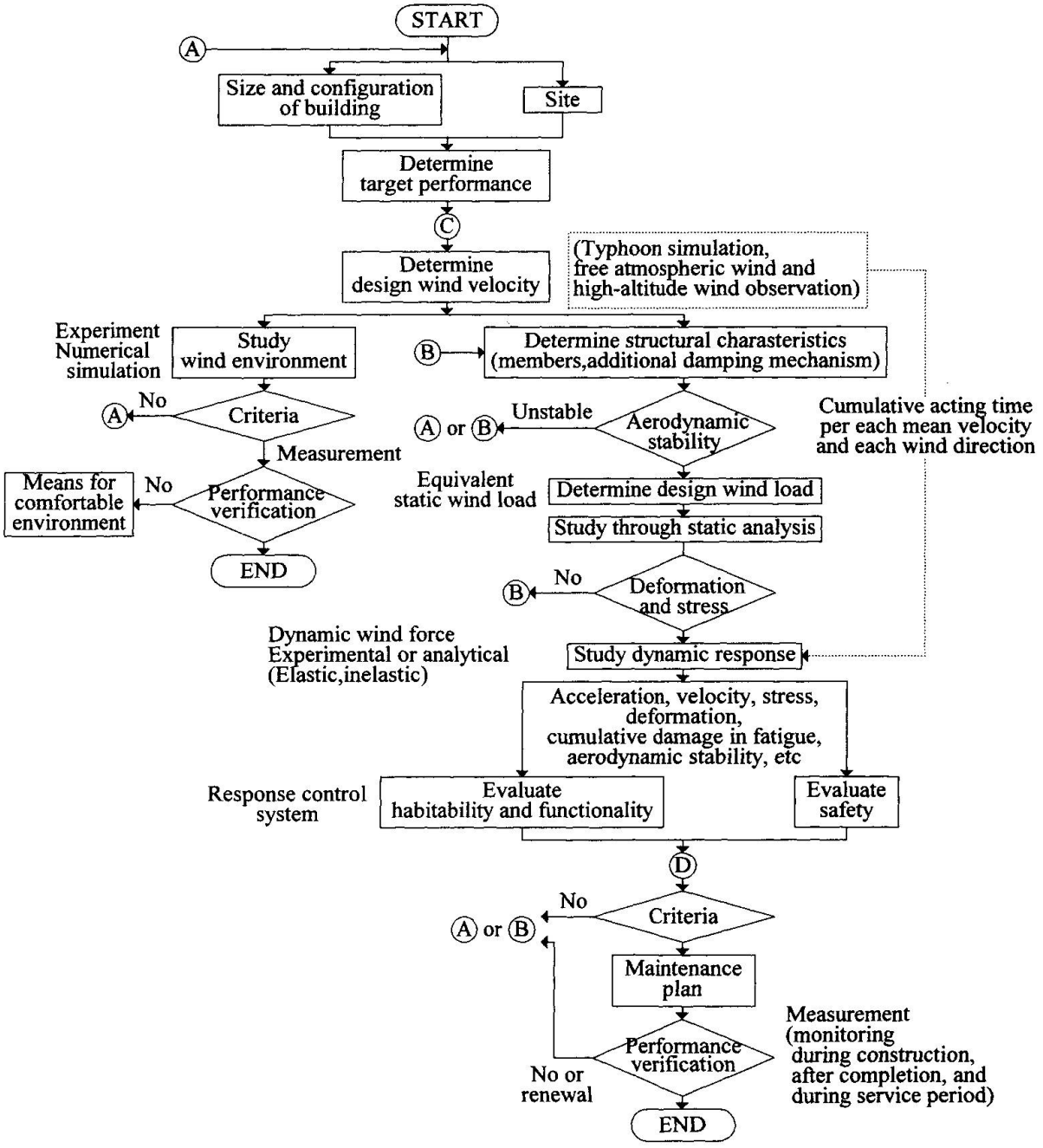

Fig.4 Flowchart for wind-redistant design

5. Conclusions

In this paper, basic concepts of what should be done to ensure the structural safety of hyper buildings against earthquakes and winds have been presented. As a result of this study, a number of subjects of further study have been identified. Among them are as follows,

1) Subjects concerning structural safety

(1) Risk level determination by use of such techniques as risk management
(2) Design recurrence interval and criteria
(3) Variations among analysis models

2) Subjects concerning design ground motion

(1) Synthesizing of broad-band (period: 0.1 to 20 second) design ground motions
(2) Zoning of predominant periods of ground based on past studies of velocity structure and on observation records of long-period strong ground motions
(3) Seismological conditions at the construction site and the determination of ground investigation areas
(4) Variations of factors affecting the maximum ground motion

3) Subjects concerning with wind-resistant design

(1) Development of wind-resistant design methods which consider elastoplasticity of structural members
(2) Development of more accurate typhoon simulation methods
(3) Observation of high-altitude winds

REFERENCE

1. J. Kanda, B. Ellingwood, Formulation of Load Factors Based on Optimum Reliability, Structural Safety, 9, 1991
2. J. Kanda et al, Construction Cost for Various Buildings with Varying Seismic Load, Proc. Annual Meeting, Architectural Institute of Japan (A.I.J.), Nagoya, 1994 (in Japanese)
3. M. Nakahara, Y. Tamura, Y. Asami, Y. Niihori and Y. Yoshikawa, Map of Japan showing Design Wind Speed, Trans. of A.I.J., No.336, Feb., 1984 (in Japanese)
4. J.Kanda, Stochastic Evaluation of Wind Load Considering Dynamic Gust Response, Proc. Symposium Wind Eng., 1982 (in Japanese)
5. T. Ishii and T. Sato, An Evaluation Methodology of Design Earthquake Motions Based on Site -Related Earthquakes, J. Struct. Constr. Eng., A.I.J. , No.462, Aug., 1994 (in Japanese)
6. Y. Meng, M. Matsui, and K. Hibi, An Analytical Model for Simulation of the Wind Field in a Typhoon Boundary Layer, J. Wind Eng. Ind. Aerdyn., No. 56, 1995
7. H. Hayashida, S. Fukao, T. Kobayashi, H. Nirasawa, Y. Mataki, K. Ohtake and M. Kikuchi, Remote Sensing of Wind Velocity by Boundary Layer Radar, J. Wind Eng., No.67, April, 1996 (in Japanese)
8. T. Amano, T. Ohkuma, A. Kawaguchi and S. Goto, The Wind Observation in Okinawa by Doppler Sodar during Typhoons, J. Wind Eng., No.67, April. 1996 (in Japanese)
9. O. Tsujita, Y. Hayabe, T. Ohkuma and A. Wada, A Study on Wind-Induced Response Characteristics and Prediction for Inelastic Structure Part1. A case of across-wind vibration, J. Struct. Constr. Eng., A.I.J., No.481, Mar., 1996 (in Japanese)
10. M. Yoshida, T. Kobayashi, T. Fukumoto, S. Hanyuuda and Y. Matuzaki, Estimation of Wind-Induced Damage Ratio of Steel Damper Controlling Structural Vibration, Steel Construction Eng., Vol.1, No.2, 1994 (in Japanese)

Wind Velocity and Building Reactions of High-Rise Structures

Gert KÖNIG
Prof. Dr
Univ. of Leipzig
Leipzig, Germany

Carl-A. GRAUBNER
Prof. Dr
Univ. of Technology
Darmstadt, Germany

Andreas BERNEISER
Civil Eng.
Elz, Germany

Summary

This paper describes the results obtained from wind velocity measurements at different heights in combination with longitudinal extensions in the main construction elements during the construction period of the new Commerzbank building in Frankfurt/Main. Additionally, a wind-tunnel test was carried out for comparison. A typical profile and other characteristics of the wind velocity plus resulting reactions of the building in an inner-city region were measured and compared with theoretical calculations and the coming European standard Eurocode 1 Part 2.4 "wind loads". The main result showed, that wind loads on high-rise buildings in inner-city regions are assumed much too high in the German and European standard, and, as such, may be reduced.

1 Introduction

From 1995 to 1997 a new high-rise building for the Commerzbank AG was erected in the city of Frankfurt (see [4], [6] and [10]). It is a 63-story building, which reaches to a height of approx. 300 m, including a 40 m high mast - making it the tallest building in Europe (see Fig. 1). It is located in an area with many other high-rise buildings.

This provided the opportunity to measure and analyze the wind velocity and resulting wind loads on a high-rise building in such an inner-city region. For tall buildings the vertical profile of wind velocity has a significant influence on the wind loads.

The wind velocities were measured on cranes at heights of 261 m, 219 m, and 216 m at the building site, at 153 m on top of a nearby high-rise building, and at 60 m in a region with only lower buildings. The measuring instruments for the longitudinal extensions were located inside 6 mega-columns on the 1st floor to get the reactions at the baseline of the building.

Thus, it was possible to measure the wind velocity at definite heights and the resulting base moment of the building from the wind loads simultaneously. Additionally, a wind-tunnel test was carried out to generalize the results.

Fig. 1: Eastern elevation of the new Commerzbank-Building

2 Description of the equipment

2.1 Measurements of the wind velocity

During the construction period three measuring points were installed: two on top of the cranes, which were raised consecutively with each constructional phase, and one on a 6 m high mast on top of the nearby Eurotower (147 m) (see Fig. 3 and Fig. 4). At each point of installation three anemometers measuring the wind velocity in three directions were implemented to determine the absolute velocity and direction. Most of the time, mainly at the end of the construction period, two installations were available, one on a crane at a height of 261 m and one on the Eurotower. The specifications of the used anemometers (see Fig. 2) are shown in Table 1. In addition to these measurements, the mean wind velocity at a height of 60 m was obtained from a weather station located 2 km from the Commerzbank tower in an area with only lower buildings.

The data were transmitted via radio signal to a PC located in a room in the second basement, and the data from all anemometers were saved simultaneously every two seconds (for detailed information see [5]).

Table 1: Specifications of the propeller anemometers

Description	Propeller Anemometer
Measuring mode	Digital (Impulses)
Range	±0.15 ~ ± 60 m / sec
Accuracy	< 1.0 % of value measured
Resolution	< 0.13 cm / sec
Length of inertia	2.0 m ± 0.1 m
Measurement cycle	Once every two seconds

Fig. 2: propeller-anemometer

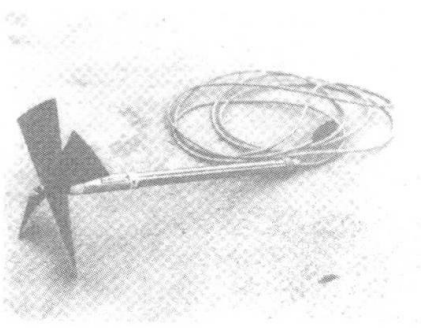

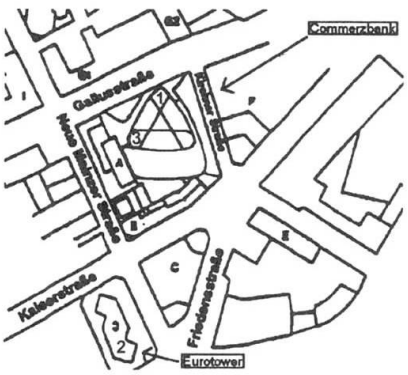

Fig. 3: Location of the measurement instrumentation (1, 2, 3)

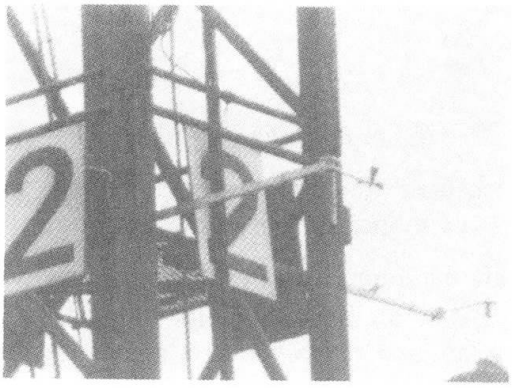

Fig. 4: Propeller-anemometer at crane 2 (Installation Number 1)

2.2 Measurements of the longitudinal extensions

The total resistance of the building against wind is provided by the six mega-columns coupled with steel frameworks. Thus, it was possible to calculate the whole reaction of the building against wind only from the measured extensions, using the modulus of elasticity and section modulus.

Strain transducers were installed at the first floor level within the six mega-columns (in addition to the instruments for the wind velocity) in order to measure the longitudinal extensions. Each column contains 5 steel bars with anchor plates at both ends (see Fig 5) and strain gauges used in a full-bridge configuration. The strain transducers were embedded in the reinforcement before casting (see Fig. 6).

The data was collected simultaneously with the wind velocities at ten-second intervals, rendering the analysis of the correlation between wind velocity and the reaction of the building possible.

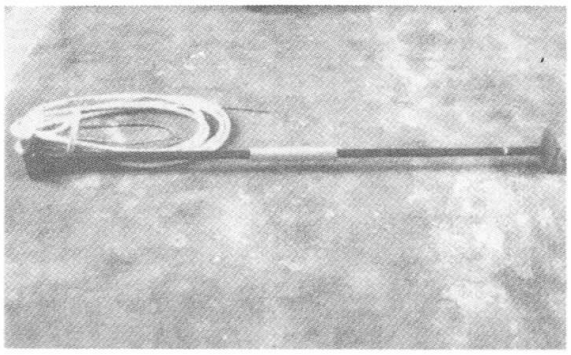

Fig. 5: Strain transducers

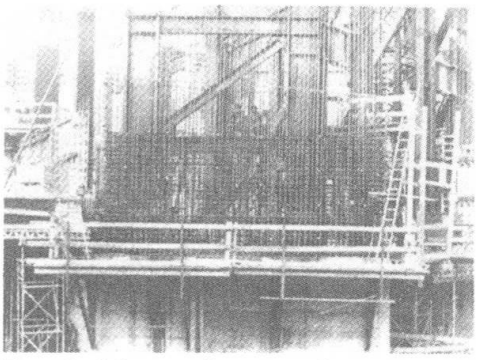

Fig. 6: Mega-column under construction

2.3 Wind-tunnel test

A wind-tunnel test was carried out to obtain additional information about the reaction of the Commerzbank-building against wind and generalize the full-scale measurements.

The pressure on the surface of the building was measured at 270 points for 12 different wind directions. Using these measurements, the base moment was calculated. The profile of the wind simulated in the test was a power-law profile with an exponent $\alpha = 0.25$. For detailed information see [7] and [9].

3 Results

3.1 Profile of the mean wind speed

The measured wind velocity was compared with the power-law model from Davenport [3] and the log-law model used in Eurocode 1.

The left diagram in Fig. 7 shows mean wind velocities measured in ten-minute intervals at heights of 60 m, 153 m, 212 m, and 261 m. The measurements are compared with the results of the log-law and the power-law model for the terrain categories "suburban" (α = 0.28, Kat. III) and "city-centers" (α = 0.40, Kat. IV). These velocities are put into relation to the velocity at the height of 261 m.

The right diagram in Fig. 7 shows the measured mean wind velocities without the values at the height of 212 m. However, the wind velocities measured on this day were the highest ones of all measurements carried out.

These figures show that the measured wind velocity is always lower than the velocities calculated with the log-law profile and also lower than calculated with the power-law profile for suburban areas. It can also be seen that the velocities calculated on the basis of Eurocode 1, categories III and IV, are greater than those calculated on the basis of the power-law model for the suburban areas (α = 0.28) and city-centers (α = 0.40). The profile of the log-law model is very flat, indicating that the velocities at the lower heights are too high.

The turbulence intensity and the spectral density of the measured wind velocities was also compared with the definitions by Davenport and Eurocode 1, but is not presented here. Detailed information is given in [1] and [2].

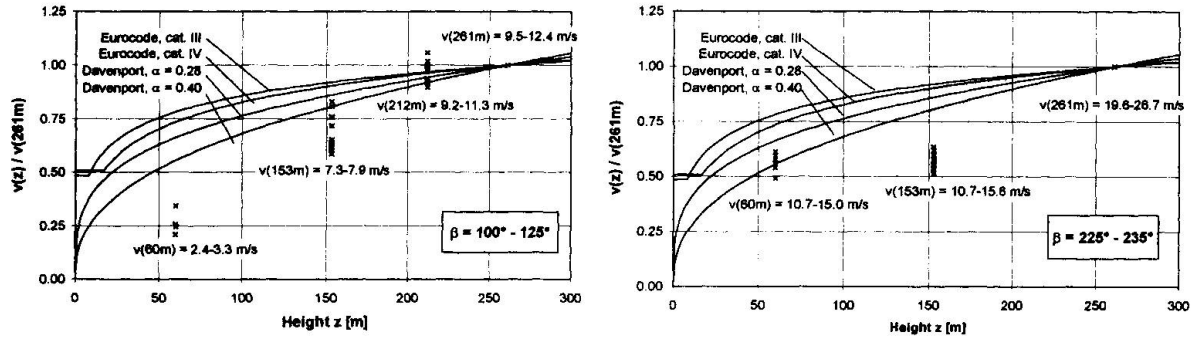

Date: 16.4.1996 Date: 29.10.1996 (storm "lilly")

Fig. 7: Comparison of the measured ten-min. mean velocity with those calculated with the power-law and the log-law model. At two different times.

3.2 Reaction of the building against wind

The dependence of the base moments on the wind direction is very strong. Therefore, the measured base moments were divided in a component around the east-west axis and the north-south axis.

Fig. 8 and Fig. 9 show the east-west and the north-south components of the base moment calculated on the basis of the wind-tunnel test and derived from the full-scale measurements. The moments are related to the wind pressure at 261 m.

The values obtained from the full-scale measurements are all similar to or lower than the wind-tunnel results. This means that the profile of the wind velocity has an higher exponent α than predicted by the wind-tunnel test. Only for the direction of 240° to 270° the wind-tunnel results and the full-scale measurements show nearly identical results due to a more precise modeling of the many high-rise buildings located in this direction and used in the wind-tunnel test.

In addition to the measurements, the reaction against wind was calculated with Eurocode 1 and Davenport. Table 2 shows the measured and calculated base moments for a similar situation. The actual reaction of the building is much lower than the calculated one according to Davenport or Eurocode 1.

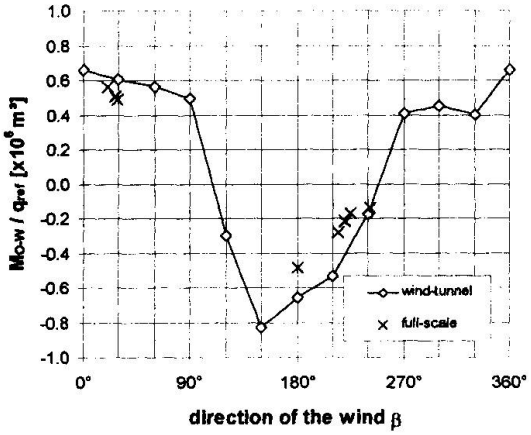

Fig. 8: Related base-moments around east-west axis

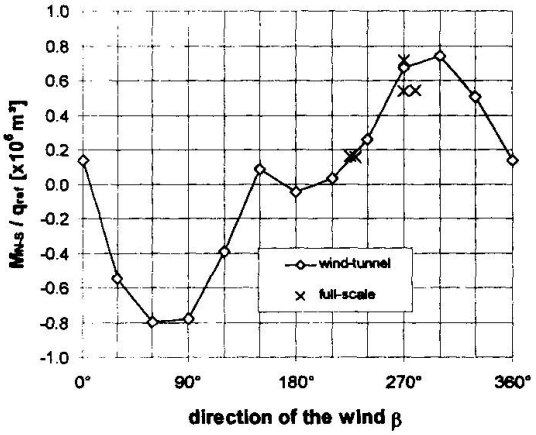

Fig. 9: Related base-moments around north-south axis

Table 2: Calculated and measured base-moments

Source	Base-Moment [MNm]
Full-scale measurements	686
Wind-tunnel test	825
Davenport, α=0.16 (=German standard)	1585
Davenport, α = 0.28	1120
Davenport, α = 0.40	727
Eurocode 1, Cat. III	1239
Eurocode 1, Cat. IV	956

4 Conclusion

The results of the measurements prove that in city regions - as, for instance, Frankfurt/Main - it seems to be permissible to use an exponential profile of the mean wind velocity with an exponent of $\alpha = 0.28$. Most measured data would also correlate to calculations with an exponent of 0.40. Also, the log-law model used in Eurocode 1 is very flat and does not correlate to the measurements. Therefore, it seems to be possible to reduce the wind loads given in Eurocode 1 for high-rise buildings.

The wind loads given in Eurocode 1 are restricted to buildings lower than 200 m. For high-rise buildings above 200 m, no standard will be given to calculate the wind loads. So it is necessary to establish another concept to describe these loads.

The measurements have proven, that a power-law model used to describe the profile of mean wind-velocity using parameters like ones described by Davenport will lead to realistic results. To generalize the results, however, measurements at other locations are necessary. Also, only little information was available regarding the dynamic characteristics of the wind velocity and the building. Further information in this field is needed.

In a next step, the "Institut für Massivbau" of the University of Technology in Darmstadt is carriging out new full-scale measurements at another new high-rise building in Frankfurt/Main, which is currently under construction.

REFERENCES

[1] Berneiser, Andreas. Windlasten im innerstädtischen Bereich – Messungen am neuen Commerzbank-Hochhaus in Frankfurt/Main –. Dissertation. Institut für Massivbau, TU Darmstadt, 1998.

[2] Berneiser, Andreas. Wind loads in city centres demonstrated at the new Commerzbank building in Frankfurt/Main. In: Darmstadt Concrete, Vol. 12, Institut für Massivbau, TU Darmstadt, 1996.

[3] Davenport, Alan G. The application of statistical concepts to the wind loading of structures. In: Proc. of the institution of Civil Engineers, 19, pages 449-472, 1961.

[4] Grüneis, H. Commerzbank-Hochhaus Frankfurt am Main: Projektentwicklung und Projektmanagement. Bauingenieur, 71, pages 305-314, 1996.

[5] Koster, Gerhard. Monitoring system for wind velocity and column strains on the new commerzbank building. In: Darmstadt Concrete, Vol. 11, Institut für Massivbau, TU Darmstadt, 1996.

[6] Ladberg, W. Commerzbank-Hochhaus Frankfurt am Main: Planung, Fertigung und Montage der Stahlkonstruktion. In: Stahlbau, 65, Seiten 356-367, October 1996.

[7] Sonntag, Ralf. Auswertung von Meßdaten aus Windkanal- und Feldmessungen am neuen Commerzbank-Hochhaus in Frankfurt am Main. Diplomarbeit am Institut für Massivbau der TU Darmstadt, 1997.

[8] Winz, Christine. Windprofilbetrachtungen und Auswertung von Meßdaten zum neuen Commerzbank-Hochhaus. Diplomarbeit am Institut für Massivbau der TU Darmstadt, 1997.

[9] Winz, Christine und Sonntag, Ralf. Windkanalversuche zum neuen Commerzbank-Hochhaus in Frankfurt/Main. Vertieferarbeit am Institut für Massivbau der TU Darmstadt, 1996.

[10] Wise, M.C. u.a. Commerzbank-Hochhaus Frankfurt am Main: Das Tragwerk. In: Bauingenieur, 71, pages 471-479, 1996.

Structural Impact on the Environment: Aesthetics

Mark LENCZNER
Structural Engineer
Tasei Co.
Tokyo, Japan

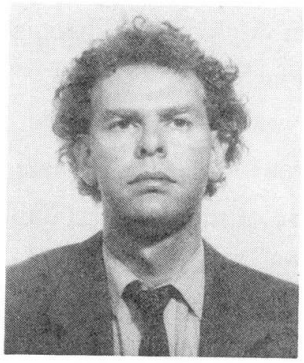

Mark Lenczner, born 1961, graduated from Imperial College in civil engineering with 1st class honours, and obtained a post-graduate DEA from the ENPC, Paris. After working in London with SOM, in 1990 he joined the structural design section of Taisei. He has worked on numerous major international and domestic projects and is also a qualified Licensed Architect.

Summary

Of the various ways that a structure can affect the surrounding environment, it is perhaps aesthetics that has the greatest impact on society. Whilst bridge engineers have recently paid increased attention to this aspect, the aesthetic aspects of building structures has generally been left to the domain of architects. Yet the role of the structure in determining the appearance of buildings can be significant, and merits increased input from engineers. This applies to all types of buildings. As most people live and work in a built environment, society has much to gain from any improvement that can be made. This paper attempts, albeit briefly, to highlight some points on how the structural engineer can readily make a difference on various types of projects, and improve both the building aesthetics and the surrounding environment.

1. The challenge to improve aesthetics

Improving the aesthetics of buildings directly enhances the built environment in which we live. It also increases the public acceptance of buildings and other structural works. The creation of technically proficient yet often dull or jarring and 'impersonal' buildings means we are not succeeding in creating a pleasant environment, albeit safe, convenient and technically advanced.

Many modern constructions are not held in high regard by society. Indeed, when the public are asked to name their preferred buildings, they will often refer to those built many years ago and considered as 'traditional'. This will typically be buildings made from 'traditional' materials in 'traditional' styles. The materials would typically be those available locally, whether in stone, wood, bamboo, brick or even dried earth. The 'style' was often a development of

function and a response to the local conditions and environment; good aesthetics often 'fell into place' in meeting these requisites, making adjustments to suit cultural styles and in providing interest to avoid monotony. The result was often buildings and a built environment in which people felt 'comfortable', an idyll which people still appreciate, despite the shortcomings of some of these constructions.

Admittedly, one common theme is, of course, the use of natural materials, and the empathy humans tend to have to them. Yet the use of modern structural materials is not necessarily a preclusion to creating 'aesthetic' structures. The recreation of new buildings in old styles can often prove unsuccessful when we sense that the materials are not being used in the same original conditions. It is more how we use them, and in particular the overall form or structure in which they form part, and how well the whole responds to the numerous needs that will determine their assessment.

Through interfacing with architects at a concept stage with and by a re-consideration of the appropriateness and potential of certain structural forms and materials, and their expression, the aesthetics of even the most mundane of buildings can be enlivened.

2. The roles structure can play

Although building aesthetics is often left to architects, they do not have a monopoly on the ability to judge aesthetics. Furthermore, the potential of structure is (usually) best understood by engineers. Structural engineers should thus not refrain from proposing solutions; most good architects would appreciate the possibilities that can result.

2.1 Form

Form, when derived from a sense of function, results in both variety in shape and a sense of aptness and belonging. The conditions which dictate the form and function depend on both the type of building and its location, and are also a response to the local environment (both human and natural). Such considerations rarely lead to the same solution, so there is rarely any standard 'right' solution. This in itself should discourage monotony, a major problem for improving the aesthetics in the built environment. This is also true for considering different parts of the same building. Time, construction and budget considerations aside, lack of inventiveness or imagination is a major impediment to attaining good solutions. The best solutions are likely to result from a holistic approach, viewing the building, its shape and surroundings, as a whole. A structural solution derived such will often produce a 3-D form that allows numerous possibilities for creative and aesthetic expression, even if only parts of

the structure are expressed.

The ability to create in 3-D is compounded somewhat by the 2-D or linear nature of most structural components (beams, slabs, etc.) that we use both in our analysis models and in actual construction. This contrasts with the 'micro-structure' elements , such as brick, used more frequently in the past. Yet think in 3-D we must. Indeed, the connection of the elements making a frame can in itself be part of the aesthetic concept, perhaps reflecting how the building is put together.

Addressing how the structural form is detailed and co-ordinated into the finished form is also important, hopefully avoiding the addition of unnecessary marring 'extras'. Similarly, the structure should not just appear 'clever' from an engineering point of view, but appear pleasant to the human eye.

2.2 Material

Expressing structure as an aesthetic thus also concerns us with exposed material. Steel and concrete have an industrial image. They are not typically viewed as 'aesthetic' materials and are usually covered by building finishes. Yet they are utilised widely in numerous other forms and media (e.g. cars, furnishings, large 'non-building' structures) with less objection.

Part of the problem lies in their mixed past-record as used in buildings. For steel, problems include providing corrosion protection, maintenance and the sometimes unsightly protrusions and 'complexity' of some members. There is also the challenge in ensuring their fire-resistance in the exposed state. For concrete, problems remain with staining, deterioration and cracking concerns. Yet we equally know that with greater attention paid to material behaviour, detailing and construction methods, most of these problems can be overcome, and appear in colours and textures to suit as required.

Indeed, with thorough investigation of possible design concepts, these materials can be expressed in attractive ways, as existing examples can testify. In Japan, exposed concrete is now accepted and frequently preferred to more 'artificial' paint-type finishes. Yet such examples are generally exceptions, rather than a standard to which we must regularly aim for. We can do more to express the numerous possibilities these, and other materials, have for aesthetic expression, and be structurally efficient. Working in tandem with architects, building service and lighting specialists etc., such structure can be made to be the 'feature' of the building design, a plus gained without the need for the additional cost of cladding, which itself can often have a pre-fabricated unnatural image. When this is combined with making not just the material but the structural form of the building the chief characteristic, then one is on the

way to creating an attractive and efficient building.

Mention should also be made of the still rather under-used structural properties of glass, timber, stone, non-ferrous metals and new composite materials. Although their potential is known, and used on occasion, it is usually as a response to an architect's requirement, and done on a case-by-case basis. Yet when we adopt their structural potential as a starting point in the concept design, we can readily produce complete 'aesthetic' structural forms, rather than as 'in-fills'.

3. SETTING

The fitting into the surrounding landscape, be it urban, rural or natural, is a major influencing factor of aesthetics, and will often be the critical factor in the success of a design. The following are just a few examples of how engineers can help address aesthetic issues.

3.1 Prime Nature

For projects in prime natural settings, it may often be preferable to blend/conceal or hide the works altogether by partly building underground or into the hillside, or create low-side walls of 'natural' structural materials. The creation of the exposed surface roof form will usually be the primary aesthetic consideration. Here the engineer can lead in designing long-span contoured structures to suit both external aesthetic and internal planning requirements, with the surface finish blending into (landscaped) or perhaps even complementing the surrounding scenery, perhaps using tensile net or contoured space trusses of wood or steel, with a translucent skin. Overtly 'regular' structures are unlikely to blend in.

3.2 Semi-rural, suburban outskirts.

In semi-rural or city outskirt-settings, the designers should similarly be expected to provide non-obtrusive solutions, though not to the same level of concealment. The track record of such developments is generally not so good; typically developers are primarily looking for commercially viable solutions to purely functional requirements. Apart from certain agricultural-related structures such as silos and the like, whose function demands tall structures, typical large developments would be low-rise commercial, warehouse or factory-type buildings. Here also the engineer can instigate improvements.

For example, the mono-pitch or low-angled flat roof is a fairly standard solution, but is often not a true expression of the actual structure inside supporting it, as they often have interior

columns, particularly where over one-storey high. Sloping roofs in three-dimensions could provide a visually more-interesting solution, with structural merit, and allow more natural daylight inside. For the case where a single clear-long span is required, exposing the spanning structure outside creates numerous possibilities for expressing a distinctive solution. The side-walls also, normally summarily clad in bland sheet-cladding, can be considered as a opportunistic mural to display geometrically attractive lateral resisting systems. Bracing need not always be concealed, nor X or V shaped. Geometric star shapes, even curves and non-rectangular solid-forms can provide vastly increased visual interest. An exposed structure of almost any form could be designed to improve upon most standard clad-solutions.

3.3 Urban

It is for urban settings, however, where the problems of improving aesthetics is most demanding. Not only can adjacent buildings distract from one's preferred objective, but the confinements imposed, be they functional, legal or technical, are stricter. One must also attend to the building as seen from a distance, and also at street level 'close-up', where the selection of material is more crucial. As such, the criteria for long or tall structures can be different to smaller structures which are less visible from afar.

For long-span, or in particular high-rise buildings, the structure is critical in defining the building's form. For very tall structures, utilisation of the whole depth of the building's volume, such as for tube or coupled perimeter frame and wall structures, is often a stability requirement. The result is often a fairly regular solid form. From a far distance, the outline of groups of such skyscrapers can give a city a 'dynamic' look. Closer-up, however, their simplistic shapes can sometimes appear harsh and dull. This problem can be addressed somewhat through the design of the cladding, or perhaps more efficiently with 'engineering expression'.

Some of the solutions used are the expression of perimeter framing and cross bracing, and the highlighting of 'megaframe' modules, belt-trusses and the like. Some of these have been successful in providing further visual interest, structural efficiency and freeing the architect to create more varied forms (or voids), to suit other requirements perhaps, between the critical structural members. The engineer is most influential in defining the 'megaframe' and can create pure and logical forms, which the public can appreciate, and preferably not muddled or concealed by the addition of less relevant elements. The structure need not always be literally 'on view' ; more subtle expressions of the 'muscular' form and shape of the structure projecting out but still enveloped by the cladding can also be effective.

The appearance at street level is also critical in creating a pleasant environment. Well-

engineered structures can often lose their potential appeal and clarity if the form of the overhead superstructure is masked at ground level, such as by ill-thought out cladding and in-fills, so losing the potential of forming a dramatic open-space framed within or around the structure. Transfer structures at lower levels can also similarly confuse the form of the main superstructure if not treated correctly. As the designers responsible for these elements, we should not passively accept inappropriate treatment.

For smaller buildings, the structure is typically less critical in moulding the form and expression of the building, yet the potential and improvements to be gained from the lack of attention to structural expression are perhaps even greater. The somewhat ubiquitous approach of designing a skeleton to support a predetermined layout normally leads to buildings of a rather 'two-dimensional' or 'hollow' character, apparently composed of facades of either overt simplicity, or featuring rather illogical ins-and-outs, belying the fact there is a structure, hidden from view, on which to develop the design. In many cases, when structure is expressed, it is too often disguised to look like something it is not.

This is partly a material problem, with reluctance to expose structural materials, and partly a lack of appreciation of the potential to be gained (including functional benefits) of encouraging expression of structural form. This is particularly so for 3-D forms, and their inherent structural efficiency and flexibility, but also for the part expression of wall or column/beam elements, and the interesting spaces they can form. Indeed, the interior expression of structure is another area where the interior environment can be similarly improved to create more inspiring living space.

Conclusions

The ways in which our built environment can be improved are many, yet attention to aesthetics is perhaps on of the most influential. The scope for structural engineers to play a leading role is significant and merits increased attention to be paid. The working relationship with architects also needs to be addressed so that this potential can be greater realised. The built environment is almost around us wherever we go. Indeed, the examples I will be taking for illustrating these points are all in the immediate vicinity of where I live, but the principles can be applicable anywhere. Attention to aesthetics does not require much additional effort, yet the rewards to be gained for society as a whole can be many.

Are There Intelligent Options in Skyscraper Design?

Valer MOCAK
President
Int. Consult. & Design Center
Fremont, CA, USA

Valer Mocak, born 1932, received his degree as an engineer architect from the Technological Univ. in Bratislava, Slovakia.

Summary

The striving to build higher and higher structures is visible throughout the entire human history. But only the last one hundred years deserve to be called as an era of the skyscraper. During this period we were witnessing an astonishing development of this building type. At the same time, there were increasing, often insane tendencies to regulate the planning of skyscrapers, mostly in forms of zoning laws. Parallel ideas were trying to circumvent the official ordinances by theoretically applying some unorthodox methods. Among the future intelligent options in skyscraper design are the concept of interconnected cluster of skyscrapers as well as shapes of towers utilizing the open, void areas in their facades.

1. The role of regulations

History teaches us that the building of the city or any large urban complex within a city can follow basically two paths. One is in maintaining a certain order, rigid compositional structure, symmetry, introduction of an axial matrix with views and controlled traffic lines. Many exceptional examples of this group are part of the cultural heritage of the mankind: Versailles, Schonbrunn, plazas in Rome and other cities, and the group of skyscrapers in Rockefeller Center in New York.

Each society is trying to impose certain regulations in order to prevent chaotic and unrestricted explosion of unwelcomed sizes and shapes of buildings on the footprint of the city. The tool for such regulation is the zoning law (A) which attempts to set up the series of conditions regarding the organization of functional elements and their image within the entire

city. Environmental concerns (the length of shadows, etc.), maintaining the street lines, setbacks, and others are also addressed here.

The rectangular plans of ancient Greek cities, often neglecting a morphology of the terrain and cutting into the stone the entire parts of the city just for the sake of maintaining the right angle grid, can be seen today as an abomination of the healthy urban planning. This grid in some American cities in larger scale has many advantages, but it also can be dull.

2. Reinterpretation of Some Undesirable Rules

Sometimes the planner has to rely on inspiration from the borderline disciplines. One such effort is based on the theory of fractals. It was described originally in the author's 1986 study "Unconventional Design Possibilities for Skyscrapers at Waterfront Lands" (B), and later refined and updated in the 1997 paper "A Quest for Sanity in Skyscraper Design" (C) for the conference in Sao Paulo. The present study will examine the interdependence of the urban design theories with some other fields.

3. Theory of Chaos

The second path in the development of the city growth is distinguished by everything but order or symmetry, or a clear geometrical concept. The seemingly chaotic image of Santorini or Venice would indicate a lack of compositional order, a disorder, but we have to admit it is a lovely, delightful and charming disorder. Here we cannot but register the following anecdote: When Le Corbusier visited the United States the first time, his ship was entering the New York harbor. Looking at the skyline of Manhattan and noticing the visual results of the first, heroic era of skyscrapers, Le Corbusier exclaimed: "What a disaster !". Then he added: "But what a beautiful disaster".

The chaotic results in some urban areas, being it a group of almost nomadic one story shanties in the "Gold Rush" time (representing an unadulterated chaos), or St. Gimignano type concentration of the medieval towers (D) nicknamed protoskyscrapers, will attract more attention when we'll start to realize that they reflect enormous physical energy as well as human psyche.

In the second half of the 20th century, mathematicians started to pay more attention to the theory of chaos (E), or disorder, later renamed as the theory of complexity. In the other fields, like economy, the systems (F) and irregular patterns that were discussed and analyzed. Not so in the probably largest area of human endeavors, in the past and present

building activities. Architectural historians like to stratify these achievements into clear periods, styles (G) and demarcation lines between them. The present times require much more background knowledge from the planners and their trainers, the academia. In the age of computers and virtual reality, the new generation of experts will have to combine the old methods with a new angle of complex evaluation of conditions and events and be ready to challenge the archaic zoning ordinances.

4. The Intricacies of Randomness

In the complexities of creative life and time, a pure randomness is to be distinguished from theoretical chaos, althought they may overlap. Randomness can even be predictable by a sharp individual used to deal with multifaceted challenges.

Let's two buildings appear as identical, complying with all the conditions of the zoning law, such as height, sky exposure curves, etc. The setting of the buildings, however, in the matrix of city might be offensive, not sensitive to basic aspects of common sense, etc. Hardly a satisfactory condition. Now let's multiply this condition several times. (There were years when on Manhattan alone 40 to 60 high-rises were under construction at the same time.) If we add to it the influences of nature and study them for a long enough time, such a status will cease to be qualified as randomness. It is on its best way to become a chaos, although recognized as such only some decades later. In the realms of physics we call it entropy. But what about the urban design, where unmeasurable categories like talent, inspiration, emotional world, intuition and creativity are involved ? In such a case, existing regulatory models are useless. Here we have to rely on the other set of tools, the theory of games.

5. The Game Theory Applied to New Urban Concepts

The classical teachings of statistics maintain that in the coin-toss game the chances of getting either heads or tails are even. Not so, says the "Gambler's Ruin" theory (H), the absolutelly unscientific speculation, according to which in the long run the gambler always looses.

In the game theory, the alternatives are being studied, one of them reminding us of the Gambler's Ruin, and called the "worst case scenario". Based on the work of John von Neumann (I), covering the model of general equilibrium, planning problems, numerical methods to determine optimum strategy and many other pertinent topics, his ideas were further developed for the economics by a Nobel Prize winner (1994) John Harsanyi (J). We know that economics as a field is a very important part of our life.

But it's still only a part of it. It touches some other fields like technology only marginally. On others, like art, religion, etc., its impact is often questionable.

In the urban sciences, the participation of economics is subordinated to the larger picture. Then why the theory of games was never studied and applied in the field of city planning ? Because of our intellectual laziness ? Or inability - or fear - to deal with something more complex than the zoning law ? In adopting some aspects from the game theory to the ways how we plan today's cities we can enhance the image of our environment.

6. Interconnected Cluster of Skyscrapers

While the environmental issues were so far concentrated on the quality of life in the surroundings of the skyscraper, mainly on the ground level of adjacent lots and city blocks, there is an unexplored field of mental state of persons living or working in the super high floors. The acrophobia (fear of heights) and claustrophobia (fear of being in an enclosed place, like elevator) are only two samples of uncomfortable feelings, many times multiplied by the swaying of the structure (K). One way to eliminate these fears is to build a cluster of interconnected skyscrapers (Fig. 1).

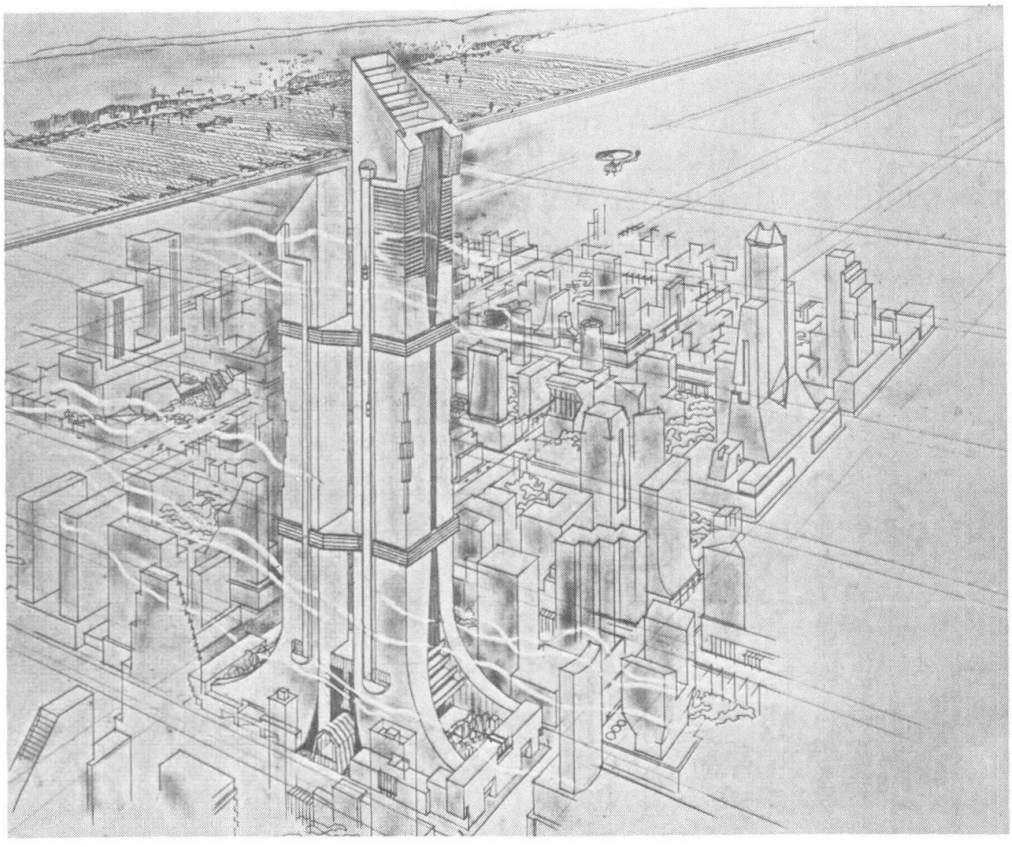

Fig. 1 : Author's study for the World's Tallest Building (1981) shows the skyconcourse at every 40 floors.

7. Skyscraper Image Revolution

The image of the building plays a decisive role in minds of people, not often valued as an important attribute in the individuality of the city. But to what degree one can always invent new shapes and images ? It's like with the music, where it is no end of combinations. The new skyscrapers in Dubai (Fig. 2 and 3) remind us of the creative fermentation of futuristic styles as strongly as the architecture of Tel Aviv did of the international style in the late thirties. Some of the latest skyscraper designs show voids, openings in their mass, as in the future World's Tallest Building in Shanghai (Fig. 4). It makes them not only more interesting but helps in easing the wind pressure on the skyscraper wall.

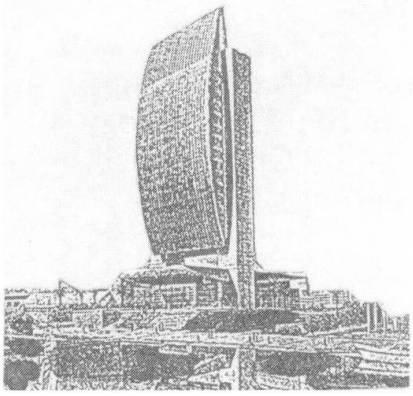

Fig. 2 :
National Bank of Dubai

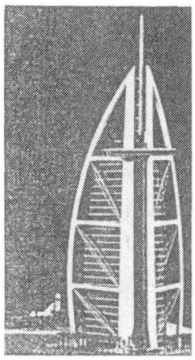

Fig. 3 :
70 story Chicago Beach Tower Hotel in Dubai

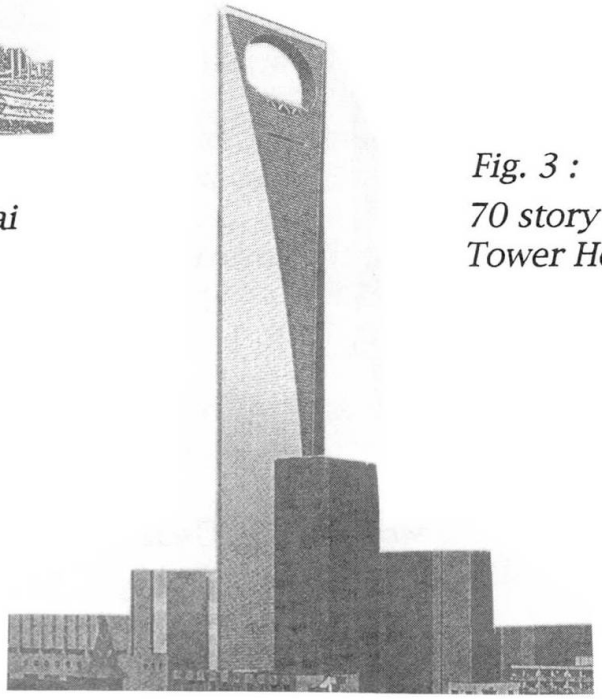

Fig. 4 : World Financial Center in Shanghai, the future (2002) World's Tallest Building

8. Conclusion

There is more than one way how to enrich our life by taking the inspiration for our creative thinking from the other fields.

9. References

(A) New York, City of: New York City Zoning Resolution. Department of City Planning, New York, 1985.

(B) Mocak, Valer: Unconventional Design Possibilities for Skyscrapers at Waterfront Lands. Paper prepared for the Council on Tall Buildings & Urban Habitat, Non-Governmental Organization of UNESCO, Bethlehem, PA, 1986.

(C) Mocak, Valer: A Quest for Sanity in Skyscraper Design. Paper for the 2nd International Conference on High Technology Buildings, Sao Paulo, 1997, published in the Proceedings of the Conference.

(D) Mocak, Valer: Development of Image Diversity in Skyscraper Design. Paper for the Sao Paulo International Conference on High Technology Buildings, Council on Tall Buildings and Urban Habitat - Grupo Brasil, Oct. 25-26, 1995. Published in High Technology Buildings, CTBUH, Bethlehem, PA, 1995, page 118, Illustration 3D.

(E) Gleick, James: Chaos: Making a New Science. Viking, NY, 1987.

(F) Bertalanffy, Ludwig von: General Systems Theory: Foundations, Development, Applications. George Braziller, NY, 1968.

(G) Mocak, Valer: Contemplating the Future Architectural Styles. Paper prepared for the Congress of the Society for Science and Art, Bratislava, Slovakia, July 5-10, 1998.

(H) Crichton, Michael: The Lost World. Alfred A. Knopf, NY, 1995, page 250.

(I) Neumann, John von, with Morgensern, Oscar: Theory of Games and Economic Behavior. Princeton University Press, 1944.

(J) Harsanyi, John, with Selton, Reinhard: A General Theory of Equilibrium Selection in Games. MIT Press, 1988.

(K) Mocak, Valer: Skylobbies as Interconnecting Links Amid the Cluster of Skyscrapers. Published in Second Century of Skyscrapers, Van Nostrand Reinhold, Inc., New York, Wokingham (Bergshire, England), Melbourne (Australia), Agincourt (Ontario, Canada), 1988, page 287.

High-Rise Tubes for Solar Chimneys

Jörg SCHLAICH
Prof. Dr
Univ. of Stuttgart
Stuttgart, Germany

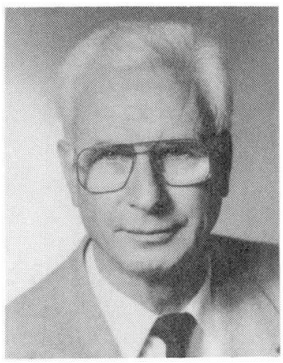

Jörg Schlaich, born 1934 received his civil engineering degree from the Univ. of Berlin and his Dr Eng. from the Univ. of Stuttgart, Germany. Since 1974 he is professor and director of the Institute for Structural Design, Univ. of Stuttgart and since 1980 partner of Schlaich Bergermann und Partner, Consulting Engineers, Stuttgart, Germany

Summary

The solar chimney combines three well-known technologies - the greenhouse, the chimney, and the turbine - in a novel way. Incident solar radiation heats the air under a large transparent collector roof. The temperature difference causes a pressure drop over the height of the chimney resulting in an upwind which is converted into mechanical energy by turbines and then into electricity via conventional generators (Fig. 1). In order to achieve competitive electricity cost, the height of the chimney should be in the order of 1.000 m.

1. Introduction

This solar energy system has many technological and physical advantages:

- Global radiation, including diffuse radiation when the sky is overcast, can be exploited.
- The natural storage medium - the ground - guarantees operation at a constant rate until well into the hours of darkness (and throughout the night with large-scale installations). If in addition black water-filled tubes are placed on the ground underneath the roof (Fig. 2), a continuous 24 hours electricity production can be achieved (Fig. 3).
- There are no moving parts, nor are there parts that require intensive maintenance aside from the turbine and the generator. Not even water is required.

Its simple, low-cost design and materials (glass, concrete, steel) make solar chimney systems applicable to less industrialised countries. Labour represents a high portion of the installation costs. This would stimulate the local labour market, while at the same time helping to keep overall costs down.

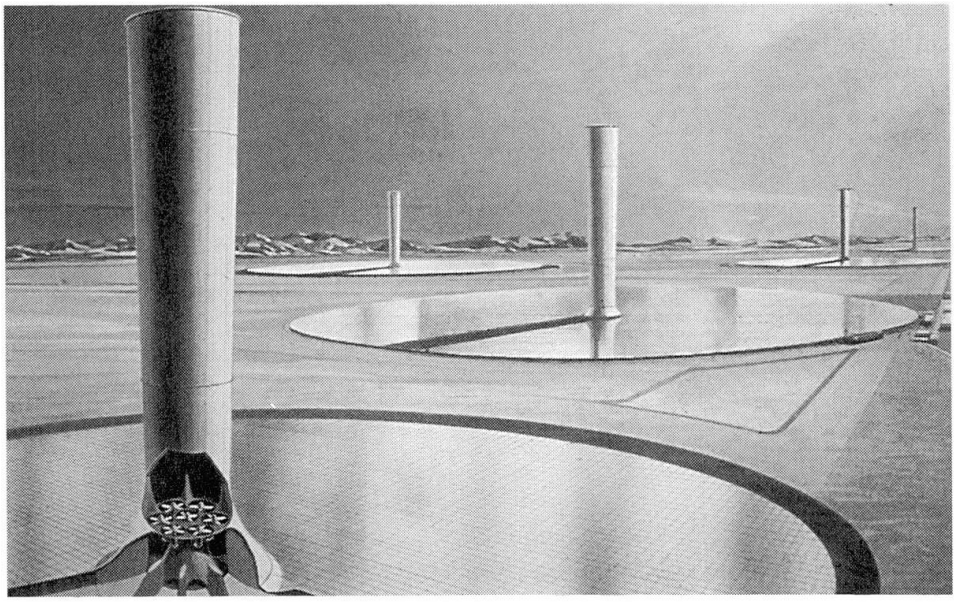

Fig. 1 Drawing of several large (100 - 200 MW) solar chimneys in a desert.

There is in fact no optimum physical size for solar chimneys. The same output may result from a large chimney with a small collector roof area and vice versa. Thus, to decide the optimum dimensions of chimney height against collector radius, the specific construction costs of these items must be known. If glass is cheap but concrete expensive, a large collector and low chimney is preferable, and vice versa. Broadly, to achieve a maximum output of (30) 200 MW at an irradiance of 1.000 W/m², the roof must have a diameter of (2.200) 4.000 m if the chimney has a height of (750) 1.500 m. If black water-filled tubes are placed on the soil underneath the roof (Fig. 2) for a continuous 200 MW full load 24 hours electricity production the diameter of the roof must be increased to 7.200 m. Now this solar chimney from a solar radiation of 2.300 kWh/m²a extracts about 1.500 GWh/a, in fact a power plant!

The collector roof, responsible for almost 50 % of the total cost must be as economical as possible. For that the glass panels are placed on suspended stress ribbons made from steel slats, spaced 1 m. They are supported by underslung girders resting on steel tubular columns 9/9 m². Tests on a prototype solar chimney in Manzanares/Spain have shown that this is a most efficient and durable structure (Fig. 4 and 5).

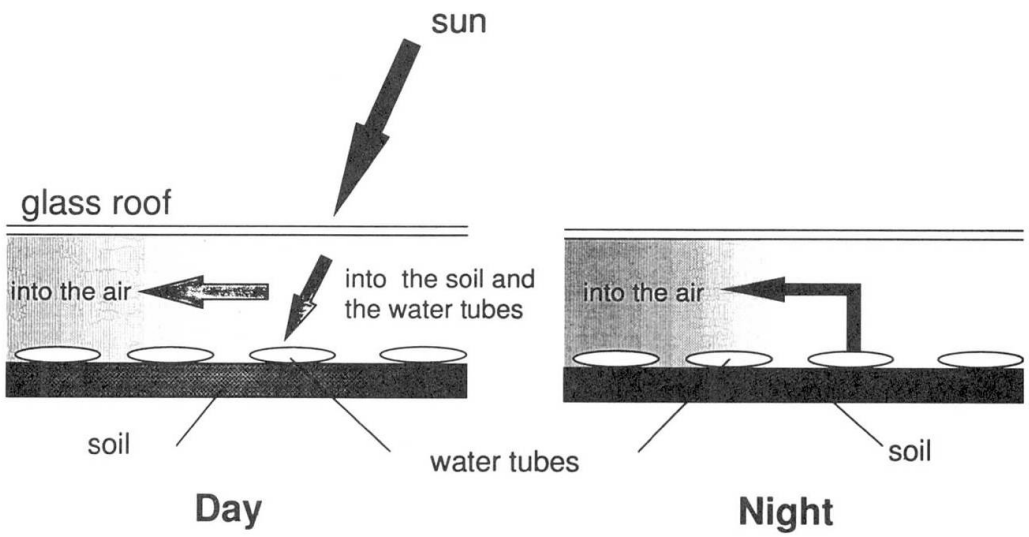

Fig. 2 Principle of heat storage underneath the roof using water-filled black tubes.

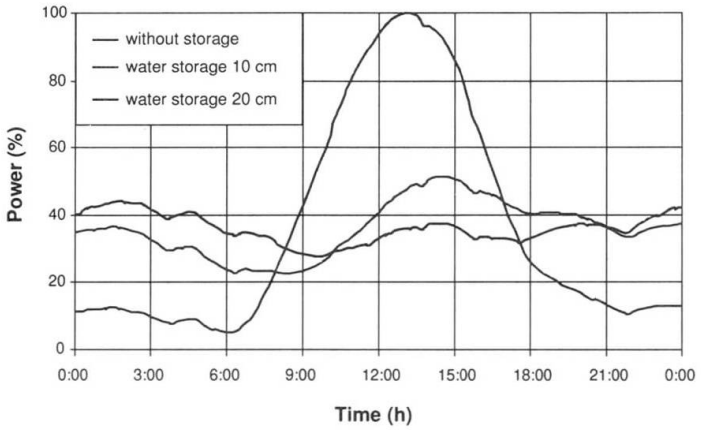

Fig. 3 Electricity output during 24 h as a function of the thickness of the water layer.

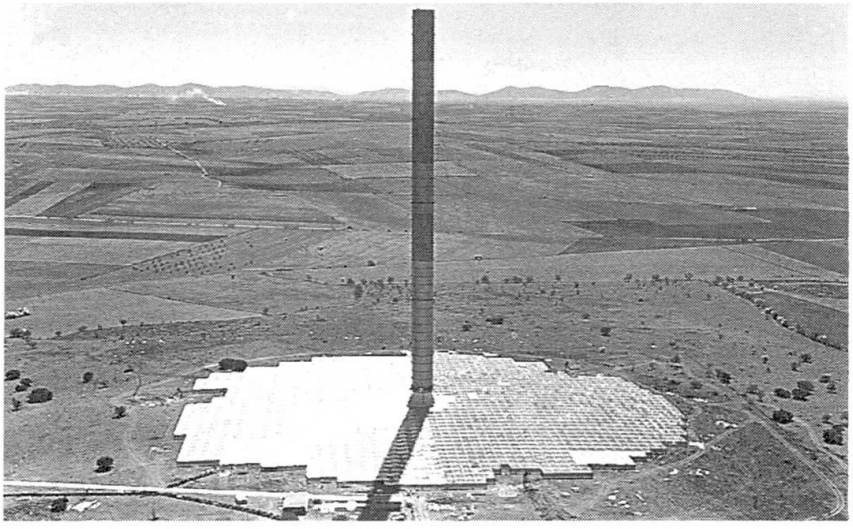

Fig. 4 The solar chimney in Manzanares/Spain.

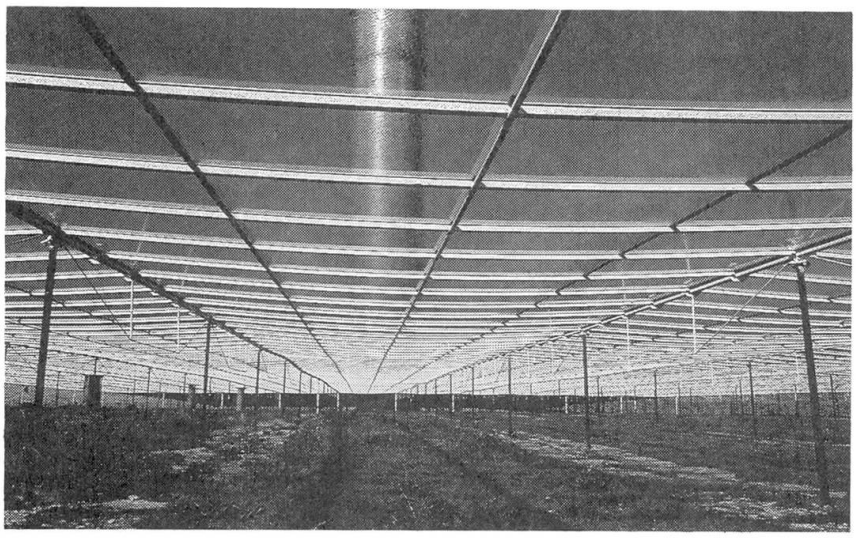

Fig. 5 The glass collector roof of a solar chimney.

The turbines are basically more closely related to the pressure-induced water turbines than to the velocity-induced natural wind power plants. Either several horizontal axis engines are placed around the chimney base or - the cheaper solution - one large, say 200 MW turbine with a vertical axis is placed in the chimney's diameter (Fig. 6).

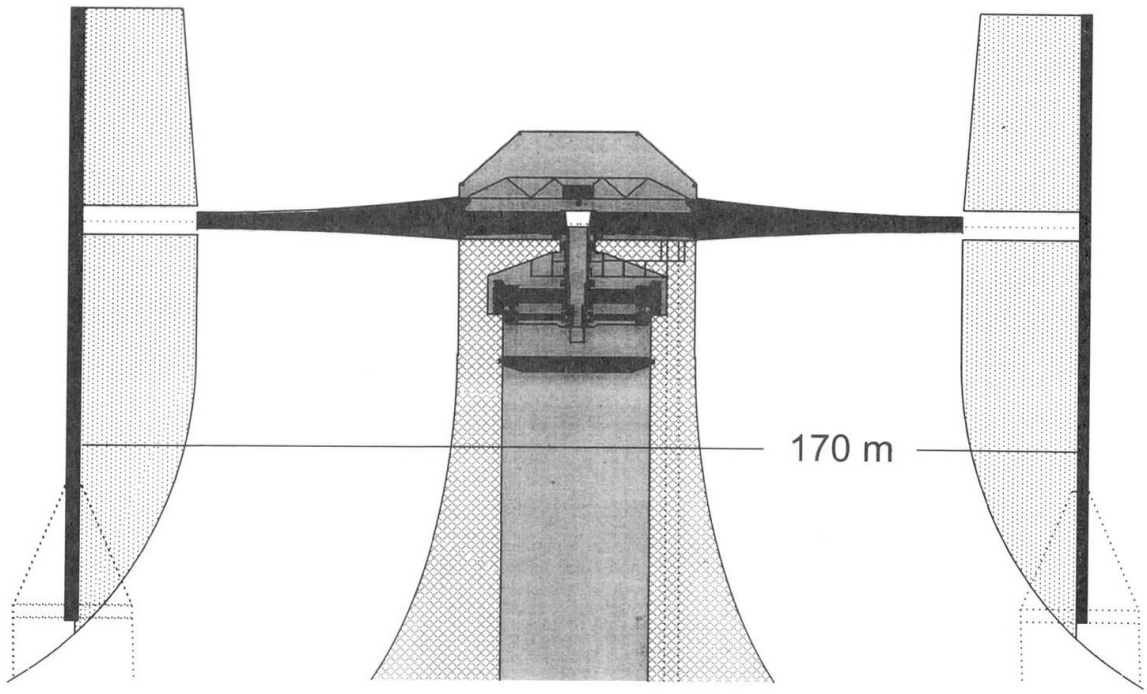

Fig. 6 200 MW vertical axis in the shaft of the solar chimney.

For the chimney itself the possible construction methods and the materials such as covered steel framework with cable nets, membranes, trapezoidal metal sheet etc. were compared to discover that for all the desert countries in question the reinforced concrete tube promises the

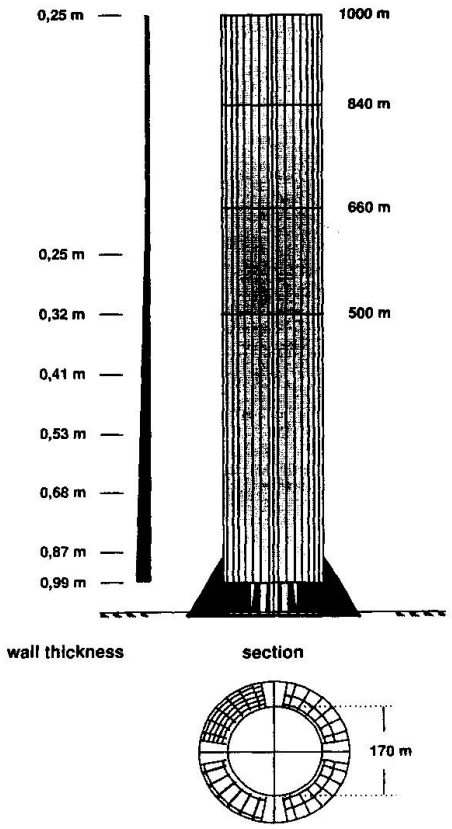

Fig. 7 Wall thickness of a chimney 1.000 m high and 170 m in diameter

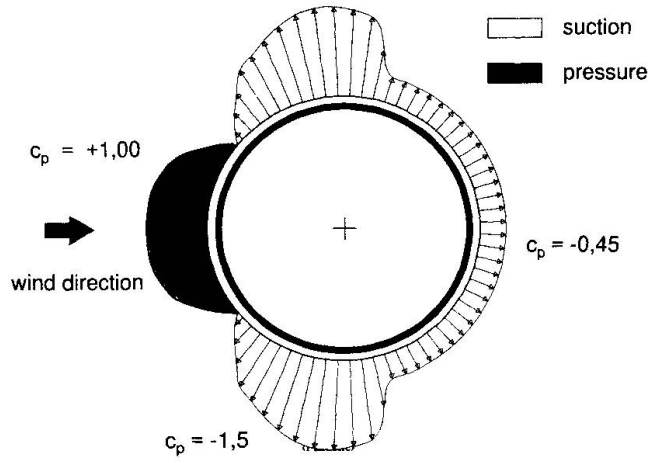

Fig. 8 Typical pressure distribution around the circumference of a cylindrical tube

longest life-span at the most favourable costs. Technologically speaking they are nothing but cylindrical natural draught cooling towers with - as shown in Fig. 7 as an example - a diameter of 170 m and height of 1.000 m. The wall thickness decreases from 99 cm just above the support on radial walls to 25 cm halfway up, then remaining constant all the way to the top. Such thin-walled tubes will oval due to the wind suction especially at the flanks (Fig. 8). This tremendously increases the meridional compressive and tensile stresses if compared with the linear bending stresses of a cantilevering beam (Fig. 9, top left). The resulting loss in stiffness due to cracking of the reinforced concrete and the danger of buckling limit the height of natural draught cooling towers to about 200 m. But this ovalling can be efficiently counteracted by stiffening spoked wheels, which have the same effect as diaphragms, hardly affecting the upwind. If the spokes are made of vertical steel slats stressed between a compression ring along the chimney's wall and a hub ring, such a spoked wheel is prestressed by its own weight, thus resulting in tension- and compression-resistant spokes (Fig. 10). It is seen from Fig. 9 that the meridional stresses in the chimney wall, shown in the diagrams across the diameter and the height, do ondulate tremendously without any spoked wheels. But one spoked wheel at the top and another one or even three more further below reduce the meridional stresses to an extent that tension disappears completely, succumb by the tube's dead load. Considering thatthe absolute volume under these stress diagrams is somehow proportional to the consumption of concrete and reinforcing steel, one finds that these spoked wheels, make such high towers for solar chimneys feasible.

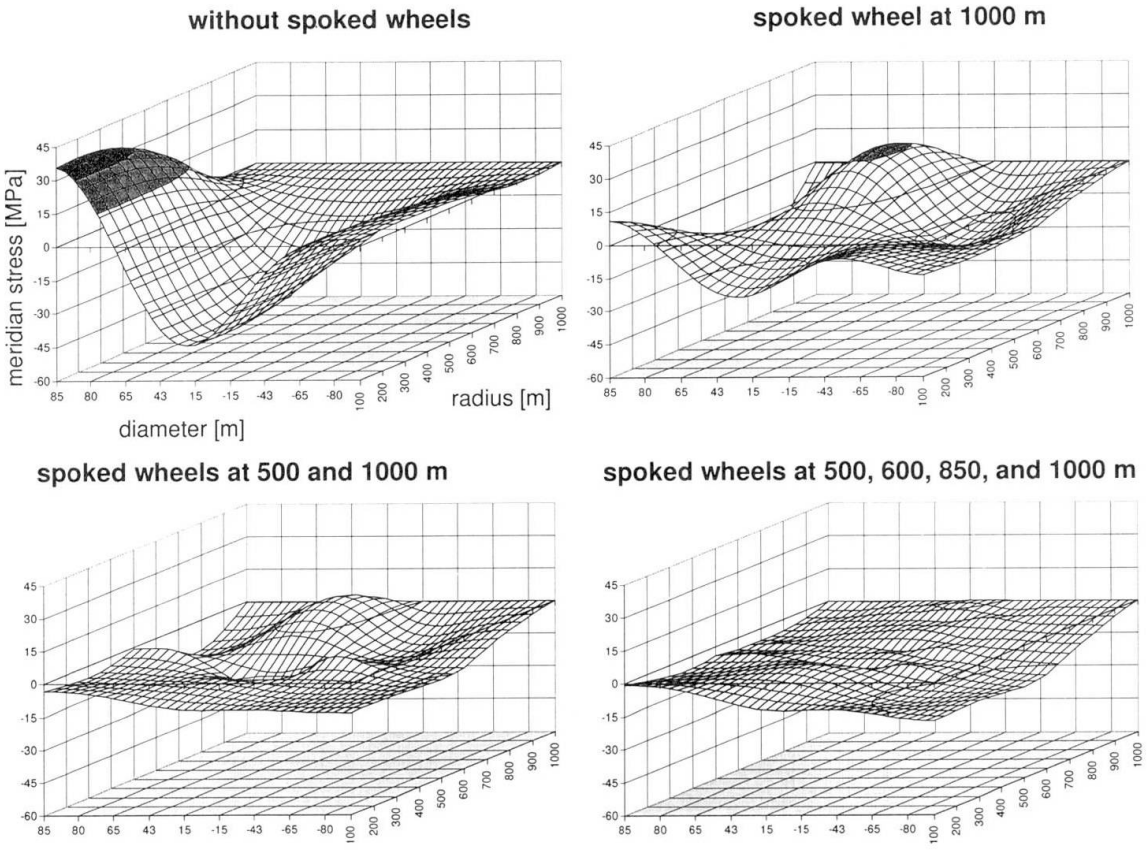

Fig. 9 Meridional stresses in the chimney according to fig. 7, around its periphery and along its height depending on the number of stiffening spoked wheels.

Thus, with the support of construction companies, turbine manufacturers and the glass industry a rather exact cost estimate for a 200 MW solar chimney could be compiled. Two big German utilities determined the electricity producing costs compared to coal- and combined cycle power plants based on equal and usual methods (Fig. 11).

This clearly shows that calculated purely under commercial aspects with a gross interest rate o' 11 % and a construction period of 4 years during which the investment costs increase already by 30 % (!) electricity from solar chimneys is just 20 % more expensive than that from coal.

In case of the solar chimney the interest on the investment governs the price of electricity, whereas in the case of fossil fuel power plants mainly the fuel costs are the deciding factor.

Merely reducing the interest rate to 8 % would make electricity from solar chimneys competitive today (Fig. 12).

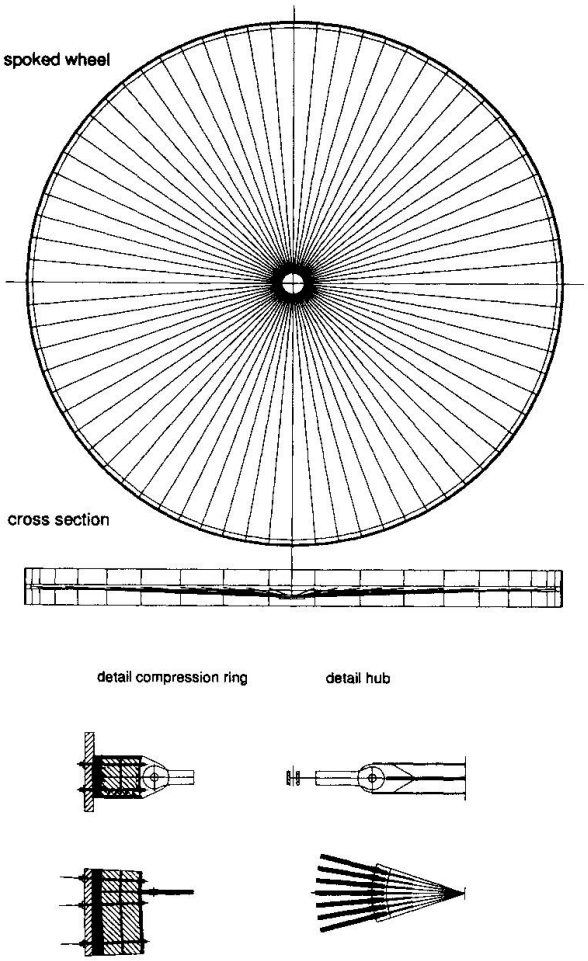

Fig. 10 Spoked wheels, the spokes are made of vertical steel slats.

Proportion of	Solar Chimney Pf/kWh	Coal Pf/kWh	2 x CC Pf/kWh
Investment	11,32	3,89	2,12
Fuel	0,00	3,87	6,57
Personnel	0,10	0,78	0,31
Repair	0,52	0,92	0,83
Insurance	0,01	0,27	0,12
Other running costs	0,00	1,16	0,03
Tax	2,10	0,69	0,37
Total	**14,05**	**11,58**	**10,35**

Commissioning in 2001
Power: 400 MW
Running hours: 7445 h/a
Yearly energy: 2978 GWh

Own investment 1/3 at 13,5%
External investment 2/3 at 8%
Total interest rate: 10,67%
Tax rate: 30%

Fig. 11 Electricity producing costs per kWh (1 Pf = 0.01 DM) from solar chimney, coal and combined cycle power plants according to the present business managerial calculation.

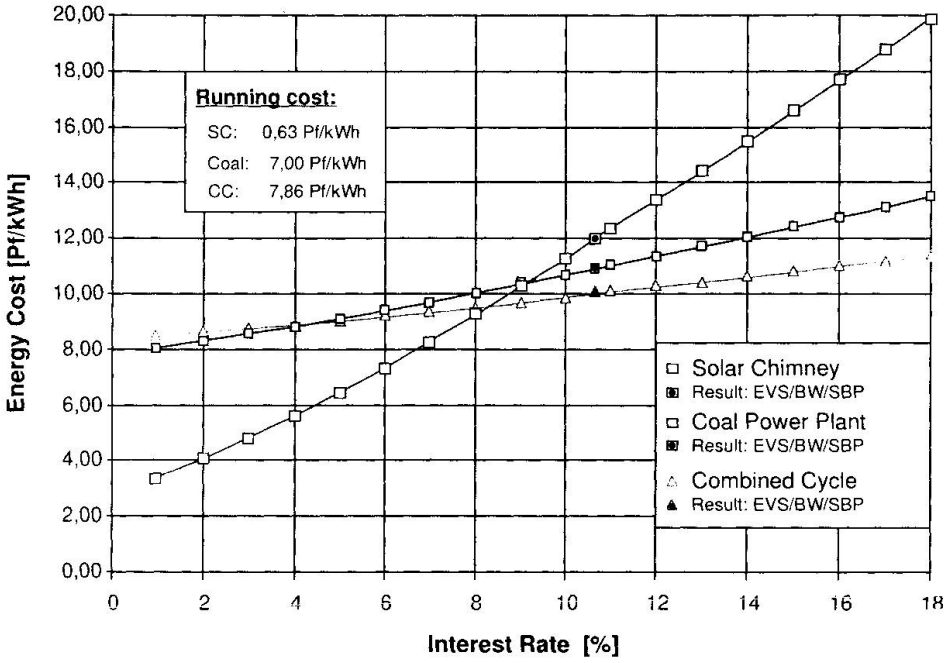

Fig. 12 Electricity producing costs from solar chimney, coal and combined cycle power plants depending on the interest rate.

The presently still higher costs of solar electricity are balanced by several advantages:

- No ecological damage and no consumption of resources, not even for the construction, because a solar chimney predominantly consists of glass and cement which is sand plus self-made energy, a really sustainable power plant.
- The (high) investment costs are almost exclusively due to labour costs. This creates jobs, and
- a high net product for the country with increased tax income and reduced social costs (= human dignity, social harmony), and in addition
- no costly imports of coal, oil, gas which is especially beneficial for the developing countries releasing means for their development.

We have no choice but to do something for the energy consent, the environment and above all for the billions of underprivileged people in the Third World. But we should not offer them hand-outs, a multiple of which we deceitfully regain by imposing a high interest rate on their debt. Instead we should opt for global job sharing. If we buy solar energy from Third World countries, they can afford our products. A global energy market with an essential solar contribution beyond hydropower is no utopian dream!

If we really want to we can do it!

References

Winter, C.-J. et al. *Solar Power Plants*. Springer Verlag, Berlin 1991.
Schlaich, J. *Renewable Energy Structures*. Structural Engineering International, pp. 76 - 81, Vol. 4, No. 2, 1994
Schlaich, S. and J. *Erneuerbare Energien nutzen*. Werner-Verlag, Düsseldorf, 1991.
Schlaich, J. *The Solar Chimney*. Edition Axel Menges, Stuttgart, 1995

Applications of Damage-Controlled Structure to Diagonal Lattice Tube Building

Kenichi HAYASHI
Structural Eng.
Nippon Steel Corp.
Tokyo, Japan

Toshio UNNO
Mgr
Alpha Structural Design
Tokyo, Japan

Mamoru IWATA
Gen. Mgr
Nippon Steel Corp.
Tokyo, Japan

Summary

This design shows an application of a damage-controlled structure to a structure having a diagonal lattice tube. The damage-controlled structure is a combination of primary structure and seismic members. This building is a diagonal lattice tube structure. The framework is exposed on the outside of the building and the floor frames are positioned inside of the diagonal lattice tube. The center portion of the diagonal lattice tube is made up of seismic members using axial hysteretic dampers. The rigidity of the entire structure, the energy-absorption initiation level, and the total amount of energy absorption are controlled by varying cross-sectional areas and materials of the seismic members. By thus decreasing the seismic responsiveness of the conventionally elastically designed, diagonal lattice tube, we have realized an economical building.

1. Introduction

This paper describes a structural design in which the concept of damage-controlled structure is applied to a diagonal lattice tube building.
The diagonal lattice tube comprises a framework of diagonal columns and a floor framing in triangles. If the diagonal lattice tube is regarded as an elastic trussed structure, it provides high stiffness for a high-rise building and the member force is of the axial force governing type. Under dynamic loads such as seismic load, however, the high stiffness induces an increase in the seismic response story shear-force and the cross-sectional area of members tends to become large.
The damage-controlled structure (Connor et al. 1997) is composed of a primary structure and seismic dampers. The primary structure constantly supports loads and behaves elastically during an earthquake. The seismic dampers absorb the input energy during an earthquake. The damage level of buildings is controlled by setting the quantity of energy absorbed by seismic dampers.
In the 1995 Hyogoken-Nanbu earthquake, the fracture phenomenon occurred in many buildings of steel-frame construction. In the high-rise housing complex "Ashiyahama Seaside Town", in particular, the fracture from the base material of extra-thick steel-frame columns posed various problems. This building is a mega-structure using a trussed structure and does not have seismic dampers for absorbing seismic input energy. On the one hand, it has become a practice since this earthquake to set an energy absorption mechanism for high-rise buildings and to examine building performance against an excessive input energy that exceeds the design load. On the other hand, the resistance of materials themselves to brittle fractures has begun to attract attention in the phenomenon where a failure occurs without the buckling of columns.
This building, planned one year after this earthquake, uses a diagonal lattice tube, which is exposed to the outside. The building is so designed that the diagonal lattice tube serves as the damage-controlled structure, and a reduction in seismic load and setting of the energy absorption mechanism are performed. Furthermore, the resistance of the members of the diagonal lattice tube to brittle fracture has been verified by tests.

2. Outline of structure

The present building has fourteen stories above ground and two below. The frame above the ground rises from the first basement. The height of the building is 63 m. The floor area of the building is 24 x 24 m above ground and 38 x 34 m underground. The structure above ground is of steel, while that underground is of SRC and RC.
The framework above ground is a diagonal lattice tube with a gradient of about 60° which is exposed outside. The floor frames are located 900 mm inside from the diagonal lattice tube. The framework and floor frames are connected by projecting members (Fig. 1).

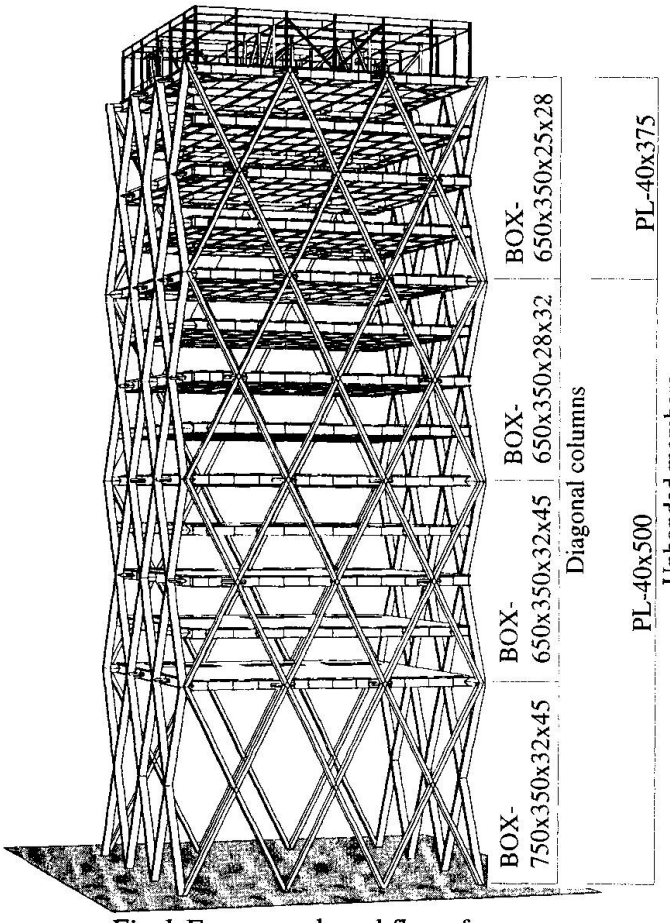

Fig.1 Framework and floor frames

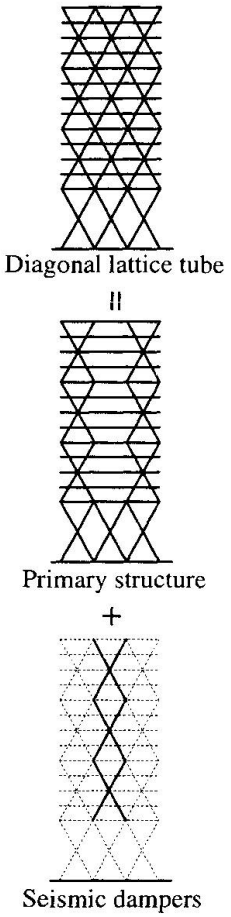

Fig. 2 Concept of seismic design

The diagonal lattice tube can be regarded as a kind of truss frame. The member force is of the axial force governing type. The concept of the seismic design of the diagonal lattice tube is shown in Fig. 2. The diagonal lattice tube consists of a primary structure and seismic dampers. The primary structure supports stationary loading and behaves in an elastic manner upon occurrence of an earthquake. The seismic dampers absorb the input energy at the time of an earthquake. The primary structure consists of the first story of diagonal lattice tube, diagonal columns at the corners, and floor frames. The other diagonal lattice tubes are the seismic dampers. For seismic dampers, unbonded members, which are hysteresis type dampers of the axial force system, are used.
In the design, the stiffness of a building can be adjusted by changing the sectional area of primary structure members and unbonded members. The level of the load at which the building starts to absorb seismic energy can be set by determining the combination of the materials and sectional areas of unbonded members.

3. Seismic design and response

3.1 Target of seismic design

The target of seismic design is to ensure that the primary structure is completely in the elastic region against an earthquake ground motion of Level 2 (50 cm/sec). For this purpose, a safety factor of 1.2 must be ensured by conducting the allowable stress design of each part using a maximum story shear-force due to an earthquake ground motion of Level 2. As with the design of general high-rise buildings, the limit of maximum drift angle is 1/200 for an earthquake ground motion of Level 1 (25 cm/sec) and 1/100 for an earthquake ground motion of Level 2.
Furthermore, a target value for an earthquake ground motion of Level 3 (100 cm/sec) is set in the present building. The load-deformation in which the members buckle and the plastic hinge occurs for each story of the principal structure is regarded as the elastic limit, and the maximum value of response to an earthquake ground motion of Level 3 must be within the elastic region. Unbonded members allow materials to become plastic under an earthquake ground motion of Level 1 or less (15 ~ 20 cm/sec). As a result, the stiffness of the building decreases and the unbonded members begin to absorb energy.

3.2 Acting direction of horizontal load and dynamic behavior of building

An examination is made into the effect of the acting direction of horizontal load on the dynamic behavior of diagonal lattice tube. In the case of the present building, the acting direction of horizontal load is in the range of 0 to 45 degrees from the X- or Y-direction in terms of plane symmetry. There is no floor framing in the first story, and there is no member that supports the diagonal lattice tube from the inside. For this reason, the effect of the acting direction of horizontal load manifests itself remarkably. A static numerical analysis of this first story is made in consideration of the nonlinearity of the stress-strain relationship of the material and geometrical nonlinearity (Fujimoto et al. 1975) when the acting directions of horizontal load are 0, 15, 30 and 45 degrees with respect to the X- or Y-direction.

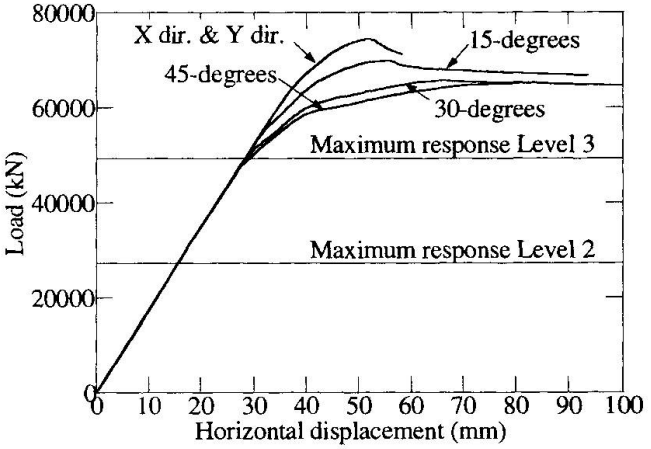

Fig. 3 Load-deformation Curve

According to the load-deformation curves in each direction of horizontal load, the strength decreases with increasing angle with respect to the X- or Y-direction, although the initial stiffness is the same in each case (Fig. 3). In view of this point, the seismic response analysis is made in the X-direction, Y-direction and 45-degrees direction.
The load-deformation curves and elastic limits of each story in the X-direction, Y-direction and 45-degrees direction are determined (Fig. 4). Buckling occurs in the diagonal columns. However, yield strength does not decrease abruptly. The hysteresis characteristics for a seismic response analysis and the elastic limit for a design target are set based on this load-deformation curve. If buckling or plastic hinge does not occur in the members before the completion of an analysis, the load-deformation upon completion of the analysis is set as the elastic limit for convenience sake.

3.3 Seismic response analysis

In the seismic response analysis, a 14 mass point system is adopted in which the floor position of the first basement of the building is fixed, and the equivalent stiffness of flexural-shear beam model is used.
The first natural period of this mass system is considerably short compared with general

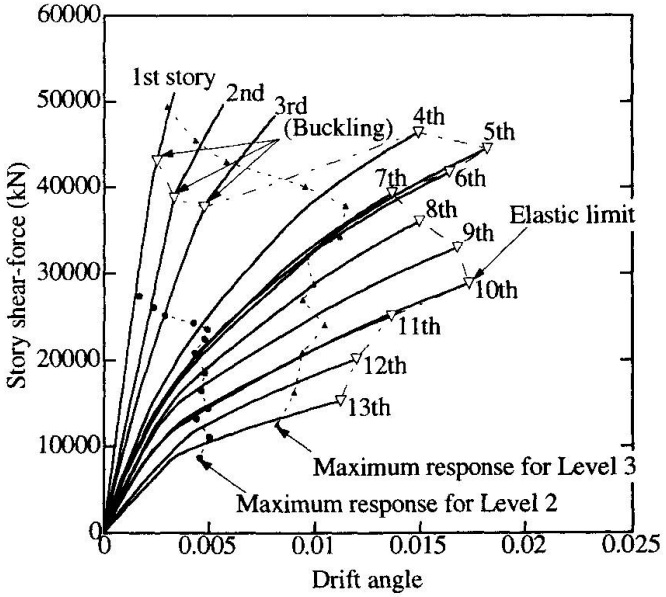

Fig. 4 Load-deformation curve and seismic response

buildings of steel-frame construction (building height x 0.03 = 1.8 seconds) and this building has high stiffness (Table 1).

Table 1 Natural period of the mass system

	X dir. & Y dir.		45-degree	
	in elastic region	all unbonded members yielded	in elastic region	all unbonded members yielded
1	0.958	1.406	0.980	1.414
2	0.387	0.540	0.408	0.550
3	0.263	0.333	0.336	0.364

The earthquake ground motions for the response analysis are the four motions of El Cento, Taft, Tokyo and Hachinohe.

This earthquake response analysis is made by paying attention to changes in the natural damping that has a great effect on the damping of the building and those in the stress-strain relationship of the energy absorbers of unbonded members.

In buildings of steel-frame construction, the natural damping coefficient is generally 2%. In the present design, however, responses when the natural damping coefficient is 1% and 0% are also determined and the effect of the damping by unbonded members is verified. The damping matrix of natural damping is assumed to be proportional to the stiffness. The shear stiffness by unbonded members is excluded from the shear stiffness matrix used to prepare the damping matrix.

For the low yield point steel plate LYP100 that is the energy absorber of unbonded members, the yield point intensity is basically set at 100 N/mm^2. The stress-strain curve shows changes in such a manner that, for example, the yield point increases 1.6 times when the temperature drops from 0°C to –40°C, and it increases 2.3 times when the strain rate increases from 0.02%/sec to 100%/sec (Nakamura et al. 1997). For this reason, four types of hysteresis characteristics of unbonded members in which the yield point intensity is 30, 60, 100 and 200 N/mm^2 are set, and the scatter of analysis is examined (Fig. 5).

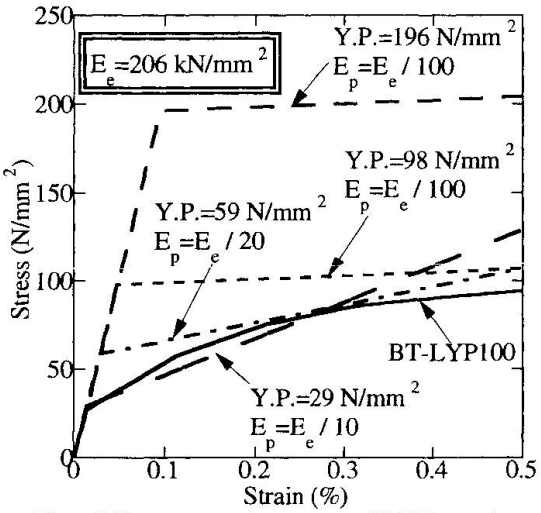

Fig. 5 Stress-strain curve of LYP steel

The yield stress intensity of LYP-100 is set at 100 N/mm^2 in the response analysis made using the natural damping coefficients of 1% and 0%, and the natural damping coefficient is set at 2% in the response analysis made using the yield point intensities of LYP-100 of 30, 60 and 200 N/mm^2.

Even with the same input earthquake ground motion, the value of response changes depending on the magnitude of natural damping. The response values of Hachinohe wave have a relatively small scatter and show the absorbed energy distribution of each story. When the natural damping coefficient is 2%, the energy absorption by the first story that has high stiffness is large. This energy absorption by the first story is gradually replaced with the energy absorption by unbonded members as the natural damping decreases (Fig. 6). Also, the maximum drift angle increases with decreasing natural damping (Fig. 7).

The maximum drift angle for each stress-strain curve of LYP-100 is shown in (Fig. 8). There is scarcely any difference at Level 1. This is because the unbonded members scarcely yield. The scatter of response increases with increasing level of input earthquake ground motion. The greatest

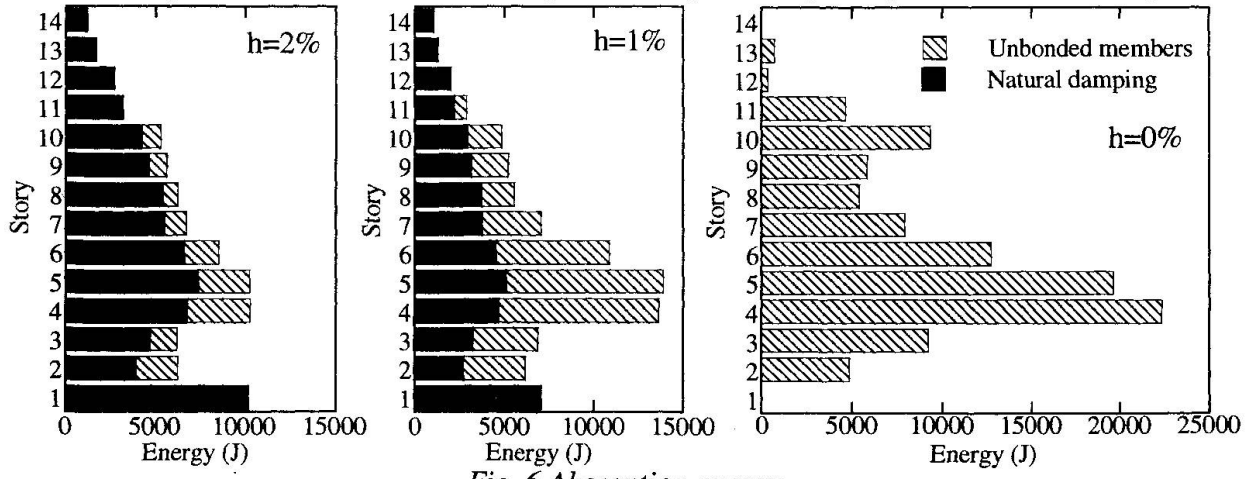

Fig. 6 Absorption energy

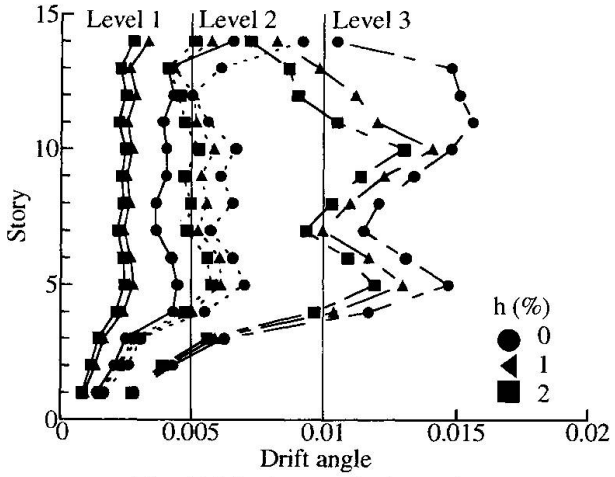

Fig. 7 Maximum drift angle

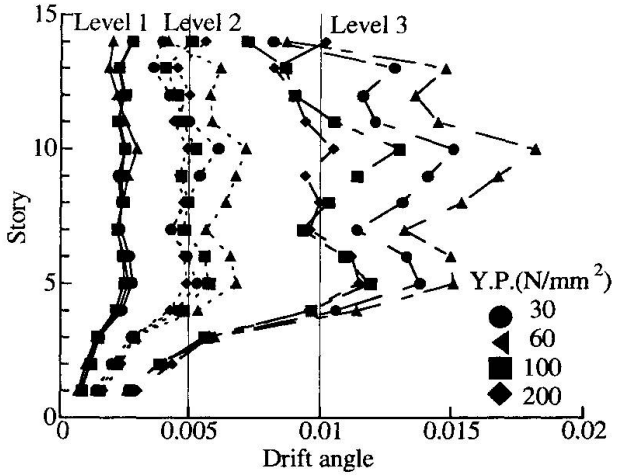

Fig. 8 Maximum drift angle

response is obtained when the yield point is 60 N/mm^2.
When the yield point is 100 N/mm^2, the maximum drift angle is 1/336 for an earthquake ground motion of Level 1 and 1/173 for an earthquake ground motion of Level 2.
The story ductility factor of maximum response, which is the ratio to the elastic limit, is 0.38 for an earthquake ground motion of Level 1, 0.68 for an earthquake ground motion of Level 2, and 1.2 for an earthquake ground motion of Level 3. For an earthquake ground motion of Level 3, the diagonal columns in part of the second story reach the buckling load in the input in the X- and Y-directions, and those in part of the first- to third stories reach the buckling load in the input in the 45-degrees direction.
The allowable stress design of each part is conducted using the story shear-force of maximum response to Level 2.

4. Diagonal lattice tube joint

Large tensile force is induced in diagonal columns upon occurrence of an earthquake. The temperature of these columns, however, drops in winter. It is, therefore, necessary to use a steel with high brittle fracture resistance for these columns.
Charpy absorption energy is used as an indicator of brittle fracture resistance. For SN and TMCP steels, this energy is specified to be higher than 27J at 0°C. According to the transition curve of HT325C-FR, for TMCP steel, used for the present building, the Charpy absorption energy is more than 280J at 0°C and its transition temperature is below -50°C. Simply put, this steel has a performance which is far higher than the specifications. SN steel also exhibits high performance.
The steel used for the diagonal columns has excellent brittle fracture resistance. According to the transition curve of the steel casting used in the joint, however, the Charpy absorption energy is higher than 100J at 0°C, but the transition temperature is about 0°C. The steel casting is inferior in brittle failure resistance to the TMCP and SN steels used for the diagonal columns.
The diagonal columns are welded to the cast steel blocks. The transition curves for the heat-affected zone (HAZ) and fusion line of the steel castings in the weld zone shift more toward the higher temperature side than the curve for the steel castings (Fig. 9).
To clarify the effect of low Charpy absorption energy of steel castings and weld zone on the dynamic behavior of the joint, static tensile test of full-size diagonal column joint was

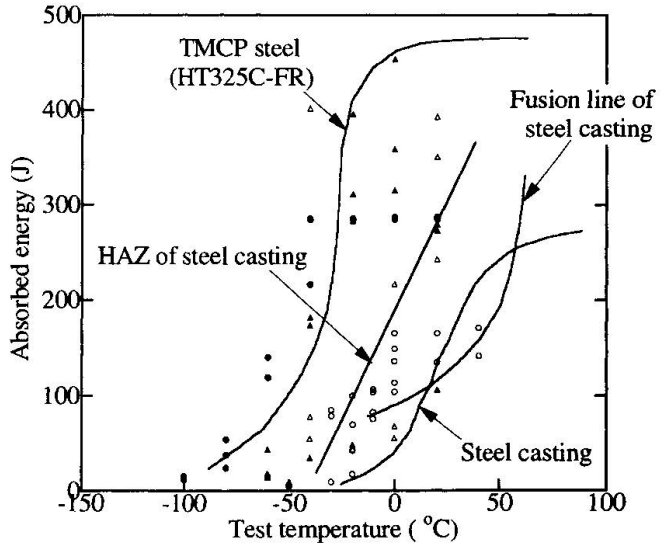

Fig. 9 Transition curves of Charpy absorption energy

conducted. The primary structure of the present building is of elastic design. According to the results of the test, design is not adversely affected so long as the maximum strength is more than 1.2 times the specified yield axial force of 24,500 kN.

Three full-size test specimens of diagonal column joints were fabricated, simulating the actual diagonal column joint. Erection pieces were set to these specimens. For the locations requiring site welding, welding was carried out with the specimens inclined obliquely. Tensile test was conducted after cooling the specimens. This was because it was estimated that brittle fracture is more likely to be caused at a low strength because of weld defects if the test is conducted at a temperature at which the Charpy absorption energy becomes very low. The cooling temperature was set at -20°C for two test specimens and at -50°C for one specimen.

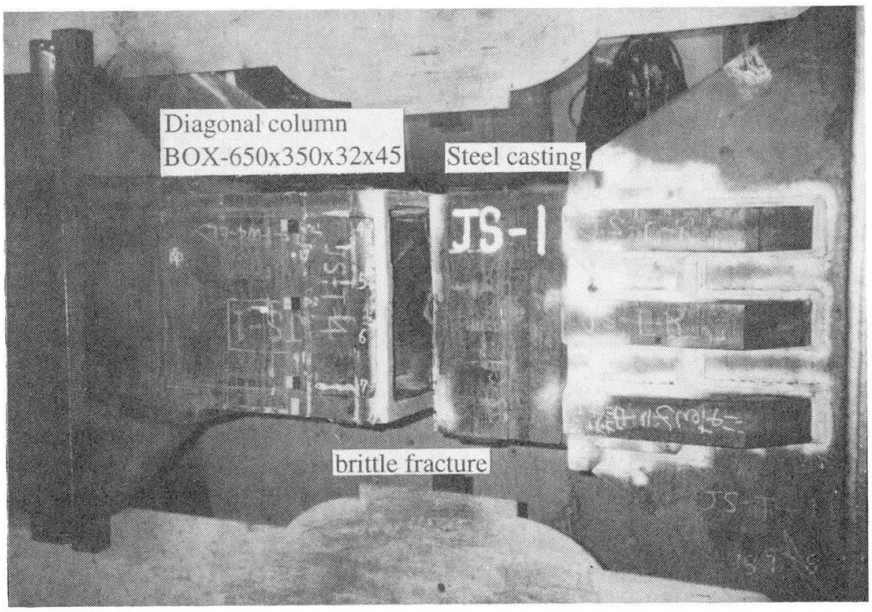

Fig. 10 Full-size test result of diagonal column joint

All test specimens failed in a brittle manner (Fig. 10). The maximum strength was 1.26 ~ 1.56 times the specified yield axial force. The fracture initiated from the weld defect. This weld defect was a small defect, acceptable according to the standards of the Architectural Institute of Japan.

Based on the results described above, it is estimated that the design of the present building is not adversely affected by the performance of steel castings and weld zone.

5. CONCLUSION

To realize seismic design for a high-rise building using diagonal lattice tubes, the building was designed on the assumption that it consisted of a primary structure and seismic dampers.

Acknowledgment

This building was designed by Plantec Architects. We wish to express our appreciation to this office for its kind cooperation in our study.

The full-size joint test was supervised by Professor Koji Morita of Chiba University. We wish to thank him for his valuable guidance and advice.

References

Connor, J. J., Wada, A., Iwata, M., and Huang, Y. H. (1997) "Damage-controlled Structures. I: Preliminary design methodology for seismically active regions.", *Journal of structural engineering*, April, 423-431

Fujimoto, M., Wada, A., Iwata, M., and Nakatani, F. (1975). "Nonlinear three dimensional analysis of steel frame structure.", *Transactions of A.I.J.*, 227, 75-90

Maeda, Y., Nakata, Y., Iwata, M., and Wada, A. (1998). "Fatigue of axial-yield type hysteresis dampers.", *Transactions of A.I.J.*, 503, 109-115

Nakamura, Y., Ono, T., Iwata, M., and Kako, Y. (1997). "The influence of notch, temperature and strain rate on the mechanical properties of steels.", *Summaries of technical papers of annual meeting A.I.J.*, 497-500

Ono, T., Kaminogo, T., Yoshida, F., Iwata, M., and Hayashi, K. (1997) " A study on material properties and hysteretic behavior of metallic material.", *Transactions of A.I.J.*, 498, 137-143

Unique Structural Engineering Solutions for China's Tallest Building

Stanton KORISTA
Dir. of Struct. Eng.
Skidmore, Owings & Merrill LLP
Chicago, IL, USA

D. Stanton Korista, Director of Structural Engineering at SOM, received his BS Degree in Civil Engineering from Bradley Univ., USA and his MS Degree in Structural Eng. at the Univ. of Illinois, USA

Mark P. SARKISIAN
Assoc. Partner
Skidmore, Owings & Merrill LLP
Chicago, IL, USA

Mark P. Sarkisian, Senior Project Structural Eng. at SOM, received his BS Degree in Civil Eng. from the Univ. of Connecticut, USA and his MS Degree in Structural Eng. at Lehigh University, USA.

Ahmad K. ABDELRAZAQ
Assoc.
Skidmore, Owings & Merrill LLP
Chicago, IL, USA

Ahmad K. Abdelrazaq, Project Structural Eng. at SOM, received his BS Degree in Civil Eng. and MS Degree in Structural Eng. at the Univ. of Texas at Austin, USA.

Summary

The site for the Jin Mao Tower located in new Pudong development district of Shanghai, The People's Republic of China, is not naturally conducive to accepting a tall building structure, especially China's tallest. Soil conditions are very poor since the site is located in the flood plain of the Yangtze River, the permanent water table is just below grade, typhoon winds exist, and moderate earthquakes are possible. Unique structural engineering solutions were incorporated into the design with the combined use of structural steel and reinforced concrete; solutions which not only overcame the adverse site conditions but also produced a very efficient structure for this ultra-tall building.

1. The Structural System

The superstructure for the 421 meter-tall, 88-story Jin Mao Tower consists of a mixed use of structural steel and reinforced concrete with major structural members composed of both structural steel and reinforced concrete (composite). Thirty-six (36) stories of hotel spaces exist over 52 stories of office space. The structure is being developed by the China Shanghai Foreign Trade Co., Ltd. and constructed by the Shanghai Jin Mao Contractors, a consortium of the Shanghai Construction Group; Obayashi Corp., Toyko: Campenon Bernard SGE, France; and Chevalier, Hong Kong. The structure was topped-out in August 1997 with an expected overall completion date of August 1998. The structure is the tallest in China and the third tallest in the world behind the Petronas Towers in Kuala Lumpur, Malaysia and the Sears Tower in Chicago, Illinois, USA.

The primary components of the lateral system for this slender Tower, with an overall aspect ratio of 7:1 to the top occupied floor and an overall aspect ratio of 8:1 to the top of the spire, include a central reinforced concrete core wall linked to exterior composite mega-columns by structural steel outrigger trusses. The central core wall houses the primary building service functions, including elevators, mechanical fan rooms for HVAC services, and washrooms. The octagon-shaped core is nominally 27 m deep with flanges varying in thickness from 850 mm at the top of foundations to 450 mm at Level 87 with concrete strength varying from C60 to C40. Four (4) - 450 mm thick interconnecting core web walls exist throughout the office levels with no web walls on the hotel levels, creating an atrium with a total height of 205 m which leads into the spire. The composite mega-columns vary in cross-section from 1500 mm x 5000 mm at the top of foundations to 1000 mm x 3500 mm at Level 87. Concrete strengths vary from C60 at the lowest floors to C40 at the highest floors.

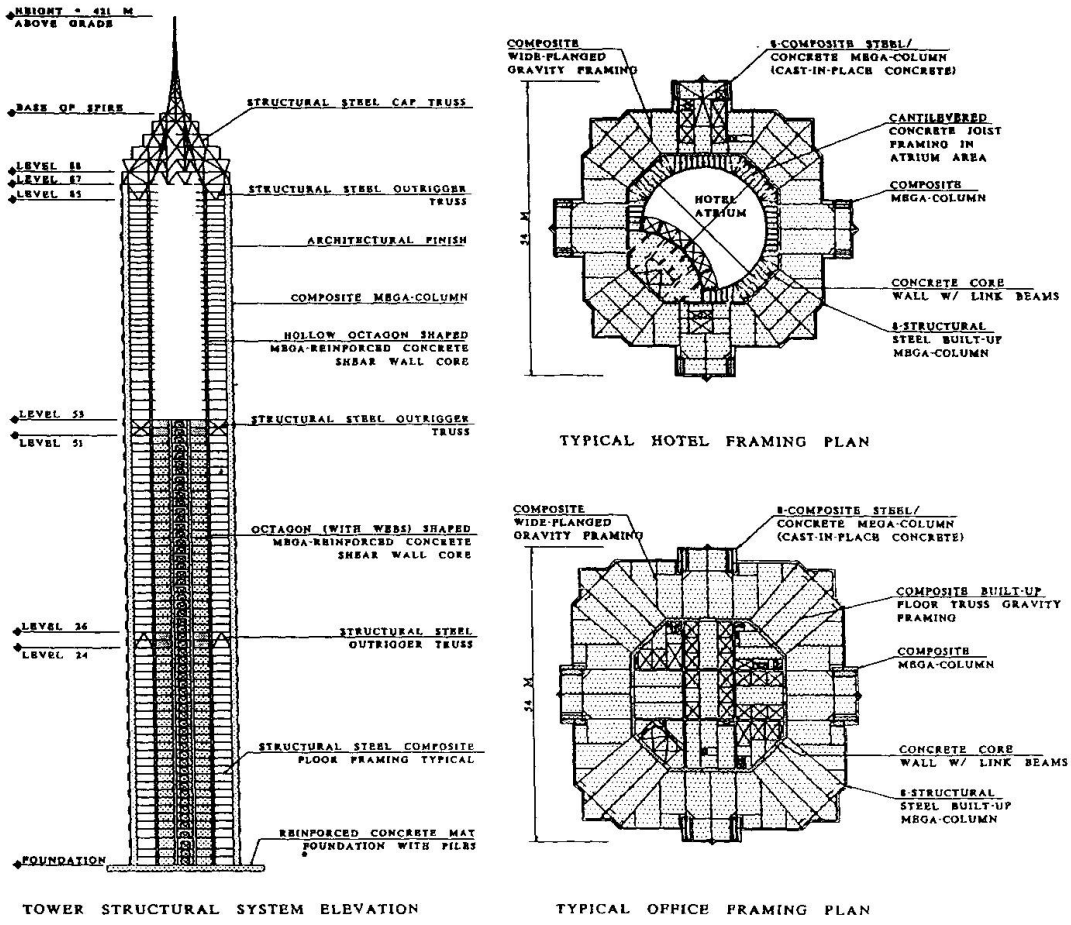

Figure 1 - Structural System Elevation and Framing Plans

Structural steel outrigger trusses interconnect the central core and the composite mega-columns at three 2-story tall levels. The interconnection occurs between Levels 24 & 26, Levels 51 & 53, and Levels 85 & 87. The outrigger trusses between Levels 85 & 87 engage the 3-dimensional structural steel cap truss system. The cap truss system which frames the top of the building between Level 87 and the spire is used to span over the open core, support the gravity load of heavy mechanical spaces, engage the structural steel spire, and resist lateral loads above the top of the central core wall / composite mega-column system.

In addition to resisting lateral loads, the central reinforced concrete core wall and the composite mega-columns carry gravity loads. Eight (8) built-up structural steel mega-columns also carry gravity loads and composite structural steel wide-flanged beams and built-up trusses are used to frame typical floors. The floor framing elements are typically spaced at 4.5 m on-center with a composite metal deck slab (75 mm metal deck topped with 80 mm of normal weight concrete) framing between the steel members. Figure 1 illustrates the components of the superstructure.

2. Poor Soil Conditions

Because of extremely poor upper-strata soil conditions, deep, high-capacity structural steel pipe piles are required to transfer the superstructure loads to the soil by friction. Open structural steel pipe piles are 65 m long with a tip elevation 80 m from existing grade. The tips of the piles rest in very stiff sand and are the deepest ever attempted in China. Pipe piles were installed in three (3) approximately equal segments, having a wall thickness of 20 mm, and having an individual design pile capacity of 750 tonnes. Piles were driven from grade with 15 m long followers before any site retention system construction or excavation had commenced. The pipe piles are typically spaced at 2.7 m on-center under the core and

composite mega-columns with a 3.0 m spacing under the other areas. The piles are capped with a 4 m thick reinforced concrete mat comprised of 13,500 m^3 of C50 concrete. The mat was poured continuously, without any cold joints, over a 48 hour period. Concrete temperature was controlled by an internal cooling pipe system with insulating straw blankets used on the top surface to control temperature variations through the depth of the mat and to control cracking.

A reinforced concrete slurry system was designed and constructed around the entire perimeter of the site (0.75 kilometer). The thickness of the slurry wall is 1 m with a concrete design strength of C40 and depth of 33 m.
The slurry wall bears on moderately stiff, impervious clay. The slurry wall acts as a temporary retention system wall, a permanent foundation wall, and a temporary / permanent water cut-off system. A tieback ground anchor system was designed and successfully tested to provide lateral support of the slurry wall during construction, however, the contractor chose to construct a locally accepted reinforced concrete cross-lot bracing system for the three (3) full basement levels which extended approximately 15 m below grade. The permanent ground water table is within 1 m of existing grade. Based on the site conditions and the slurry wall depth, a sub-soil drainage system was designed to carry 18.5 liter/sec of water. An overall description of the foundation system is shown in figure 2.

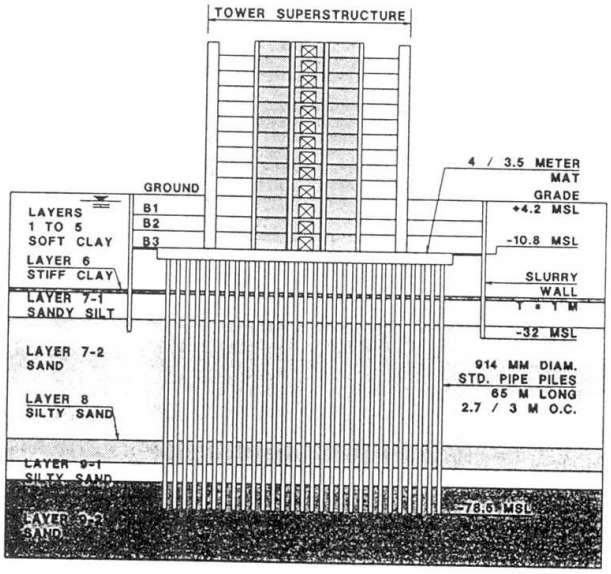

Figure 2 - Tower Foundation Systems

3. Extreme Winds

Typhoon winds as well as strong extratropical winds exist in the local Shanghai environment. Multiple analytical and physical testing techniques were used to evaluate the behavior of the Tower. Since ultra-tall structures had not been previously constructed in China, the Chinese wind design code did not address structures taller than 160 m. Therefore, code requirements were extrapolated for the Tower and wind tunnel studies were performed to confirm Code extrapolations and to study the actual, "rational" local wind climate. Wind tunnel studies, performed under the direction of Dr. Nicholas Isyumov at the University of Western Ontario in conjunction with the Shanghai Climate Center, were conducted for the building located in the existing site condition and considering the future master plan development termed the "developed Pudong" condition. The existing site context essentially consisted of low-rise buildings (3-5 stories in height) with the fully "developed Pudong" environment consisting of 30 - 50 story buildings surrounding the Jin Mao Tower with two (2) ultra-tall towers located within 300 m of Jin Mao. Wind tunnel investigation included a local climate study, construction of proximity models, a force balance test, an aeroelastic test, an exterior pressure test, and a pedestrian-level wind study. All tests considered both typhoon and extratropical winds as well as the existing and "developed Pudong" site conditions.

The final design of the Tower considered both the People's Republic of China Building Code as well as the "rational" wind tunnel studies. Strength design for all lateral load-resisting components is based on the Code-defined 100-year return wind with a basic wind speed of 33 m/s for a 10 minute average time at 10 m above grade. The basic wind speed corresponds to a design wind pressure for the Tower of approximately 0.7 kPa at the bottom of the building and 3.5 kPa at the top of the building. Results from the wind tunnel studies, considering the existing site condition and the "developed Pudong" condition as well as extratropical and typhoon winds confirmed that the Chinese Code requirements for design were conservative.

Serviceability design, including the evaluation of building drift and acceleration, was based on the "rational" wind tunnel study results. Wind tunnel studies were performed for 1-year, 10-year, 30-year, 50-year and 100-year return periods. The studies considered the actual characteristics of the structure. The fundamental translational periods of the structure are 5.7 seconds in each principal direction and the fundamental torsional period is 2.5 seconds. The overall building drift, with comparable inter-story drifts, for the 50-year return wind with 2.5% structural damping is H/1142 for the existing site condition and H/857 for the "developed Pudong" condition. It was determined that the two (2) ultra-tall structures proposed to be located near the Jin Mao Tower would have a significant effect on the dynamic behavior resulting in significantly higher effective structural design pressures. Building drifts are well within the internationally accepted building drift of H/500. Considering 1.5% structural damping and a 10-year return period, the expected building acceleration ranged from 9 - 13 milli-g's for the top floor of the occupied hotel zone. In addition, expected building acceleration ranged from 3 - 5 milli-g's for a 1-year return period considering 1.5% structural damping. The internationally acceptable accelerations for a hotel structure are 15 - 20 milli-g's for a 10-year return period and 7 - 10 milli-g's for a 1-year return period. Because of the favorable serviceability behavior of the building, the passive characteristics alone could be used to control dynamic behavior with no additional mechanical damping required.

Wind tunnel study results determined that the Code requirements for lateral load design was equivalent to a 3000-year return wind. The overall building drift based on this conservative wind loading is H/575 which also meets internationally acceptable standards for drift.

4. Moderate Seismicity

The approach for evaluating seismic loadings for the Jin Mao Tower considers both Chinese Code-defined seismic criteria and actual site-specific geological, tectonic, seismological and soil characteristics. Actual on-site field sampling of the soil strata and engineering evaluations were performed by Woodward-Clyde Consultants, the Shanghai Institute of Geotechnical Investigation and Surveying, and the Shanghai Seismological Bureau.

All lateral load resisting systems, including all individual members, were designed to accommodate forces generated from the Chinese Code-defined response spectrum as well as site specific response spectrums. Extreme event site-specific time history acceleration records (10% probability of occurrence in a 100-year return period) were used in time history analyses to study the dynamic behavior of key structural elements including the composite mega-columns, the central core, and the outrigger trusses.

The site specific response spectrums used to describe the Tower's dynamic behavior included analyses for a most probable earthquake with a 63% probability of occurrence in a 50-year return period and a most credible earthquake with a 10% probability of occurrence in a 100-year return period. In addition, the Tower was evaluated using a 3-dimensional dynamic time history analysis for a most credible earthquake with a 10% probability of occurrence in a 100-year return period.

In all cases, the Chinese-defined code wind requirements governed the overall building behavior and strength design; however, special considerations were given to the outrigger trusses and their connections. In all design cases, these structural steel trusses were designed to remain elastic.

5. Unique Structural Engineering Solutions

The structural design for the Jin Mao Tower created an opportunity to develop unique structural engineering solutions. These solutions included the practical development of theoretical concepts, unusual detailing of large structural building components, and comprehensive monitoring of the in-place structure.

The overall structural system utilizes fundamental physics to resist lateral loads. The slender cantilevering reinforced concrete central core is braced by the outrigger trusses which act as levers to engage perimeter composite mega-columns, maximizing the overall structural depth. The overall structural redundancy is limited by engaging only four (4) composite mega-columns in each primary direction. Structural materials are strategically placed to balance the applied lateral loads with forces due to gravity. Very little structural material premiums were realized because of the structural system used. Lateral system premiums essentially related to material required for the outrigger trusses only without measurable structural material premiums required for central core wall and composite mega-column elements. The combination of structural elements provides a structural system with 75% cantilever efficiency.

Even after equalizing the stress level within the central core and composite mega-columns, the expected relative shortening between the interconnected central core and composite mega-columns was large. By calculation, considering long-term creep, shrinkage, and elastic shortening, the expected relative movement between these elements at Levels 24-26 was as much as 50 mm. The magnitude of relative movement would have induced extremely high stresses into the stiff outrigger truss members weighing as much as 3280 kg/m. Therefore, structural steel pins with diameters up to 250 mm were detailed into the outrigger truss system (see figure 3). These pins were installed into circular holes in horizontal members and slots in diagonal members to allow the outrigger trusses to act as free moving mechanisms for a long period during construction. This allowed a majority of the relative movement to occur free of restrain, therefore, free of stress. After a long period of time, high strength bolts were installed into the outrigger truss connections for the final service condition of the lateral load resisting system. The expected relative movement after the final bolting was performed was a maximum of 15 mm at Levels 24-26. Considering the flexibility of the long composite mega-columns, the final forces attracted to the trusses did not appreciably increase the member and connection sizes.

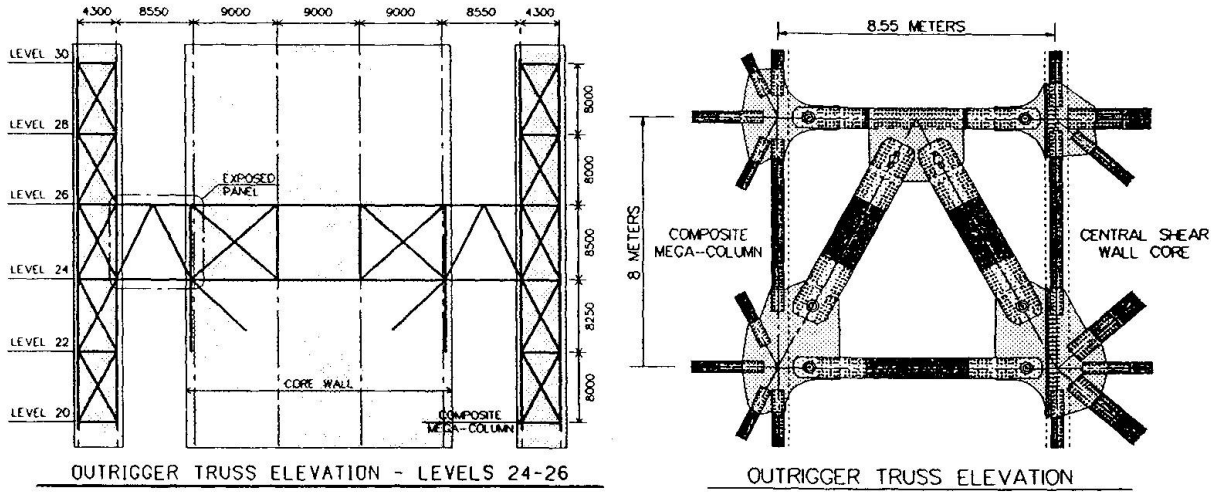

Figure 3 - Elevation and Detail of Outrigger Truss System

A comprehensive structural survey and monitoring program was designed and implemented into the Jin Mao Tower. Extensometers were placed on the reinforced concrete central core and on the reinforced concrete of the composite mega-columns. In addition, strain gages were placed on the built-up structural steel mega-columns as well as on the wide-flanged structural steel columns location within the concrete encasement for the composite mega-columns. Sample results of measured strain versus calculated strain are shown in figure 4. In addition to the gaging of the superstructure, the mat was periodically surveyed for long-term settlement. The mat foundation system under the Tower was initially surveyed just after pour completion in October 1995 and is currently still being surveyed. Based on a sub-structure / soil analysis, the expected maximum long-term Tower mat settlement is 75 mm. The latest Tower mat settlement is shown in figure 5. Laser surveying techniques were used for both lateral and vertical building alignment. Floor levels of the structure were typically built to drawing design elevation, compensating for creep, shrinkage, and elastic shortening which

occurred during construction. Lateral position of the Tower was constantly monitored from off-site benchmarks and was found to be well within acceptable tolerances.

6. Conclusions

Incorporating fundamental structural engineering concepts into the final design of the Jin Mao Tower lead to a solution which not only addressed the adverse site conditions but also provided an efficient final design. The final structural quantities included the following for the Tower superstructure from the top of the foundation to the top of the spire (gross framed area = 205,000 m^2):

Structural Concrete	0.37 m^3/m^2
Reinforcing Steel	30.4 kg/m^2
Structural Steel	73.2 kg/m^2

A final evaluation of monitoring and survey data will be performed. Data from the as-built structure subjected to actual imposed loads will be correlated with theoretical results. This comparison will prove to be invaluable for the future design and construction of ultra-tall occupied structures.

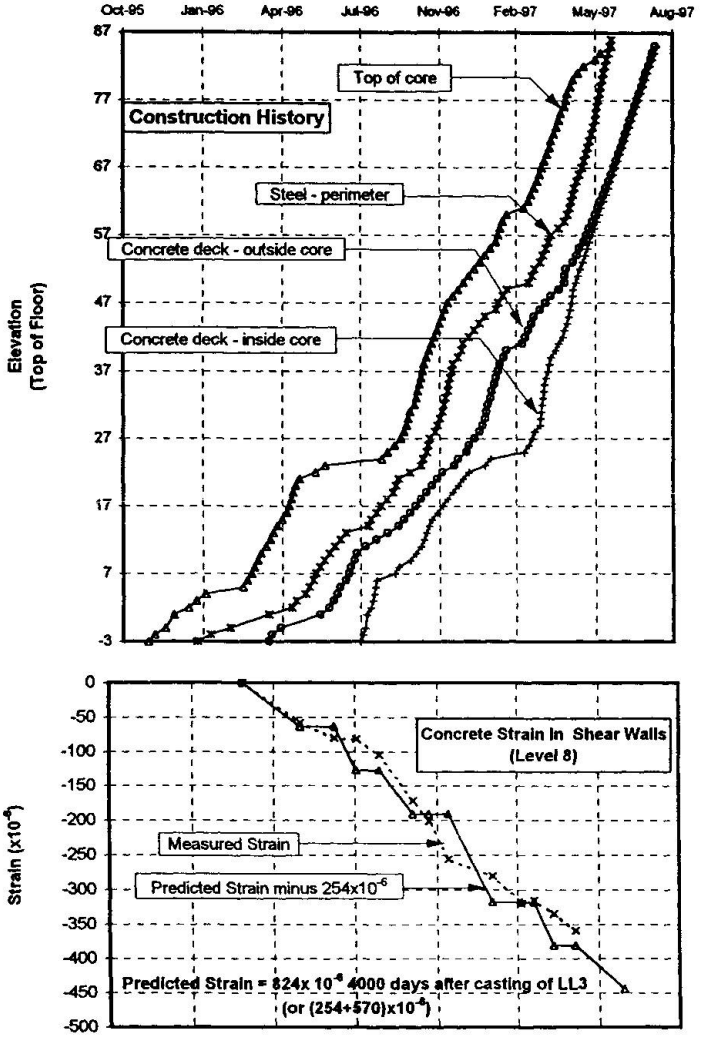

Figure 4 - Comparison of Measured Strain Versus Predicted Strain in Shear Walls (Level 8).

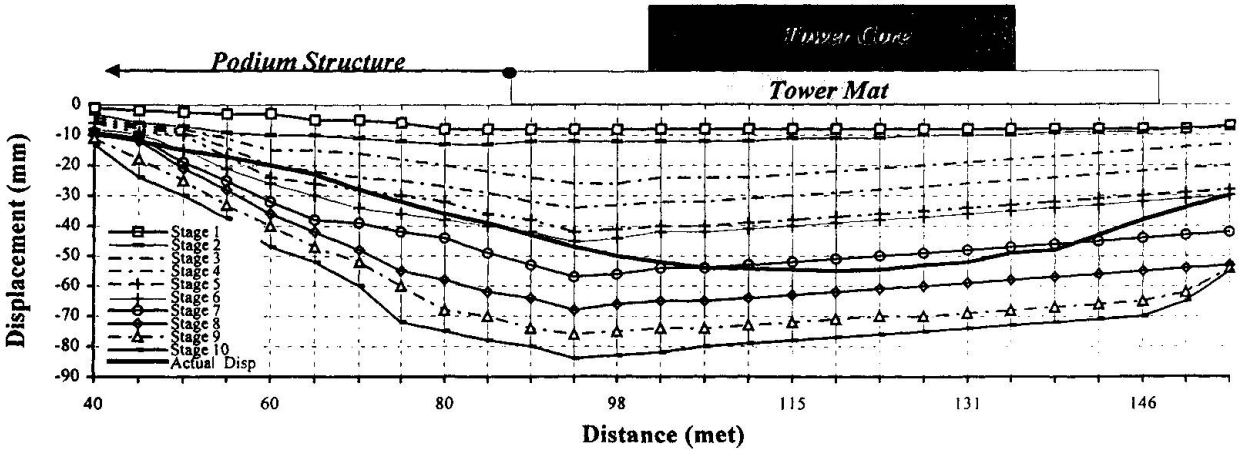

Figure 5 - Comparison of Estimated Versus Actual Tower Mat Settlement

High-Rise Condominium with Concrete Filled Steel Tubular Column and Visco-Elastic Damper

Hiroshige MORI
Structural Eng.
Konoike Constr. Co. Ltd
Osaka, Japan

Yasuo KUROKI
Senior Eng.
Konoike Constr. Co. Ltd
Osaka, Japan

Yasuhiro KAWASAKI
Mgr
Housing and Urban Dev. Corp.
Osaka, Japan

Kenichi KATAGIHARA
Dir.
Konoike Constr. Co. Ltd
Osaka, Japan

Masakazu OKAMOTO
Senior Specialist
Housing and Urban Dev. Corp.
Osaka, Japan

Summary

At present, a 40 story high-rise condominium is under construction in Osaka, Japan for completion in 1999. One of main features of the structure is that high strength and substantial ductility are secured with cross-tube arranged frames consisting of concrete filled steel tubular columns and steel girders. In the condominium, structural control system with visco-elastic dampers, VED, is employed for improvement of habitability under gusts or typhoons while seismic performance is also enhanced. In order to verify damping improvement effect by the VED, response analysis with time series excitation of wind and earthquake has been performed. In the paper, effect of the VED is clarified by outcome of the response analysis, as well as is peak-cut system which is not to input excessive stress into the surrounding frames.

1. Design Concept

Since the Hyogo-ken Nanbu earthquake on the 17th of January, 1995, how to secure redundancy of earthquake response capability of structural system has become a hot issue in Japan. On the other hand, high-rise building, especially of resident use, needs a capability to decrease uncomfortable vibration. The authors believe that upgrading the viscous damping capacity of building by installing the VED is efficient method to meet the request. Single equipment like Tuned Mass Damper installed at uppermost floor may give improvement of the habitability, but there is a possibility to harm the building in case of unpredictable situation like excessively intense earthquake. Passive system consisting of a large number of small devices which are relatively undersized and easy to exchange, is considered to be safe and the surest technique for securing redundancy of seismic capability and good habitability of high rise building.

2. The building outline

The structural system is mainly cross-tube arranged frames with standard span of 6.5 m by 9.0 m, adaptable for architectural arrangement. The structural frame consists of steel girders and concrete filled steel tubular columns, with reinforced concrete frames and walls under ground. Typical structural plan and

framing elevation are shown in figures 2, 3. The steel tubes of the CFT columns have weld built-up box section with SN490B steel and the girders have weld built-up H-shape of SN490B steel. Girders to columns joints have inside diaphragm and girder brackets fabricated by shop welding. Joints of bracket and girder element are field welding for flange and high strength bolt joint for web. Filling concrete of the CFT column is high flow concrete of 60 N/mm^2 strength for the first through the 12th story and 42 N/mm^2 for higher stories. The arrangement of the VED for each story has been determined not to cause twisting in the plan as well as sudden change of stiffness between stories. Dwelling unit plan, emergency check of the VED and influence of temperature to the VED are also of consideration. In the first through the 19th story, eight VEDs are placed between dry wall sidings in symmetrical arrangement for both axes, and four VEDs are placed as well in the 20th through the 38th story, as shown in figures 2,3.

Figure 1 Persepective

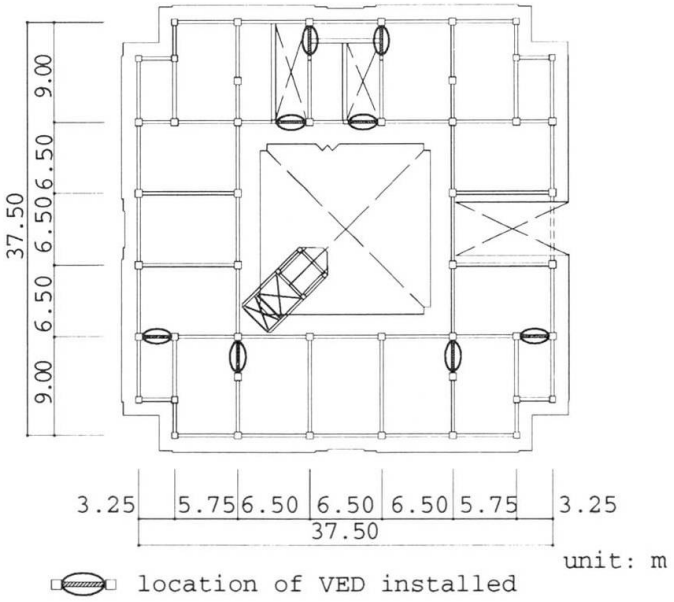

Figure 2 Structural plan, lower stories

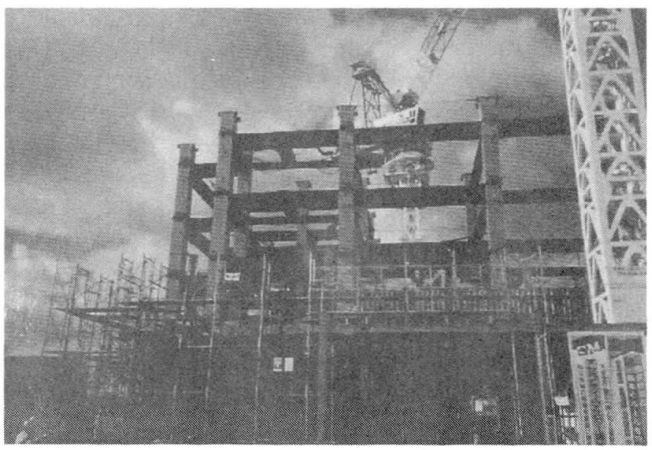

Photo 1 Steel erection of lower stories

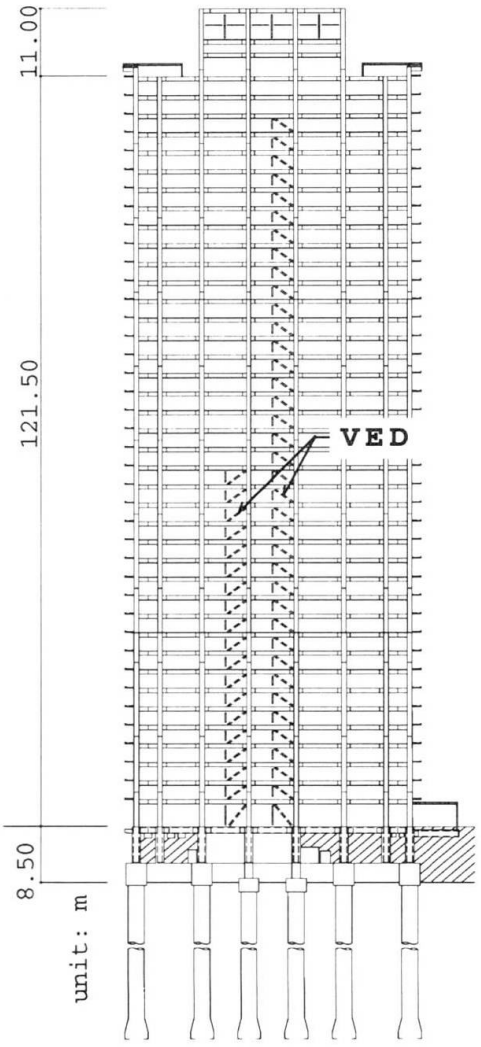

Figure 3 Framing elevation

3. The visco-elastic damper, VED

The VED makes use of hysteretic property of rubber-like visco-elastic substance, VES, when it is subjected to cyclic shear strain. The VED consists of the VES held between five steel sheets as shown in figure 4. From load-shear deformation relationship of experiments, figure 5, it is seen that hysteresis loop of the VED is quite similar to an elliptic from low amplitude to large ones, which suggests that those dampers are possessed of almost linear mechanical properties. When earthquake or gusts occurs, the steel sheets shift causing shear deformation to the VES, which then absorb energy. The property of the VED can be represented by a Voight model. Assuming that the VED has perfectly linear properties, its hysteresis loop becomes an inclined elliptic as shown in Figure 6[1]. The angle between the horizontal axis and the line from the origin to the point where the deformation shows its maximum is defined as equivalent stiffness Keq. Equivalent damping coefficient Ceq then is given as:

$$Ceq = \Delta W / (2 \pi^2 \cdot a^2 \cdot f)$$

where , ΔW , a and f are the area of the hysteresis loop, the amplitude and the frequency respectively. Keq and Ceq are to be corrected for temperature in practical use because of the VES's temperature-dependent property. The temperature correction can easily be performed just by multiplying rigidity and viscosity by temperature correction factors [1]. Because the VED is also velocity-dependent, there may occur excessive force under impulsive

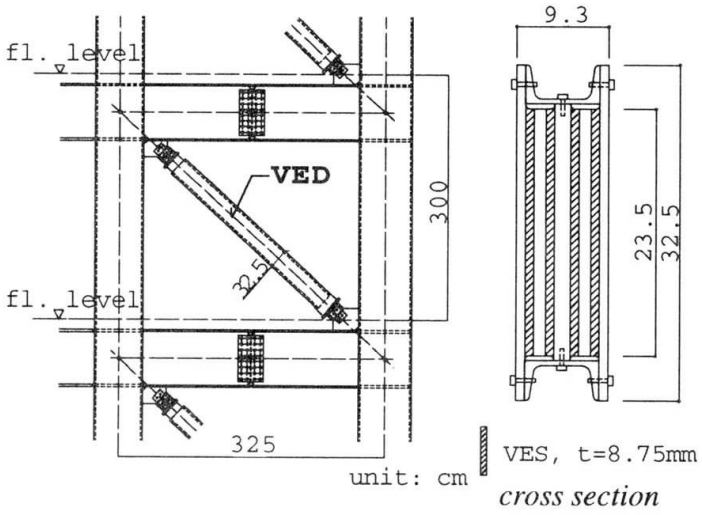

Figure 4 Visco-elastic damper

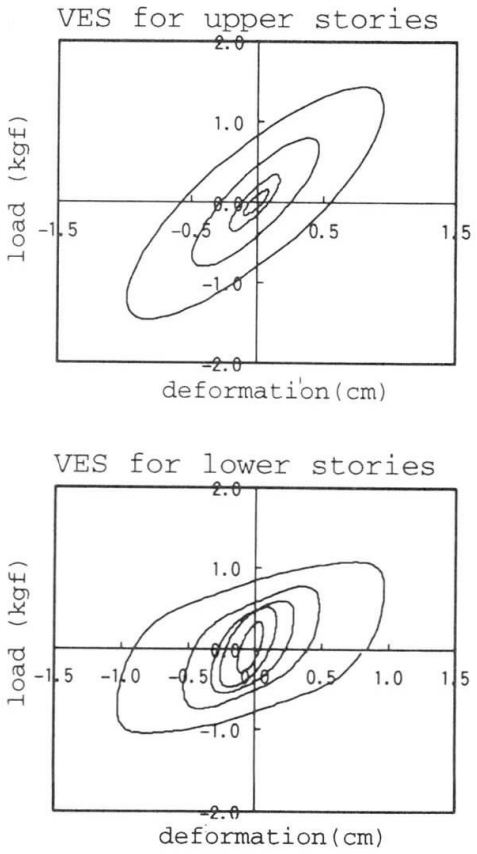

Figure 5 Hysteresis loops of experiment

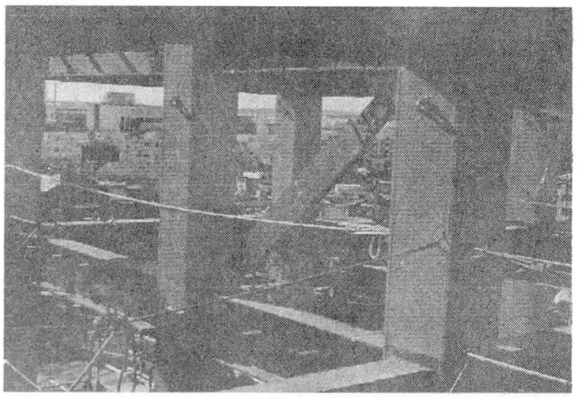

Photo 2 Installation of VED

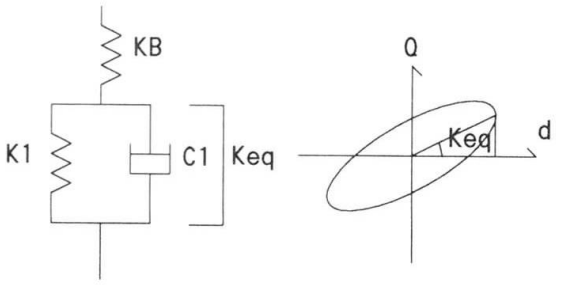

Figure 6 Voight model

input like earthquake excitation. Then the force imposed on the VED is to be controlled by so-called peak-cut system, a set of high strength bolts and slotted holes which is equipped on one end of the VED. It avoids excessive force working on the VED and damaging the surrounding frames.

4. Study of habitability under gusts

4.1 The wind response analysis

To confirm the improvement effect of the habitability under gusts by the VED, wind response analysis has been performed. Wind external force was formed as time series load with experimental data of wind pressure measured in wind tunnel tests. These are for wind direction and orthogonal direction to the wind with condition of wind velocity of one year return period, that is 25.3 m/s at the top of the building, 141.8 m high from neighboring river surface.

The primary natural period of the building is 3.43 seconds of one direction, 3.38 seconds of another direction. Consequently the property of the VES is employed for 3 Hz of frequency. The property of the VES is also for 20 degree, 25 degree and 30 degree in Celsius of temperature, because the monthly average temperature of August through October, when gusts or typhoons usually happen at Osaka, are 28.2 ℃, 24.2 ℃ and 18.3 ℃, respectively [2].

Time-history response acceleration at the uppermost 40th floor is shown in figure 7 for with and without the VED. Root mean square, RMS values of 10 minutes duration for response quantities are employed to evaluate, because shake or vibration of building perceived is considered to be related to response quantities of a certain duration rather than a momentary response. The RMS values of the response acceleration with the VED installed are decreased about 20% and 35% for 30 ℃ and 20 ℃ respectively, compared with the response acceleration without the VED.

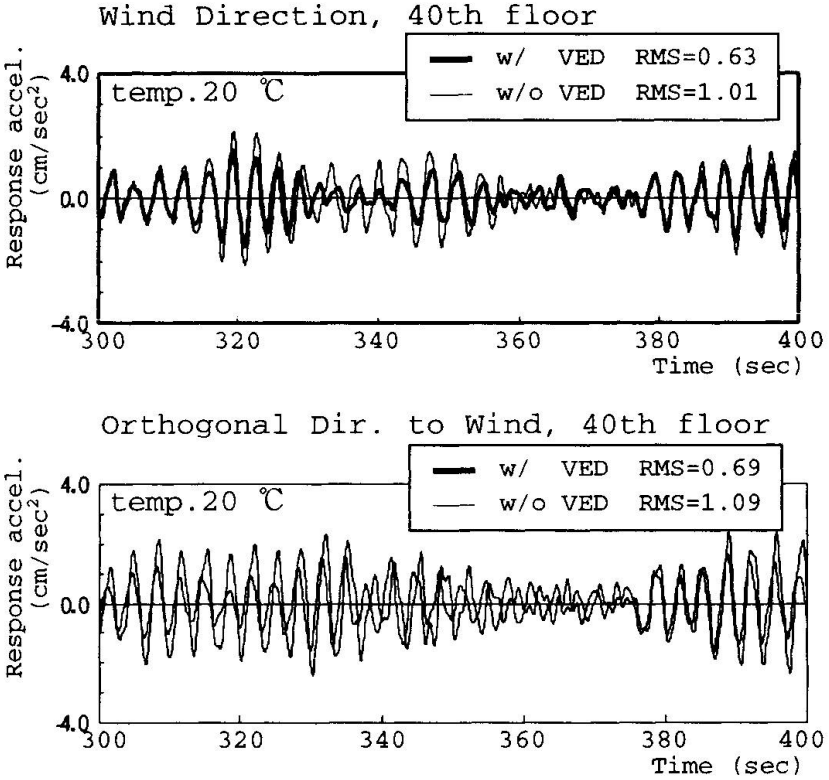

Figure 7 Response acceleration at the 40th floor

Table 1 Equivalent damping with the VED

	20··	25··	30··
heq (wind dir.)	3.4 %	2.3 %	1.9 %
heq (orthogonal dir. to wind)	5.0 %	3.0 %	2.0 %

Including original structural damping of 1 %

The response analysis has been performed also for solely structural model without the VED but of series of structural damping factor changed from 1% through 6%, where original damping factor of the structure itself is assumed 1%. With comparing the outcome of the damping factor series with the outcome of the VED installed, damping effect of the VED is estimated to be equivalent with 1% to 4% of structural damping factor, as shown in Table 1.

4.2 Evaluation of habitability

Evaluation of habitability under gusts of one year return period has been worked on the uppermost 40th floor according to official recommendations [3]. Response acceleration are estimated by a method of a

guidelines [4] rather than the outcome of the response analysis, and equivalent structural damping in Table 1 are employed for the evaluation.
Evaluation chart is shown in Figure 8. The structural control effect of the VED is conspicuously expressed both in the wind direction and the orthogonal direction to the wind, meeting rank II and rank III. It confirmed that it met rank III even in case of 30 ℃ temperature which is the most unfavorable condition in viewpoint of temperature-dependent property of the VES. The performance about habitability indicates almost equal to the one of the same scale reinforced concrete structure.

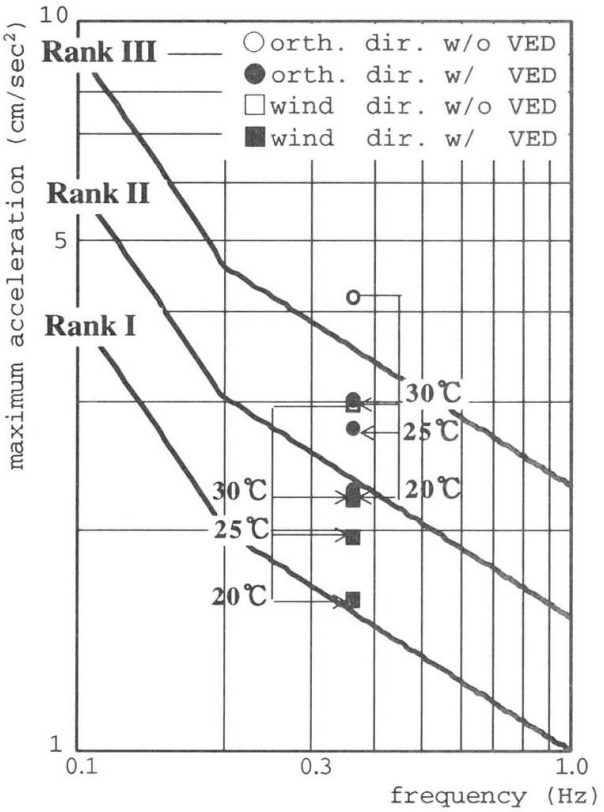

Figure 8 Evaluation of habitability

5. Behavior of earthquake response

5.1 The peak-cut system

It provides so-called peak-cut system, a set of high strength bolts and slotted holes which is equipped on one end of the VED, in order to avoid excessive force occur in the VED in case of intensive earthquake. Load and deformation relationship of dynamic shear loading tests for 16mm diameter high strength bolts, M16, is shown in Figure 9. The maximum load at friction slip shows the value which is about 75 % of design load for the conventional friction joint with normal bolt hole, while the hysteretic loop shows rigid-plastic behavior. Therefore, combination of the Voight model (Keq and C1) and rigid-plastic bi-linear model (K_B) for the VED as shown in figure 6, is employed in the earthquake response analysis.

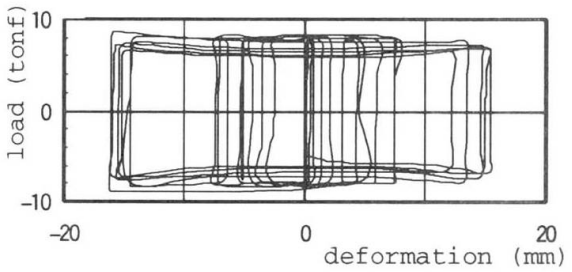

Figure 9 Dynamic behavior of peak-cut system

5.2 Earthquake response analysis

In order to clarify earthquake response behavior due to the installation of the VED, response analysis have been performed for maximum ground velocity of 25 cm/sec as Level I and of 50 cm/sec as Level II. Earthquake records are El Centro NS 1940, Taft EW 1952, Hachinohe NS 1968 and TKMF061 1995. TKMF061 is a site record of another Housing and Urban Development Corp. condominium, about 2 km apart from the concerned site, obtained at the time of the Hyogo-ken Nanbu earthquake on January 17, 1995. The temperature is specified to be 20 ℃ as the year average temperature at Osaka. The response quantities of the analysis shows about 10% decrease for Level I and about 5% decrease for Level II by the VED in overall view. The response for the TKMF061 solely is shown in Figure 10, conspicuously representing decrease of response quantities for each floor uniformly due to the VED. The time history of force-deformation relationship of a VED installed in the 10th story is shown for Level II earthquake in Figure 11. It is clearly recognized that excessive force working on the VED should be avoided and undesirable influence onto the surrounding frames are controlled by the peak-cut system.
The maximum shear strain of the VED and maximum slip deformation of the peak-cut system under Level II earthquake are shown in Table 2. The maximum shear strain of the VED are 100% through 160 % and is in

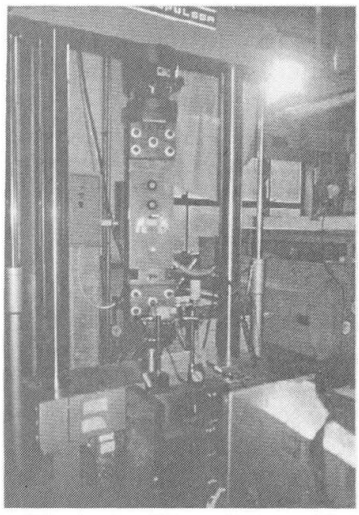

Photo 3 Experiment of peak-cut system

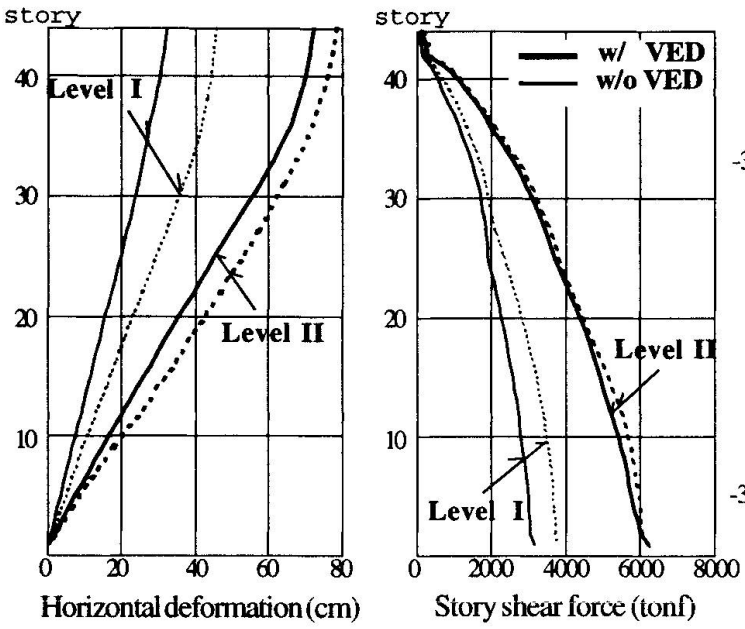

Figure 10 Earthquake response

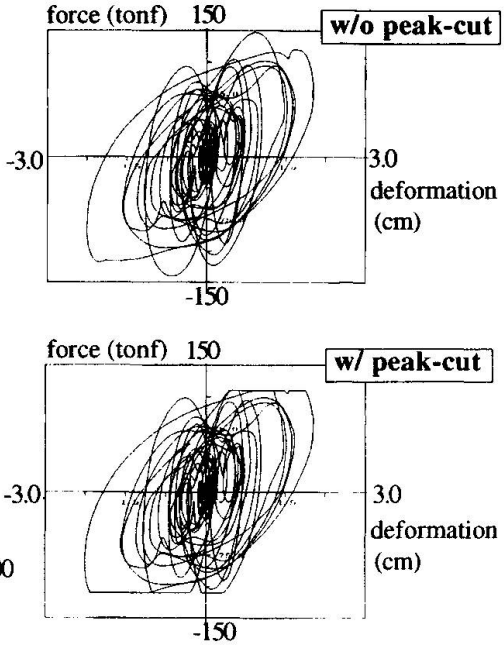

Figure 11 Response of the VED

Table 2 Response strain and deformation

	10th story	20th story	30th story	38th story
Maximum shear strain of VES	101 %	159 %	158 %	132 %
Maximum slip deformation of peak-cut system	0.69 cm	0.18 cm	0.62 cm	0.50 cm

the range of stable behavior of the VES experiment result, that is, the elliptic loop remain linear mechanical properties. The maximum slip deformation of the peak-cut system shows approximately 0.7 cm indicating a design detail for 1 cm or more slip deformation to be required. The detail in the VED actually installed in the building is designed as adequate for 3 cm slip in both direction.

6. Conclusions

The VED has already been used for vibration control in the skyscrapers in the U.S., since 30 years ago and has results applied in a large number of buildings. Recently, research and development has moved for feasible use in seismic retrofit of conventional reinforced concrete structures, and the number of practical use has increased in Japan. The VED has its particular property of energy dissipation capability for every magnitude of amplitude, while it is easily manufactured resulting in low cost. Manufacturer of the VES are carrying forward the development of substances with higher damping and less temperature-dependent property. Two kinds of the VES which are newly developed by different manufactures should be used in the concerned building. The building is now under construction for completion in June of 1999. Measurement system in the building consisting of seismometers, wind observation devices and VED measurements, is expected to clarify furthermore the behavior of the structure and the VED.

References

[1] Satsuya Soda, Jyun-ichi Wada et. al., Visco-Elastic Damper: Cyclic Loading Test to Construct Mechanical Model, Journal of Struct. Constr. Engng., Architectural Institute of Japan, No. 457, Mar., 1994 [in Japanese]
[2] The science chronological table, Japanese national observatory volume, 1994 edition [in Japanese]
[3] Recommendations for Loads on Buildings, AIJ, 1993 edition [in Japanese]
[4] Guidelines for the evaluation of habitability to building vibration, AIJ, 1991 edition [in Japanese]

The Concept of the Parts Oriented Production System

Takashi KUNUGI
Mgr
Shimizu Corp., Technol. Dev. Div.
Tokyo, Japan

Takashi Kunugi, born 1958, has devoted the last 15 years in the development of structural analysis software, production planning and control software

Hiroo TAKADA
Gen. Mgr
Shimizu Corp., Technol. Dev. Div.
Tokyo, Japan

Hiroo Takada, born 1942, obtained Doctor of Eng. at Tokyo Science Univ. and has devoted the last 30 years in the study of new construction methods.

Naoto MINE
Dep. Gen. Mgr
Shimizu Corp., Technol. Dev. Div.
Tokyo, Japan

Naoto Mine, born 1946, obtained Doctor of Eng. at Waseda Univ. and has devoted the last 26 years in the study of construction productivity issues.

Summary

The authors propose the PARTS ORIENTED PRODUCTION SYSTEM (POPS) as a revolutionary concept to solve the various problems currently being faced by the construction industry in Japan. The ultimate goal of this system is the pursuit of transparency of all information and all processes in construction production. It does not stop at construction performance processes but aims at reform in the construction production process as a whole, including design at the early stages, and at the parts procurement stage. At present, partial testing and application to construction sites is being carried out in order to verify the benefits of this system.

1. Introduction

Currently, the construction industry in Japan must struggle with problems related to productivity improvement and responses to the diversification of customer needs. It is predicted that in ten years twice the current level of productivity will be required. Meanwhile, customer needs are diversifying and becoming more sophisticated. The level of social requirements to buildings becomes higher and the trend of building requirements changes faster. This therefore results in the major problem of how quickly companies can provide buildings which satisfy these complex and diverse conditions. In order to do so it is necessary to break away from the labor intensive construction production systems of the past, and to undertake radical reform which incorporates all processes of construction production into the perspective.

The goal of the Parts Oriented Production System proposed by the authors is to make lower subsystems transparent in the early stages. Furthermore, by clarifying the mutual relationships between a variety of information, it will be possible to control quality, cost and work duration earlier than usual. This system makes it possible to rapidly realize buildings which satisfy the demands of customers.

2. The Concept of the Parts Oriented Production System

This system comprises three major subsystems. The first subsystem is design. Considering a building to be made up entirely of parts, it is possible to describe the building in terms of the properties of each part, i.e. the qualities and shapes of parts, and part unit prices. The designer then decides on the volume of the building as a whole, and the structure and layout of each space, taking into account the restricting conditions such as the demands from the customer, the site conditions and the laws and regulations which apply to the site. Next, in order to achieve the performance of each space, the designer selects the materials to be used in the parts which make the space, and decides on the dimensions after considering individual demands for each space and the building as a whole, based on existing design cases and the designer's knowledge gained from experience. In parts oriented design, the designer advances the design process by selecting the parts one by one based on his or her knowledge gained through experience and the attribute information of each part. If a designers wishes to make the most of his individuality in building or space, or if a conscious attempt is made to differentiate that building or space from others, original parts may be developed. It is also possible to use designs which intend parts replacement to extend the building's life. Through such processes as these, a list of the parts to be used in the building as a whole is completed, and it is easy to obtain the total numbers of each part including a total of each type of part, and a total unit cost.

The second subsystem is procurement and distribution. Procurement plans are formulated by referring to the parts list for each building provisionally decided upon in the design subsystem, and taking into account the process for each building. The design subsystem entails review of each individual item, but in the procurement and distribution subsystem, review is carried out to bring together the lists of parts for each building and to increase the quantity of parts purchased as much as possible. If it is judged that the performance of particular parts are roughly the same, but the quantitative effect against cost is higher for the parts of a different manufacturer, review must be carried out once more to establish whether it is possible to make changes in the design subsystem. If it is impossible to make one order due to slight differences in the delivery date, at the same time as reviewing the possibility to changes in delivery date at the construction site, the possibility of provisionally setting up a temporary stockyard at the company or the manufacturer should be reviewed. In addition, in order to purchase parts more cheaply, production planning of parts manufacturers shall be considered. It is necessary to constantly exchange information with parts manufacturers, and possess low-cost parts information in real time.

The distribution subsystem reviews how the procured parts will be delivered to the construction site. Up until now, there has been a high degree of reliance on manufacturers for the distribution of each part, and the distribution costs of parts have been tacitly added onto part unit costs. In the distribution subsystem, it is important to review conventional customs, to clearly differentiate part unit cost and distribution costs, and to develop a mechanism which enables cost control of the two. The necessary parts must be delivered to each construction site at the necessary time (just in time), but if parts ordered all at one in large quantities are shipped at the one-sided convenience of the manufacturer, the management at each site becomes confused. Two methods available to prevent this from happening are that the manufacturer maintains a temporary inventory, or the company provides a temporary storage area. Taking a look at the conventional state of carrying in materials to construction sites, there are many cases in which a large truck comes only carrying a minuscule quantity of materials. It

is also important to review the ideal packing method and form of packaging for transportation based on the dimensions, shape, weight and material of each part. This would then make it possible to select a truck in accordance with the quantity, thereby improving distribution efficiency. Additionally, using the return trips of trucks which have carried in parts to recover temporary parts which are no longer necessary, and patrolling other sites located nearby will also contribute to improving distribution efficiency.

The third subsystem is pre-assembly. Most of the assembly systems in current construction production entail carrying out work continuously one by one on a final assembly line leading to completion. i.e. the straight line production system. Taking a close look at this production process, it is not necessarily the case that it must be implemented on a final assembly line. That is to say, there are a considerable number of parts which can be unitized or assembled into panels in a place inside or outside the site, before being installed on the final assembly line. If this parallel production system (hereinafter referred to as "pre-assembly") is used, it becomes possible in principle to divide up and carry out in parallel the production processes in accordance with the required work duration, thereby dramatically reducing the work duration. In unitizing parts or assembling panels, there is the method in which a production yard is set up and operated within the construction site, the method which uses the factories of manufacturers of related parts, and the method which uses a temporary storage area discussed in the distribution subsystem above. Whichever method is used, it is separated from the final assembly line (sub-line), and a good work environment may be expected. That is to say, an attitude which is easy to work in is adopted by creating tools to fit the parts, or deciding on supply routes for parts which minimize the walking distance of workers. Improvements in the work environment will also make it possible to simplify the work which conventionally requires highly developed skills. For example, if work done facing upwards is changed to work done facing downwards, that alone makes work easier to perform. This makes it possible to use unskilled labor, which in turn enables companies to keep the cost of labor down. In addition, when different occupations perform work one after the other, it becomes possible for workers from different occupations to perform simplified work. That is to say, it makes workers multi-skilled. The same may be said if machines are used on the sub-line. If simple regular position work is adopted, and processing machines are used, sophisticated machinery becomes totally unnecessary. Unlike conventional construction robots, there is no need for the machines to automatically approach the parts. Machines should be operated using cheap labor, with a mobile pedestal for the machines or the parts to be assembled.

A further benefit of the pre-assembly method is the prevention of unproductive waiting time. Conventionally in locations related to equipment and the interiors of buildings a variety of occupations become jumbled, and there is a tendency for workability to suffer. In such locations, by breaking away from a final assembly line, and assembling at a sub-line, not only is it possible to achieve a more spacious working area, but by establishing multiple sub-lines and making workers patrol on cycles which correspond with the cycles of the final assembly line, it is possible to prevent unproductive waiting time from occurring and to achieve dramatic improvements in workability.

The content of the main three sub-systems has been described above, and while these three processes have a slight time differential, work can be advanced simultaneously in parallel through cooperation. As mentioned at the beginning of the design subsystem section, by adopting an approach which recognizes that the individual parts which make up a building are separate and have their own unique attributes, it suggests the possibility that matters which

may have seemed extremely complex in the conventional macro perspective may be able to be organized clearly.

3. Application

In order to verify the effectiveness of this concept, the authors are carrying out construction testing assuming actual construction, and are applying this concept to construction sites. Two cases are presented here.

3.1 Utilization of Multi-skilled Labor in Interior and Equipment Works for Multiple Dwelling Housing

Conventionally, the systematization of construction of interior and equipment work is lagging behind that of structural work, and there is a tendency for processes to become complicated and the working efficiency to suffer as a result of the work of different occupations becoming intricate in confined areas such as plumbing areas. This case was an attempt to overcome this problem by making carpenters who were conventionally specialists into multi-skilled workers, and having them implement part of the equipment work. In this test, the carpenter carried out wiring and plumbing, mounting of ventilation fans, and mounting of electronic equipment in the presence of specialist workers. In order to make it possible for the carpenter to also carry out the water and hot water plumbing, parts made of cross-linked polyethylene pipe, which is lightweight and can be bent, were pre-assembled at the factory in accordance with the residential layout. In addition, in an effort to improve productivity of partition walls, half panel parts constructed from plasterboard and wooden studs were used. By using cross-linked polyethylene pipes it becomes possible for the carpenter to carry out woodwork and plumbing alone, which in turn makes it possible to reduce the ineffective work time caused by jumbling of different occupations. Photographs taken during the test are shown from Fig. 1 to Fig. 6. The cross-linked pipe parts and partition wall half-panels pre-assembled in this case both have unique attribute information (materials, dimensions, unit price, constructability, etc.) It is without a doubt that the act of referring to some of this attribute information in the design subsystem and focusing on the construction stage to decide on part of the attribute information, makes lower subsystems transparent in the design subsystem. This case made multi-skilling possible by the utilization and development of parts which can be constructed without highly developed skills, thereby improving productivity. At the same time, this case actively made lower subsystems transparent in upper subsystems.

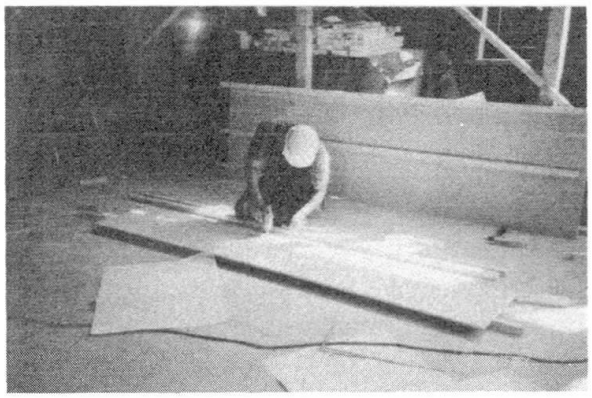

Fig. 1 Production of half-panel parts

Fig. 2 Installation of half-panel parts

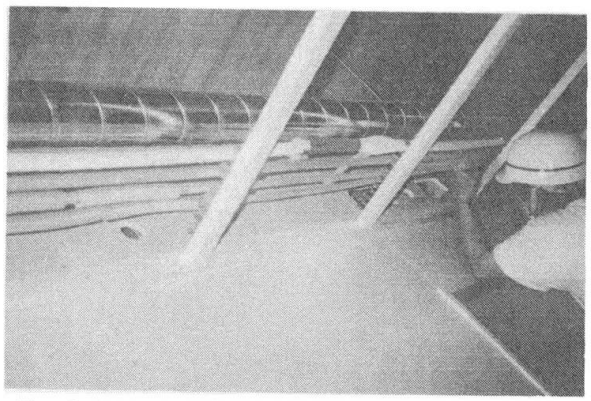

Fig.3 Laying of crosslinked polyethylene pipes

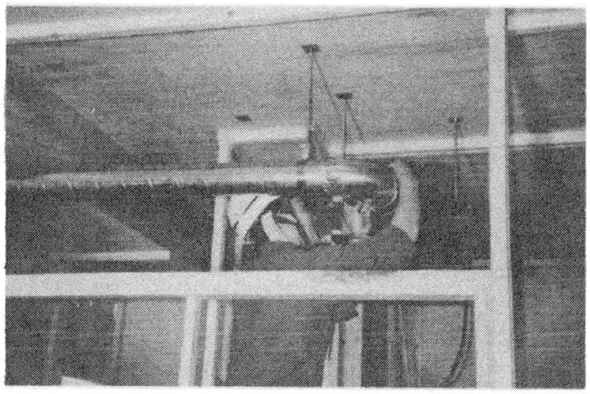

Fig.4 Mounting of ventilation fan and duct

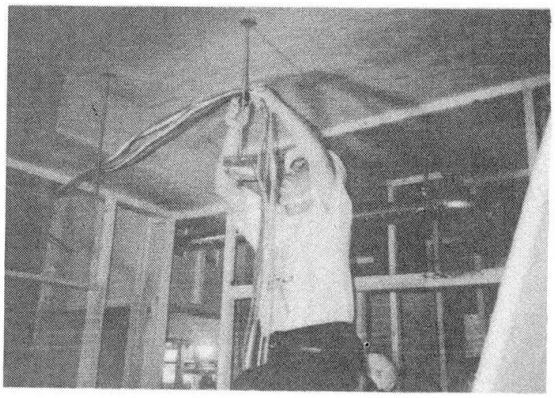

Fig. 5 Electric wiring

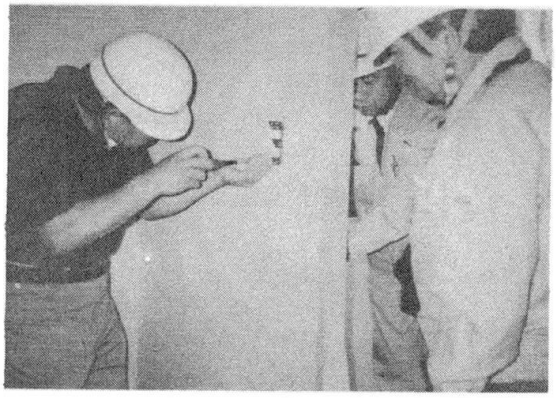

Fig. 6 Installation of switch box

3.2 Parts Oriented Assembly of Meter Boxes for Multiple Dwelling Housing

This case entails the parts oriented assembly of the pipes and the precast concrete panel which supports such pipes inside the meter box for multiple dwelling housing, and it is currently being applied to actual construction. This multiple dwelling housing in this case is a 17 floor building with a total of 332 residences, and construction is being carried out in four construction areas. Fig. 7 shows a plan of a typical residence. The area around the meter box shown in the plan is a confined area in which the work of different occupations becomes jumbled, as was the case in 3.1. The decision was therefore made to remove the work around the meter box from the main work in an effort to level out and improve the efficiency of labor. The production of precast concrete panels is implemented on site, and pipes pre-assembled at the factory are mounted at the same time as the precast concrete panels are completed. This production cycle is planned to be synchronized with the structural construction process and to reduce the number of steel forms in this cycle process and the stockyard area. Steel form onto which fittings for inserts have been mounted is used to enable the production of precast concrete panels by unskilled labor. This production of meter box parts by pre-assembly becomes parallel with main works, and not only contributes to reducing the input of labor, but also makes it possible to keep labor costs down by utilizing unskilled labor in parts production itself. Fig. 8 to Fig. 12 show photographs of the meter box parts and the state during construction.

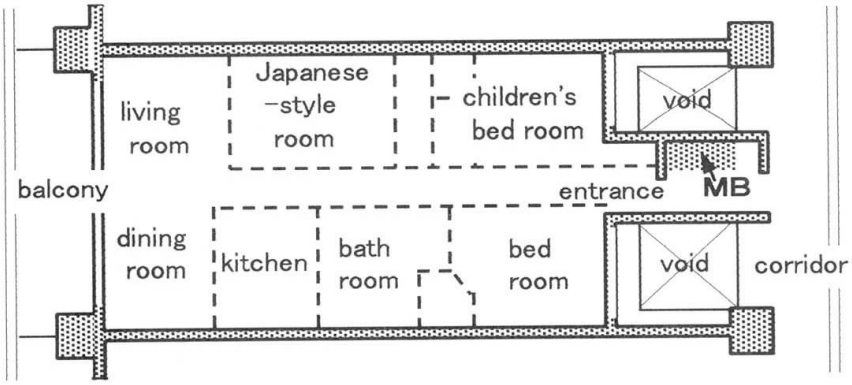

Fig.7 Plan of a typical residence

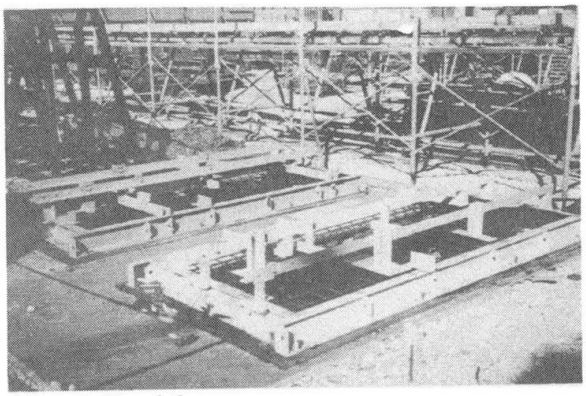

Fig. 8 Steel form

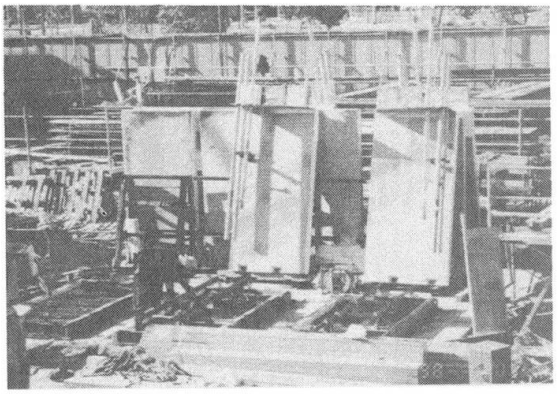

Fig. 9 Site yard for production of precast concrete panel parts

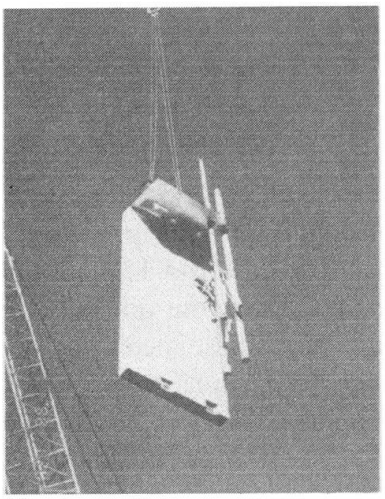

Fig.10 Lifting of precast concrete panel parts

Fig.11 Installation of precast concrete panel parts

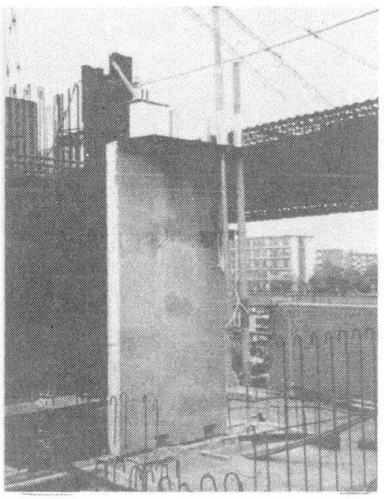

Fig.12 Installed precast concrete panel parts

4. Conclusion

The authors propose the Parts Oriented Production System as a mechanism to solve the problems faced by the construction industry in Japan, and have discussed the content of the three major subsystems which make up this system. By focusing on the attributes unique to each part and having the three subsystems cooperating simultaneously and in parallel, it is possible to achieve greater transparency and control than conventional construction production processes. Partial testing and application to construction sites is currently being carried out in order to verify the effectiveness of this system. In the future the authors hope to carry out further testing and application to construction sites for the rapid realization of this system as a whole.

Performance of Framed-Tube Structures under Vertical Forces

Bishwanath BOSE
Lecturer
Univ. of Abertay Dundee
Dundee, Scotland, UK

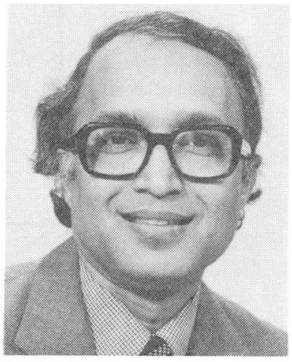

Bishwanath Bose, born 1939, received his civil engineering degree from Patna Univ., India in 1960 and PhD from the Univ. of Strathclyde, Scotland in 1976. He is currently a lecturer at the Univ. of Abertay Dundee, Scotland.

Summary

This paper reports the summary of a simplified analysis of framed-tube structures subjected to vertical forces.

1. Introduction

The framed-tube structure consists of a closely spaced exterior columns tied at each floor level by spandrel beams to produce a system of four orthogonal rigidly jointed frame panels forming a rectangular tube system (see fig 1(a)). The most significant framed-tube structure are the 110-storey twin towers for the World Trade Centre in New York, USA. The analysis of framed-tube structures supported on rigid and elastic bases and subjected to lateral wind load were considered in two papers[1,2]. By replacing the discrete structure by an equivalent orthotropic tube (see fig 1(b)), and making simplifying assumptions regarding the stress distribution in the substitute structure simple closed solutions were obtained. In addition to the lateral load, the framed-tube structure is subjected to vertical forces due to the dead load of the structure and the imposed load acting on the floor areas.

2. Method of analysis

Detailed analysis of a framed-tube structure of rectangular cross-section, subjected to vertical forces, is given in Reference 3. In this paper a framed-tube of square section, of side 2b, is considered (see fig 2). The vertical force caused due to the weight of the structure itself may be considered as a uniform force ρ_s per unit volume of the equivalent tube structure. The weight of the floor system and the imposed load acting on the floor areas are transferred equally to the four panels at every floor level, which for the panel AD may be expressed as

$$\rho = \rho_f \left[1 - \left(\frac{y}{b} \right)^2 \right] \qquad (1)$$

where ρ_f is a constant term independent of the height coordinate z.

The simplest approximation which may be made for the symmetrical distribution of vertical stress σ_z in the panel AD may be expressed as

$$\sigma_z = f_1 + \left(\frac{y}{b} \right)^2 f_2 \qquad (2)$$

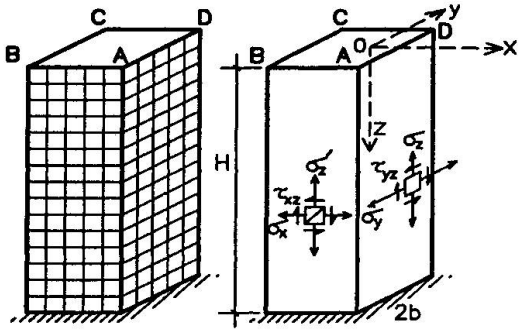

Fig 1 Framed tube (a) real and (b) substitute structure

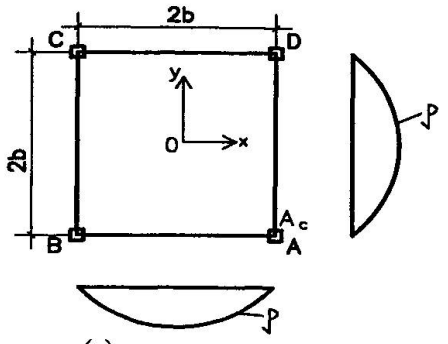

Fig 2 Vertical forces due to floor load

in which f_1 and f_2 are functions of the height coordinate z only.

By considering the condition of vertical force equilibrium at any level z the function f_1 is given as

$$f_1 = -\frac{W}{A} - \frac{3n+2}{3(n+2)} f_2 \qquad (3)$$

in which W is the total vertical force at that level, given by

$$W = 4tz\left[\frac{4}{3} b\rho_f + \left(2b + \frac{Ac}{t}\right)\rho_s\right] \qquad (4)$$

$n=A_c/bt$, A is the area of the equivalent tube section, given by $A=8bt+4\,A_c$, t is the thickness of the equivalent tube and A_c is the area of the corner column.

By applying the laws of equilibrium and the principle of least work the function f_2 is determined as

$$f_2 = \frac{\rho_f \sinh m_2 H\xi}{m_2 \cosh m_2 H} \qquad (5)$$

in which m_2 is constant and $\xi = z/H$.

The distribution of vertical stress in each panel may be expressed as

$$\sigma_z = -\frac{W}{A} - \left[\frac{3n+2}{3(n+2)} - \left(\frac{y}{b}\right)^2\right] f_2 \qquad (6)$$

The normal stress σ_y ($=\sigma_x$) and shear stress τ_{yz} ($=\tau_{xz}$) may also be found. The results from the substitute continuum system must then be transferred into the real discrete structure to give shears, and thus moments, and axial forces in beams and columns.

References

1. Coull, A and Bose, B. Simplified analysis of frame-tube structures. Journal of the Structural Division, ASCE, November 1975, 2223-2240.
2. Bose, B. Analysis of framed-tube structures supported on elastic base. Proceedings of the 2nd International Conference on high-rise buildings, Nanjing, China, March 1992, 69-74.
3. Bose, B. Analysis of framed-tube structures for high-rise buildings. PhD thesis, University of Strathclyde, Glasgow, 1976.

Loss of Workability of Superplasticized Concrete in High Rise Construction

K.B. PRAKASH
Assist. Prof.
T.K. Inst. of Eng. & Technology
Warananagar, India

K.T. KRISHNASWAMY
Head, Dept of Applied Mech.
Walchand College of Eng.
Sangli, India

Summary

In the construction of high rise buildings, sometimes it may so happen that the superplasticized concrete which is mixed may have to wait for a longer time before entering the form, either due to some machinary/pump failure or due to some dispute. If this superplasticized concrete is kept for a longer time, it will loose its workability. To increase the workability, one more dosage of superplasticizer may have to be applied just before the pouring of this concrete into the forms. Thus the application of repeated dosages of superplasticizers become important in such circumstances. Thus the application of repeated dosages of superplasticizer is one of the solutions for counteracting the loss of workability. This paper presents the results of an experimental investigation carried out on the effect of repeated dosages of superplasticizers on the properties of concrete produced from 43 grade & 53 grade cements.

1. Experimental Work

The primary aim of this experimental programme was to study the effect of repeated dosges of superplasticizers on the properties of fresh and hardened concrete produced from 43 grade & 53 grade cements and hence to know how many repeated dosages of superplasticizers can be applied without sacrificing the strength & workability properties of concrete.

The tests were conducted on a mix of proportion 1:2:4 with a w/c ratio of 0.40. Two superplasticizers with their recommended dosages as follows were used in the experimentation.

Conplast 430 - 0.5 %
Zentrament Super BV - 0.5 %

2. Experimental Results

Table 1 - Shows the effect of repeated dosages of Conplast 430 & Zentrament Super BV on the properties of concrete produced from 43 grade & 53 grade cement.

Table - 1 Results of repeated dosage application.

Particulars of concrete	Dosages of superpla - sticizer	Slump (mm)		% flow		V.B. Degree (Sec)		Avg. Density (N/cum	Avg. Compressive Stg. (MPa)	Avg. Flexural Stg. (MPa)
		Before Dosage	After Dosage	Before Dosage	After Dosage	Before Dosage	After Dosage			
Concrete produced from 43 grade cement with Conplast 430	No Dosage (after 0 min)	-	20	-	1.5	-	80	26890	19.89	8.00
	1st Dosage(after 30 min)	14	80	1.3	4.2	98	45	27960	29.56	8.40
	2nd Dosage (after 60 min)	13	85	1.3	4.5	105	42	28070	32.00	8.80
	3rd Dosage (after 90 min)	10	90	1.0	5.0	112	40	28140	33.28	9.10
	4th Dosage (after 120 min)	8	80	0.0	4.5	130	50	27700	32.00	8.80
Concrete produced from 53 grade cement with Conplast 430	No Dosage (after 0 min)	-	20	-	2.0	-	80	27300	23.11	8.65
	1st Dosage(after 30 min)	17	80	1.5	4.8	96	55	29000	36.77	8.70
	2nd Dosage (after 60 min).	12	90	1.2	6.0	100	45	27620	39.34	9.00
	3rd Dosage (after 90 min)	12	95	1.2	7.0	114	40	28230	40.78	9.10
	4th Dosage (after 120 min)	10	85	0.0	6.0	130	50	27770	37.77	8.60
Concrete produced from 43 grade cement with Zentrament Super BV	No Dosage (after 0 min)	-	20	-	1.5	-	80	26890	19.89	8.00
	1st Dosage(after 30 min)	13	60	1.0	7.0	90	70	27630	24.56	8.20
	2nd Dosage (after 60 min)	13	90	1.2	8.0	95	60	27450	26.20	9.00
	3rd Dosage (after 90 min)	12	92	0.0	8.5	105	55	27510	30.34	9.60
	4th Dosage (after 120 min)	12	75	0.0	4.5	120	80	27180	26.78	8.40
Concrete produced from 53 grade cement with Zentrament Super BV	No Dosage (after 0 min)	-	20	-	2.0	-	80	27290	23.11	8.65
	1st Dosage(after 30 min)	15	90	1.5	7.0	90	65	27430	30.56	9.00
	2nd Dosage (after 60 min)	15	100	1.2	8.6	95	60	27700	32.00	9.50
	3rd Dosage (after 90 min)	12	110	1.0	8.7	110	55	27700	33.00	9.90
	4th Dosage (after 120 min)	10	100	0.0	6.5	120	75	26870	30.66	9.10

3. Conclusions

The following conclusions can be drawn -

a. The strengths (compressive & flexural) and workability as measured from slump, flow and vee bee degree on concrete produced from 43 grade & 53 grade cements both, using Conplast 430, show an increasing trend upto the application of third repeated dosage, each dose being applied at an interval of 30 minutes. After the third dosage there is no increase in strengths and workability.

b. The strengths (compressive & flexural) and workability as measured from slump, flow, and vee Bee degree on concrete produced from 43 grade & 53 grade cements both, using Zentrament Super BV, show an increasing trend upto the application of third repeated dosage, each dose being applied at an interval of 30 minutes. After the third dosage there is no increase in strengths & workability.

c. Loss of workability of superplasticized concrete can be controlled through the repeated dosage application. But at the same time, it should be remembered that more number of repeated dosage application of superplasticizer will bring down both workability and strengths of concrete. Thus every superplasticizer has a definite number of repeated dosage application, after which it may produce ill effects in concrete. Therefore superplasticizers have to be used cautiously during their repeated applications. Otherwise they may induce undesirable properties to concrete.

Again, Shear Failure of RC Columns in 1995 Kobe Earthquake

Minoru YAMADA
Prof. Emeritus
Kobe Univ.
Osaka, Japan

Minoru Yamada, born 1930, received Dr Eng. from Kyoto Univ. 1959. Prof. Kobe Univ., 1964 - 1992. He received Meritorious Paper Award from AIJ for his finding of shear explosion of RC short columns and its verification at Tokachi-Oki EQ 1968. He founded Disaster Mitigation Council in Hyogo-Pref, 1978 and given warning and advised urgent retrofitting of RC buildings in Kobe.

Summary

Explosive cleavage shear failure of reinforced concrete short columns was found by the author in 1966 and reported at the 8. Congr. IABSE, New York, 1968 [1]. He had given his warning on the danger of collapse of buildings under earthquake and advised to retrofit existing buildings [2][3][4]. His warning were verified shortly after at the Tokachi-Oki EQ; Japan 16 May. In spite of his repeated warning to check and retrofit of old RC buildings and piers of high ways, designed before 1968, retrofittings were not carried out and at last many such old RC buildings with short columns were destroyed again at Kobe EQ. 1995 by shear explosion [5]. The author would like to give by this report his serious warning again on the urgent necessity of retrofitting of existing old RC buildings with short columns. This is the best way to mitigate the earthquake disasters.

1. Shear Explosion of RC Short Columns [1]

RC columns in rigid frames show three typical facture modes according to their shear span ratios *(H/D)*, i.e.shorter columns with smaller shear span ratio show shear explosion under predominant shear force *V*, medium length columns with medium shear span ratio show bending yield under predominant bending moment *M* and longer columns with longer shear span ratios show buckling under predominant axial load *N* such as shown in *Fig.1*, *Photo 1* and *2*. Critical value of shear span ratio $(H/D)_{cr}$ between shorter and medium length column i.e. shear explosion and bending yield is expressed as a function of axial load level ratio $X=N/N_y$ and reinforcing index $f_y p/f'_c$ [2][3][4] by :

$$\left(\frac{H}{D}\right)_{cr} = \frac{2[X+2(1+X)f_y p/f'_c](0.5-d_1)}{\frac{7}{8}(1-d_1)\sqrt{-0.10X^2+0.09X+0.01}}$$

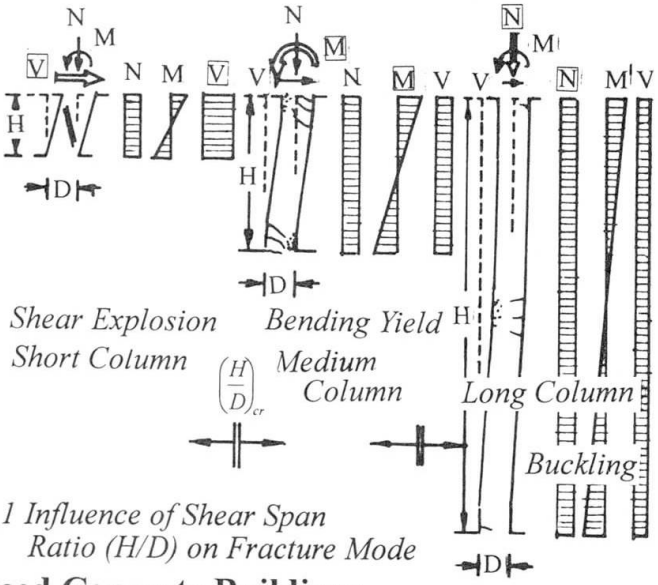

Fig.1 Influence of Shear Span Ratio (H/D) on Fracture Mode

2. Earthquake Damages of Reinforced Concrete Buildings

Explosive cleavage shear failure of reinforced concrete short columns were verified shortly after the warning of author [1] by the collapse of many RC buildings at the Tokachi-Oki EQ Japan, 16. May.1968 and reported at the 8.Congr., IABSE, New York, Sep. 1968 [1], and then at the Miyagiken-Oki EQ Japan, 12. Jun. 1978.

3. Urgent Necessity of Inspection and Retrofitting of RC Buildings

In spite of the warning of the author [2][3][4] on the existences of dangers of collapse by the explosive shear fracture of short columns in reinforced concrete, many buildings and piers of high ways were broken down again and again at the Loma Prieta EQ US. 17.Oct. 1987, the Northridge EQ US. 17. Jan. 1994 and at last the Kobe EQ Japan, 17. Jan. 1995. Such buildings and piers of high ways were designed and built according to the old stractural design codes and standards with no consideration of the shear explosion of short columns.

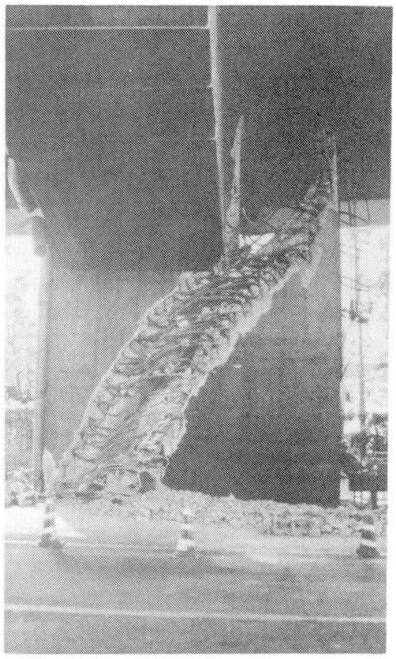

Photo 3 Highway Pier 1995 [5]

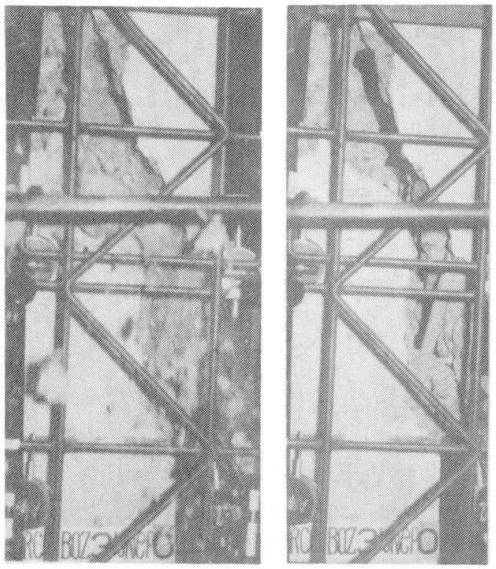

Photo 1 Shear Explosion [1]

4. Warning

There are yet very many old reinforced concrete buildings which were designed by old structural design codes and standerds without consideration of shear explosion and far lower assumed seismic load than really excited load. These old buildings and piers of highways must be inspected and retrofitted as soon as possible. This is the most urgent and necessary way to mitigate the seismic disasters. The author would like to give his serious warning again on the necessity of retrofitting of existing old RC building with short columns.

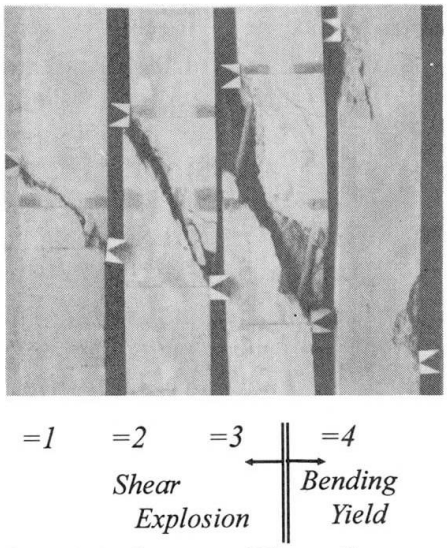

Photo 2 Influence of Shear Span Ratio(1968) [1]

References

[1] Yamada, M., Furui, S.,: Shear Resistance and Explosive Cleavage Failure of Reinforced Concrete Members Subjected to Axial Loads, Final Rep., 8. Congress IABSE, New York, 1968, pp.1091-1102.

[2] Yamada, M., : Ultimate Deformation of Reinforced Concrete, ASCE-IABSE-International Conf., Planning and Design of Tall Buildings, Lehigh, 1972, Vol.DS. pp.699-703.

[3] Yamada, M., Kawamura, H., : Simplified Calculation Method for Flexural and Shear Strength and Deformation of Reinforced Concrete Columns under Constant Axial Loads, IABSE-Symposium, Quebec, 1974, pp.153-160.

[4] Yamada, M., : Shear Strength, Deformation and Explosion of Reinforced Concrete Short Columns, ACI, SP-42, Vol.2, 1974, pp.617-638.

[5] Yamada, M., : Das Hanshin-Awaji-Erdbeben, Japan 1995, Bauing., Vol.71, 1996, Jan. pp.15-19, Feb.pp.73-80, Mar.pp.106-119.

Seismic and Wind Actions on the Asinelli Tower in Bologna

Giorgi CROCI
Prof.
Univ. La Sapienza
Rome, Italy

A. VISKOVIC
Structural Eng.
Univ. La Sapienza
Rome, Italy

A. ORSINI
Structural Eng.
Univ. La Sapienza
Rome, Italy

Summary

The Asinelli Tower, built in 1081 in Bologna, considered an outstanding monument for its slenderness and height, shows a significant out of plumb in western direction. Its great historical importance and bold masonry structure are a source of worry for its stability in presence of most frequent ambient disturbances like wind or seismic events. The seismic actions and the longitudinal and transversal (the vortex shedding phenomenon) effects of the wind have been analysed using a finite three-dimensional elements model.

1. Historical notes and structural peculiarities

To understand the structural behaviour of Asinelli Tower, it's important to revue its history that is full of events like earthquakes, fires, lightning and wind gusts; this events caused a number of serious but not irreparable damages. The Tower was built in 1081 (date fixed through the thermoluminescent method) up to 60m of height; its was built mainly for defence and prestige just in the time of the contrasts between Papacy and the Sacred Roman Empire. In 1200 the Municipality increased the height of other 40m up to 97.2m of height. In 1398, after an earthquake and a following fire, consolidation and restoration works were realised. Some horizontal solid diaphragms and structural reinforcements, consisting in a masonry vault at the middle floor, in a rib-groined vault at the top floor and in a more solid basement, were added afterwards. The base portico with ornamental function and a restraining of the Tower's lower part through two horizontal circumferencial chains, were built about in 1480. The number of horizontal chains was increased by other nine, placed at several heights, in 1913. The structure presents a hollow square section that has a side dimension included between 8.7 and 6m. The vertical walls are made of sack masonry that has an external-facing wall in «selenite» masonry up to 3 m of height and in brick masonry up to 60m; the upper parts are made by full brick masonry. One of its peculiarities consists in a significant out of plumb (2.25 m in western direction) due to constructional defects. Surveys of the damage has shown a considerable fragility of the corners and some cracks in the East and the West sides up to 35m of height.

2. The mathematical models and the results of the studies

The structural behaviour has been analysed using a finite three-dimensional elements model (fig. 1 and 2a,b), taking into account wind and seismic actions according to the Italian Code and the EC1. First of all, the dead load analysis (fig. 2c), which shows as the out of plumb effect produces an unbalancing of compression tensions (until 1.7 N/mm^2), has been carried out.

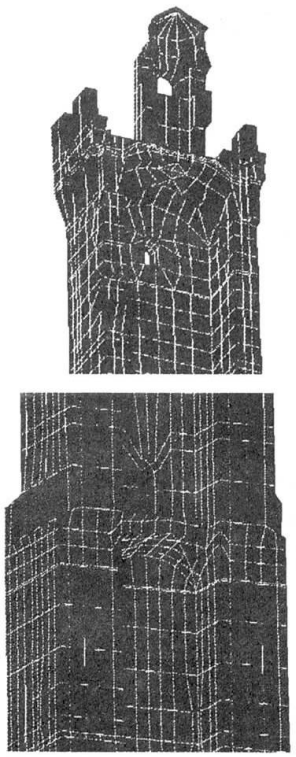

Figure 1

The dynamic behaviour of the structure has been defined through a modal analysis (T_1=3.68s), and then two kind of dynamic analyses have been carried out: a response spectrum analysis as regard the earthquake and time-history analyses concerning the longitudinal turbulent wind. Seismic actions have also been considered in the diagonal (S-W) and normal (W) direction, through linear and non-linear static equivalent analyses based on a 3D masonry failure domain (fig.2d). The results show that earthquakes only a little stronger than those expected by the Codes may seriously damage the tower and cause the collapse when the horizontal ground acceleration reaches 0.07g. Similarly it has been analysed the longitudinal and transversal effects of the wind, the last due to the vortex-shedding phenomenon. As regard the longitudinal turbulent wind (fig. 2e), the effects are much less dangerous than earthquakes and the structure remains substantially in the elastic field, preserving sufficient safety margins. On the contrary the vortex shedding phenomenon (fig. 2f), evaluated according to the EC1, seems to produce serious effects comparable with those of the expected earthquakes. Nevertheless the Code seems too much severe and not well defined in case of square section masonry towers; thus the vortex-shedding phenomenon probably doesn't generate an actual risk of collapse.

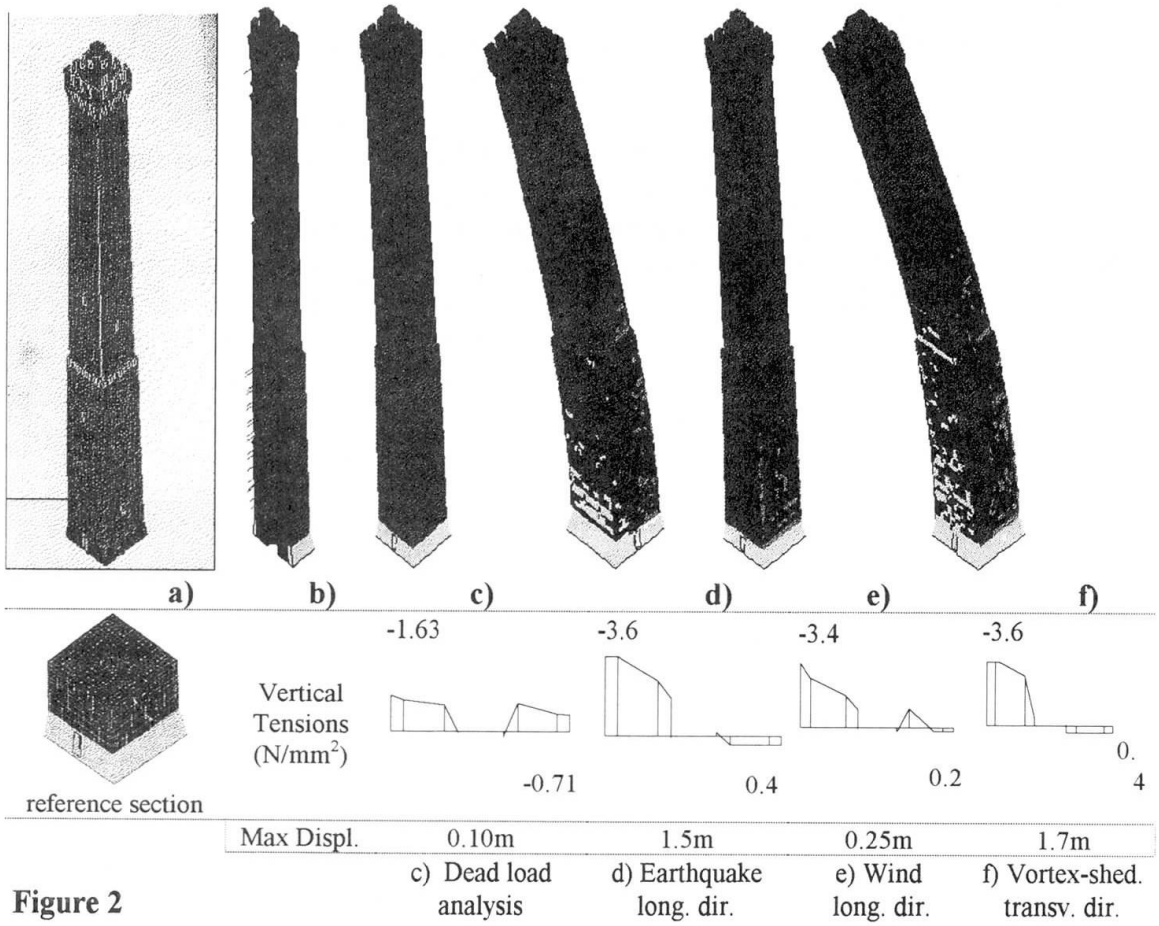

Figure 2

Seismic Upgrade by Base Isolation System and Visco-Elastic Damper

Hiroshi OHTA
Senior Eng.
Konoike Constr. Co. Ltd
Osaka, Japan

Kenichi KATAGIHARA
Dir.
Konoike Constr. Co. Ltd
Osaka, Japan

Taichi TANABE
Struct. Eng.
Konoike Constr. Co. Ltd
Osaka, Japan

Tetsuro ONO
Dir.
Konoike Constr. Co. Ltd
Tokyo, Japan

Mitsuo NAKAYAMA
Dir.
Konoike Constr. Co. Ltd
Tokyo, Japan

Summary

After the Hyogo-ken Nanbu earthquake on 17 January,1995, many existing buildings have been strengthened in Japan for surviving during severe earthquake in the future. In this paper, we introduce two buildings that employed innovative strengthening techniques.
One is the new reinforced concrete building that replaced the existing building suffered serious damage during the Hyogo-ken Nanbu earthquake. We employed a base isolation system in this building for adding high seismic capacity.The other is the historical wooden building in Kyoto that was constructed in the 18th century. We employed visco-elastic dampers in this building.
We used each technique to control and dissipate input energy from ground motion. Both techniques are useful for new and old buildings. We wish structural engineers and researchers further study and widely utilize new structural systems like energy dissipation system and base isolation system.

1. Seismic Upgrade by Base Isolation System

A condominium located in Takarazuka city was steel structure, which suffered severe damage during 1995 Hyogo-ken Nanbu earthquake. For seismic repair of this building , we have studied several methods, as adding new braces or welding steel plates. But it is evident that we can't obtain good habitability and seismic safety by these methods. So we decided to reconstruct this building of reinforced concrete structure with using base isolation system, so that the building doesn't change the original plan and feature(photo 1).
In this project, we have used the laminated natural rubber as isolator under high compressive axial stress over $10N/mm^2$ for lengthening natural vibration period, and two different types of damper, namely steel bar damper and lead damper(photo 2). The natural vibration period without damper is about 3.0 second. We could reduce the response of first floor shear coefficient from about 0.3 to 0.14 and maximum story drift angle from more than 1/100 to 1/800 in case of 40cm/s maximum ground motion.

2. Seismic Upgrade by Visco-elastic Damper System

The historical wooden building, which was constructed about 250 years ago, is strengthened using visco-elastic dampers(VED). This is one of the buildings in Zen-shu temple "Tenryu-ji" located in Kyoto. Photo 3 shows the appearance of the building. Because this is historical building, we couldn't be allowed to change the appearance. Under this condition, conventional technique couldn't add enough performance to this building, so we put inside the building the steel frame with visco-

elastic dampers in knee-bracing type as shown in photo4. By installing visco-elastic dampers in steel frame(figure 1), we could reduce response story drift angle to smaller than 1/80 and displacement to about 70 percents of displacement without damper in case of 50cm/s maximum ground motion(figure 2).

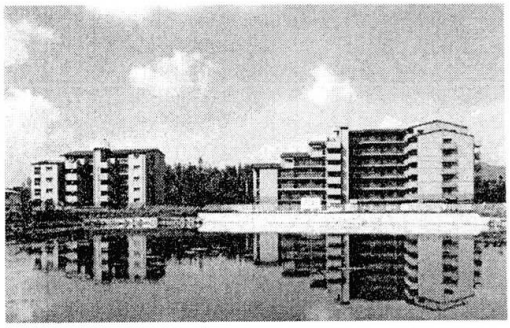

Photo 1. Reconstructed condominium located in Takarazuka city

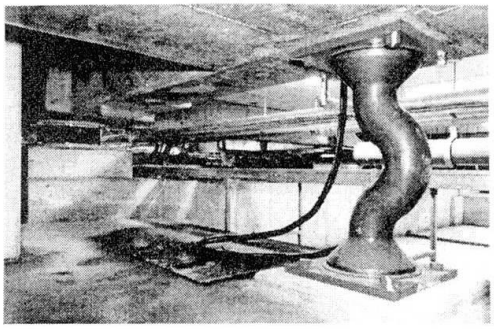

Photo 2. Base Isolation System

Photo 3. Hatto of Tenryuji-temple in Kyoto

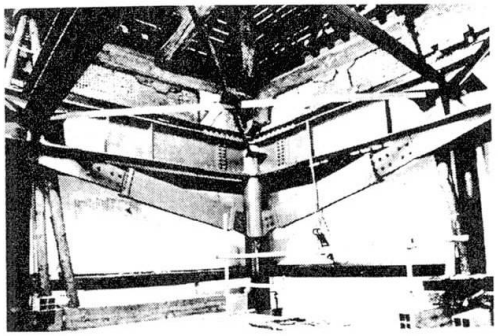

Photo 4. Installed VED in Knee-bracing Type

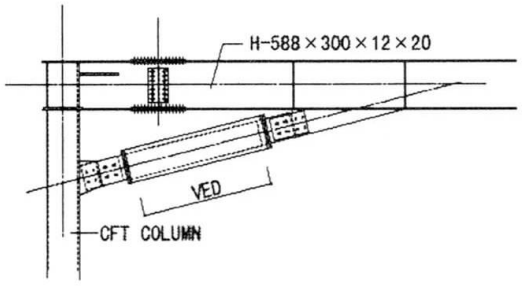

Figure 1. Detail Drawing of VED

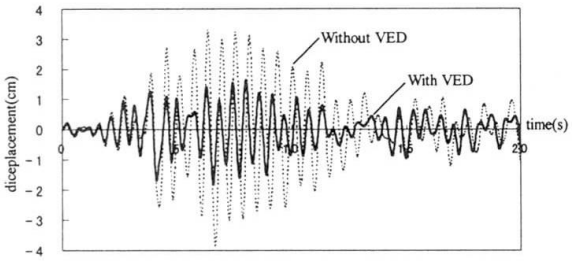

Figure 2. Time-history Diagram of Earthquake Response Analysis

References

[1] K.Katagihara et al,Seismic Strengthening with Visco-Elastic Dampers for Historic Wooden Architecrure,Summaries of Technical Papers of Annual Meeting,AIJ,Sept.,1997,in japanese.
[2] S.Soda et al,Study of Visco-Elastic Damper(part1),Summaries of Technical Papers of Annual Meeting,AIJ,Sept.,1996,in Japanese.
[3] S.Soda and Y.Takahashi,Application of Visco-Elastic Damper to Seismic Strengthening of RC Buildings,Proceedings of the Japan Concrete Institute,Vol.18,No.2,pp.191-196,in japanese.
[4] H.Yamanouchi and S.Soda and K.Katagihara,Seismic Strengthening with Visco-Elastic Dampers, Proceedings of Structual Engineers World Congress,July ,1998,San Francisco.

Anti-Seismic Behavior of a Multi-Tower Building Model

Xiang-Yu Gao
South China Constr. Univ.
Guangzhou, China

Fu-Lin ZHOU
South China Constr. Univ.
Guangzhou, China

Wen-Xiu CHEN
Huayi Arch. Design Inst.
Shenzhen, China

Summary

This paper introduced a shaking table test research on anti-seismic behavior of a multi-tower building model. The prototype is Futian Commercial Building that use the new technique of RC transfer plate and steel tube columns. The details of the columns are specially designed and the load bearing capacity of columns-beams joint models was proved by series static tests. The anti-seismic behavior (such as dynamic characteristics, cracking procedure, etc.)of the global tructure is studied here through the test results. Some suggestions for structural design are raised.

Introduction

Futian building group on a rigid foundation has four commercial buildings (39 floors, 100m high) and one official building (39 floors, 139m high). Because a commercial market occupies its first 6 floors, the structural system is changed by means of a reinforced concrete transfer plate(at 7th floor). Frame and RC tube are used under the plate, above which, are the four independent shear wall structures. The official tower (frame-tube structure) does not connect with the plate. Fig.1 is the plane layout of 2nd floor. For increasing the market area, steel tube concrete columns are used. A specially designed beam-column details was put forward for simplifying construction. Static tests(Fig.2) conducted in EERTC indicated that the details were reliable. Considering both of the special columns and the complicated building, structural analysis is very difficult. Therefore, a shaking table test of micro concrete model is necessary for the design and analysis. Some aspects of the anti-seismic behavior are presented later according to the tested results.

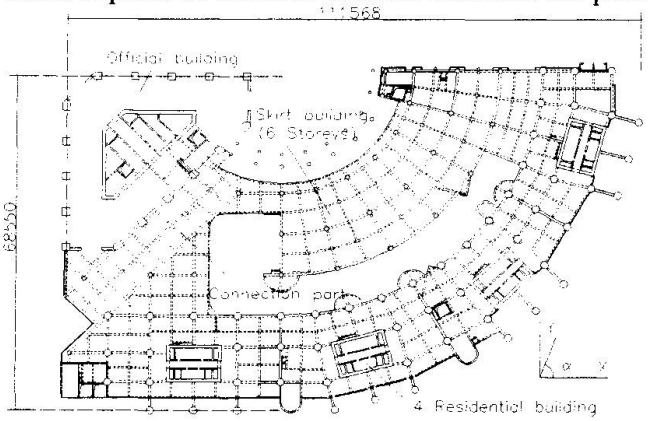

Fig.1: 2nd floor of Futian Building

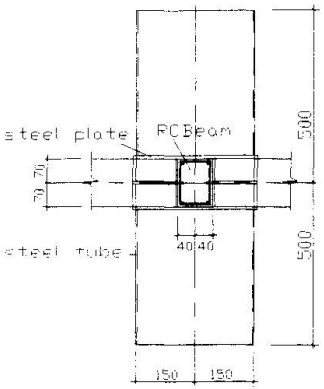

Fig.2: Beam-Column Joint Model

Design of the Model

Considering the table condition and the test requirements, the simulation coefficients are listed in table 1. Fig.3 is the testing model. Different angles are required to input earthquakes. Tree waves, thirteen different input angels and tree grades of intensity (plus white noise and biaxial tests) of total 32 tests are included.

Table1 Simulation of Futian Building

Item	*Parameter*	*Scale*	*Note*
length	C_l	38	thickness adjusted as E_c
elastic model	C_e	3.06	
strain	C_ε	1.00	
density	C_ρ	0.46	table bearing condition
acceleration	C_a	0.18	inertia force equivalence
gravity	C_g	1.00	
time	C_t	14.65	
mass	C_m	24967	

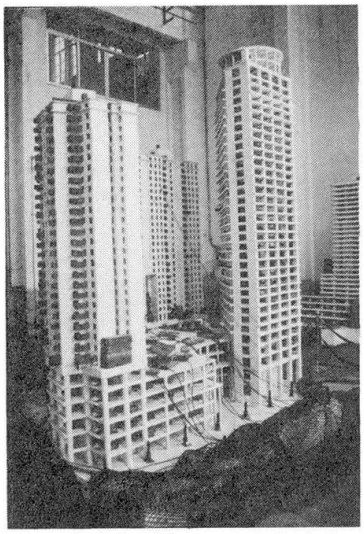

Fig.3: The Testing Model

Anti-Seismic Behavior

Table2 shows the comparison between the calculated and tested frequency. Fig.4 gives the analytic model and vibration modes. Fig.5 is the tested result. It is clear that the analytic mode is a kind of "plane vibration", while the tested one is "space vibration". All the earthquake tests (inputted from different angle) proved that the entire torsional movement was the dominant mode. Comparing the responses of different input angles, α=45° and 135° were the worst. The connection part cracked at moderate intensity. Steel tube columns and the transfer plate were reliable during the different tests.

Table 2 Comparison of frequencies (model)

Items	*Calculated*		*Tested*	
	X direc.fre.	Y direc.fre.	Frequency	Note
1st mode	4.48	4.31	6.72	entire torsion
2nd mode	7.51	7.07	8.72	move slantwise

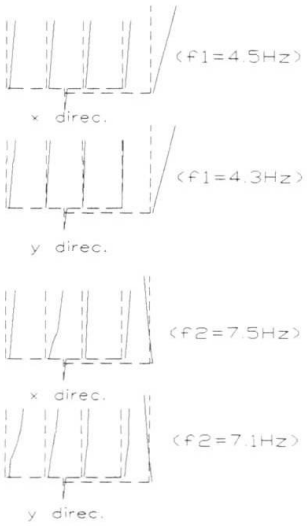

Fig.4: Analytic model and modes

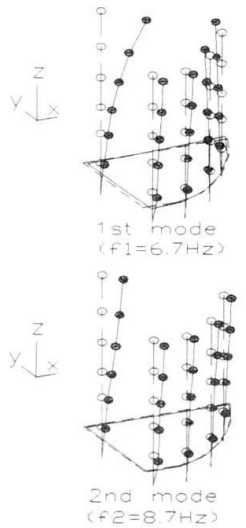

Fig.5:Tested modes

Conclusion and Suggestions

The details of steel tube concrete columns and the RC transfer plate are reliable. The dominant vibration mode is the torsional mode because of the structural layout. The response of Elcentro (ns+ew) wave is the most severe than other waves. The difference between the tested and the analytic result comes mainly from the analytical model that needs to be improved. Cracks appeared at the connection part of the official tower and the 4 residential buildings, which was the weakest part and need to be strengthened or totally separated.

Reference

[1]G.M.Sabnis,H.G.Harris,R.N.White,M.S.Mirza,Structural Modeling and Experimental Techniques, Prentice-Hall, 1983.

[2] Structural Design and Construction Standard for High-rise Buildings in Reinforced Concrete, JGJ 3-91, 1991, China.

[3]. Design Code for Earthquake Resistant Building, GBJ11-89, April,1990, China.

Ductility Design of Earthquake Resistant High-Rise RC Building

Kai MEN
Prof.
Qingdao Inst. of Arch. Eng.
Qingdao, China

Kai Men, born 1931, received his civil engineering degree from W-N-Indru. Inst. in 1955 and professor Qingdao Inst. of Arch. Eng.

Maode QIU
Senior Eng.
Huiyang Building Design Inst.
Huiyang, China

Maode Qiu, born 1944 received his civil engineering degree from S-C. Univ. of Tech in 1968 and president, general Engineer of Huiyang Building Design Inst.

Summary

In the Large city that high-rise building are concentrated in China , the seismic intensety is height , the wind load is larger , the engneering geology is led , and building plan and elevation size and form is complex , high -width ratio larger , structural period long , some building is more towery , these privet more new and more high demand for resistance earthquake design .Regulated in national standard 《 The Resistance Earthquake Design Code of Building 》 in China , standard for Resistance earthquake hagard protection is "not damaged in minor seismic , repairable in mdium seismic and no collapes in major seismic". How to ensure these demand ? code main adopt approximated and Practical method that regulated internal force of memler section.Based on summing-up the research results of resistance earthquake ductility design of high-rise RC building sturcture , this paper discusses ductility demand of resistance earthguake of high-rise RC building structure and regulated principle and method of interal force of memher section .

1.Ductility demand for resistance earthquake of high-rise RC building sturcture

Resistance earthquake design of high-rise RC building sturcture should ensure whole property resistance earthquake of sturcture,take in learing capaity ,rigity and ductility of sturcture each other coordinate, so that the focal point of resistance earthquake design of high-rise RC building sturcture is ductility design. Ductility demand of resistance earthquake of high-rise RC building structure is :

- Strong column and soft beam of RC frame
- Shear-pressure ratio in column of RC frame
- Moment regulate in beam end of RC frame
- Shear-pressure ratio in point of RC frame
- Shear-pressure ratio in beam of RC frame
- Axial pressure ratio in column of RC frame
- Stromg shear and soft curve in column of RC frame
- Strong connect and soft member of RC frame point
- Rigity discount of connecting beam of shear wall
- Shear-pressure ratio of shear wall
- Axial-pressure ratio of shear wall
- Shear pressure ratio of connecting beam of shear wall

- Strong shear and soft curve of connecting beam of shear wall
- Strong shear and soft curve of under strong area of shear wall
- Axial force incyease for frame suported column
- Moment increase for column base in base story of coumm

2. Prin ciple and method of regulation interal force of memler section

For example strong column and soft beam of RC frame sturcture should be had follow requirement:

$$\Sigma M_{ca} \geq \eta_R \Sigma M_{ba} \qquad (1)$$

Code comprehensive considered resistance earthquake safety,economic and design work possibility of sturcture ,based on theory ,test study and engneering design and economic etc condition ,considered learing capacity resistance earthquake uegulate coefficient ,difference not alike resistance earthquake degree of RC sturcture ,adopt comprehensive method,for class 3 or class 4 of sturcture, not regulated interal force of memler section,only adopt sturctural measure to ensure ductilityof structure,for class 1 or class 2 of sturcture,adopt in rugulated interal force of member section ,code used method :

$$\Sigma Mc = 1.1\Sigma M_{bua} \qquad (2)$$

$$\Sigma Mc = 1.1\lambda j \Sigma M_b \qquad (3)$$

$$\Sigma Mc = \eta_M \Sigma M_b \qquad (4)$$

In equation,λj — Practial setting coefficient for class 2 of RC frame λj=1.0,for class 1 of RC frame ,may be adopt 1.1 time of ratio of practical tension reinforcement total area and area of calculating reinforcement Increace coefficient of moment of column end η_M=1.1λj or adopt 1.35 ~ 1.5 interal with huilding hight.

For example resistance earthquake class 1 of RC framce,λj calculate following:

$$\lambda j1 = 1.1\frac{1964+1520}{1632.2+1411.7} = 1.26(clockwise)$$

$$\lambda j2 = 1.1\frac{1964+1520}{1691.9+891.4} = 1.48(clockcounter)$$

Point of RC frame and section of beam and column see Fig.1.

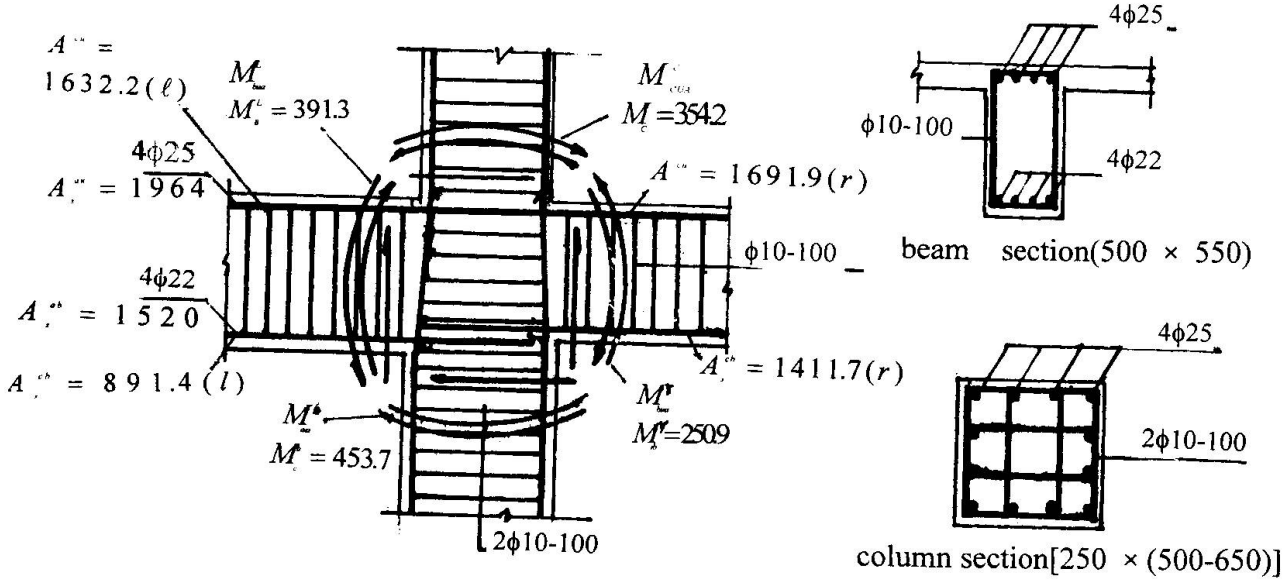

Fig1. Point of RC frame

Analysis and Design of a High-Rise Reinforced Concrete Structure

Milivoje STANKOVIC
Prof.
Civil Engineering Faculty
Nis, Yugoslavia

Milic MILICEVIC
Prof.
Civil Engineering Faculty
Nis, Yugoslavia

Marina MIJALKOVIC
Assistant
Civil Engineering Faculty
Nis, Yugoslavia

Summary

The structure of a tall building, which is aimed to be a hotel with restaurant and casino, is considered in this paper. This structure is under construction in Moscow and is going to be high 106m, with 34 stories. The floor plan of higher part of the structure is in the shape of rectangle of size 36.00m x 17.40m. The analysis of the structure as a spatial one, by use of the first order theory in accordance with Russian code, as well as the analysis of representative frames in two orthogonal directions is carried out. The mathematical model consists of 918 joints and 2298 members. A new software package for static analysis, as well as dynamic analysis, based on the response spectrum analysis of the earthquake engineering, with comprises interaction of the structure and soil, is developed.

1. Structure concept

Hotel "Centrosojuz" is going to be high-rise building with restaurant and casino. It is under construction in Moscow and is going to be high 106m. The floor plan of higher part of the structure is in the shape of rectangle of size 36m x 17.40m. Structure of this building is designed as reinforced concrete structure, composed of concrete and high-quality steel. The caring system is spatial, mixed one, and it consists of columns, beams and plates. The structure is design according to IMS (Serbian Institute for Materials) precast prefabricated reinforced concrete system, which is widely applied all over the world (Yugoslavia, Hungary, Russia, Cuba, India, i.e.). IMS system is proved for 30 stories. As this hotel is planed with 34 stories, designer has predicted nine stories as monolithic, reinforced concrete, casted at the site (two of them are cellar under ground), while the other 25 are precast prefabricated. In the case of tall buildings torsion imperfection increases with increasing of the number of stories. It is necessary to pay attention on this effect in designing, as in the case of structure that is object of this paper.

The transmission of vertical load is performed by two-way slabs on longitudinal and transversal beams of the frames and finally on vertical caring elements of structure.

Reinforced concrete wall-plates in transversal direction at the ends of structure, as well as reinforced concrete core in the zone of elevator are to accept wind forces. Those elements and columns carry vertical load as well.

2. Analysis of loading

Loading is analyzed in accordance with Russian code SNiP (Stroiteljne Norme i Pravila), which consider separately weight of the structure itself and long-term vertical useful movable load (about 30% of the whole load) and whole useful load. Horizontal wind load contains of two components: static and dynamic action

3. Static and dynamic design

A new software package, similar to STRESS, is developed by use of Finite element method for purpose of static and dynamic design, which comprises the interaction of the structure and soil. The static analysis of the structure as a spatial one, by use of the first order theory in accordance with Russian code, as well as the analyses of the representative frames in two orthogonal directions, is carried out. The mathematical model consists of 918 joints and 2298 members.

Interaction between foundation structure and soil is taken into account by assuming that slab foundation is boundless rigid and placed in an elastic soil. Data about soil properties are taken from available geomechanics report.

The adopted simplified dynamically model is cantilever beam with masses in the level of the floors. Such model is chosen because static model with 918 joint and 2298 members is to complicated for dynamic analysis.

Reinforced concrete foundation plate is design by means of Finite element method as plate on elastic foundation using nodal points as boundary elements.

All calculations are carried out for five types of loading and appropriate superposition:

1. weight of structure itself;
2. vertical long-term useful load;
3. whole vertical load;
4. wind load in longitudinal direction;
5. wind load in transversal direction.

4. Proportioning

Three programs in FORTRAN are developed for the porpoise of proportioning of the structure elements, as are floor plates and foundation plate, beams and columns of frames.

According to mentioned Russian code for concrete and reinforced concrete the two phases are required:
- I - design of caring capacity and stability of structure;
- II - design for serviceability phase.

5. Conclusion

Design concept that is presented in this paper is proved by numerical results. Our experiences point out that IMS system is rational, economical and constructively safe enough for high-rise structures. In the case of tall buildings torsion imperfection increases with increasing of the number of the stories and that why it is necessary to pay attention on this effect in designing as it is in case of the structure which is object of this paper. Such structures can be recommended for application because they are very economical, not expensive and fast for construction.

Working Session

Innovative Design against Vibration of Tall Buildings

Papers

Leere Seite
Blank page
Page vide

Deformation Behaviour of Base-Isolated Buildings in Near-Fault Earthquake

Masayoshi NAKASHIMA
Assoc. Prof.
Kyoto Univ.
Kyoto, Japan

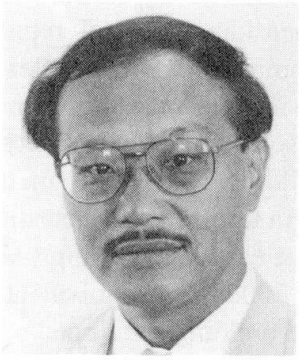

Masayoshi Nakaashima received his B.S. and M.S. from Kyoto Univ., Japan and Pd.D. from Lehigh Univ., USA. He has been involved with analysis and seismic design of steel buildings structures and development of experimental techniques for earthquake response simulation.

Summary

Response behavior of base-isolated buildings subjected to near-fault earthquakes was examined. Recorded, synthesized, and simplified ground motions were used in the analysis. It was found that (1) a large ground motion component appearing at a particular time tends to control the maximum deformation and (2) dynamic amplification and increase in ductility demand is most significant when the natural period of buildings under smaller vibration is 0.4 to 0.8 times the period of a large ground motion component.

1. Introduction

The 1995 Hyogoken-Nanbu (Kobe) Earthquake revealed much damage to modern building structures [1]. Although many of those damaged escaped from collapse, their functionality was severely impaired, resulting in significant loss in capital. Since that experience, importance on the control of functionality (in addition to collapse prevention) has been emphasized greatly. One solution toward this end is considered as "base-isolation." Japan has a history of construction of base-isolated buildings for nearly fifteen years [2], but the construction was limited, remaining about a dozen new base-isolated buildings annually. After the Kobe Earthquake, the construction has grown significantly, and more than 150 new base-isolated buildings were built for a single year of 1997 [3]. On the other hand, ground motion specialists address the possibility of a very large pulse-like ground motion in near-fault regions, particularly in the direction perpendicular to the fault [4,5] and warn that such large ground motion can induce very large deformations to structures with long natural periods such as base-isolated buildings. On one hand, construction of base-isolated buildings has grown with the belief that they are effective in damage control against large earthquakes; on the other hand, base-isolation may be useless for near-fault earthquakes; this rather conflicting argument has to be resolved. To provide some information on this issue, numerical response analysis was carried out for base-isolated buildings represented as SDOF systems, with the type of ground motion, type of hysteretic behavior, and natural period as major variables, and their effects on the response were examined. To understand the basic behavior of base-isolated buildings subjected to near-fault earthquakes, the ground motion was simplified as a one-cycle sinusoidal ground motion (acceleration), and the response of SDOF systems subjected to the motion was investigated in terms of the dynamic amplification of maximum deformations.

2. Numerical Analysis

In base-isolated buildings, it is a common practice to make the base-isolation devices much more flexible (in the horizontal direction) than the super-structure, and the super-structure would not go beyond its elastic limit. Therefore, an SDOF representation (Fig.1) is reasonable, with the super-structure assumed to be completely rigid and flexibility provided only by the base-isolation devices. Thirty eight base-isolated buildings previously designed were surveyed for the hysteretic behavior of their base-isolation devices. (Necessary information was obtained from the data presented in [3].) In all buildings, the maximum deformation under ambient and small vibrations was limited to 5 to 10% in terms of the shear strain (γ) of the rubber bearings, and the maximum deformation under large earthquakes (approximately 0.5 m/s in the maximum ground velocity) was limited to γ= 150 - 200%. The equivalent natural period (estimated based upon the secant stiffness) of base-isolated buildings equipped with rubber bearings with lead dampers (14 buildings surveyed) ranged from 1.2 to 1.8 sec for a deformation corresponding to γ = 15 - 20%, and the tangential stiffness under large deformations (corresponding to γ = 100 - 300%) was about 10 to 15 % of the secant stiffness at γ = 15 - 20%. The equivalent natural period of base-isolated buildings equipped with high damping rubber bearings (14 buildings surveyed) ranged from 1.1 to 1.7 sec for a deformation corresponding to γ = 20 %, and the tangential stiffness under large deformations was about 20 - 25 % of the secant stiffness at γ = 20%. The equivalent natural period of base-isolated buildings equipped with a combination of natural rubber bearings and lead and steel dampers (10 buildings surveyed) ranged from 1.7 to 1.9 sec for a deformation corresponding to γ = 10 % (at which steel dampers were expected to yield), and the tangential stiffness for large deformations was about 15 - 20% of the secant stiffness at γ = 10%. From these observations, the hysteresis of base isolation devices can reasonably be approximated to be bilinear (Fig.1), with the first stiffness corresponding to the equivalent natural period of 1.0 - 2.0 sec and the second stiffness equal to 10 - 25 % of the first stiffness. Considering these values, bilinear SDOF systems having the elastic natural period

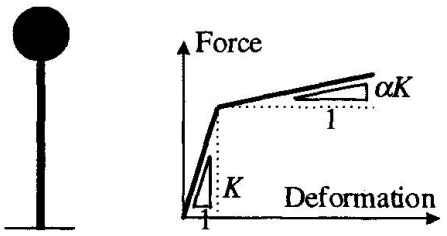

Fig.1 SDOF and bilinear representation of base-isolated building

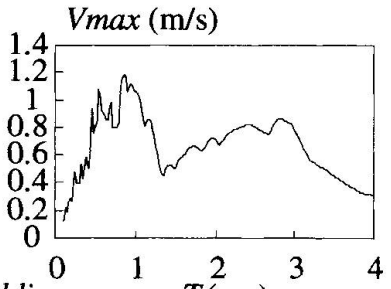

(a) El Centro (1940)

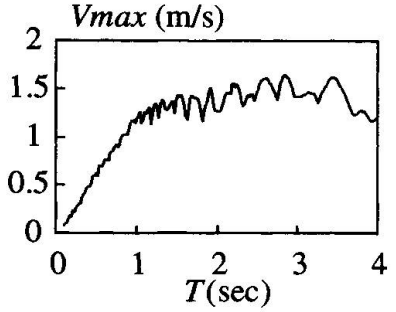

(b) Yokohama

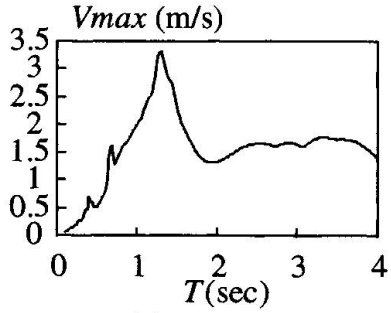

(c) NTT (1995)

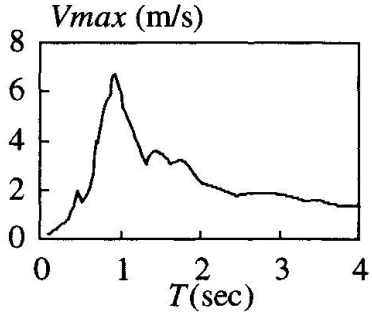

(d) Point-B

Fig.2 Elastic pseudo velocity spectra of ground motions analyzed

(T) of 1.0, 1.5 and 2.0 sec and the second stiffness that is 15 and 25 % of the initial stiffness were analyzed. The following four ground motions were selected: El Centro NS (1940), Yokohama (1995), NTT (1995), and Point-B(1996). El Centro record was selected as the basis of comparison because the record has been used extensively for earthquake response investigations. Yokohama (1995) is a synthesized motion having almost a constant pseudo ground velocity over a large range, developed for the simulation of ocean-ridge earthquakes. NTT (1995) is a ground motion recorded during the Kobe Earthquake, and Point-B is a synthesized motion that simulated the ground motion at downtown Kobe during the Kobe Earthquake [6] The last two motions were selected as representatives of near-fault ground motions. The elastic pseudo velocity (*Vmax*) spectra of these four motions are shown in Fig.2.

Figure 3 shows examples of input and dissipated energies in terms of the equivalent velocities (*VE* and *VP*), and Fig.4 shows the maximum deformations (*Dmax*), ratios of the maximum plastic deformation relative to the cumulative plastic deformation [$(\mu - 1)/\eta$], and the number of inelastic excursions (N). These figures are for the second stiffness equal to 25 % of the initial stiffness. In the figure, f indicates the yield force, defined as the yield force relative to the maximum force exerted if the system would respond only elastically under the same ground motion. The energy behavior is summarized as follows. In El Centro and Yokohama both input and dissipated energies are relatively constant regardless of the yield force and do not change significantly for the three natural periods (1.0, 1.5, and 2.0 sec). This supports the energy constant concept advocated in [7]. In NTT and Point-B the energy terms fluctuate with respect to the yield force and are different significantly for the three natural periods. According to Fig.4(a), the maximum deformation does not change so significantly with respect to the yield force in El Centro and Yokohama, supporting the maximum deformation constant rule [8], whereas the maximum deformation in NTT and Point-B change significantly with the yield force. Figure 4(b) shows that the ratio of maximum plastic deformation to cumulative plastic deformation is largest in NTT, followed by Point-B, El Centro, and Yokohama. The larger ratio means that the energies exerted and dissipated for one large response cycle is more significant relative to the total input and dissipated energies. This suggests that the response is more dominated by a large, single shock rather than accumulated by smaller but multiple shocks. This statement is supported by Fig.4(c), in which the number of inelastic excursions is significantly smaller in NTT and Point-B. It was also observed that in NTT and Point-B the maximum deformation was achieved around the same time regardless of the yield force and natural period, indicating that the maximum deformation was induced by a large ground motion component appearing at a particular time, whereas in El Centro and Yokohama the time at attainment of the maximum deformation varied from case to case. In summary, the response behavior for near-fault earthquakes (represented by NTT and Point-B) is characterized as follows. (1) The maximum deformation tends to be induced by a large ground motion

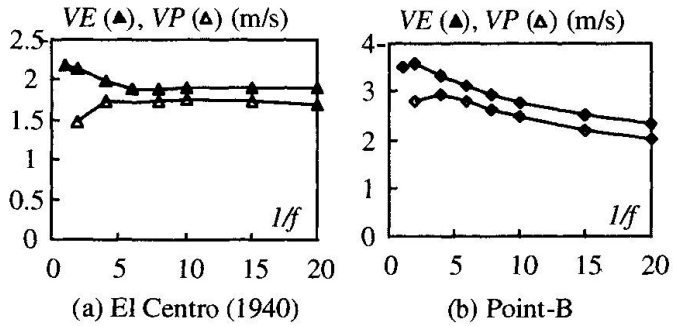

(a) El Centro (1940) (b) Point-B

Fig.3 Input and dissipated energies of SDOF bilinear systems (T=1.5 sec)

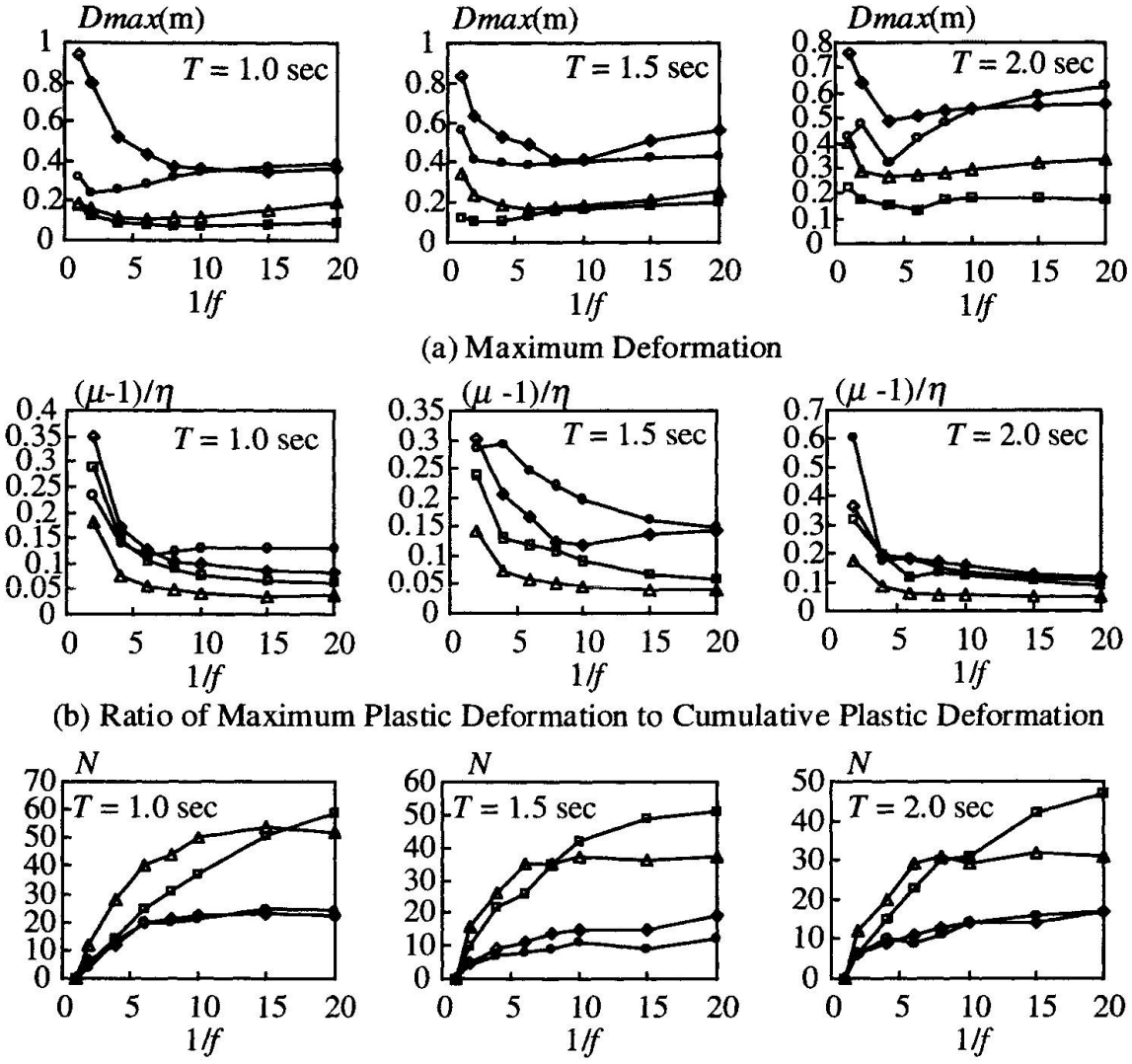

Fig.4 Response characteristics of bilinear SDOF systems

component appearing at a particular time, (2) the input and dissipated energies vary significantly with respect to the yield force and natural period, leading the energy constant concept less certain, and (3) the maximum deformation is dependent much on the yield force, making the constant maximum deformation rule less applicable.

3. Behavior of SDOF Systems Subjected to One-Cycle Sinusoidal Motion

In reference to the above discussion, it is interesting to examine how the system would behave under a large ground motion component. As a most simplified form of such motion, one cycle sinusoidal ground motion was considered (Fig.5), and the response of bilinear SDOF systems subjected to the motion was obtained.. Figure 6 shows the maximum deformation in terms of the ductility ratio (μ), defined as the maximum deformation relative to the elastic limit rotation, for various natural periods (T/Te) and the yield force (f). Here, Te is the period of the sinusoidal ground motion, and the yield force f is defined as the yield force relative to the maximum force exerted for the equivalent elastic system subjected to one-half cycle sinusoidal motion. Figure

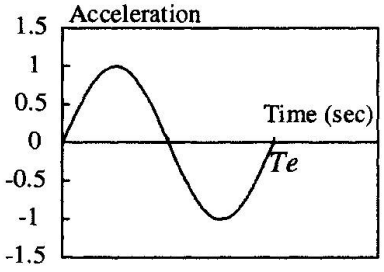

Fig.5 One-cycle sinusoidal ground motion analyzed

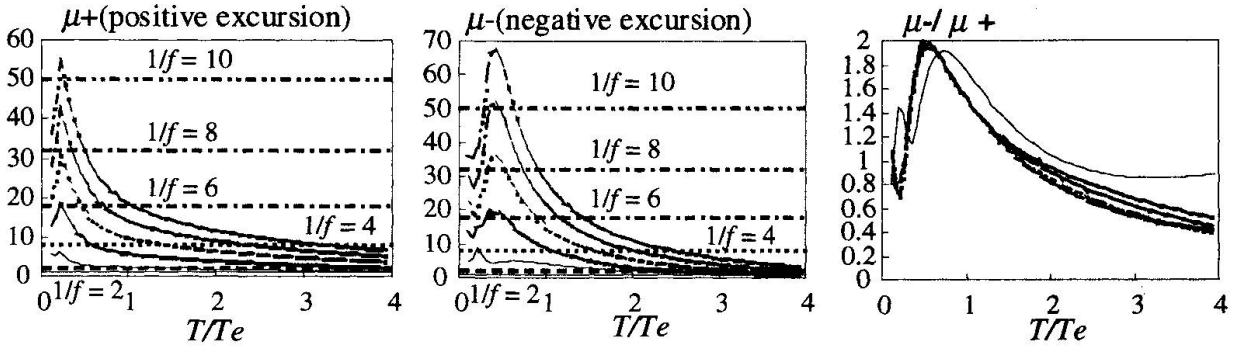

(a) ductility ratio for positive excursion

(b) ductility ratio for negative excursion

(c) Ratio of positive to negative ductility ratio

Fig.6 Response characteristics of bilinear SDOF systems subjected to one-cycle sinusoidal ground motion

6(a) is the maximum deformation obtained for the positive excursion, Fig.6(b) the maximum deformation for the negative excursion, and Fig. 6(c) is the ratio of the negative maximum to the positive maximum, indicating that the maximum deformation is achieved in the negative excursion for $T/Te \leq 2.0$. Most notable is that the ductility ratio is largest around $T/Te = 0.4$ and significantly reduces with the increase of T/Te. In reference to the definition of f, this figure provides an answer to the following question; i.e. if the yield force is reduced to f times the maximum force exerted in the elastic system, how much ductility should we consider? Figure 6 also shows the ductility ratios estimated based on the energy equivalent rule [8]. The obtained ductility ratios are much larger than those estimated for about $T/Te = 0.4$. Figure 7 shows another form of ductility ratio, this time the maximum deformation is normalized by the maximum deformation if the system receives the motion statically, thus enabling the direct comparison of maximum deformation. When $T/Te \leq 1.0$, the difference is significant with respect to the yield force, indicating that the maximum deformation rule is less reliable. These observations reveals that dynamic amplification and increase in ductility demand is very large for $T/Te = 0.4 - 0.8$. Earlier discussion demonstrated that the equivalent natural period of previously designed base-isolated buildings ranged from 1.0 to 2.0 sec for small deformations, which means that if a near-fault ground motion contains a large component having a period of 1.25 (= 1/0.8) sec or more, base-isolated buildings would sustain very large dynamic amplification.

A separate study is underway to derive approximate closed-form equations for estimating the ductility ratio (μ) of bilinear SDOF systems subjected to one cycle sinusoidal ground motion. The equations are applicable for $0.5 \leq T/Te \leq 2.0$, the range of most importance in terms of dynamic amplification and increase in ductility. In formulating the equations, the deformation shape was assumed to be sinusoidal, and the energy balance between the input and absorbed

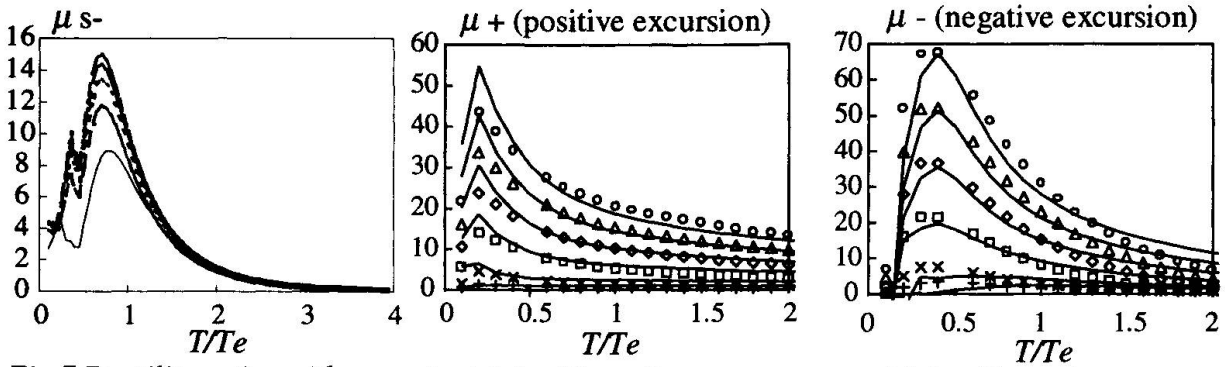

Fig.7 Ductility ratios with respect to static deformation

(a) ductility ratio for positive excursion

(b) ductility ratio for negative excursion

Fig.8 Comparison between estimated and analyzed ductility ratios

energies was considered [9]. Figure 8 shows comparison between the estimated and numerically ductility ratios, demonstrating reasonable agreement between the two.

4. Conclusion

Response behavior of base-isolated buildings subjected to near-fault earthquakes was examined. The behavior was found to be characterized such that: (1) a large ground motion component appearing at a particular time tends to control the maximum deformation and (2) energy constant concept, energy equivalent rule, and maximum deformation constant rule are less applicable. Response behavior when subjected to one-cycle sinusoidal ground motion was examined. Dynamic amplification and increase in ductility demand was found to be most significant when the equivalent natural period of buildings in small vibrations is 0.4 to 0.8 times the period of the motion.

References

[1] The Architectural Institute of Japan (AIJ) (1995). English Edition of Preliminary Reconnaissance Report of the 1995 Hyogoken-Nanbu Earthquake, 215pp.
[2] Menshin (1996). Japan Society of Seismic Isolation, No.16, pp.20-31.
[3] Building Letters (1996). The Building Center of Japan, No.348 to 359.
[4] Hall, J., et al. (1995). Near-source ground motion and its effects on flexible buildings, Earthquake Spectra, Vol.11, pp.569-605.
[5] Heaton, T. H., et al. (1995). Response of high-rise and base-isolated buildings to a hypothetical Mw 7.0 blind thrust earthquake, Science, Vol.267, pp.206-211
[6] Hayashi, Y. and Kawase. H. (1996). Strong motion evaluation in Chuo Ward, Kobe, during the Hyogoken-Nanbu Earthquake of 1995, Journal of Structural and Construction Engineering, the Architectural Institute of Japan, No.481, pp.37-46 (in Japanese).
[7] Akiyama, H. (1985). Earthquake-resistant Limit-State Design of Buildings, University of Tokyo Press, Tokyo.
[8] Newmark N. M. and Hall, W. J. (1975). Earthquake Spectra and Design, Earthquake Engineering Research Institute.
[9] Nakashima, M. (1998). Prediction of Maximum Deformation of Base-Isolated buildings subjected to pulse-like ground motions, Report to Grant-in-Aid for Scientific Research on Mitigation of Urban Disasters by Near-Field Earthquakes, Ministry of Education, Japan, 87pp.

Active Structural Seismic Control Including Ground Rigidity Effects

Jinmin ZAI
Prof.
Nanjing Arch. & Civil Eng. Inst.
Nanjing, China

Guoxing CHEN
Prof.
Nanjing Arch. & Civil Eng. Inst.
Nanjing, China

Dong YANG
PhD
Nanjing Arch. & Civil Eng. Inst.
Nanjing, China

Dajun DING
Prof.
Southeast Univ.
Nanjing, China

Summary

The characteristics of active structural control, namely active pulse control (APC) and active anchor rope control (AARC), on the six-storey frame structure considering soil-structure interaction (SSI) effects were examined. The results show that the effect of APC is better and the AARC may take no effect at all on soft ground due to the SSI effects. The APC force can be greatly reduced by 1/3 to 1/2 when the SSI effects are considered in comparison with the result of rigid-foundation assumption. The extent of control force reduced will be increased as the soil becomes softer. It seems unnecessary in some conditions to use active control facilities if the SSI effects are considered in the earthquake resistant design of building.

1. Introduction

The research carried out on structural seismic control so far was almost based on the assumption of rigid-foundations, but in reality, the interaction between superstructure and ground is always existent except for constructions directly built upon a well-integrated bedrock, which can be considered approximately as rigid-foundations. Therefore, it is worthy to investigate that whether or not the regular pattern of structural seismic control on rigid-foundations will reflect the real behavior of a building during earthquake. According to references [1][2], the rigidity of ground has an effect on passive seismic control that cannot be neglected and the optimum seismic design can take place only under considerations of the SSI effects as well as ground conditions. Hence, it may be inferred that the SSI effects also have a significant influence on the result of active seismic control. According to references [3][4], in order to achieve the goal of active seismic control there must be a modification in original control arithmetic when the SSI effects are to be considered. And changes needed for the control force are relevant to vibration characteristics of the soil-structure system. The research mentioned above is all based on such assumptions: the superstructure is a linear elastic system of single degree of freedom; the ground is elastic half-space and the input motion is simple harmonic waves. This paper will discuss the active seismic control of structure with emphasis on the effect made by using APC and AARC methods when the SSI effects are considered. The earthquake record is inputted under premise of inelastic structure and a real simulation of actual structural dynamic characteristics.

2. Computational model and method

In the research, the soil-building system is simplified to be two-dimensional, the ground soils are treated as viscoelastic medium which would be a plane strain subject and the lateral boundary of soil mass is treated as a simple boundary. The superstructure is simplified as a plane structure of bar system being composed of variable-section beam elements so that the rigidity difference on different sections of beams or columns caused by differential stress condition can be considered (the details of the rigidity matrix of varying rigidity beam element and the trilinear elasto-plastic constitutive model of reinforced concrete members can be found in references [2][5]

The research was based on the real six-storey frame structure and its sketch drawings of structural computation are shown in fig. 1. The foundation is regarded as a rigid block and the details of building design can be found in reference [2]. The softness and hardness of ground are represented by Vs of shear-wave velocity with which hard soil Vs = $160H^{0.30}$(m/s) and soft soil Vs = $120H^{0.30}$(m/s). Here H stands for the depth of soil layers. The depth of bottom boundary of the soil layer was taken as 40m and the damping ratio of the soil mass was taken as 5%. The soil dynamic nonlinear effects essentially soften soils thus the soil nonlinear behavior can be indirectly considered by changing soft-hard conditions of ground.

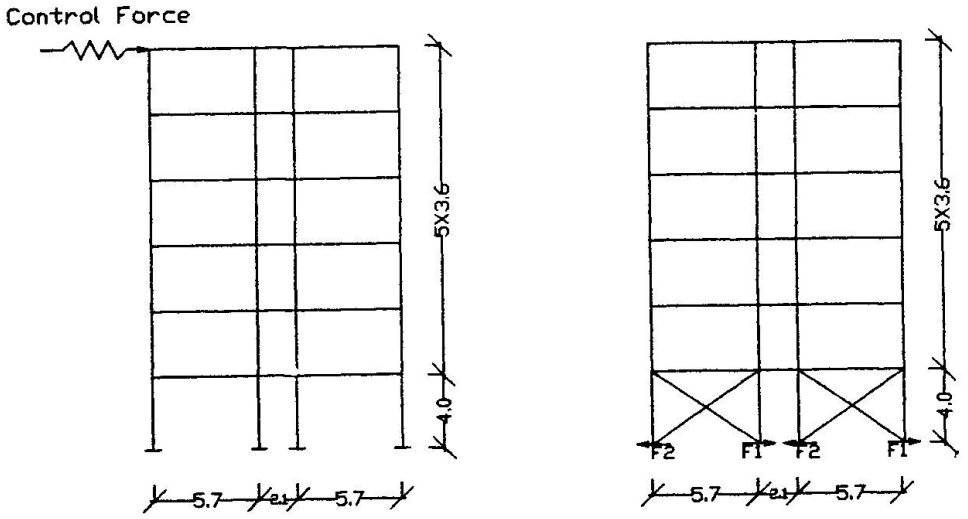

(a) Case of APC (b) Case of AARC

Figure 1, sketch for computational model of superstructure (unit: m)

The input motion is an El Centro earthquake acceleration record. Taking into account of small, medium and strong earthquakes, the maximum peak value is correspondingly taken as 70, 200 and 400cm/s^2. Under the condition of rigid-foundations the input motion was simply controlled by regulating the value of actual motion proportionally. When the SSI effects are considered, the intensity of input motion determined by the acceleration peak value of the mass center of foundation which is unknown before the numerical analysis. For this reason the value adjustments of the input motion are needed in order to compare with the condition of rigid-foundation assumption.

Any measurements of earthquake response of structure can be easily calculated by solving the dynamic equation of the SSI system using Newmark-β method [6][7]

3. Active Pulse Control (APC) Of Structure Considering SSI Effects

The pulse generator is placed on the top of structure (see fig.1). The control arithmetic adopted is that the direction of the control force generated by the pulse generator is opposite to the relative displacement direction of the top structure and the amount of the control force is equal to the relative displacement of the top structure multiplied by the gain factor.

With the consideration of the SSI effects the earthquake response was analyzed in 27 combined cases on the basis of the small, medium and strong motion; rigid, hard and soft ground; and gain factor being taken respectively as 600, 800 and 1000kN/m. The value of relative displacement under the motion is illustrated in fig. 2 to 4. The illustrations also include results of earthquake response analysis for 9 combined cases of non-control facilities, so they can be compared with the results of the APC. The results show that the earthquake displacement of structure was reduced by the SSI effects, and the softer the ground, the smaller will be the earthquake response. In other words, the softer the ground, the greater will be the earthquake response of superstructure influenced by the SSI effects and the smaller will be the earthquake response of superstructure in comparison with the condition of rigid-foundations. The table 1 shows the maximum value of the APC force needed. In general, the result of active control is better when the gain factor K equals to 800kN/m. In comparison with the APC force under assumption of rigid-foundations, the SSI effects cause the use of less APC force, and the softer the ground, the smaller the control force needed. The APC force needed will become greater when the gain factor K is increased.

Since the amount of the control force is determined by the earthquake displacement response of structure in the APC mothed, thus there are two important meanings to consider the SSI effects during the structural aseismic design. Firstly, as the objective of active seismic control is to confine the earthquake response of superstructure to a certain extent and the SSI effects would lessen the earthquake displacement of structure, so the condition of displacement control will be satisfied automatically without the need of extra active seismic control facilities. Secondly, as the SSI effects greatly reduce the APC force needed, so the power for the APC system would be lowered enormously with which the cost could be cut down.

Table 1 Maximum Control Force Needed

		For APC (kN)			For AARC (kN)	
gain factor K (kN/m)		600	800	1000	4000	6000
small earthquake	rigid ground	32.0	39.4	53.8	65.2	94.8
	hard ground	20.0	24.6	34.3	53.2	78.6
	soft ground	14.8	18.2	23.9	49.6	71.4
medium earthquake	rigid ground	88.4	112.7	153.8	186.4	270.6
	hard ground	57.3	70.6	98.1	144.8	208.8
	soft ground	42.4	52.1	68.2	141.2	203.4
strong earthquake	rigid ground	174.7	215.5	268.1	334.8	499.8
	hard ground	114.5	141.0	196.0	296.4	426.6
	soft ground	83.6	102.6	132.6	280.8	399.6

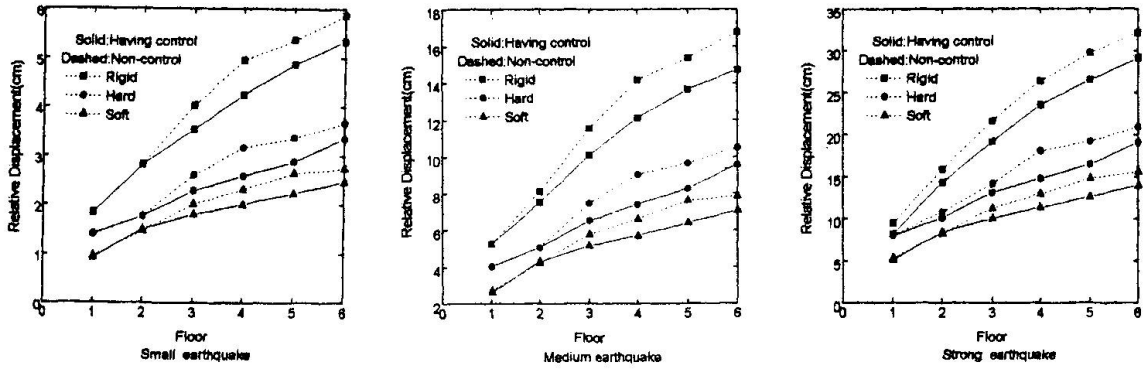

Fig.2 Comparison of relative displacement between non-control and APC for K=600 kN/m

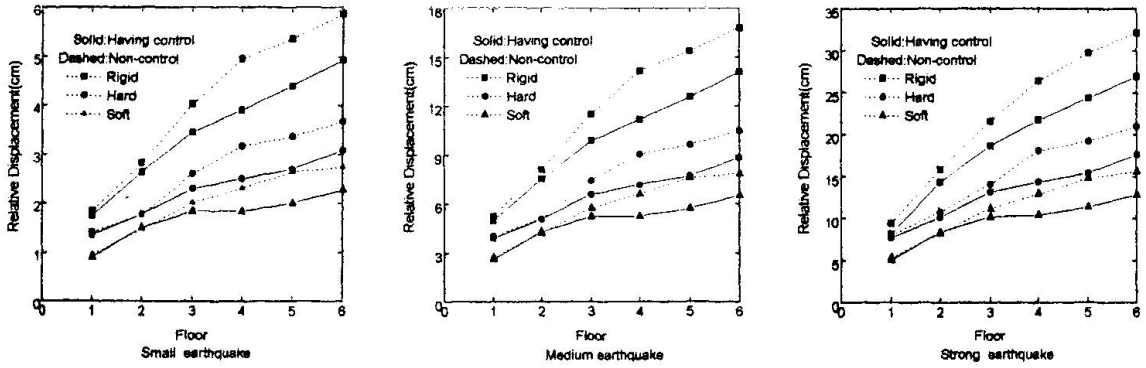

Fig.3 Comparison of relative displacement between non-control and APC for K=800 kN/m

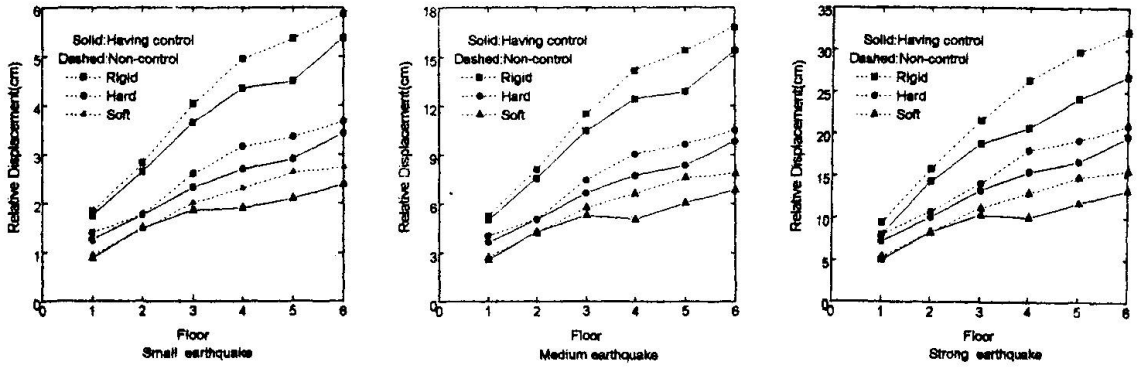

Fig.4 Comparison of relative displacement between non-control and APC for K=1000 kN/m

4. Active Anchor Rope Control (AARC) Considering the SSI Effects

Fig. 1(b) shows the computational model for the AARC. The control force was generated by a servosystem pulling the anchor rope and the amount of the control force equaled to the storey displacement of bottom structure multiplied by the gain factor K. The direction of the control force was determined by the following method: if the displacement of superstructure moves to left, then $F_2 = 0$; if it moves to right, then $F_1 = 0$.

Fig. 5 and 6 show that there are 18 combined cases of storey displacement with the consideration of input motions as the small, medium and strong one; the ground condition as the rigid, hard and soft ground; and the gain factor K taken as 4000 and 6000kN/m. In order to compare with the cases of non-control facilities, the storey displacement of non-control facilities was also given in the figures. Table 1 shows the AARC force needed and the storey displacement of structure lessened by the SSI effects, and the softer the ground, the greater will be the influence caused by the SSI effects. The SSI effects decreased the efficiency of AARC of structure, and the softer the ground, the greater will be the extent decreased. But the SSI effects affected on AARC was limited under the condition of hard ground. That the SSI effects can decrease much control force means the cost could be reduced.

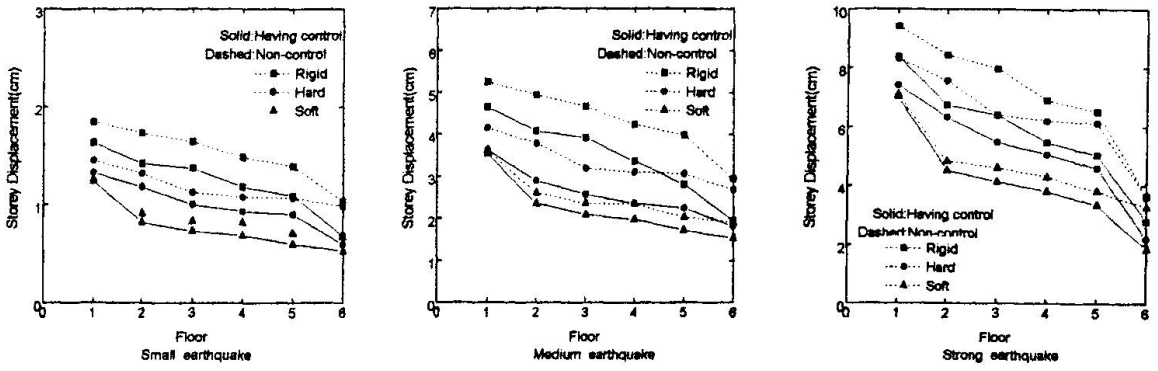

Fig.5 Comparison of storey displacement between non-control and AARC for K=4000 kN/m

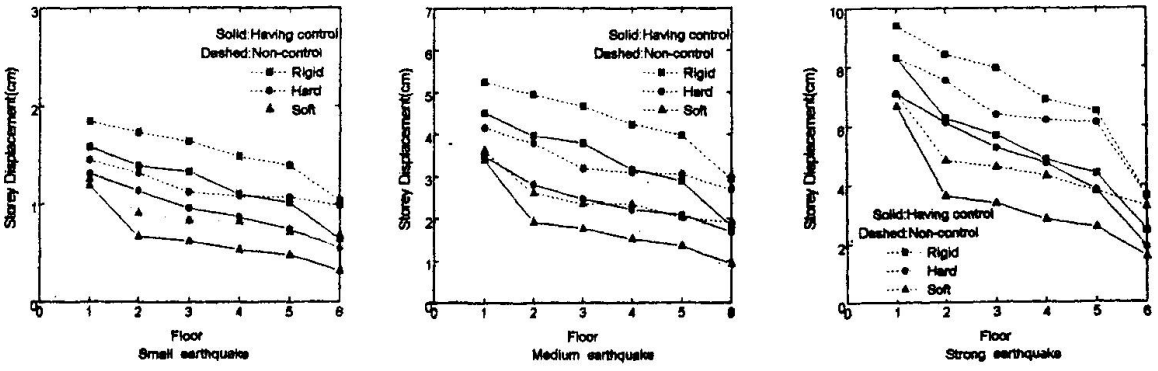

Fig.6 Comparison of storey displacement between non-control and AARC for K=6000 kN/m

5. Conclusion

The active seismic control of inelastic structure under considerations of the SSI effects has been first time analyzed by using the two-dimensional finite element method. After the investigation of the active aseismic control of structure effected by the SSI effects in detail, the conclusion can be reached as follows.

Firstly, since the purpose of active control is to control the earthquake response of structure within a safe extent and for multistorey shear frame structure the SSI effects would significantly decrease the earthquake response of structure, so the actual earthquake displacement of structure would be automatically contented with the purposed degree on rigid-foundation assumption without setting up active seismic control facilities if the SSI effects are to be considered during the structural aseismic design.

Secondly, comparing the two control methods, namely APC and AARC, the APC method needs less control force than the other and its result is quite contented with any type of ground by just regulating the gain factor K to an appropriate value. The result of the AARC on soft ground, however, is not so good, even taking no effect at all. In other words, for multistorey frame structure the earthquake displacement on top storey is controlled in a relatively effective way.

Third, the SSI effects reduce greatly the control force needed for the APC of structure and on hard and soft ground it would be reduced by 1/3 and 1/2 on the frame structure mentioned above, thus, the power consumption is decreased and the cost then could be cut down.

The research is based on specific structure and input earthquake motion, and the ground condition is relatively simple, therefore, it is a initiative and further research is needed.

References

1. Yang D., Chen G. X., and Zai J. M. Study on shock absorbing characteristics of primary and secondary structure. Earthquake Engineering and Engineering Vibration, 1996 (1), 100-109 (in Chinese).
2. Yang D., Chen G. X., and Zai J. M. A study on the effects of SSI on the aseismic characteristics of artificial plastic hinge. Journal of Nanjing Architectural and Civil Engineering Institute, 1997 (2), 15-22 (in Chinese).
3. Wong H. L., Luco J. E. Structural control including soil-structure interaction effects, ASCE, 117 (EM10), 2237-2250.
4. Smith H. A., Wu W. H. and Borja R. L. Structural control considering soil-structure interaction effects, EESD, 23(6), 609-626.
5. Yang D., Ding D. J. and Cao S. Y. A study on the influences of behaviors of new artificial plastic hinge on aseismic character of frame structures. Building Structure, 1994(4), 11-15 (in Chinese).
6. Chen G. X. An integrated system analysis procedure and application software package for analyzing the aseismic behavior of the soil-structure system. Journal of Nanjing Architectural and Civil Engineering Institute, 1992(2), 1-7 (in Chinese).

Experimental Study on Isolation System with Friction Damping

Kazushi OGAWA
Senior Mgr, Bridge Eng. Div.
Kawasaki Heavy Ind. Ltd
Akashi, Hyogo, Japan

Jun-ichi YABE
Senior Officer, Bridge Eng. Div..
Kawasaki Heavy Ind. Ltd
Tokyo, Japan

Tooru NISHIDA
Assist. Mgr, Akashi Techn. Inst.
Kawasaki Heavy Ind. Ltd
Akashi, Hyogo, Japan

Dong-Ho HA
Res. Eng., Bridge Eng. Div.
Kawasaki Heavy Ind. Ltd
Tokyo, Japan

Toshihrio TAMAKI
Staff Officer, Bridge Eng. Div.
Kawasaki Heavy Ind. Ltd
Tokyo, Japan

Fujikazu SAKAI
Dir., Kanto Techn. Inst.
Kawasaki Heavy Ind. Ltd
Noda, Chiba, Japan

Toshio SAITOH
Assist. Mgr , Bridge Eng. Div.
Kawasaki Heavy Ind. Ltd
Akashi, Hyogo, Japan

Summary

The displacement response of seismic-isolated bridges supported on the lead rubber bearings (LRB) or the high damping rubber (HDR) bearings can be very large to great earthquake like the Great Hanshin Earthquake. New type of seismic-isolation system to reduce the displacement response has been developed by the auhors. This new system consist of friction damping bearings, which contain permanent displacement control mechanism by water pressure, and horizontal rubber springs. A series of shaking table experiment had been conducted for the performance verification of a new frictional damping device for seismic isolation of bridge. The excellent energy dissipation effect of friction was identified as the small displacement response with acceptable acceleration response. The comparison of the results of the experiment and the numerical simulation shows the suitability of the simulation.

1. Introduction

The Great Hanshin Earthquake in 1995 caused severe damages on the highway bridges. The seismic isolation systems are used to reduce the response during the earthquake by shifting the natural period of the structure out of the range of dominant earthquake energy and increasing the damping capacity. The isolation systems are recognized as efficient device to reduce the earthquake resopnse. However, the displacement response of the bridges isolated by usual rubber bearings can be 30cm to 70cm to the great earthquake. The design of expansion joints and falling prevention system are difficult to such a large displacement. Therefore the isolation systems with less displacement response are desired. In this paper, the new seismic-isolation system[1,2], the results of measurement of friction elements and the shaking table experiments of the similitude model are discussed. The results of the experiments show the efficiency of the isolators.

2. Isolation system with friction damping

The configuraton of the isolation system with friction damping is shown in Fig. 1. The system consists of the horizontal rubber springs to lengthen the natural period of the bridge structure, and the friction bearings which support the weight of the structure and dissipate the vibration energy by friction. The characteristics of the isolation system with friction damping is as follows.

(a) The vertical load is beared by the friction bearings, traffic vibration does not occur.
(b) The acceleration response of the structure is almost same as the rubber bearings but the displacement response of the structure is well suppressed than by the rubber bearings.
(c) If the residual displacement may occure after the earthquake, the restoration mechanism installed in the device using the water pressure can restore the residual displacement easily.

The isolation system with friction damping can be deformed in horizontal and rotational direction as shown in Fig. 2. The horizontal rubber springs need not bear the vertical force and need not energy dispersion and it is easy to design.

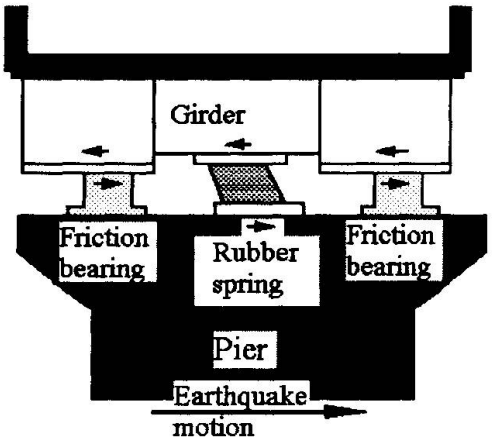

Fig. 1 Configration of isolation system with friction damping

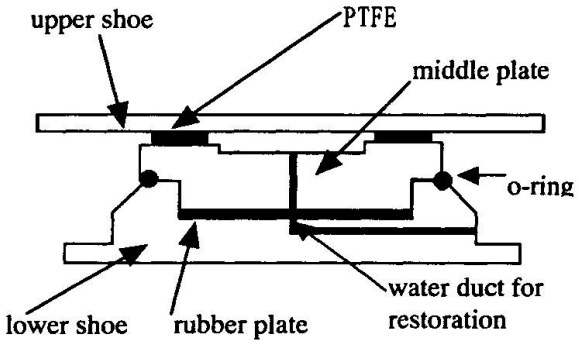

Fig. 2 Friction Bearing

3. Measurement of friction element

3-1 Experimnetal equipments

As shown in Fig.3, one SUS (stainless steel) plate inserted between the two lower shoes pressed each other is moved by the actuator. The water pressure induced into the cavity in the PTFE (Polytetrafluoroethylene) ring plate reduce the bearing pressure on the ring and the friction force. In this experiment, vertical force, horizontal force, relative displacement and water pressure are measured. The specification of the equipment and the measurement condition are shown in Table 1.

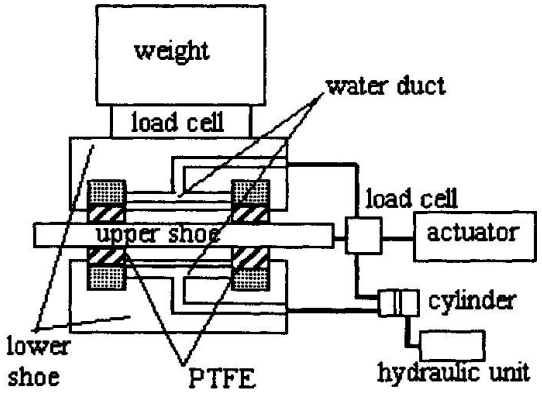

Fig. 3 Equipment for friction measurement

Table 1 Measurement condition

sliding plate	amplitude	135[mm]
	velocity	5~212[mm/s]
PTFE	bearing pressure	9.4,126[MPa]
	area	80[cm^2]
cavity	water pressure	0~58 [MPa]
	area	64[cm^2]

3-2 Results of measurement

The maximum sliding velocity of the PTFE to the SUS are obtained from the time history of the skiding displacement. The coefficients of friction are computed as the ratio of the horizontal force to vertical force. The relation of the friction coefficient and the sliding velocity is shown in Fig. 4. The friction coefficient of PTFE and SUS is small in low velocity region and 0.10 to 0.16 in the region higher than 5cm/sec.

The relation of the sliding velocity and the friction coefficient at each water pressure are shown in Fig. 5. The figure shows the tendency that the higher water pressure makes the friction coefficient smaller in spite of the sliding velocity. Therefore the residual displacement of the bridge can be restored easily by the water pressure. In the case of water pressure higher than 4.6-4.9[Mpa], a little water leakage was observed and the water on the interface of PTFE and SUS reduce the friction coefficient with lubrication effect.

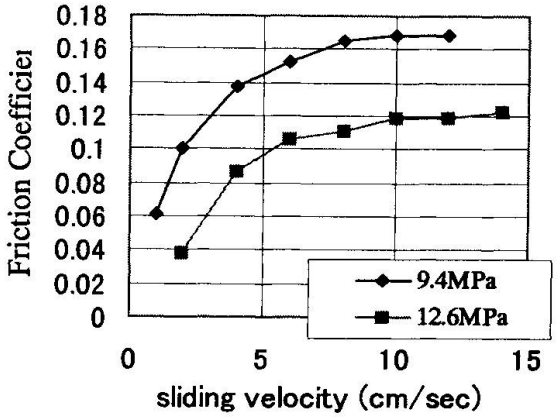

Fig. 4 Velocity and Friction Coefficient

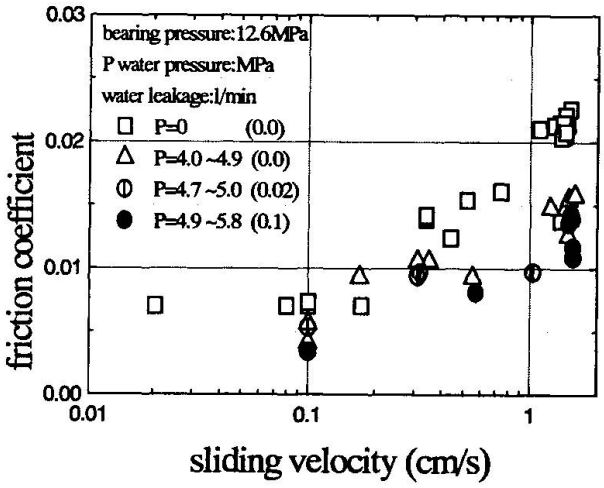

Fig. 5 Water pressure and Friction Coefficient

4. Shaking table experiment

4-1 Experimental model

The objective bridge of this study is a 5-span continuous steel box-girder with concrete piers as shown in Fig. 6. The shaking table model simulates the dynamic property of the first mode in the logitudinal direction, and of the one span of the girder supported on the isolators above the pier in scale of 1/5. The mass of the model is 10 tons. The natural frequency of the model supported on the horizontal rubber springs is 1.2[Hz] ($\sqrt{5}$ times of the prototype). The dimension of the model is shown in Fig.7 and the photograph of the model on the shaking table in Fig. 8.

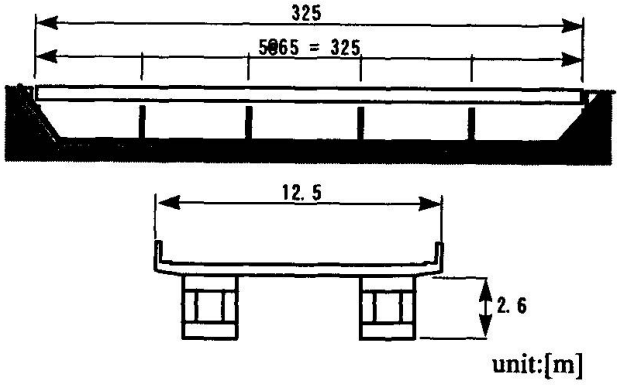

Fig. 6 General view of 5-span continuous steel box-girder bridge

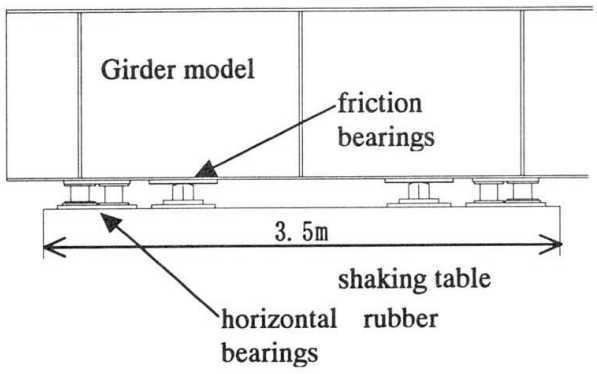

Fig. 7 Model for shaking table experiment

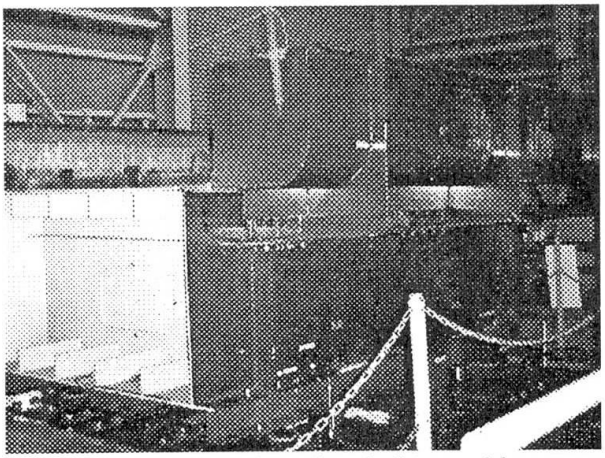

Fig. 8 Model on the shaking table

4-2 Input wave

The sinusoidal waves to investigate the basic characteristics of the model and the earthquake waves to investigate the response of the isolated bridge are used as the input to the shaking table. The earthquake inputs are computed as the response of the pier-girder 2DOF system subjected ground acceleration. The ground motions used for shaking table input are standard time history records for checking design ultimate horizontal strength[3] and the record of the Great Hanshin Earthquake[4]. In Fig. 9 an example of the time history of the acceleration is shown.

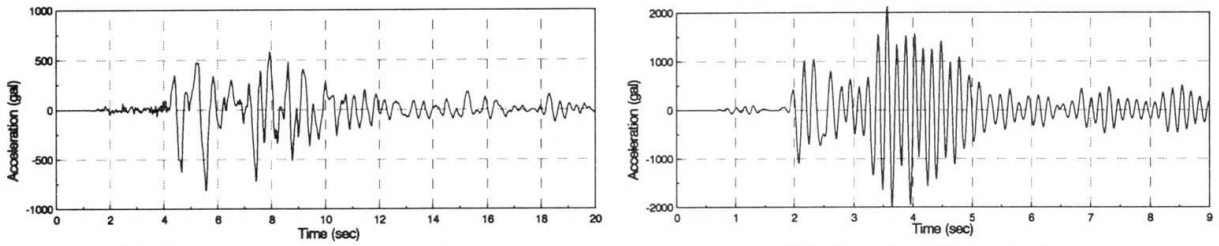

(a) Acceleration at ground (b) Acceleration at pier

Fig. 9 Input Acceleration (JMA Kobe NS)

4-3 Numerical Simulation

The numerical model of the experimental model is described as a SDOF mechanical vibration system with Coulomb friction as Fig. 12. The equation of motion of the system in Fig.13 is written as follows.

$$\begin{cases} M\ddot{x} + C\dot{x} + Kx = -M\ddot{z} + F_r \\ F_r = -\mu_d Mg\,\mathrm{sgn}(\dot{x}) \end{cases} \quad (1)$$

When

$$\begin{cases} \dot{x} = 0 \quad \text{and} \\ |-M\ddot{z} - C\dot{x} - Kx| \le \mu_s Mg \end{cases} \quad (2)$$

simulation is restarted with the condition

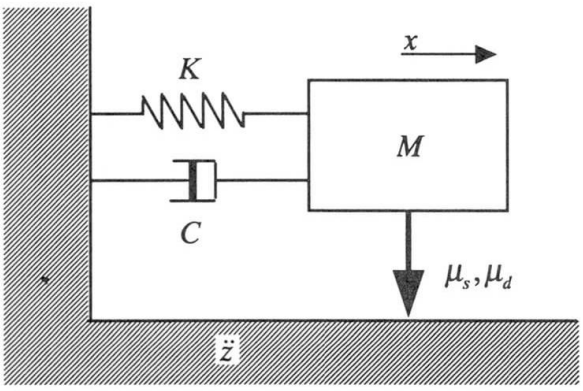

Fig. 10 SDOF simulation model

$\dot{x} = 0$. It means that when the relative velocity is zero and the acting force less than the static friction force, the motion will stop. In the numerical solution procedure of differential equation (1), it is difficult to judge the condition (2) exactly. We evaluated the condition by eq. (3) insetead of eq. (2) using a small value ε and restart with the condition $\dot{x} = 0$.

$$\begin{cases} |\dot{x}| \le \varepsilon \\ |-M\ddot{z} - C\dot{x} - Kx| \le \mu_s Mg \end{cases} \tag{3}$$

Based on the results of measurement of the friction elements, we set the dynamic friction coefficient μ_d =0.14 and static friction coefficient μ_s as 0.04. Solution scheme by Adams-Gear method with variable time step (0.0001~0.001[sec.]) and $\varepsilon = 10^{-5}$ are used.

4-4 Results of shaking table experiment

a) Harmonic Excitation

Firstly harmonic excitaions of the girder model supported on the horizonal rubber spring are measured. The acceleration amplitude of the shaking table was set to 4, 8, 16, 20 gal. The frequency response is shown in Fig.11. The resonanse frequency changes from 1.42 Hz to 1.26 Hz with increse of input amplitude and it shows that horizontal rubber springs have slightly nonlinear stiffness. The damping ratios were from 0.025 to 0.031 and almost linear.

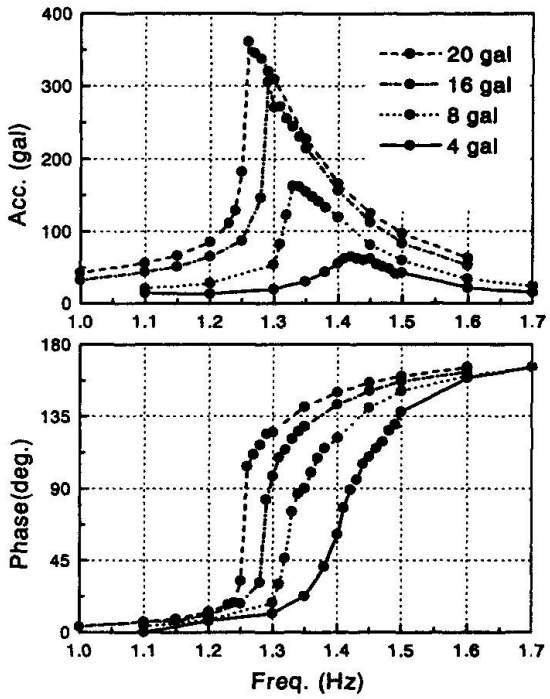

Fig.11 Frequency response of girder on rubber spring

Next, in the case of girder supported on the friction isolator and horizontal rubber spring, the time history of acceleration is obtained as Fig. 12. In this figure the measurement results (solid line) and results of the numerical simulation (dashed line) are compared. The results of experiment and simulation are in good agreement and the simulation method and parameters are appropriate.

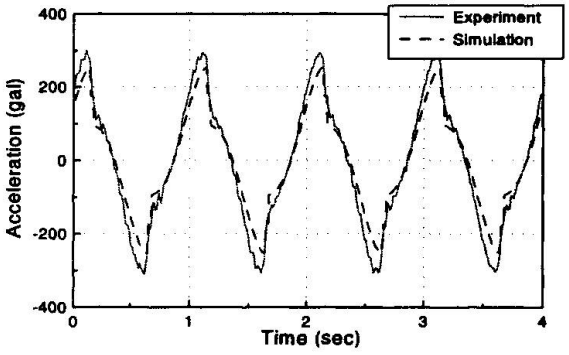

Fig. 12 The time history of the gider supported on isolators

b) Earthquake Excitation

The comparison of time history of the girder on the horizontal rubber spring is shown in Fig.13. In this figure solid line indicates the experimental results and dashed line the simulated results of bi-linear SDOF model. Input wave is based on Kobe JMA NS record (Fig. 9). The difference of the maximum acceleration response is 1.7% and it shows that the property of the horizontal rubber spring is well described by bi-linear model.

The comparison of the time histories of the experiment and the simulation is shown in Fig. 14. This figure shows good agreement of the responses by the shaking table experiment and by the simulation considering Coulomb damping.

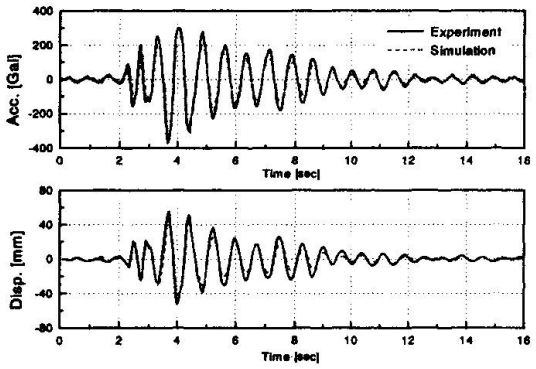

Fig. 13 Response of girder supported on rubber springs

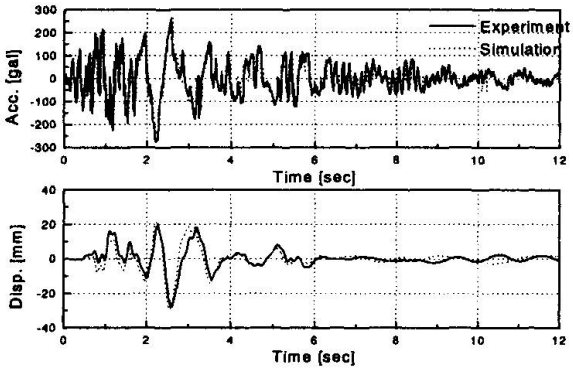

Fig. 14 Response of girder supported on isolation system with friction damping

4-5 Comparison of the isolation effect

Based on the results of the shaking table test, we compare the isolation effect of the isolation system with the friction damping and usual rubber isolator by the numerical simulation of the 2DOF model consists of the girder and the pier. In the simulation isolator with the friction damping is treated as a linear spring and Coulomb damping and usual rubber bearing is linear spring and dashpot of 15% of the critical damping. The maximum response of the girder to the earthquake waves are comparerd in the table 2. In this table it is shown that the acceleration response of both isolators are almost same, but the displacement response of the new isolator are much smaller than that of rubber bearings. This shows that the efficiency of the new isolator to suppress the displacement response.

Table 2 The comparison of isolation effect

Input wave	Isolator with Friction		Rubber bearing	
	Acc.	Disp.	Acc.	Disp.
Kaihoku	357	222	377	363
Itajima	373	239	438	415
Tsugaru	389	255	552	532
JMA Kobe	308	170	337	306
JR Takatori	735	604	725	685
Higashi Kobe	403	268	538	528

unit Acc.:gal, Disp. :mm

5. CONCLUSION

The authors discussed the friction measurement and shaking table test of the seismic isolation system with friction damping. The excellent energy dissipation effect of friction was identified as the small displacement response with acceptable acceleration response. A simple simulation with Coulomb damping model was achieved by using the experimental result. The comparison of the results of experiment and numerical simulation shows the suitability of this simulation.

References

(1)Doi Y. et al,"Earthquake isolation of bridge using friction damping shoes", proc. of 1st Colloquim on seismic isolation and control, JSCE 1996.(in Japanese)

(2)Tamaki T. et al, "Experimental study on the seismic isolation system", proc. of JSCE Ann. 1997.(in Japanese)

(3)Civil engineering reserch center, "Temporaly mannual of design method for base-isolated highway bridges ", 1992.(in Japanese)

(4)Japan meteorological agency, "Strong motion record in 1995 Great Hanshin Earthquake", 1995.

Damage Control Design Based on Hysterisis Damping Effect

Masaaki YASUI
Struct. Eng.
Obayashi Corp.
Osaka, Japan

Katuyosi ITAGAKI
Struct. Eng.
Obayashi Corp.
Osaka, Japan

Kiichiro SAITO
Struct. Eng.
Obayashi Corp.
Tokyo, Japan

Sanae FUKUMO
Struct. Eng.
Obayashi Corp.
Osaka, Japan

Summary

Recently, in Japan, remarkable progress has been made in the field of structural response control, after the Hanshin-Awaji Earthquake of 1995 caused many steel structure buildings to fail. This paper reports on the design of a 15-story steel structure building employing two types of hysteretic damper systems. One is composed of a steel bearing wall skirted by boundary beams on either side. The other is composed of a boundary beam passing between two braced mega-columns. In the case of a big earthquake, these boundary beams work as hysteretic dampers through plastic deformation, thereby preventing damage to the main beams and columns bearing vertical loads.

1. Structure Design

1. 1 Outline of Structure

The building reported on in this paper is an office building with a 15-story steel structure. The perspective drawing of the building is shown in figure 1. The plan of a typical floor of the building is a rectangle spanning 37.8 by 23.6 meters. The height of the building is 59.3 meters. The plan and section of the building are shown in figure 2 and figure 3. The basic structural system of the building above ground is a moment frame with damper system.

figure 1 A perspective drawing of the building

1．2 The mechanism of the damper system

Two types of hysteretic damper systems are applied in the structural design. One consists of the combination of steel shear walls and boundary beams. Henceforth this system will be referred to as the shear wall type. The other consists of the combination of braced mega-columns and boundary beams, and will henceforth be referred to as the brace type.

The shear wall type is made of a steel plate with boundary beams on both sides. The design concept is for the boundary beams to behave as dampers, absorbing seismic energy mainly through plastic deformation in the web, as a result of shear stress. Therefore the web plate is made of low yeild-point steel (LYP235 has a yield strength of about 235 MPa). LYP235 exhibits little deviation of yield strength and good elongation. The architectural advantage of this system is that it allows floor to ceiling openings between boundary beams on both sides of the shear wall.

The brace type is composed of a boundary beam passing between two braced mega-columns, each mega column being composed of two columns joined by cross bracing. In this system the boundary beams dissippate seismic energy mainly through plastic deformation of the flange plates, as a result of bending moment. These beams are made of normal steel material (SM490A, which has a yield strength of about 330 MPa). The design advantage of this system is that floor to ceiling openings can be arranged between boundary beams.

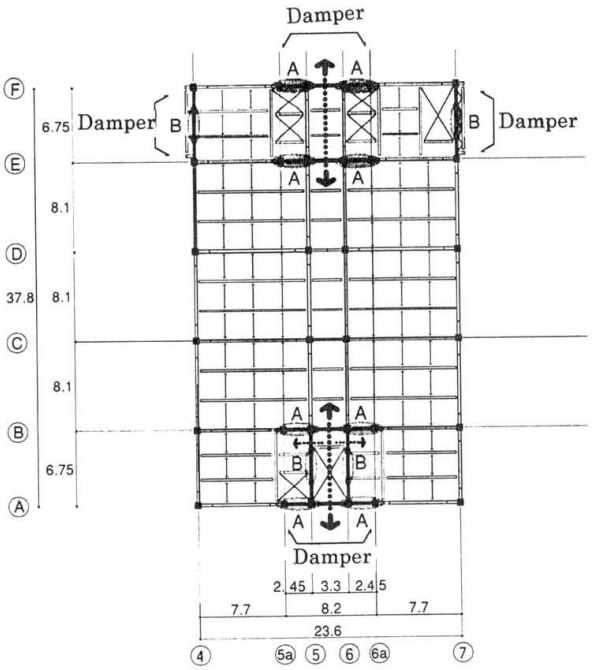

figure 2 The plan of the building

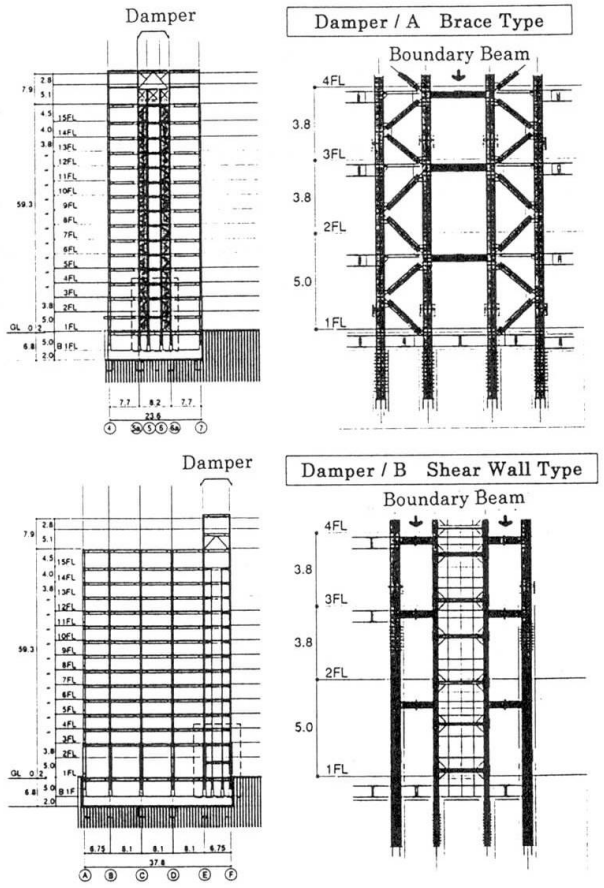

figure 3 The section of the building

1. 3 Strctural Design Concept

The building is designed according to Japanese architectural standards. In the case of a big earthquake, the boundary beams will work as the hysteretic damper through plastic deformation, thereby preventing damage to main structural members bearing vertical loads. The damper resists about 10% to 50% of the seismic force (average about 30%) at each floor. The target structural performance is shown below.

Table-1 The target structural performance

		Level I (25 cm/s)	Level II (50 cm/s)
Slope by relative storey displacement		under 1/ 200	under 1/ 100
Ductility factor of a general beam		Elastic	under 4.0
Ductility factor of a boundary beam	Shear yield type	Elastic	under 20.0
	Bending yield type	Elastic	under 4.0
Column · brace steel plate shear wall		Elastic	Elastic

2. Inspection of Damper Effect by Dynamic Analysis

2. 1 Static Elasto-Pastic Analysis

Static elasto-plastic analysis was carried out with a plane frame model. The skeleton curve of each story is modeled on a tri-linear curve as defined below. The upper limit of resistance force at each story is defined through the method of virtual work. The hysteresis characteristic was modeled to Normal Tri-Linear type.

First bending point: point at which any beam at a given story first yields

Second bending point: point at which half of the beams at a given story yield

2. 2 Dynamic Analysis

The response analysis was performed in the cases of the following earthquakes: El Centro 1945 NS, Taft 1952 EW, and Hachinohe 1968 NS, each on both level I (25 cm/s) and level II (50 cm/s). Furthermore, the seismic wave (with a maximum velocity of 85 cm/s) observed during the Hanshin-Awaji Earthquake in 1995 was input for the simulation. The seismic wave was recorded at the NTT Kobe Building (B3F) located in front of the JR Kobe Station. The first natural period of the building studied in this report is 1.95 seconds in both directions. The

result of response analysis is shown in table 2 and figure 4. The plastic hinges which occured in the building during simulation of the Hanshin-Awaji Earthquake are shown in figure 5. The maximum ductility factor is 2.70 for main beams, 11.5 for boundary beams of shear wall type, and 4.20 for boundary beams of brace type. It is confirmed that the structure satisfies the target performance through these analyses. The ductility factor of the typical main beam is smaller than that of a boundary beam.

Table-2 result of earthquake response analysis

		Level I (25 cm/s)	Level II (50 cm/s)	Hanshin-Awaji Earthquake (85 cm/s)
Slope by relative storey displacement		1/ 196	1/ 102	1/ 74
Ductility factor of a general beam		Elastic	2.05	2.70
Ductility factor of a boundary beam	Shear yield type	Elastic	7.80	11.5
	Bending yield type	Elastic	2.95	4.20
Column・brace steel plate shear wall		Elastic	Elastic	Elastic

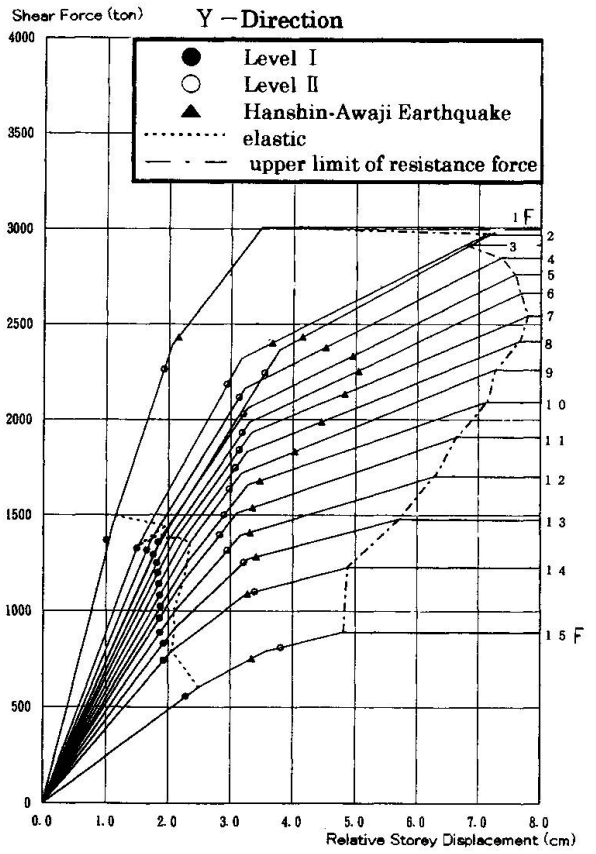

figure 4 Skeleton curve and Result of response analysis

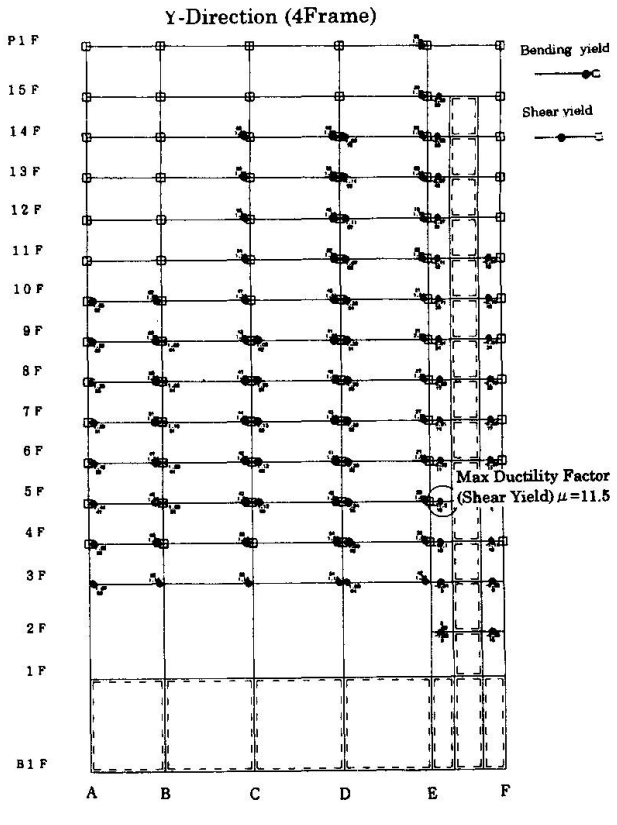

figure 5 The plastic hinges in the building (Hanshin-Awaji Earthquake)

2．3 Evaluation of Damping Effect

The total dissipated seismic energy is broken down into viscous damping energy, hysteretic damping energy of damper, and kinematic energy, in order to evaluate the damper's performance.

In the case of the shear wall type damper (long span direction of the building), viscous damping is 2.0%, hysteretic damping of framework is 0.33%, and hysteretic damping of damper is 0.67%.

In the case of the brace type damper (short span direction of the building), viscous damping is 2.0%, hysteretic damping of framework is 0.20%, and hysteretic damping of damper is 0.53%.

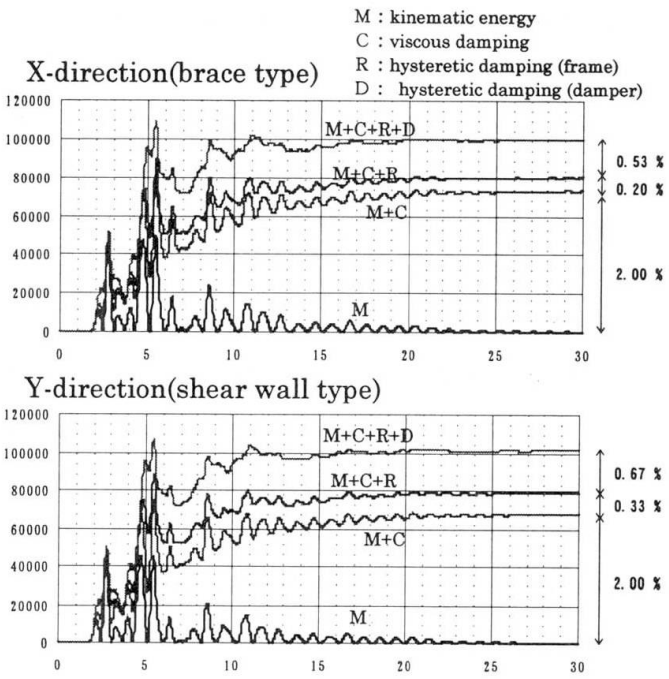

figure 6 Evaluation of Damping Effect

2．4 FEM Analysis of steel plate shear wall and boundary beam

An FEM analysis of the shear wall system was used to minutely evaluate the stress condition of boundary beams in a state of maximal deformation. Von Mieses stresses for the case of design shearing force and the Hanshin-Awaji Earthquake, respectively, are shown in figure 7. Each member is elastic in the case of design shearing force. The boundary beams yield entirely in the case of the Hanshin-Awaji Earthquake.

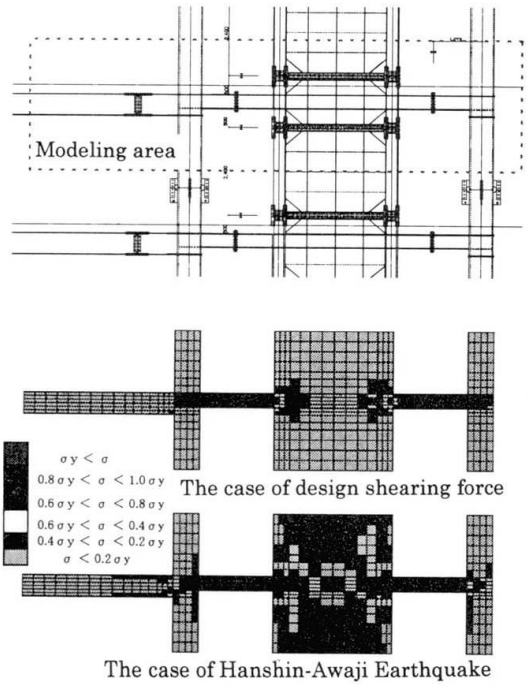

figure 7 Result of FEM analysis

3. Conclusion

In general, it is difficult to arrange braces or shear walls in a structural design because they put restriction on the floor plan or to natural lighting. The damper systems presented in this paper are, however, of significant advantage to architectural performance, because they can be placed so that openings will accomodate the requirements of a given floor plan. This flexiblility makes these systems widely applicable in the realm of structural response control.

References

1) Kotaro Tanaka, Katuyosi Itagaki, Yosihiko Takahasi : Damage control design based on hysteretic damping effect of 14-story office building with Y-formed brace damper, JSSC annual paper, The 4th volume, pp.396~376, 1996.11

2) Yosihiko Takahasi, Yuuji Sinabe : Empirical research related to a hysteresis characteristic of thin steel plate of shear yield type Architectural Institute of Japan paper selection of structural section, The 494th, pp.107~114, 1997.4

Damage Control Design Based on Attenuation Mechanism by Unbonded Brace

Masanori FUJII
Struct. Eng., Design Dept
Obayashi Corp.
Osaka, Japan

Koutarou TANAKA
Design Team Mgr, Design Dept
Obayashi Corp.
Osaka, Japan

Katuyoshi ITAGAKI
Design Mgr, Design Dept
Obayashi Corp.
Osaka, Japan

Yasuhiro NAKATA
Senior Mgr, Steel Structure Div.
Nippon Steel Corp.
Tokyo, Japan

Summary

This paper shows a damage control design of 19-stories office building by ' Unbonded Brace '. Unbonded brace is a buckling-resistant structural member consisting of steel core members enclosed in a concrete-filled square steel tube. The unbonded braces consisting of steel core member using low yield strength steel become plasticized even at moderate seismic level. At large seismic level, the unbonded braces absorb a large quantity of seismic energy. Moreover, after a large earthquake, unbonded braces can be replaced as required.

Introduction

Since the Hanshin-Awaji Earthquake (1995.1.17) in Japan, studies on seismic energy isolation and damping structures abound and a number of attenuation mechanisms have been proposed. It is noteworthy that the realization of structures with high energy absorption is possible through early plasticization of seismic members (hysteretic damper).

In accordance with this concept, the authors proposed a damping structure. The damage control design for this building is based on attenuation mechanism produced hysteresis damping effect by unbonded brace using low yield strength steel (LYP100 : yield strength $\sigma y \fallingdotseq 100$ Mpa). This paper outlines the damage control design of a 19-stories office building, which was designed based on attenuation mechanism by unbonded brace and is currently under construction in Osaka.

1. Outline of the Building

Designed building is 19-stories steel structure as shown overall-view in Fig 1. As illustrated Fig 2 and 3, the building consists of main frames with three spans of 9.6 m, and hysteretic dampers (unbonded braces) are situated in common space located at north and south sides. The typical story heights are 3.85 m and 3.8 m, and the height of the building is 85.8 m.

This structure is furthermore characterized by:

(1) mega-structure frame taken advantage of rescue to enhance the hysteresis damping effect by unbonded braces,

(2) concrete filled tubes to enhance the capacity to absorb earthquake energy and the rigidity of 1 and 2 stories with taller height (4.8 m).

Fig 1 Overall-View

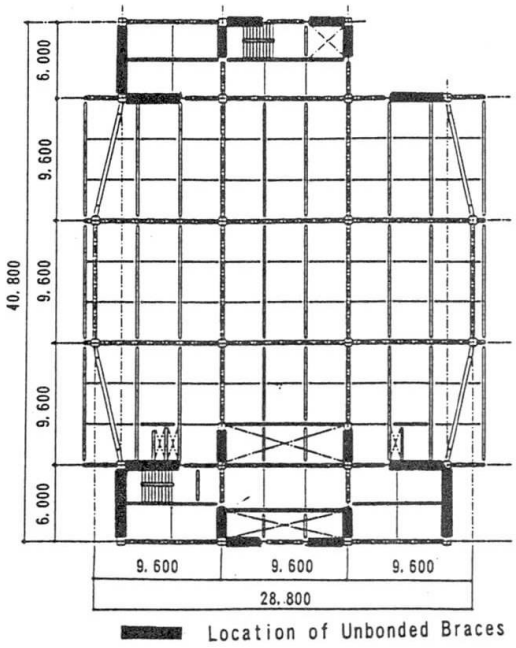

Fig 2 Typical Floor Plan

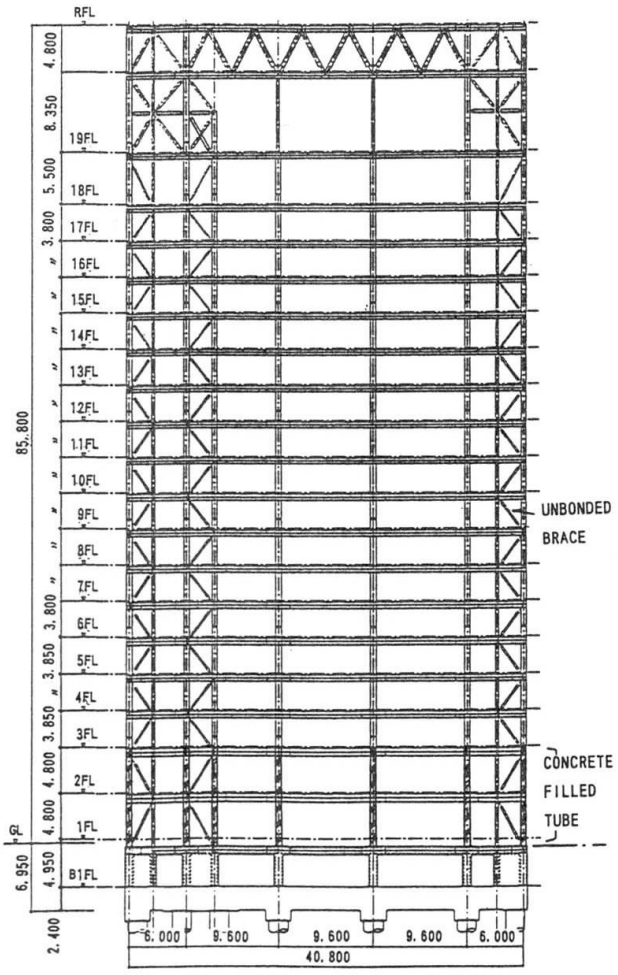

Fig 3 Framing Elevation (N-S dir.)

2. Seismic Design

2.1 Damping Mechanism

'Unbonded brace' is a buckling-resistant structural member consisting of steel core member enclosed in a concrete-filled square steel tube (Fig 4). The steel core member is coated with a non-bonding material, so that no axial force works on the concrete and the steel tube. Consequently, this brace shows stable hysteresises if the yielding load working on the core member is smaller than the buckling load of the steel tube. Besides the stable hysteresis, this brace shows excellent energy absorption. Because the steel core member is made of low yield strength steel (LYP100: $\sigma y \fallingdotseq 100$ Mpa) and the hysteresis energy of low yield strength steel is much greater than ordinary steel (Fig 5).

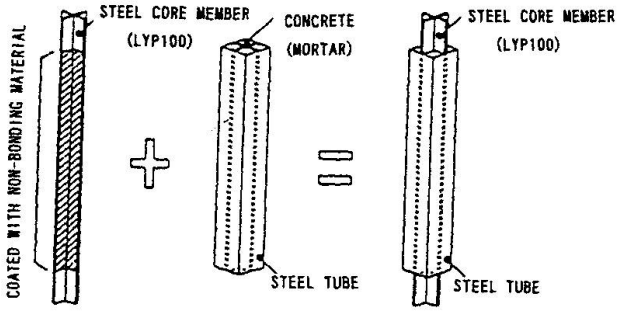

Fig 4 Unbonded Brace

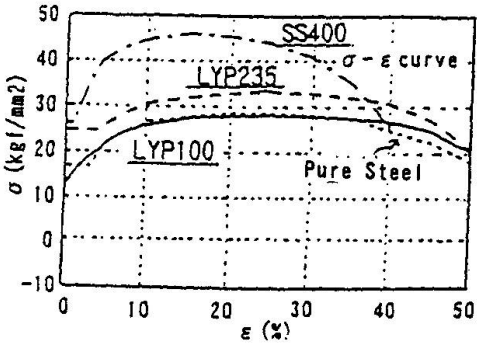

Fig 5 Stress-Strain Curve of Low Yield Strength Steel (LYP100)

2.2 Design Philosophy

In order to assure earthquake resistance of this structure, it was designed according to the following criteria. Table 1 gives the target values of structural performance obtained from the dynamic response analysis. The axial strength of unbonded braces was designed by aiming at that almost columns and beams are not yielding at seismic level 2 (the ground velocity of 50 kine). At that time, the end joints of unbonded braces are elastic.

Table. 1 Target Values of Structural Performance

Earthquake Ground Velocity	Target Values			
	Story Drift	Ductility Factor of Members		Strain of Members
		Beam	Column	Steel Core Member of Unbonded Brace
25 kine	≦ 1/200	≦ 1.0	≦ 1.0	≦ 0.005
50 kine	≦ 1/100	≦ 2.0	≦ 1.0	≦ 0.015

3. Seismic Response Analysis

3.1 Three-Dimensional Static Analysis

A three-dimensional nonlinear static analysis was carried out by the step-by-step method in order to identify the elasto-plastic characteristics of the designed frame, and confirm that the collapse mechanism is determined by flexural yield of beams. As shown in Fig 6 , unbonded braces were analyzed using three divided axial model consisting of ordinary steel (joint) and low yield strength steel (core member). The hysteresis curve of low yield strength steel to harden by repetition was approximated by the result of specimen test (Fig 7) . On the assumption that the floor is rigid, analysis was carried out by applying to the gravity center of each floor incremental load with the same distribution pattern as that of the design shear force.

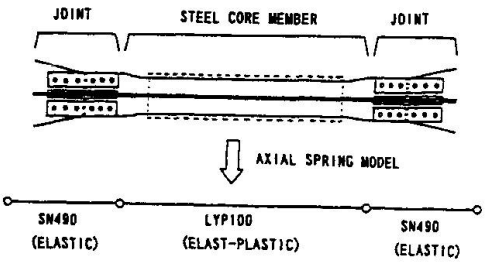

Fig 6 Modeling of Unbonded Brace

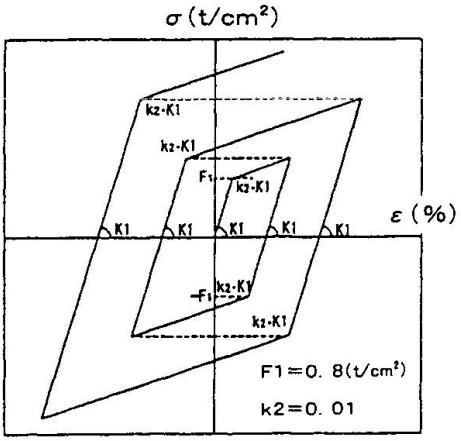

Fig 7 Hysteresis Curve of Low Yield Strength Steel (LYP100)

3.2 Time History Seismic Response Analysis

The time history seismic response analysis included: a shear-mode Lumped Mass System Response Analysis which was designed to grasp the response characteristics of the whole structure; a Plane Frame Response Analysis which was designed to grasp the elasto-plastic behavior of structural members (columns, beams, and braces).

In the Lumped Mass System Response Analysis, a model was defined that had 20 mass points (one for each story) on a rigid foundation. Internal viscous damping effect proportional to frequency was assumed, and the damping factor was assumed to be 2% for the first mode frequency. The maximum story drift angle for 25 and 50 kine responses were shown in Table 2 respectively, which are smaller than their respective target values, 1/200 and 1/100.

Table. 2 Maximum Story Drift angle by Lumped Mass System Response Analysis

Ground Velocity	X-direction	Y-direction
25 kine	1/245	1/208
50 kine	1/125	1/117

The Plane Frame Response Analysis was carried out using the wave recorded at the Hanshin-Awaji Earthquake (1995.1.17) with the velocity of 50 kine. Fig 8 shows the distribution of yield hinges produced in Y direction frame. The maximum ductility factor of beams was 1.16, and yield of columns was not observed. The maximum axial stress and strain of unbonded braces was 1.5 (t/cm^2), 0.005, respectively (Fig 9 and 10).

For investigating response at largest seismic level, the Plane Frame Response Analysis was carried out using the same wave with the velocity of 75 kine. The maximum ductility factor of beams was 2.6, the maximum strain of the steel core members in unbonded braces was 0.098, and yielding columns was not observed.

From the above results it was confirmed that the response values were within the target range of structural performance. The unbonded braces using low yield strength steel become plasticized even at moderate seismic level. At large seismic level, the unbonded braces absorb a large quantity of seismic energy.

Moreover, numerical analyses on unbonded braces fixed in a frame were made using the non-linear finite element method. The maximum strain of the end in steel core at maximum axial deformation was 0.016. It was confirmed that unbonded braces fixed in a frame can absorb a large quantity of seismic energy.

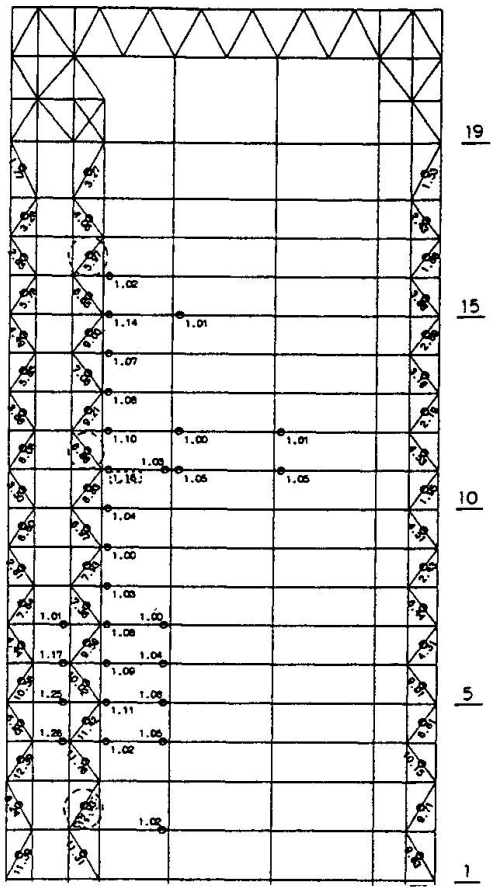

Fig 8 Distribution of Plastic Hinges (Y-dir. 50 kine)

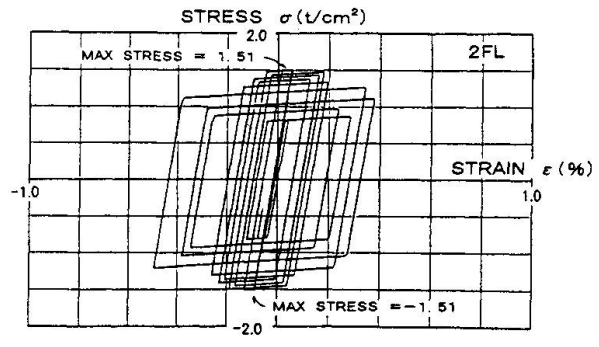

Fig 9 Stress-Strain Curve of Steel Core Member (50 kine)

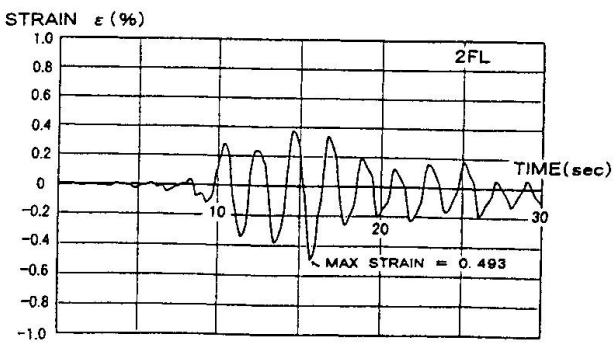

Fig 10 Strain Time Response of Steel Core Member (50 kine)

4. Conclusion

The authors designed 19-stories office building which unbonded braces using low yield strength steel was first extensively adopted. According to this attenuation mechanism by unbonded braces, columns and beams was little damaged at large earthquake. Moreover, after a large earthquake, unbonded braces can be replaced as required.

In view of the results of the seismic response analysis, the authors believe that the building designed according to the hysterisis damping effect by unbonded braces using low yield strength steel will prove to be excellent in seismic resistance.

In closing, the authors believe that this damage control design will help to develop 'Structural response control'.

References

1) E.Saeki, Y.Maeda, H.Nakamura, M.Midorikawa, A.Wada: Experimental Study on Practical-Scale Unbonded Braces , J.Struct.Constr.Eng., Architectural Institute of Japan, No.476, pp.149~158,1995.10

2) E.Saeki, M.Sugisawa, T.Yamaguchi, H.Mochizuki, A.Wada: A Study on Low Cycle Fatigue Characteristics of Low Yield Strength Steel , J.Struct.Constr.Eng., Architectural Institute of Japan, No.472 , pp.139~147,1995.6

3) E.Saeki, Y.Maeda, K.Iwamatsu, A.Wada: Analytical Study on Unbonded Braces fixed in A Frame, J.Struct.Constr.Eng., Architectural Institute of Japan, No.489 , pp.95~104,1996.11

4) M.Iwata, Y.Nakata, Y.Maeda, A.Wada: Study on Fatigue Properties of Restoring Dampers Part1,Part2, Summaries of Technical Papers of Annual Meeting Architectural Institute of Japan, StructuresⅢ, pp.733~736,1997.9

Design S-N Curves for Axial Fatigue of Spiral Strands

Mohammed RAOOF
Prof.
Loughborough Univ.
Loughborough, UK

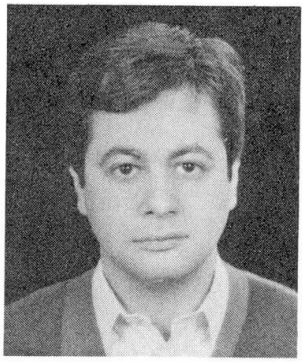

Mohammed Raoof, born 1955, is a graduate of Imperial College where he obtained his BSc, MSc, and PhD. He is the winner of a number of British awards for his research efforts.

Summary

Based on an extensive series of theoretical parametric studies on some very substantial spiral strands with realistic construction details, a new set of S-N curves for predicting the axial fatigue life of spiral strands to first outer (or inner) wire fractures have been proposed. The theoretical model based on which these parametric studies are conducted, has been verified extensively against a very large number of carefully conducted and large-scale test data using specimens with diameters ranging from 25 to 164mm, as produced by different manufacturers and tested by a number of Universities/Research Institutions. The proposed S-N curves are compared with others recommended by API, Chaplin, and Tilly, which are the ones that are currently most commonly referred to and certain shortcomings of previously available recommendations by others are identified.

1. INTRODUCTION

In recent years there has been considerable interest in the tensile fatigue of wire ropes (and spiral strands) for use in both offshore and onshore applications. On the offshore scene, there has been a growing need for longer and stronger elements with larger diameters for use as components in mooring systems for oil exploration, production, and accommodation platforms. As regards onshore structural applications, steel cables are extensively used in bridges and as tension elements for suspended and stayed structures generally.

With the increasing number of available large scale test data for a wide variety of cable constructions, design S-N curves for steel cables have been included in some recent codes of practice in the field of Structural Engineering. One example is API (American Petroleum Institute) recommended S-N curve, another the design S-N curves currently in preparation for the Health and Safety Executive by the Transport Research Laboratories, U.K. Work is also in progress for Eurocode 3. The API and HSE attempts at codifying the S-N curves have taken the form of suggesting lower bound curves to published S-N data with no due attention paid to the specific cable construction details and detrimental termination effects of test specimens which can both be of prime importance.

The present paper presents newly developed S-N curves which take the construction details of large diameter (i.e. realistic) spiral strands into account, and also cater for the effects of end terminations. The proposed S-N curves are based on extensive theoretical parametric studies using a newly proposed model. Finally, the proposed S-N curves are compared with others recommended by API, Chaplin, and Tilly, which are the ones that are currently most commonly referred to, and it is shown that in certain cases, these S-N curves provide unconservative results. As a pre-requisite to this, however, a brief description of the theoretical model follows next, which will, then, enable the reader to better understand (and appreciate) the results presented later.

2. THEORY

Using the orthotropic sheet model (1) it is now possible to obtain reliable estimates of interwire contact forces (and stresses) throughout multi-layered helical strands. Experimental observations suggest that individual wire failures are largely located over the trellis points of interlayer contact and it is now believed that this is as a result of high stress concentration factors in these locations.

Once the maximum effective Von-Mises stress, $\bar{\sigma}'_{max}$, over trellis points of contact, for a given mean axial load on the strand is calculated, the stress concentration factor, K_S, is defined as

$$K_S = \frac{\bar{\sigma}'_{max}}{\bar{\sigma}'} \tag{1}$$

where $\bar{\sigma}'$ is the nominal axial stress in the helical wires which may be calculated using the method developed by Raoof (1).

Raoof (1) deals with the topic of strand axial fatigue at some length. Using the so-obtained values of K_S in conjunction with axial fatigue data on single wires, a theory has been developed which predicts the axial fatigue life of strands (under constant amplitude cyclic loading) from first principles.

For carbon steel wires the fatigue stress-number of cycles plot (S-N curve) possesses an endurance limit, S′, below which no damage occurs. Traditionally the magnitude of S′ is compared to the ultimate wire strength, S_{ult}: tests on single galvanised wires suggest an approximate value of $S' = 0.27\ S_{ult}$. The reduced magnitude of the endurance limit, S_e, which takes interwire contact and fretting plus surface conditions and size effects, etc., into account may be defined as

$$S_e = K_a K_b S' \tag{2}$$

where, $K_b = \frac{1}{K_S}$, and K_a is a constant.

The so-obtained values of the parameters S_e, then, are used to produce the S-N curves for fatigue life to first outer (or inner) wire fractures in spiral strands using the S-N curves available in the literature for axial fatigue life of individual wires of a given grade (1).

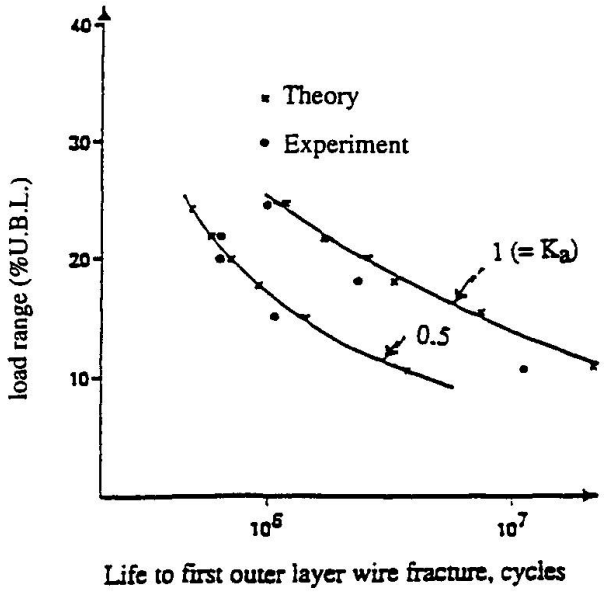

Fig. 1 Axial fatigue of 51mm O.D. strand-comparison of theory and test data.

Fig. 1 compares the theoretical predictions with experimental data for a 51mm diameter spiral strand. The criterion for fatigue initiation has been the occurrence of first wire failure in the outer layer. A fairly significant degree of scatter was found in the experimental data which may be covered by an empirical surface finish factor K_a in the range $0.5 \leq K_a \leq 1.0$. The ultimate tensile strength of the wire material is S_{ult} = 1640 N/mm^2. With the strands having epoxy resin end terminations, all the initial wire failures in this strand occurred away from the ends. However, as discussed elsewhere (2), for the end terminations to have no detrimental effects on the wire fractures remote from the ends the minimum length of test specimens must be around 10 lay lengths with the wire fractures occurring within the central region which extends by 2.5 lay lengths on either side of the middle of the test specimen (i.e. within the central portion with a length of 5 lay lengths). It then follows that due to the total length of the tested 51mm O.D. strands being significantly less than 10 lay lengths, even for the wire fractures away from the ends, certain test data points in Fig. 1 have been influenced by the detrimental end effects with the correlations between the theory and such test data suggesting $K_a = 0.5$ as an appropriate factor in the presence of end effects. Otherwise, for wire fractures which happen away from the ends and, in addition, are not influenced by end effects, one may assume $K_a = 1.0$: this, then, provides the reader with an insight into the role of the parameter K_a in the proposed theoretical model.

The theoretical predictions have been supported by a very extensive set of large scale test data relating to spiral strands with diameters equal to 25, 35, 39, 40, 44, 51, 53, 63, 100, 127, and 164mm as produced by different manufacturers and tested by Bridon Ropes, Imperial college, Transport Research Laboratories, and National Engineering Laboratories in U.K., and University of Alberta in Canada, with lay angles within the wide range $11^\circ \leq \alpha \leq 21^\circ$, and wire diameters covering the range 3mm $\leq D \leq$ 7.10mm, which very nearly embody the presently adopted manufacturing limits. In all cases, the correlations between the theoretical predictions and such an extensive set of large scale test data has been very encouraging. Space limitations do not allow a full reporting of such good correlations here: these have been reported fully in the references cited elsewhere (3). This, then, provides ample support for the general applicability of the recently proposed theoretical model which can predict both initial outer and/or inner wire breakages with the initial inner wire fractures generally having a lower fatigue life than the outer wires (1).

3. THEORETICAL PARAMETRIC STUDIES

3.1 Background

Recently, Bridon Ropes made the construction details for three realistic types of 127mm diameter spiral strands available to the present author. In particular, three different levels of lay angles (12°, 18° and 24°) were used for designing these strand constructions with each strand having the same lay angle in all its layers and their other geometric factors (such as number and diameters of the helical wires) were kept very nearly the same. As discussed elsewhere (3) following extensive theoretical and experimental work, the lay angle has been found to be the primary factor which controls a number of strand overall structural characteristics with the other geometrical factors being of secondary importance. It should be emphasised that the 12-24 degrees range of presently adopted lay angles cover the full practical range of this parameter as currently used by cable manufacturers. Ref. (3) gives the construction details for 127mm diameter spiral strands used in the following theoretical parametric studies. The assumed Young's modulus for galvanised steel wires E = 200 kNmm^{-2} and the Poisson's ratio for wire material ϑ = 0.28. The Ultimate Breaking Load (U.B.L.) of the strands was assumed to be the same, equal to 13510 kN, while tensile ultimate strength of the wire material S_{ult} =1520

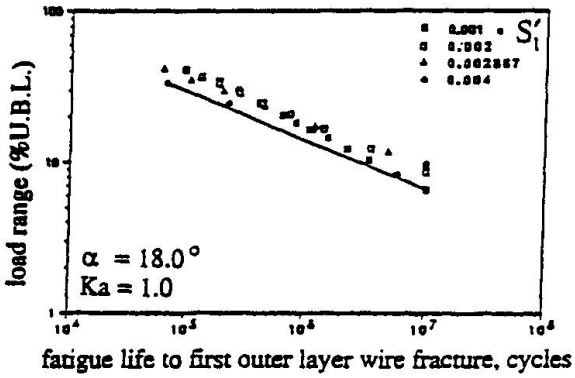

Fig.2
Theoretical effects of changing S_1' on axial fatigue life for a given lay angle, α.

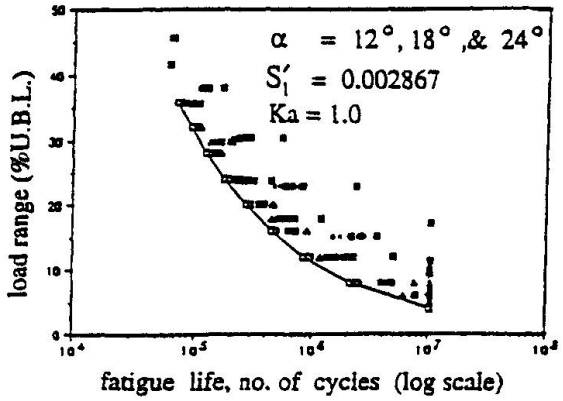

Fig.3
Theoretical effects of changing α on axial fatigue life for a given S_1' .

Nmm^{-2}.

For the purposes of theoretical parametric studies, four values of strand mean axial strains S_1' = 0.001, 0.002, 0.002867, and 0.004 were assumed which cover the usual practical working ranges for structural applications. Axial fatigue life was defined as the number of cycles to first wire fracture.

3.2 Design Recommendations

Fig. 2 presents (as a typical example) the plots (in log-log scale) of load range (as a percentage of U.B.L.) against axial fatigue life to first outer layer wire fracture for the 127mm diameter spiral strand with a lay angle of 18 degrees. The assumed value of K_a for this figure is 1.0 - i.e. the initial wire fractures are assumed to happen in the free field and are not affected by end terminations. The plots cover a wide range of $0.001 \leq S_1' \leq 0.004$. This figure includes a lower bound straight line to all the individual theoretical data points which compared to those in Fig. 3 are found to exhibit a much less degree of scatter. The composite data points in Fig. 3, on the other hand, relate to all the three types of 127mm diameter spiral strands with the lay angles of 12, 18, and 24 degrees and K_a = 1.0 (although, only one value of S_1' = 0.002867 has been assumed for all the results in this figure and changing the value of S_1' will cause significantly more degree of scatter in the results). Comparing the scatter of results in Fig. 2 with those in Fig. 3, therefore, strongly suggest the merits in separating the results for each individual value of lay angle: in this way, much more sensible lower bound S-N curves may be obtained with the individual data points relating to each lower-bound S-N curve exhibiting reasonable degrees of scatter. The above exercise may, therefore, be repeated for other cases of practical importance: (a) when K_a = 0.5 -i.e. when individual wire fractures are assumed to be affected by the end terminations; and (b) when the criteria for fatigue failure is changed to that corresponding to the other extreme condition - i.e. when fatigue life is defined as the number of cycles to first wire fracture in the innermost layer of helical wires. In case (b), two separate sets of plots may be obtained: (ii) those with K_a = 1.0; and (ii) another set using K_a = 0.5. Space limitations do not allow presentation of all the plots for cases (a) and (b) in the above, here. Suffice it to say that in all cases, the scatter of the individual theoretical data points (to which a lower-bound S-N curve is added) is similar to those presented in Fig. 2.

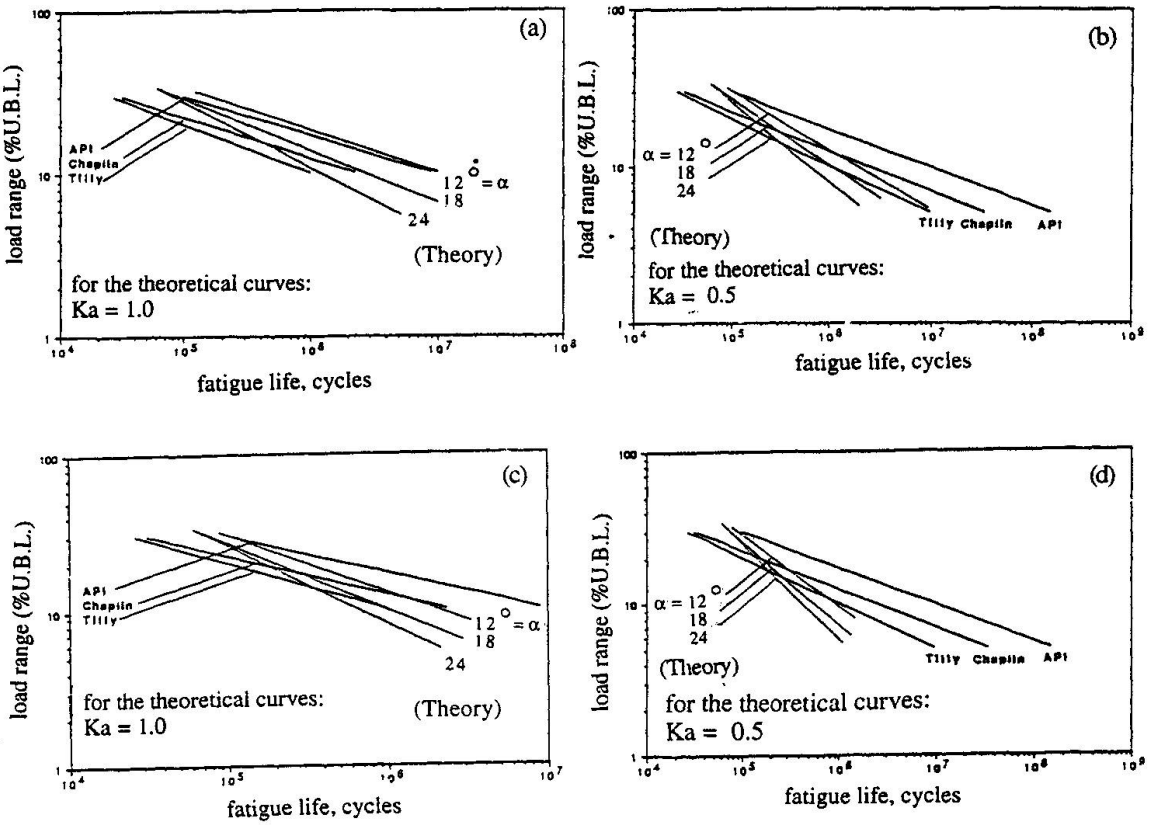

Fig. 4. Comparison of alternative design S-N curves for different values of K_a: (a) and (b) K_a = 1.0 and 0.5, respectively, for the fatigue life to first outer layer wire fracture; (c) and (d) K_a = 1.0 and 0.5, respectively, for the fatigue life to first wire fracture in the innermost layer.

Figs. 4a-d present all the so-obtained theoretical lower bound S-N curves. Figs. 4a,b correspond to the plots based on K_a values of 1.0 and 0.5, respectively, with the fatigue life defined as number of cycles to first outer layer wire fracture; while in Figs. 4c,d (which, again, assume K_a = 1.0 and 0.5, respectively), fatigue life is defined as the number of cycles to first wire breakage in the innermost layer. In each figure, three theoretical lower bound S-N curves corresponding to lay angles of 12, 18, and 24 degrees are presented and, considering that the plots are in log-log scale, the significant influence of lay angle on the axial fatigue life of spiral strands is obvious, with increasing values of lay angles in various layers leading to decreasing magnitudes of fatigue lives (for a given axial load range).

As mentioned previously, the assumed values of strand Ultimate Breaking Load (U.B.L.) and grade of wire for producing the theoretical lower bound S-N curves in Figs 4a-d are 13510kN and 1520 Nmm^{-2}, respectively. However, as discussed at some length elsewhere (3), because the strand axial load range in these plots is non-dimensionalized with respect to U.B.L., all the theoretical lower bound S-N curves are of general applicability irrespective of the magnitude of U.B.L. and grade of wire in practice. Included in Figs. 4a-d are also lower bound empirical S-N curves recommended by API (4), Chaplin (5), and Tilly (6), which are the ones most commonly referred to in the available literature. In producing these purely empirical S-N curves non of these references have differentiated between various types of strand (or, indeed, rope)

constructions used in their experiments. Moreover, different types of failure criterion have been adopted by these references: the failure criteria adopted by Chaplin is number of cycles to total collapse, while Tilly has chosen number of cycles to 5% wire fracture (i.e. life to fatigue initiation). The failure criteria chosen by API is not defined in the code, and there does not seem to be any background literature (available in the public domain) for this recommendation.

The potentially unsafe nature of the previously reported lower bound S-N curves of API, Tilly, and Chaplin for certain (i.e. smaller) levels of axial load range (depending on the magnitude of lay angle), as shown in Figs. 4a-d, is noteworthy. One thing is clear: the API recommended S-N curve can be unconservative for certain practical cases. As regards Tilly's or Chaplin's recommended S-N curves, the situation depends on the failure criteria adopted in practice, and the magnitude of the lay angle for the wires of the strands which are to be used in a given construction. In this context, one should also decide as to whether fatigue failures are to happen at (or in the vicinity) of end terminations or in the free field, away from the ends.

4. CONCLUSIONS

Using extensive theoretical parametric studies (based on a fully verified theoretical model) on some substantial (large diameter) multi-layered spiral strands with realistic construction details and covering the full manufacturing limits of lay angles which are the primary (controlling) parameter, a set of design S-N curves for axial fatigue life prediction of spiral strands are proposed. Unlike previously available and purely empirical S-N curves, the present recommendations cater for the influence of changes in lay angles on the strand axial fatigue life and also can account for the detrimental termination effects. Comparisons are made between the presently recommended design S-N curves and those recommended by others, and the previously available S-N curves are found to suffer from certain shortcomings.

REFERENCES

1. RAOOF, M., "Axial fatigue of Multi-Layered Strands", J. Engrg. Mech., ASCE, Vol.116, No. 10, 1990, 2083-2099.
2. RAOOF, M., and HOBBS, R.E., "Analysis of Axial Fatigue Data for Wire Ropes", Int. J. Fatigue, Vol. 16, Oct., 1994, 493-501.
3. RAOOF, M., "Recommendations Regarding Design of Spiral Stands Against Axial Fatigue Failure", accepted for inclusion in the Proc. of 8th (1998) Int. Offshore and Polar Engrg. Conf., Montreal, May, 1998.
4. API 2FP1 (RP2FP1), API Recommended Practice for Design, Analysis, and Maintenance of Moorings for Floating Production systems, 1992.
5. CHAPLIN, C.R., "Prediction of Offshore Mooring Ropes", Proc. Round Table Conf. on Applications of Wire Rope Endurance Research, OIPEEC, Delft, Netherlands, Sept., 1993, 50-75.
6. TILLY, G.P., "Performance of Bridge Cables", 1st Oleg Kerensky Memorial Conf.held at Queen Elizabeth II Conference Centre, Instn. Structural Engrs., London, U.K., June, 1988, Session 4, 22/4-28/4.

Welded High Strength Low Alloy Steels in Seismic Design

Mikael LORENTZON
Graduate Student
Lulea Univ.
Lulea, Sweden

Kjell ERIKSSON
Assoc. Prof.
Lulea Univ.
Lulea, Sweden

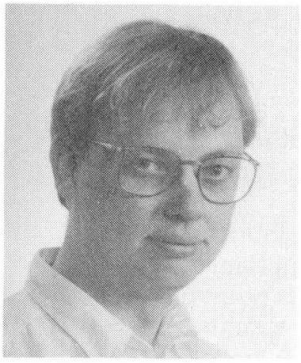

Kjell Eriksson, born in 1941, received his Ph.D. in fracture mechanics in 1975 at the Royal Inst. of Technology, Sweden. His research field is fracture and fatigue of heavy welded steel structures.

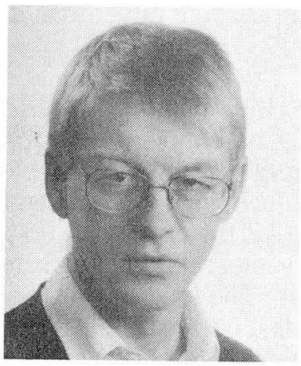

Mikael Lorentzon born in 1967, received his M.Sc. degree in mechanical eng. 1992. He is now at Lulea Univ., Div. of Solid Mechanics for research studies in fracture mechanics.

Summary

High strength low alloy steels (HSLA) are frequently used in applications when high strength properties enable weight reduction, e.g. in long span bridges. Results of an experimental investigation show that the HAZ fracture toughness in HSLA depends strongly on the loading rate and temperature. At low and static loading rates ductile behaviour is enhanced and at increased loading rates there is a transition to brittle behaviour. Loading rates that reduce the fracture toughness significantly are frequent in buildings and bridges during a seismic event. This means that surprisingly short fatigue cracks become critical so that dissipative zones may fracture rather than deform and prevent structural collapse.

1. Introduction

In regions of high seismic risk steel structures are usually preferred because of their often superior performance in terms of strength and ductility. Structural ductility is achieved by allowing yielding in selected parts of the structure upon loading beyond a certain level, so-called dissipative zones. During severe seismic events such zones absorb seismic energy through ductile behaviour and hysteresis. Current design methods [1] recommend that connections in dissipative zones shall have sufficient strength to allow yielding of connected parts. In order to ensure this, butt welds or full penetration welds are recommended. It is obvious that this design philosophy assumes that structural elements are free from starting points for fracture, i. e. severe stress concentrators such as sharp defects and fatigue cracks. Despite current seismic design codes, serious failures of steel structures have not ceased to occur. Post-earthquake investigations [2]-[3] have pointed out that welded connections are critical locations for several types of structures. The most typical damages reported from the Kobe earthquake may be summarised as following: 1) fracture of fillet welded joints of beam to column connections, 2) column-to-column with partial joint penetration weld and 3) fillet welded joints of column to through diaphragm. Another interesting observation was that surprisingly short cracks and geometrical discontinuities provided starting points for brittle fracture.

In this work it is assumed that some insight into the cause of some of these failures can be gained through a fracture mechanics approach. Small fabrication defects, e.g. weld undercuts and slag inclusions, are almost always present in welded joints. Fatigue cracks may initiate and grow from such initial defects during normal service. Under normal service loading conditions, short fatigue cracks may exist without seriously affecting the load carrying capacity of a structure. During a seismic event structures are in general subjected to both inertia loads and high loading rates. In a previous investigation [4] it was found that loading rates just above the maximum limit prescribed in the fracture toughness testing standard ASTM E813 [5] significantly affect the fracture toughness of ordinary C-Mn structural steels. In practice that means that shorter cracks become critical and that dissipative zones may fracture rather than deform and absorb energy at increased loading rates.

The observations in [4] raised the question if similar rate effects exists in HSLA steels, particularly in HAZ material. These modern structural steels are frequently used in applications when high strength properties allow weight reduction, e.g. in long span bridges. In this paper the results of an experimental investigation of the fracture toughness of both base and HAZ material of an HSLA steel are presented. The crack driving force in terms of the J-integral [6] is evaluated for an edge cracked beam flange with the finite element method. The loading rates are, from a fracture mechanics point of view, estimated in a simple elastic frame subjected to ground acceleration. The results are discussed in connection to fracture toughness testing requirements in current design codes.

2. Material

The test material comprised both base and HAZ material of an HSLA steel. Two 16 mm plates were joined with a 1/2 V-butt weld. In order to achieve as good toughness properties as possible and to reduce residual stresses welding was performed with multi-run welds and the submerged metal arc process. The chemical composition of the base material is shown in Table 1 and the tensile properties in Table 2. The Charpy-V notch toughness of the base material is typically 30 J at -60 °C.

Table 1. Chemical composition of the base metal (wt %).

C	Mn	P	S	Si	Mo	N	B
.15	1.40	.025	.01	.45	.10	.015	.002

Table 2. Tensile properties of base metal at 20 °C.

ReH [MPa]	R_m [MPa]	A_5 [%]
700	780-930	14

Proportional single edge notched bend specimens (SENB) according to ASTM E813 were taken from both base and HAZ material. The notch plane was perpendicular to the rolling direction of the parent material and in the case of HAZ material, parallel to the longitudinal direction of the weld. The HAZ is usually divided into number of subzones depending on the material being welded. Each sub-zone refers to a different type of microstructure and different mechanical properties [7]. In this investigation the interest was focused on the coarse grained material adjacent to the weld metal.

3. Experimental

The quasi-static fracture toughness testing were performed in a servo hydraulic testing machine. Testing was performed at + 20 °C and -30 °C. The low temperature tests were

carried out in a climate chamber. The tests were carried out under displacement control and at different displacement rates. The loading rate in this work is defined as the linear elastic stress intensity rate and is taken as a measure of how fast the crack tip region is loaded. In each test the load and load point displacement signals were recorded with a high speed data acquisition equipment. According to ASTM E813, the critical value of the J-integral, denoted J_C, characterises the onset of crack growth. The J_C values were calculated from the area under the load-displacement curves to the maximum load using the equation for three-point bend specimens:

$$J_c = 2A / Bb \qquad (1)$$

where A is the area under the load-displacement curve, B specimen thickness and b remaining ligament. A test is considered valid if the specimen thickness meets the requirement:

$$B \geq 25 J_c / \sigma_Y \qquad (2)$$

where σ_Y is the yield strength.

4. Results

For the base metal, no significant loading rate effect on the fracture toughness was observed. This material was ductile at -30 °C over the entire loading rate range investigated. Some typical load versus load point displacement recordings are shown in Fig. 1a. Crack growth was preceded by significant lateral contraction of the material ahead of the crack tip. In all tests pop-in was observed and none of the specimens fractured completely. The obtained fracture toughness is typically greater than 300 kN/m.

The HAZ material showed a brittle behaviour already at low loading rates. From an engineering point of view, all these tests were brittle. The load-displacement curves were almost linear up to the fracture load, Fig. 1b. The fracture toughness was reduced to one third of the fracture toughness at the static loading rate. For the HAZ material, all fracture surfaces showed two distinct regions, a central flat region and a region of shear lips. The central flat region was shiny and faceted and typical for brittle fracture. All tests on the HAZ material at -30 °C are summarised in Fig 2. Only one single test was performed with HAZ material at room temperature and slow loading rate. Surprisingly, this test showed brittle behaviour and the obtained fracture toughness J_C was 86 kN/m.

5. Discussion

5.1 Material behaviour

Modern methods for producing high strength structural steels with yield strength in the range 420-500 MPa are based on thermo-mechanical rolling (TM) and accelerated cooling process. For steels with yield strength in the range 600-960 MPa the QT method (quenching and tempering) is usually preferred. This is in fact the only realistic method to achieve high yield strength without adversing weldability [8]. In practise, both these methods means tightly controlled manufacturing conditions. Welding is in fact a process with quite the opposite effect. As a result of the welding thermal cycle the original micro-structure and properties of the metal in a region close to the weld metal are strongly affected. It is of common knowledge that the microstructure of the grain coarse zone, above all other zones in the HAZ, determine the properties of the weld. In ordinary C-Mn structural steels, low fracture toughness is usually associated with the coarse grained HAZ and the intercritically reheated HAZ. The tests in this investigation show that the fracture toughness at the increased loading rate is further reduced of the order two thirds in the heat affected region. This result was somewhat unexpected considering the excellent properties of the base material. In fact, the fracture toughness values at the increased loading rate are of the same magnitude of order as those of the older C-Mn structural steels reported in [4].

5.2 Application of results

Steel frameworks have many practical applications, such as buildings and bridges. A steel frame essentially consists of beams and columns joined by connections. For the design of structures, the maximum values of relative displacement, relative velocity and absolute acceleration of the response vibration are the most important parameters. Consider for example a simple elastic frame with two columns of height L and with a rigid top beam subjected to a piecewise linear acceleration spectrum, Fig 3. The mass of the top beam is here assumed 8 ton and the total stiffness 900 kN/m. The input load is a total period of 3 s of strong ground motion with a peak ground acceleration of 0.3 g. A numerical solution routine based on the central difference method [9], can be used to solve the equation of motion provided that the time step is considerably smaller than the natural period of the structure. The calculated displacement versus time is shown in Fig. 3. The maximum loading rate in terms of linear elastic stress intensity rate can be estimated from the slope of the displacement curve for some different crack lengths. According to elementary frame analysis, the stress rate at the beam ends can be expressed as

$$\dot{\sigma} = \frac{\dot{M}}{W_x} = \frac{6EI}{W_x L^2}\dot{u} \qquad (3)$$

where E is the elastic modulus, I the moment of area, du/dt the displacement rate and W_X the bending resistance. The linear elastic stress intensity rate for a beam flange with an edge crack is approximately given by

$$\dot{K}_I = \dot{\sigma}\sqrt{a\pi} f(a/W) \qquad (4)$$

where a is the crack length, W the flange width and $f(a/W)$ a dimensionless geometry function. With W_X = 1680 cm^3, I = 25 166 cm^4 and L = 11.2 m, the maximum loading rate for the case investigated is typically 242-343 MPa$\sqrt{}$m/s for crack lengths 25-50 mm. Even if the response of a real structure is more complicated, this simple example indicates that the loading rate in an elastic frame work is higher than the maximum rate prescribed in current fracture toughness standard (ASTM E813) and within the range of reduced fracture toughness.

5.3 Crack driving force J

The path independent J-integral, is widely used as a criterion in fracture mechanics to determine the onset of crack growth. In this work a finite element model of a beam flange with an edge crack was used to investigate the influence of crack length and stress level on the crack driving force J. For the calculations the finite element program ADINA [10] was employed. The model was composed of 286 eighth-nodes elements and plain strain conditions were adopted. In the crack tip elements 1/r strain singularities were obtained by collapsing the crack side nodes on to one point in the unloaded state. The material model was plastic-multilinear and with data points in general agreement with typical tensile tests on HSLA. About 100 time increments were used through one loading history. The J-integral was calculated for eight contours through the Gauss integration points of the elements surrounding and at different distances from the crack tip.

The calculated value of J versus nominal stress is shown in Fig. 4 for different crack lengths. The lowest fracture toughness data observed in this investigation is marked by a dashed line. Assume that a 25 mm deep fatigue crack exists in a beam element and that the fracture toughness is approximately $J_C \approx 20$ kN/m. That means that a nominal stress level of $\sigma_O/\sigma_Y \approx 0.3$ is sufficient to initiate crack growth. This example shows that already short fatigue cracks are critical and that sufficient fracture toughness is a necessary requirement to achieve global ductility.

6. Conclusions and further work

Further experimental work is necessary to determine the fracture toughness of HAZ material under different welding conditions, loading rates and temperatures. One single test indicated brittle material behaviour already at room temperature. This indication is, if general, of importance for most applications. To determine loading rates from a fracture mechanics point view in some typical structures subjected to ground motion, is another interesting study in prospect. However, based on the findings in this investigation, the following conclusion can be drawn:

The fracture toughness of HSLA base and HAZ material depends strongly on the loading rate.

Fracture toughness is strongly reduced at loading rates above the maximum limit prescribed in ASTM E813.

In common structures loading rates caused by earthquakes often exceed the maximum loading rate prescribed in fracture toughness testing standards.

A necessary condition for global ductility of structures is sufficient local fracture toughness properties of structural elements and connections.

References

1. Mazzolani F. M. and Piluso V., Theory and Design of Seismic Resistant Steel Frames. St Edmundsbury Press, Bury St Edmunds, Suffolk, 1996.

2. Toyoda M., How Steel Structures Fared in Japan's Great Earth quake. Welding Journal, December 1995.

3. Nakashima S., Kadoya H. and Igarashi S., A Report Concerning Damage to Steel Structures Caused by the Hanshin Earthquake. Nordic Steel Construction Conference, Malmö, Sweden, 1995.

4. Lorentzon M. and Eriksson K., The influence of intermediate loading rates and temperature on the fracture toughness of ordinary carbon manganese structural steels. To appear in Fatigue Fract. Engng Mater. Struct.

5. ASTM E813-89, Standard Test Method for J_{Ic}, a Measure of Fracture Toughness, American Society for Testing and Materials, Philadelphia, 1987.

6. Rice J. R., A Path Independent Integral and the Approximate Analysis of Strain Concentration by Notches and Cracks. Journal of Applied Mechanics, Vol. 35, 1968, 379-386.

7. Easterling K., Introduction to the Physical Metallurgy of Welding, Butterworths, London, 1983.

8. Ahlbom B., Modern Fine Grain High Strength Steels for Structural Applications. Nordic Steel Construction Conference, Malmö, Sweden, 1995.

9. Irvine H. M., Structural dynamics for the practising engineer, Allen & Unwin Ltd, London, UK, 1986.

10. ADINA, Theory and modelling guide, Report ARD 92-8, 1992, ADINA R&D, Inc., Watertown, MA.

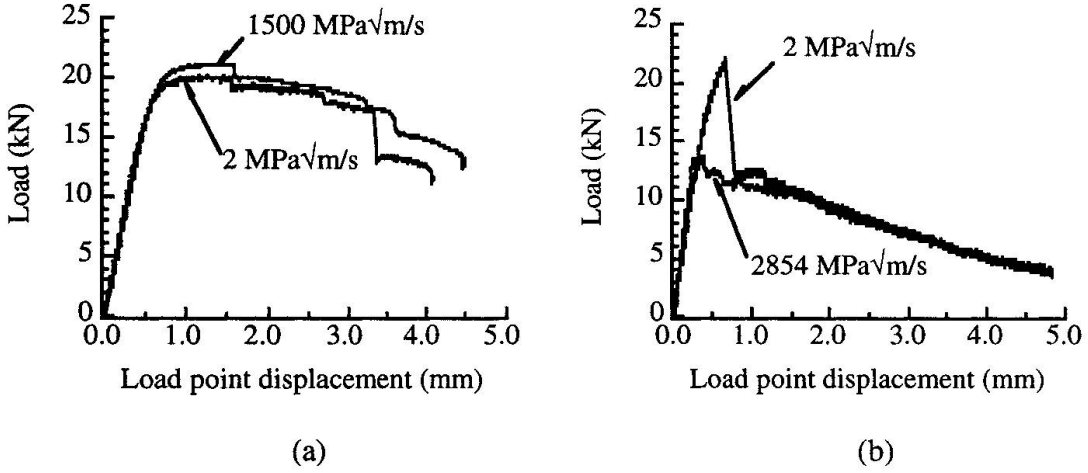

Fig. 1 Load versus load point displacement, a) base metal and b) HAZ material.

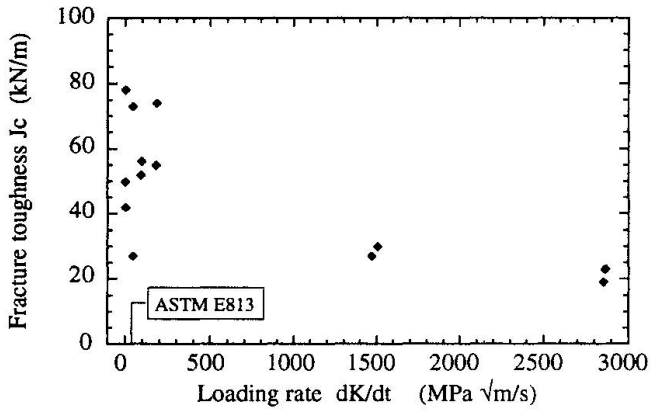

Fig. 2 Influence of loading rate on HAZ fracture toughness at temperature -30 °C.

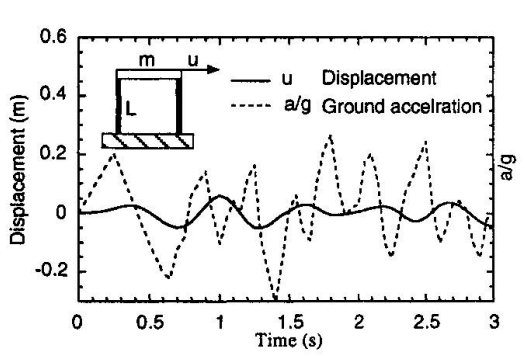

Fig. 3 Response of a simple elastic frame work subjected to ground acceleration.

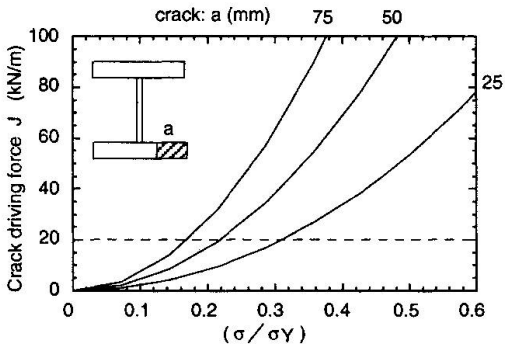

Fig. 4 Crack driving force J versus stress for some different crack lengths, σY = 700 MPa.